ENDOCANNABINOID AUGMENTATION THROUGH SUBSTRATE-SELECTIVE COX-2 INHIBITION: BEHAVIORAL AND SYNAPTIC EFFECTS IN AN ANIMAL MODEL OF STRESS-INDUCED ANXIETY

By

Joyonna Carrie Gamble-George

Dissertation

Submitted to the Faculty of the

Graduate School of Vanderbilt University

in partial fulfillment of the requirements

for the degree of

DOCTOR OF PHILOSOPHY

in

Neuroscience

August, 2016

Nashville, Tennessee

Approved:

Martin J. Gallagher, M.D., Ph.D.

Andrew Holmes, Ph.D.

Christine Konradi, Ph.D.

Sachin Patel, M.D., Ph.D.

To those who paved a way for me to pursue my dreams and aspirations.

ACKNOWLEDGEMENTS

This work would not have been possible without the generous financial and career development support from the National Institutes of Health (NIH) Grants K08MH090412 (Sachin Patel), R01MH100096 (Sachin Patel), GM15431 (Lawrence J. Marnett), the NIAAA Intramural Research program (Andrew Holmes), the NIH Initiative for Maximizing Student Diversity (IMSD) Program (Joyonna Gamble-George), Vanderbilt Brain Institute (VBI) Scholars Program (Joyonna Gamble-George), Southern Regional Education Board (SREB)-State Doctoral Scholars Program (Joyonna Gamble-George), UNCF/Merck Graduate Science Research Dissertation Fellowship (Joyonna Gamble-George), and the Society for Neuroscience (SfN) Neuroscience Scholars Program (Joyonna Gamble-George).

Also, I would like to thank those that collaborated with my lab on this research project, the laboratory of Dr. Andrew Holmes at the National Institute on Alcohol Abuse and Alcoholism (NIAAA) and the laboratory of Dr. Lawrence Marnett at Vanderbilt University. In particular, I would like to give a special thanks to Dr. Lindsay Halladay for conducting the *in vivo* electrophysiological experiments and analyses in the laboratory of Dr. Andrew Holmes (see CHAPTER III) and the Vanderbilt University Neurochemistry Core Laboratory for performing neurochemical profiling of our brain tissue samples. Moreover, I would to thank my dissertation committee for their suggestions and advice concerning my research project.

I would also like to thank those individuals that truly made a difference in my life as I completed my PhD degree program and continue to pursue my career aspiration of becoming a scientist. First, I would like to acknowledge my ancestors, who traveled thousands of miles from the shores of Africa as they were taken tragically from their homeland to one that was foreign. It still amazes me how they were able to make a way for future generations to fulfill their life dreams

in the United States despite slavery, continuous oppression and discrimination due to their skin complexion, and limited support. As I continue my journey to become a scientist, I hope I have the courage and willpower to standup for my values of integrity and respect and love for myself and thy fellow man that were passed down from my ancestors. My great great great grandmother Julia Jackson, who was a midwife during slavery in the United States, is a great example of such bravery and resolve. She taught my family the true meaning of sacrifice when she refused to be a victim of sexual exploitation at the hands of her slave master by saying she would not be "a slave in the day and [his] lover at night." As a result, she was separated from her husband and children, sent "as far as wind and water could take her" away, and eventually sold to another slave owner. She truly embodied the sacrifices my ancestors had to make at times in order to survive the psychological and physical tortures of slavery. I hope her resilience to standup for what was right will serve as a reminder of the strength I must maintain as I pursue a career, where females and African-Americans are underrepresented and continue to face injustices due to the ignorance of others. I would also like to thank my grandparents in Alabama, Joseph Pettway, Sr., and Menda Pettway, for always instilling in me the importance of acquiring a quality education, treating others with respect, compassion, and dignity, and how the acquirement of knowledge leads to self-empowerment. To my aunt and second mother, Judge Jo Celeste Pettway, thanks for letting me know that I can do anything I put my mind to, even if it involves working in a male-dominated career. I still remember that one Christmas when you bought me Barbie dolls along with G.I. Joes and Teenage Mutant Ninja Turtles. You let me know back then that the world could be my canvas to create whatever fulfilling life I would want to achieve one day. To my parents, Lay'wan Gamble and Kelvin George, thanks for all the advice you gave me when faced with life's challenges and allowing a village to raise me and help me grow into the woman I am today. Thank you Linda

Sealy and Roger Chalkley, who are co-directors of the NIH Initiative for Maximizing Student Diversity (IMSD) Program at Vanderbilt University, for always being there for me and uplifting me and believing in me when many did not do the same. You have no idea how you two have inspired me to keep pursuing my dream of becoming an academic scientist. You two made my love for science and the pursuit of understanding science through research much deeper and everlasting. Thanks to my colleagues at the University of South Florida College of Public Health for always supporting and encouraging me even after I finished my Master's degree in Health Administration. You always made me feel like a member of a close-knit family. I will cherish you throughout my life. Also, thanks to all my friends and relatives that I did not mention by name that were my cheerleaders and listening ears as I pushed forward through the years to complete my PhD degree program. Last but not the least, I would like to give thanks to a higher power (who else but GOD) for getting me through times of uncertainty and confusion and helping me to maintain my steadfast drive to pursue and achieve my career goals no matter what hindrances life inflicted upon me.

TABLE OF CONTENTS

LIST OF FIGURES

ABBREVIATIONS

AEA, anandamide
2-AG, 2-arachidonylglycerol
ANOVA, one-way analysis of variance
BCA, bicinchoninic acid
BLA, basolateral nucleus of the amygdala
BNST, bed nucleus of stria terminalis
CB_1R, cannabinoid type 1 receptor
CB_2R, cannabinoid type 2 receptor
CD-1, caesarean derived-1
CeA, central nucleus of the amygdala
cAMP, cyclic adenosine monophosphate
CORT, corticosterone
COX-2, cyclooxygenase-2
CS, conditioned stimulus
DAGLα, diacylglycerol lipase
Δ^9-THC, delta-9-tetrahydrocannabinol
DMSO, dimethyl sulfoxide
DOPAC, dihydroxyphenylacetic acid
1-EBIO, 1-ethyl-2-benzimidazolinone
eCB, endocannabinoid
ECS, endocannabinoid system
EDTA, ethylenediaminetetraacetic acid
ELISA, enzyme-linked immunosorbent assay
FAAH, fatty acid amide hydrolase
GABA, gamma-aminobutyric acid
GAD, generalized anxiety disorder
GPCR, G protein-coupled receptors
5-HIAA, 5-hydroxyindoleacetic acid
HPA, hypothalamic-pituitary-adrenal
HPC, hippocampus
HPLC, high performance liquid chromatography
5-HT, 5-hydroxytryptamine or serotonin
HVA, homovanillic acid
K-S, Kolmogorov-Smirnov
LA, lateral nucleus of the amygdala
LC-MS/MS, liquid chromatography coupled with tandem mass spectrometry
LMX, lumiracoxib
MAGL, monoacylglycerol lipase
3-MT, 3-methoxytyramine
NAPE-PLD, *N*-arachidonoyl phosphatidyl-ethanolamine phospholipase D
NIFS, novelty-induced feeding suppression
NS, no stress or not significant
NT, neurotransmitter
OCD, obsessive compulsive disorder

PFC, prefrontal cortex
PGE_2, prostaglandin E2
PVN, paraventricular nucleus
PTSD, posttraumatic stress disorder
S, stress
SK, small conductance calcium-activated potassium
SR141716, rimonabant
SSCI, substrate-selective COX-2 inhibition or substrate-selective COX-2 inhibitor
TCA, trichloroacetic acid
TRPV1, transient receptor potential cation channel, subfamily V, member 1
US, unconditioned stimulus

CHAPTER 1

THE ENDOCANNABINOID SYSTEM AND STRESS-INDUCED ANXIETY: A CASE OF MODERATION IN THE AMYGDALA

Introduction

At least once in an individual's lifetime, anxiety, a natural response to a stressful event, will be encountered. However, for some individuals, anxiety can become so maladaptive and a daily burden that it can eventually develop into a psychiatric disorder. Millions of people worldwide are affected by psychiatric disorders that are classified as an anxiety, trauma-related, or stressor-related disorder. Some examples of these psychiatric disorders are GENERALIZED ANXIETY DISORDER (GAD)[1], PANIC DISORDER[2], POSTTRAUMATIC STRESS DISORDER (PTSD)[3], SOCIAL PHOBIA[4], OBSESSIVE COMPULSIVE DISORDER (OCD)[5], AGORAPHOBIA[6], and other SPECIFIC PHOBIAS[1-4]. In the United States, anxiety, trauma-related, and stressor-related disorders are the most common mental health problems, imposing a social and economic challenge on the U.S. health care system and society. Affecting about 20% of the U.S. population aged 18 or older[1] and about 10% of teenagers between the ages of 13 and 18[2], these psychiatric disorders cost the U.S. over $40 billion annually due to prescribed medications, repeated hospitalizations[5], reduced productivity, absenteeism from the workplace, and suicide[6]. More effective and inexpensive treatment options to manage the negative effects of

[1] **GENERALIZED ANXIETY DISORDER**: An anxiety disorder that consists of constant, excessive, and impractical worry and tension about everyday concerns that lasts up to six months.
[2] **PANIC DISORDER**: An anxiety disorder that is characterized by spur-of-the-moment panic attacks and persistent worry about the fear of experiencing another panic attack.
[3] **POSTTRAUMATIC STRESS DISORDER**: An anxiety disorder that involves enduring recurrent nightmares following reminders of a single or repeated traumatic occurrence experienced directly or witnessed in others.
[4] **SOCIAL PHOBIA**: An anxiety disorder, also known as social anxiety disorder that is characterized by an intense fear of being judged by others in social settings.
[5] **OBSESSIVE COMPULSIVE DISORDER**: An anxiety disorder that is characterized by continuous, unwelcomed thoughts (e.g., obsessions) that compels an individual to enact routines repeatedly (e.g., compulsions) in order to lessen anxiety resulting from the obsessions.
[6] **AGORAPHOBIA**: An anxiety disorder that involves avoidance of situations or places where an individual experienced a panic attack as a result of fear of experiencing another panic attack.

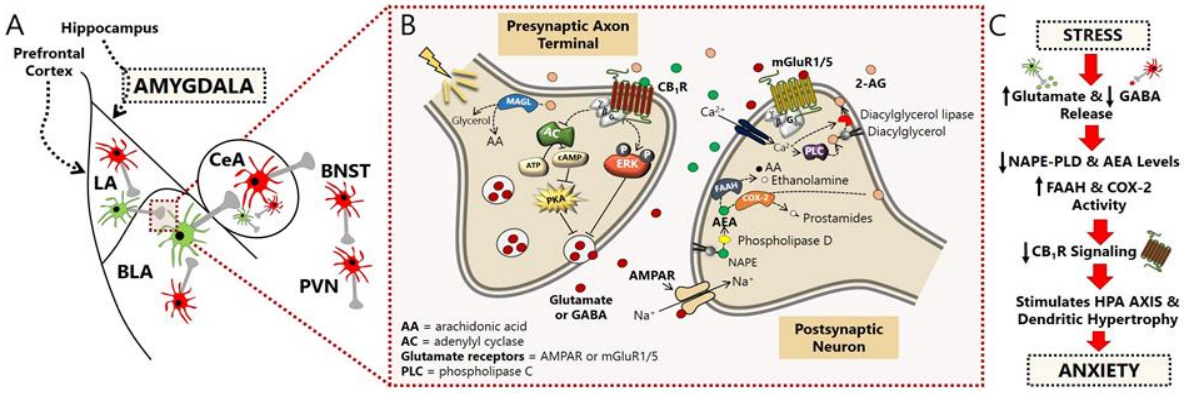

Figure 1. Intraamygdalar stress circuits and molecular mechanisms in stress-induced anxiety. a. In response to stress, the neuronal circuit that includes the amygdala and involves the hippocampus or prefrontal cortex sending glutamatergic projections (GREEN) to the LA or directly to the BLA is activated. The LA then sends glutamatergic inputs that project onto glutamatergic pyramidal neurons in the BLA, which then sends glutamatergic afferents to the CeA. Next, the CeA sends inhibitory inputs (RED) to the PVN of the hypothalamus indirectly via the BNST, where the HPA axis is activated. **b.** Upon increases in excitation or depolarization, glutamate is released from the presynaptic axon terminal. Glutamate then activates glutamate receptors on the postsynaptic neurons, initiating the synthesis of the endocannabinoids (eCBs), anandamide (AEA) and 2-arachidonylglycerol (2-AG), which are released and travel to a presynaptic axon terminal, where the eCBs activate cannabinoid receptors. Activation of the cannabinoid receptor, CB_1R, triggers downstream signaling which induces a reduction in synaptic transmission of either glutamate or GABA. [Figure adapted from Hill, M. and Patel, S. (2013). Translational evidence for the involvement of the eCB system in stress-related psychiatric illnesses. *Biology of Mood & Anxiety Disorders*. **3** (19): 1-14.] **c.** In the amygdala, stress causes increased synaptic glutamate release and decreased synaptic GABA release, inducing amygdalar excitability. This causes a reduction in AEA synthesis via NAPE-PLD and an increase in its degradation via FAAH and COX-2, reducing signaling through the CB_1R. Consequently, the HPA axis is stimulated and dendritic hypertrophy occurs. These biochemical and morphological changes induce the development of anxiety-like behaviors. HPA, hypothalamic-pituitary-adrenal.

anxiety are needed. Molecular targets involved in the endocannabinoid (eCB) system (ECS) have provided a promising alternative to treat individuals burdened by anxiety. Cannabinoid receptor agonists have proven to be effective in lessening anxiety-like behaviors caused by stress in experimental animals and humans[7-12]. However, preclinical animal studies provide evidence that these ligands produce adverse motor responses and cognitive impairments and bimodal control of anxiety, which is dependent upon many variables, including, but not limited to, dosage, time of drug administration, and the context in which a stressor is applied[13-21]. Thus, other molecular targets, such as eCB degradative enzymes, that can enhance signaling through cannabinoid

receptors by augmenting eCB levels in the brain upon pharmacological inhibition, are being investigated for their potential for combating anxiety and stress responses[22-28].

Retrograde Endocannabinoid Signaling

Endocannabinoids (eCBs) are lipid derived molecules that activate endogenous G PROTEIN-COUPLED RECEPTORS (GPCR)[7], called cannabinoid receptors, in the central nervous system. The eCBs, anandamide (AEA) and 2-arachidonylglycerol (2-AG), are synthesized "on demand" at postsynaptic sites in brain structures, such as the amygdala, as a result of elevations in neuronal excitation or calcium levels caused by depolarization[29]. Upon synthesis, eCBs are released and transported in a retrograde fashion from postsynaptic sites to presynaptic axon terminals, where they activate cannabinoid receptors (Fig. 1b)[30-34]. One of the endogenous cannabinoid receptors is the cannabinoid type 1 receptor (CB_1R)[35]. CB_1R mRNA and protein have been identified in many brain structures, including, but not limited to, the cerebral cortex, hippocampus, AMYGDALOID COMPLEX[8], hypothalamus, thalamus, olfactory-associated structures, brainstem, and the cerebellum[36-43]. The amygdala is comprised of several nuclei with three prominent nuclei: the lateral (LA), basolateral (BLA), and central (CeA) nuclei[36]. More CB_1R mRNA and protein are expressed in the BLA and LA than in the CeA[42,44-46]. CB_1Rs are located on axon terminals that contain gamma-aminobutyric acid (GABA) or glutamate[47,48]. In the amygdala, where the majority of neurons are excitatory pyramidal neurons followed by GABAergic interneurons[36,49-57], CB_1Rs are highly expressed in interneurons as opposed to

[7] **G-PROTEIN-COUPLED RECEPTOR**: A receptor that interacts with a group of integral membrane proteins that bind to guanosine triphosphate (GTP) in its active form (G proteins), catalyze the hydrolysis of GTP to GDP when activated, and relay signals from the receptor to other molecules and downstream effectors.

[8] **AMYGDALOID COMPLEX**: A brain structure comprised of the following nuclei: the basolateral nuclei (e.g., lateral nucleus (LA), basolateral nucleus (BLA), and the accessory basal nucleus (AB)), corticomedial nuclei (e.g., nucleus of the lateral olfactory tract (NLOT), bed nucleus of the accessory olfactory tract (BAOT), anterior and posterior cortical nucleus (CoA and CoP, respectively)), centromedial nuclei (e.g., central (CeA), medial (M), and amygdaloid part of the bed nucleus of stria terminalis (BNST)), and other amygdaloid nuclei (e.g., anterior amygdale area, amygdalo-hippocampal area, intercalated nuclei, and the ventral pallidum.

projecting pyramidal neurons[58]. When activated, the CB_1R inhibits cyclic adenosine monophosphate (cAMP) formation via inhibition of adenylyl cyclase, which downregulates protein kinase A signaling, and activates extracellular signal-regulated kinase by signaling through $G_{i/o}$ proteins[35,59-68]. Such effects on downstream effectors result in activation of potassium ion channels, inhibition of calcium channels, and subsequently, reduced synaptic transmission of glutamate or GABA from amygdalar axon terminals (Fig. 1b)[69]. Reduced GABA release from axon terminals of interneurons has been suggested to increase the excitability of pyramidal neurons in intraamygdalar pathways, targeting brain regions which mediate stress responses and anxiogenic behaviors, such as the bed nucleus of stria terminalis (BNST) and the paraventricular nucleus (PVN) of the hypothalamus (Fig. 1a)[70,71].

Endocannabinoid System Modulation of Anxiety-Like Behaviors in the Amygdala

Stress, whether induced by physical or psychological means, can alter the form and structure of neurons as well as their biochemical makeup. These morphological and biochemical alterations caused by stress can be manifested in the form of anxiety-like behaviors[72-76]. One brain structure that plays a role in emotional processing and mediates stress responses is the amygdala. The amygdala, which is located within the medial temporal lobe of the brain, processes visual, auditory, olfactory, and somatosensory information originating from the external environment that is transmitted from cortical brain areas. It then assigns emotional significance to such external stimuli by activating efferent neuronal projections from the amygdala to other brain structures and, subsequently, produces corresponding behavioral responses to the stimuli.[36,77-81].

Effects of Stress on Amygdalar Morphology and Biochemistry. In studies involving experimental animals, physical stress in the form of acute and chronic immobilization stress has been reported

to cause anxiety-like behaviors. Under chronic stress conditions (5, 10, or 21 days), these behavioral manifestations of anxiety accompany enhanced dendritic hypertrophy and spine density in excitatory pyramidal neurons of the BLA and decreased dendritic arborization in GABAergic interneurons of the LA and BLA[28,74,82-85]. This morphological phenotype is analogous to that observed in the BLA of mice with CB_1R gene disruption[86]. With reference to altering neuronal biochemistry, chronic immobilization stress also induces neuronal activation and excitotoxicity by increasing glutamate release at excitatory synapses and decreasing inhibitory tone in the amygdala, causing activation of glutamate receptors and loss of local calcium-activated potassium channels[43,76,87-96]. These findings correspond to studies which found increased amygdalar activity in patients with PTSD, social anxiety disorder, or specific phobia[97]. Changes in amygdalar morphology and biochemistry as a consequence of stress have been suggested to be the result of stress-induced increases in corticosterone, a glucocorticoid hormone that modulates stress responses[98-100]. In addition, immobilization stress applied acutely or chronically can alter eCB levels in the brain. Acute and chronic immobilization stress causes decreases in AEA content in the amygdala, whereas only chronic immobilization stress causes increases in 2-AG content in the amygdala[28,101]. These changes in eCB content correspond to changes in the levels of eCB biosynthetic and degradative enzymes in the amygdala as a consequence of stress. Rats exposed to the odor of a cat, its natural predator, induce decreases in genes that code for the AEA biosynthetic enzyme, *N*-arachidonoyl phosphatidyl-ethanolamine phospholipase D (NAPE-PLD), and the 2-AG biosynthetic enzyme, diacylglycerol lipase (DAGLα), and increases in the AEA degradative enzyme, fatty acid amide hydrolase (FAAH), in the amygdala[102,103]. Also, chronic immobilization stress causes increases in amygdalar FAAH activity[28]. Collectively, these findings support the hypothesis that stress increases mobilization of eCB degradative enzymes, decreases

eCB signaling through the CB_1R, and enhances excitability in the amygdala to drive anxiogenic behaviors (Fig. 1c).

Endocannabinoid System Regulation of Stress Effects on Anxiety-Like Behaviors. Data from preclinical animal studies provide evidence for the biphasic effects of cannabinoid receptor ligands on anxiety-like behaviors, where high doses of cannabinoids can illicit anxiogenic behaviors and low doses of cannabinoids can cause anxiolytic behaviors[104]. Thus, substantial increases or decreases in eCB signaling through cannabinoid receptors appear to induce anxiety, whereas minute enhancements or reductions in eCB signaling appear to lessen anxiety. Onaivi and others demonstrated that under basal conditions a high dose of the psychoactive component found in marijuana, Δ^9-tetrahydrocannabinol (Δ^9-THC), a partial CB_1R agonist[61,105], administered systemically (10 mg/kg) or microinjected (100 μg) into the CeA elicit anxiogenic-like behaviors in rodents[15,106]. Comparable results were obtained in rats administered systemically with a high dose of HU-210 (100 μg/kg), a full CB_1R agonist[61,105], for 12 consecutive days before exposure to acute immobilization stress as well as in humans that orally ingested marijuana (5-10 g)[104,107]. In contrast, a low dose of Δ^9-THC ($\leq$ 0.75 mg/kg) or WIN 55,212-2 (1 and 3 mg/kg), a full CB_1R agonist[61,105], administered systemically or microinjected into the BLA (Δ^9-THC, 1 μg) under basal conditions induced anxiolytic-like responses in rodents[14,64,108,109]. Similar results occurred when WIN 55,212-2 was microinjected into the BLA (5 μg) before acute stress in the form of a footshock and before and after a single episode of prolonged stress, a rodent model of PTSD that is comprised of restraint stress, forced swim stress, and isoflurane-induced loss of consciousness[110,111]. These findings parallel a study on recreational cannabis users that did not use marijuana on a daily basis but had used marijuana at least 10 times in their lives. Phan and others demonstrated that these subjects after orally ingesting Δ^9-THC (7.5 mg) had decreased threat-related amygdala reactivity

when exposed to social signals of threat[112]. Moreover, previous studies have shown that blockade of the CB_1R with rimonabant (SR141716)[61,105] can generate anxiogenic behaviors at high doses administered systemically (3 or 10 mg/kg) and microinfused in the CeA (0.5 μg)[113-116] similar to CB_1R gene disruption[108,116] and anxiolytic behaviors at low doses (1 mg/kg) in animals and humans[115,116]. These pharmacological effects can be context dependent at times, where brightly illuminated, novel or stressful environments induce anxiety as opposed to unstressful, familiar environments lessening anxiety in both animals and humans[115,117-120]. Nevertheless, bimodal control of anxiety by cannabinoid receptor ligands can be alleviated when the stressor applied is increased in intensity, suggesting intense stress can enhance CB_1R responsiveness to these ligands. Hill and Gorzalka demonstrated that rats subjected to chronic unpredictable stress and, subsequently, administered HU-210 (10 and 50 μg/kg) systemically appeared less anxious in the elevated plus maze[21]. Apparently, depending on the time or dosage at which a drug is administered, the potency of a drug, and the environment in which stress is induced, activation or blockade of CB_1Rs by psychoactive or synthetic cannabinoids in the brain can produce very different and complex effects on anxiety-like behaviors in both animals and humans[119,121]. These bimodal effects of cannabinoids on anxiety have been suggested to be mediated through CB_1Rs located on cortical glutamatergic neurons when animals exhibit anxiolytic behaviors and on GABAergic axon terminals when animals exhibit anxiogenic behaviors[122]. Moreover, the effectiveness of cannabinoid receptor ligands in alleviating anxiety may depend on the magnitude at which stress increases CB_1R levels[123] or activity, making more CB_1Rs available to be acted upon by the cannabinoid ligands or eCBs synthesized as a consequence of stress. Another alternative to the bidirectional effects of cannabinoids on anxiety is that depending on the magnitude of a

ligand's potency or stress, sensitization of one of the CB_1R downstream effectors may increase or decrease upon activation or inhibition of the CB_1R.

Endocannabinoid Augmentation Strategies Can Regulate Anxiety

Using psychoactive cannabinoids or synthetic cannabinoid analogs to activate or inhibit cannabinoid receptor activity in the brain is not the only approach that can control anxiety-like behaviors in animals and humans. Another method for modulating anxiety is pharmacologically and genetically targeting enzymes involved in the eCB system in order to augment eCB levels in the brain. Previous studies have demonstrated that genetic removal of genes for enzymes that degrade eCBs or pharmacologically inhibiting these enzymes can cause increases in eCBs in the brain[27,124,125]. It is assumed that elevating eCB levels in the brain will result in enhanced eCB signaling through cannabinoid receptors. This endocannabinoid augmentation strategy may possibly counteract the morphological and biochemical effects of stress on the brain, particularly the amygdala, and, subsequently, on anxiety. This hypothesis has been implied by several research studies that target eCB degradative enzymes, such as FATTY ACID AMIDE HYDROLASE (FAAH), MONOACYLGLYCEROL LIPASE (MAGL), and CYCLOOXYGENASE-2 (COX-2), in order to regulate anxiety-like behaviors in animals and humans.

Fatty acid amide hydrolase. FAAH is a postsynaptic, membrane-bound enzyme that catalyzes the hydrolysis of AEA to ethanolamine and a free fatty acid and the hydrolysis of 2-AG, to a lesser extent, to arachidonic acid and glycerol[126-128]. FAAH mRNA is located predominantly in the lateral, basal, and basomedial nuclei of the amygdala[129,130]. FAAH is localized to somata and proximal dendrites of glutamatergic neurons in the amygdala with greater distribution in the LA and BLA as opposed to the CeA[129,131]. This pattern of FAAH protein expression is similar to the

distribution of CB_1Rs in the amygdala[42,70,131,132]. Morphological and biochemical changes as a consequence of stress can be reduced or reversed by genetically removing or inhibiting FAAH. Patel and others illustrated that neuronal activation in amygdalar structures, such as the BLA and CeA, can be prevented when FAAH is genetically removed in mice ($FAAH^{-/-}$) that are subjected to acute immobilization stress[43]. Hill and others showed that chronic immobilization stress inflicted upon $FAAH^{-/-}$ mice prevented dendritic remodeling in the amygdala[28]. With respect to altering eCB levels in the brain, under basal conditions, inhibition of FAAH by URB597 at low doses (1 mg/kg) can induce increases in AEA levels in whole brain[23]. Interestingly, animals subjected to stress and administered a FAAH inhibitor can produce similar results[22,133,134]. Moreover, microinjections of a low dose (0.1 μg) of the FAAH inhibitor, URB597, in the BLA reduced stressed-induced increases in serum corticosterone. In addition, this effect was not observed when the CB_1R was pharmacologically blocked with a CB_1R antagonist, AM251, suggesting that the reduction in stress-induced corticosterone levels as a consequence of FAAH inhibition was CB_1R mediated[100]. Similar to that observed in $FAAH^{-/-}$ rodents subjected to acute immobilization stress, the genetic removal of FAAH abolishes stress-induced increases in FAAH activity and decreases in AEA content in the amygdala of $FAAH^{-/-}$ mice subjected to chronic immobilization stress[28,135]. FAAH inhibition by drugs or removal of the FAAH gene in mouse strains can lessen the effects of stress on anxiety-like behaviors. Systemically, pharmacological FAAH inhibition at low doses (URB597, 0.05-1 mg/kg) has been shown to evoke anxiolytic-like behaviors in rodents, which has been reversed by blockade of the CB_1R with rimonabant, a CB_1R antagonist and inverse agonist when it reverses adenylyl cyclase inhibition[27,136-139]. Similar behavioral effects can be observed when the aversiveness of an animal's environment (e.g., increase in illumination and removing habituation of an animal to an experimental room) is

increased and FAAH is pharmacologically inhibited[140]. In addition, genetically eliminating FAAH in mice subjected to chronic immobilization stress has been shown to prevent anxiogenic-like behaviors as compared to wildtype littermates subjected to the same stress paradigm[28]. These findings parallel studies examining threat processing in human carriers of polymorphisms in the FAAH gene that renders FAAH vulnerable to proteolytic degradation, causing reduced protein expression of FAAH and FAAH activity[141,142]. Human subjects that are carriers of the FAAH gene variant C385A have decreased threat-related amygdala reactivity and associated trait anxiety, possibly contributing to enhanced habituation and reduced sensitivity to perceived threats or harm from the external environment[141-144].

Monoacylglycerol lipase. MAGL is a presynaptic enzyme that catalyzes the hydrolysis of 2-AG to arachidonic acid and glycerol[24,31,127,128,145]. As observed with FAAH, the regional distribution of MAGL is analogous to CB_1Rs in the BLA and CeA, localized to axon terminals in the amygdala with greater distribution in the BLA as opposed to the CeA[12, 25, 42,132]. Under basal conditions, MAGL inhibition by JZL 184 at acute and low or high doses (8, 16, or 40 mg/kg) can induce increases in 2-AG levels in whole brain and anxiolytic-like behaviors in rodents in a time-dependent manner[26, 32-34, 23,24,26,146]. In addition, chronic JZL 184 treatment at a high dose (40 mg/kg/day for 6 days) induces greater increases in 2-AG levels and increases in AEA levels in whole brain from rodents but causes desensitization of CB_1Rs in the amygdala[147]. Similarly, whole brains from mice injected with a high dose of JZL 184 (16 mg/kg/day for 10 days) 1h before being exposed to restraint stress showed increases in 2-AG levels and anxiolytic-like behaviors in the novelty-induced hypophagia assay[24]. However, such increases in 2-AG content in whole brain may exhibit brain region specificity since another study by Rademacher and others showed that chronic instead of acute restraint stress (30 minutes/day for 10 days) subjected to mice resulted in

elevated 2-AG levels in the amygdala[28, 135]. In addition, chronic stress in contrast to basal conditions has been shown to reduce membrane-bound levels of MAGL in the BLA of mice chronically stressed via restraint in a conical tube for 10 days, demonstrating changes in eCB content parallel changes in eCB degradative enzyme levels in the amygdala as a consequence of stress[24, 32]. These results were illustrated again in the BLA, but only during the first 20 min of a 1h restraint stress episode on the 10th day, suggesting the short-lived or phasic nature of changes in 2-AG levels[36, 87]. Similar to previous studies involving pharmacological FAAH inhibition, acute and chronic pharmacological MAGL inhibition at low doses (8 mg/kg) in rats only produce anxiolytic effects when the rats were subjected to a more aversive environment (e.g., high illumination). This observation was blocked by co-administration of JZL 184 with rimonabant, suggesting the anxiolytic effects detected were mediated through the CB_1R[37, 148]. Also, another study showed similar results under basal conditions when JZL 184 (8 mg/kg) was administered acutely or chronically (6 days). However, the anxiolytic effects of acute JZL 184 treatment at a low dose was blocked in mice injected with a cannabinoid type 2 receptor (CB_2R) antagonist, SR144528, or mice genetically altered such that the gene for the CB_2R, was removed[23, 26]. Differences in observations between these two studies may be the result of variations in the context in which the rodents were subjected to before and during experimental testing.

Cyclooxygenase-2. COX-2 is a postsynaptic enzyme that catalyzes the hydrolysis of AEA to prostamide E_2 and 2-AG to prostaglandin E_2 glyceryl ester[128,149-154]. COX-2 is localized to dendritic arbors of excitatory neurons in the amygdala[154]. Stress-induced excitotoxicity has been shown to induce activation of downstream effectors that can upregulate COX-2 protein expression. Acute cold swim stress or immobilization stress can cause a prolonged elevation in COX-2 mRNA or protein levels and PGE_2 levels, a biomarker for COX-2 activity, as well as stimulation of the

HYPOTHALAMIC-PITUITARY-ADRENAL (HPA) AXIS[9] as observed through elevated serum corticosterone levels (Fig. 1c)[94,155-158]. These biochemical alterations can be reduced upon administration of low and high doses of the COX-2 inhibitor, NS-398 (0.5-10 mg/kg)[94,155]. Also, subchronic immobilization or acoustic stress has been shown to induce increases in COX-2 protein levels and activity in the brain. These changes in COX-2 activity after stress were mediated via CB_1Rs since activation of CB_1Rs by the CB_1R agonist, arachidonyl-2'-chloroethylamide, reduced PGE_2 levels in the brain[123]. Although there is limited information as to whether or not selective COX-2 inhibitors can reduce or reverse the biochemical, morphological, and behavioral changes caused in the brain, particularly the amygdala, after stress, some studies have demonstrated the anxiolytic potential of selective COX-2 inhibitors under normal, unstressful conditions and before the onset of stress. In one study, under basal conditions, the inhibition of COX-2 pharmacologically has been shown to result in reduced anxiety-like behaviors in mice and increased AEA and 2-AG levels in the brain. These effects are removed when mice are co-injected with the COX-2 inhibitor (LM-4131, 10 mg/kg) and rimonabant or have been genetically altered such that the gene for COX-2 has been eliminated, suggesting the increased levels of eCBs and anxiolytic behaviors as a result of COX-2 inhibition is CB_1R mediated[125]. Other studies have demonstrated that COX-2 inhibitors can prevent stress-induced anxiogenic behaviors. These studies illustrate that acute or chronic pretreatment with selective COX-2 inhibitors (rofecoxib, 2-10 mg/kg or valdecoxib, 5-10 mg/kg) before the onset of immobilization stress (1 day or 7 days) can decrease anxiety-like behaviors in mice[159,160]. Nevertheless, further evidence for which cellular and molecular mechanisms are involved in anxiolytic behaviors after stress as a

[9] **HYPOTHALAMIC-PITUITARY-ADRENAL (HPA) AXIS**: A feedback system involving the paraventricular nucleus (PVN) of the hypothalamus, the anterior lobe of the pituitary gland, and the adrenal glands that mediates stress responses. In response to stress, the PVN of the hypothalamus synthesizes corticotrophin-releasing factor (CRF), which bind to the CRF receptor on the pituitary gland. This triggers release of adrenocorticotropic hormone (ACTH), which binds to the melanocortin receptor in the adrenal gland, and, subsequently, induces the synthesis of glucocorticoids, which decrease further activation of the HPA axis.

consequence of COX-2 inhibition and the limitations of COX-2 inhibitors in modulating anxiogenic behaviors in animals and humans is needed.

Conclusion

Direct activation or inhibition of cannabinoid receptors has been shown to modulate anxiety-like behaviors under basal and stressful conditions in preclinical animal studies and humans. Nevertheless, previous studies have demonstrated that direct stimulation of cannabinoid receptors pharmacologically provides bidirectional results on controlling stress-induced anxiety. In addition, levels of eCBs and cellular expression and activity of degradative enzymatic have been shown to vary with age in preclinical studies with mice[129,156,161]. Increasing eCB levels by pharmacologically inhibiting FAAH, MAGL, or COX-2 may provide a better alternative to inducing eCB signaling through cannabinoid receptors than by direct activation of cannabinoid receptors with psychoactive cannabinoids or synthetic cannabinoid analogs. Given the potential clinical and societal importance of reducing stress-induced anxiety in humans by pharmacologically elevating eCB levels in the brain, it is essential to comprehend the biological, morphological, and physiological effects of such pharmacological manipulations under basal and stressful conditions, particularly in a brain structure, such as the amygdala, that is known to store fearful memories and regulate stress responses.

CHAPTER II

ANXIOLYTIC POTENTIAL OF SUBSTRATE-SELECTIVE COX-2 INHIBITION IN ANIMAL MODELS OF ACUTE AND CHRONIC TRAUMATIC STRESS

Introduction

Few studies have addressed the association between the eCB system, anxiety disorders induced by trauma or stress, and the underlying mechanisms that contribute to their persistence and severity for many reasons. For one, the eCB system has only been investigated for its role in modulating stress and emotional behavior for little over a decade. As a result, the pathways for eCB synthesis and how they are altered by stress or trauma exposure is still being elucidated. Moreover, much remains unknown about the neurobiological consequences of anxiety, trauma-related, and stressor-related disorders. There are huge gaps in knowledge because an individual's reaction to stress or trauma depends on a multitude of factors, such as the stressor or trauma characteristics and inter-individual variability. Also, neurobiological systems that regulate stress responses, including endocrine and neurotransmitter (NT) pathways, as well as a network of brain regions known to regulate fear behavior are complex and interconnected. In the following chapters, a unique research approach will be discussed. This research approach will provide insight into how the eCB system is affected after acute and chronic stress exposure and can be tailored using a novel molecular drug discovery approach, termed substrate-selective COX-2 inhibition (SSCI)[162], to alleviate anxiety-like behaviors in an animal model of stress-induced anxiety. SSCI, which increases brain AEA levels by pharmacologically inhibiting COX-2, will be described in the context of testing the hypothesis that endocannabinoid augmentation via SSCI can counteract stress-induced anxiety-like behaviors by elevating AEA levels in the brain, resulting in enhanced eCB signaling through cannabinoid receptors located on glutamatergic neurons. This

hypothesis was examined by determining the anxiolytic potential of SSCIs in animals subjected to acute and chronic traumatic stress (CHAPTER II) and its relation to eCB synaptic signaling in the amygdala (CHAPTER III).

Experimental

Animals. Male or female ICR (CD-1) mice between 4-7 weeks of age (juvenile) or between 12-15 weeks of age (adult) were used for all experiments (Harlan, Indianapolis, IN) unless otherwise noted. For some contextual fear conditioning, extinction, and recall experiments, male C57BL/6J mice between 4-7 weeks of age were used (The Jackson Laboratory, Bar Harbor, ME). All mice were housed on a 12:12 light-dark cycle (lights on at 6:00 a.m.) with food and water available *ad libitum*. All studies were carried out in accordance with the National Institute of Health Guide for the Care and Use of Laboratory Animals and approved by the Vanderbilt University Institutional Animal Care and Use Committee. All behavioral testing was performed during the inactive light phase of the mouse circadian cycle (between 6:00 a.m. and 6:00 p.m.).

Drugs and treatment. The following drugs were used for the experiments: the COX-2 inhibitors, LM-4131 (10 mg/kg; gift from Dr. Lawrence Marnett laboratory), lumiracoxib (1 mg/kg; Selleck Chemicals, Houston, TX), and celecoxib (10 mg/kg; Cayman Chemical, Ann Arbor, MI), the SK channel antagonist, apamin (0.4 mg/kg; Tocris Bioscience (Bio-Techne), Minneapolis, MN), the SK channel agonist, 1-EBIO (5 mg/kg; Tocris Bioscience (Bio-Techne), Minneapolis, MN), the TRPV1 antagonist, capsazepine (10 mg/kg; Cayman Chemical, Ann Arbor, MI), the CB1 receptor antagonist, rimonbant (2 mg/kg or 5 mg/kg), and the CB2 receptor antagonist, SR144528 (3 mg/kg). The CB1 receptor antagonist, rimonabant, and the CB2 receptor antagonist, SR144528, were gifts from the National Institute of Mental Health Drug Supply Program. Drugs or vehicle

(dimethyl sulfoxide or DMSO) were administered by i.p. injection. Drugs were dissolved in DMSO at a volume of 1 mL/kg. Drug pretreatment times were two hours prior to behavioral testing.

Endocannabinoid quantification. Endocannabinoids were quantified and detected using LC-MS/MS on a Quantum triple-quadrupole mass spectrometer in positive-ion mode using selected reaction monitoring as previously described[125].

Behavioral testing.

A. ***Novelty-induced feeding suppression (NIFS) or novelty-induced hypophagia (NIH) test.*** Individually-house mice were habituated to a novel, palatable food (Ensure® Homemade Vanilla Shake) in their home cages for 30 min/day for 3 days under red light conditions (40 lux) before testing. The day after habituation, mice were presented with the shake in their home cages under red light conditions. For each mouse, we measured the latency to begin feeding (an indicator of anxiety-like behavior) and the amount consumed (an indicator of anhedonic behavior). On the following day, mice were moved to a holding room adjacent to the test room for fear conditioning and acclimated for 1 h before testing under bright light conditions (175-177 lux). For fear conditioning procedures, mice were moved to the test room under bright light conditions (175-177 lux) and placed in the conditioning chamber for 30 seconds. After the initial one-half minute of habituation, mice were presented with six conditioned stimulus-unconditioned stimulus (CS-US) pairings (e.g., tone-footshock pairings) separated by a 30 second interval. Each tone (80 dB, 3000 Hz) lasted 30 seconds. Mice were presented with the electric footshock at 0.7 mA the last two seconds of the 30 s tone. At the end of the fear conditioning protocol, mice were returned to the holding room and their home cages. Two hours or six hours later on the same day, 22 hours later on the following day, or 70 hours later,

mice were administered a drug by i.p. injection two hours before being presented with the shake in a novel cage without bedding and with a white bottom under bright light conditions (295 lux). Latency to feed in the novel cage and the amount of Ensure® consumed were reported.

B. ***Elevated plus maze.*** The elevated plus maze apparatus was elevated 47 cm from the ground, and consisted of two open arms (30 × 5 cm; 90 lux) and two closed arms (30 × 5 × 15 cm; 20 lux) extending from a 5 × 5 cm central area (San Diego Instruments). The walls and floor were made from black ABS (acrylonitrile butadiene styrene) plastic. To begin the 5-min test each mouse was placed in the center, facing an open arm. Total distance traveled and time spent, latency to enter, and total entries into the open and closed arms were recorded and analyzed using Any Maze tracking software. The mouse was considered to be in an arm when all four paws were in the arm.

C. ***Tail suspension test.*** The tail suspension test was performed as previously described[115] using six chambers that interfaced with the Tail Suspension software (Version 3.30, MED Associates) for five minutes.

D. ***Sucrose preference test.*** Before testing, each mouse was given 24 hours to choose freely between a 2% sucrose solution and tap water contained in a 50-mL clear plastic conical tube that was closed by a rubber stopper encasing a metal sipper. To prevent side preference bias, the position of the two tubes was switched at every measurement of the amount of fluid consumed (e.g., 2-4 hours). No previous water or food deprivation was applied before testing. The consumption of the 2% sucrose solution or water was measured by weighing the conical tubes containing the fluids. Percentage sucrose preference was calculated as the ratio of 2% sucrose consumed over total fluid consumption multiplied by 100.

E. ***Open field assay.*** Open field locomotor activity was analyzed and performed as previously described[115] for one hour.

F. ***Acoustic startle and prepulse inhibition.*** Percentage acoustic startle response and prepulse inhibition of the startle response was measured. During all experimental testing, the background was set at 70 dB white noise. The acoustic startle response test consisted of several trial types, each of which was presented in a pseudorandom order. The trial types consisted of a single startle stimulus of 70, 76, 82, or 88 dB.

G. ***Y maze.*** Each mouse was placed at the end of an arm and allowed to explore the maze freely for 10 min. The number of entries into each arm, the total arm entries, mean speed, the total distance traveled in the Y maze, and spontaneous alternation percentage were measured. The percentage of spontaneous alternation was defined as a ratio of the number of arm entries that differed from the previous two arm entries to total number of arm entries during each testing session.

H. ***Cued and contextual fear conditioning, extinction, and recall.*** All fear conditioning and extinction procedures were adapted from Hefner and co-workers[163]. A video fear conditioning system and software from Med Associates, Inc. was used to measure freezing in the mice while in a conditioning chamber (dimensions: 30.5 cm x 24.1 cm x 21.0 cm), which was cleaned in between testing with Vimoba, a chlorine dioxide solution. Freezing was defined as no movement other than breathing and measured when mouse movement fell below a preset motion threshold of 18. Mice were moved to a holding room adjacent to the test room and acclimated for 1 h before testing under bright light conditions (175-177 lux). For fear conditioning procedures, mice were moved to the test room under bright light conditions (175-177 lux) and placed in the conditioning chamber for 30 seconds. After the initial one-half

minute of habituation, mice were presented with six conditioned stimulus-unconditioned-stimulus (CS-US) pairings (e.g., tone-footshock pairings) separated by a 30 second interval. Each tone (80 dB, 3000 Hz) lasted 30 seconds. Mice were presented with the electric footshock at 0.7 mA the last two seconds of the 30 s tone. At the end of the fear conditioning protocol, mice were returned to the holding room and their home cages. Twenty-two or six hours later, mice were administered either vehicle or a COX-2 inhibitor with or without rimonabant (5 mg/kg) by i.p. injection two hours before being placed in the conditioning chamber for extinction training. Mice were placed in the conditioning chamber with or without a white smooth floor contextual insert that was positioned over the grid floor and a white curved wall contextual insert for cued fear extinction and contextual fear extinction training, respectively. Vanilla extract was used as a distinctive olfactory cue in the conditioning chamber for the cued extinction training. After 30 seconds of habituation in the chamber, mice were presented with 20 tones (80 dB, 3000 Hz) with a duration of 30 seconds each and each separated by a 30 second interval. After 20 minutes and 30 seconds, mice were returned to a holding room and their home cages. The extinction protocol was repeated the 16 hours later or the following day to measure extinction recall.

High performance liquid chromatography (HPLC). Tissue sections were homogenized using a tissue dismembrator in 100-750 μl of 0.1M TCA, which contained 10^{-2} M sodium acetate, 10^{-4} M EDTA, and 10.5 % methanol (pH 3.8). Twenty microliters of homogenate was used for the protein assay. Then samples were spun in a microcentrifuge at 10,000 g for 20 minutes. The supernatant was removed for analysis on HPLC. Remaining samples were stored at –80^{o}C. Biogenic amines were determined using an Antec Decade II (oxidation: 0.65) electrochemical detector operated at 33°C. Twenty microliter samples of the supernatant were injected using a Water 2707 autosampler

onto a Phenomenex Kinetix C18 HPLC column (2.6 μm, 4.6 x 100 mm). Biogenic amines were eluted with a mobile phase consisting of 89.5% 0.1 M TCA, 10^{-2} M sodium acetate, 10^{-4} M EDTA and 10.5 % methanol (pH 3.8). Solvent was delivered at 0.6 ml/min using a Waters 515 HPLC pump. Using this methodology, the biogenic amines eluted in the following order over 30 minutes: norepinephrine, epinephrine, DOPAC, Dopamine, 5-HIAA, HVA, 5-HT, and 3-MT. HPLC control and data acquisition were managed by Empower software. Amino Acids were determined by the Waters AccQ-Tag system utilizing a Waters 2475 Fluorescence Detector. To prepare for HPLC analysis, 10 μl samples of the supernatant were diluted with 70 μl of borate buffer to which 20 μl aliquots of 6-aminoquinol-N-hydroxysuccinimidyl carbamate were added to form the fluorescent derivatives. After heating the mixture for 10 minutes at 55°C, 10 μl of derivatized samples were injected into the HPLC system, consisting of a Waters 2707 Autosampler, two 515 HPLC pumps, column heater (35°C), and the fluorescence detector. Separation of the amino acids was accomplished by means of a Waters amino acid column and supplied buffers (A – 19% sodium acetate, 7% phosphoric acid, 2% triethylamine, 72% water; B – 60% acetonitrile) using a specific gradient profile. HPLC control and data acquisition was managed by Empower 2 software. Amino acid concentrations were normalized by the amount of protein in tissue. Protein concentration was determined by a BCA Protein Assay Kit (Thermo Scientific). Ten microliters of the tissue homogenate was distributed into a 96-well plate (in duplicate) and 200 μl of mixed BCA reagent (25 ml of Protein Reagent A is mixed with 500 μl of Protein Reagent B) was added. The plate was incubated at room temperature for two hours for color development. A bovine serum albumin (BSA) standard curve was ran at the same time. Absorbance was measured by the plate reader (POLARstar Omega, BMG LABTECH Company).

Corticosterone levels assay. Trunk blood samples were obtained from mice at the end of the NIFS assay under basal and acute and chronic stress conditions. Blood samples were centrifuged at 1500 × *g* for 10 min at 4°C. The plasma was separated and stored at −80°C until assayed for corticosterone (CORT). CORT levels in the plasma were determined using a commercially available corticosterone enzyme-linked immunosorbent assay (ELISA) kit (Assay Designs, Inc., Ann Arbor, MI) according to the manufacturer's instructions.

Statistical analyses. For all experiments, statistical significance was calculated by two-tailed unpaired Student's *t*-test or Kolmogorov-Smirnov test (only for frequency plots) or one-way or two-way ANOVA with post hoc Holm-Sidak's multiple comparisons test.

Results and Discussion

Effects of substrate-selective COX-2 inhibition on stress-induced anxiety

We have previously shown that pharmacologically increasing AEA levels in the brain with a fatty acid amide hydrolase inhibitor can enhance CB_1R signaling and reverse anxiety-like behaviors in animals subjected to acute electric footshock stress[133]. Also, we have discovered that substrate-selective COX-2 inhibitors (SSCIs) can increase whole brain AEA levels and reduce anxiety in animals under basal conditions[125]. Thus, SSCIs may have the capacity to reduce anxiety-like behaviors in animals subjected to acute and chronic stress. To test this hypothesis, we first performed liquid chromatography-tandem mass spectrometry (LC-MS/MS) to measure AEA levels in amygdala tissue sections from juvenile male ICR (CD-1) mice subjected to no stress (controls) or acute (1 day) electric footshock stress and, subsequently, injected intraperitoneally (i.p.) with vehicle (dimethyl sulfoxide or DMSO) or the SSCI, LM-4131 (10 mg/kg). We observed a significant increase in AEA levels in the lipid extracts from the brain tissue of LM-4131treated

mice under stressed conditions (unpaired, two-tailed *t* test: ****$p < 0.0001$, $t = 6.854$, df = 14, LM-4131 (mean ± s.e.m.: 152.5 ± 6.828, $N = 8$) vs. vehicle (mean ± s.e.m.: 84.47 ± 7.197, $N = 8$); Fig. 2a). Surprisingly, we did not observe similar changes in AEA levels in the lipid extracts from the brain tissue when the mice were not exposed to acute electric footshock stress (unpaired, two-tailed *t* test: $p = 0.3316$, *ns* (not significant), $t = 1.006$, df = 14, LM-4131 (mean ± s.e.m.: 179.4 ± 25.43, $N = 8$) vs. vehicle (mean ± s.e.m.: 139.0 ± 31.12, $N = 8$); Fig. 2a). This discrepancy may be due to variability in the amygdala tissue samples. Increasing the number of samples used in quantifying AEA in the amygdala lipid extracts could have increased the chance of detecting a difference between the vehicle- and LM-4131-treated sample populations. Thus, an increase in the sample size of the amygdala tissue sections could have increased the statistical power of the comparison being made, reduce random sample variation, and thus improve the reliability of the *p* value for the comparison[164]. Since we were not able to reproduce similar increases in AEA levels in the amygdala lipid extracts under basal conditions as we have shown previously with the SSCI, LM-4131, in whole brain lipid extracts[125], another alternative to this inconsistency in amygdala AEA levels is possible. The subregions of the amygdala may have different roles when responding to the degree of aversiveness from external stimuli and whether or not such aversiveness can evoke a negative emotion. This may explain the differences in the amygdala AEA levels when an animal is subjected to a non-aversive stimulus in comparison to one that is aversive and capable of inducing fear or anxiety-like behavior, such as an electric footshock[133,165]. Several studies in humans and rodents have suggested that amygdala subregions respond differently to emotional and non-emotional stimuli. Using diffusion tensor imaging (DTI) and high-resolution blood oxygenation level-dependent (BOLD) imaging, Balderson and others identified the basolateral subregion of the amygdala as responsive to all external stimuli and the centromedial subregion of

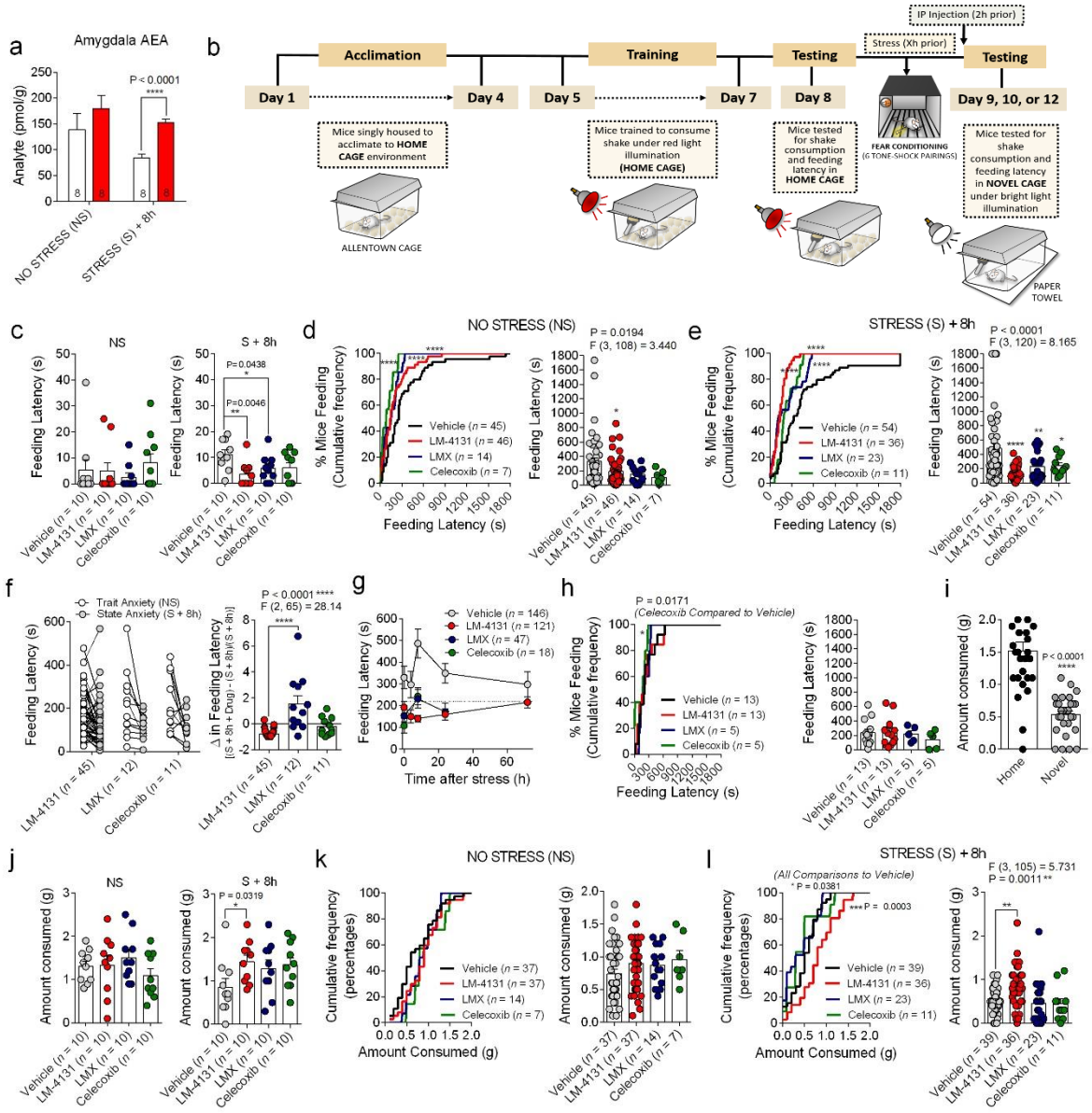

Figure 2. Stress-induced anxiety and anhedonic behavioral effects of substrate-selective COX-2 inhibition. (**a**) Quantification of the endocannabinoid, anandamide (AEA), in amygdala lipid extracts using LC-MS/MS and after mice were exposed to non-stressful and acute stress conditions. (**b**) Diagram of experimental design for NIFS. (**c**) Latency to feed in home cage environment under red light illumination and non-stressful or acute stress conditions. (**d, e**) Cumulative frequency of mice feeding and latency to feed in NIFS test under non-stressful and acute stress conditions, respectively. (**f**) Feeding latency before acute stress exposure (trait anxiety) and after acute stress exposure (state anxiety) for respective COX-2 inhibitor treatment groups but prior to treatment (left in novel cage environment). Change in feeding latency between state anxiety prior to treatment and after acute stress exposure and treatment of COX-2 inhibitor (right) in novel cage environment. (**g**) Latency to feed at different time points after acute stress exposure in novel cage environment. (**h**) Cumulative frequency of mice feeding and latency to feed in NIFS test under acute stress conditions after administering drugs two hours prior to stressor in novel cage environment. (**i**) Total amount of shake consumed compared between home cage and novel cage environment under non-stressful conditions. (**j**) Total amount of shake consumed in home cage environment under red light illumination and non-stressful or acute stress conditions. (**k, l**) Cumulative frequency of mice consuming shake and amount of shake consumed in NIFS test under non-stressful and acute stress conditions, respectively, in novel cage environment. Data are shown as the mean ± s.e.m. NS = no stress, S = stress (e.g., stress exposure in the form of an electric footshock administered 8h prior to testing), *P<0.05, **P<0.01, ***P<0.001, ****P<0.0001.

the amygdala as responsive to external stimuli that predicts an aversive outcome[166]. Animal studies have shown that the basolateral nucleus of the amygdala (BLA) plays a role in determining the aversive value of an external stimulus, such as an electric footshock, whereas the basomedial amygdala (BMA) functions in distinguishing between environments that are assigned a safe or aversive value[167].

To determine if the increases observed in amygdala AEA levels showed a relationship with the anxiolytic nature of SSCIs, we assessed anxiety-like behavior in the mice using the novelty-induced feeding suppression (NIFS) assay (Fig. 2b). To do this, we measured feeding latency (e.g., time lapsed from the start of the NIFS assay to the first consumption of a palatable vanilla ENSURE® shake) in a home cage environment under red light illumination and in a novel cage environment under bright illumination after the mice were exposed to either basal (no stress) or acute footshock conditions. Since LM-4131-induced increases in amygdala AEA levels were more robust under stressed conditions, this enabled us to ascertain if the SSCIs ability to reduce anxiety-like behavior in the mice depended on the degree of aversiveness or novelty of the cage environment used in the NIFS assay, the degree of aversiveness of stress exposure, or a combination of the two. When the mice were tested in a safe, familiar cage environment (e.g., home cage) under basal conditions, we observed no changes in feeding latency between all COX-2 inhibitor treatment groups and the vehicle treatment group (one-way ANOVA: $F_{(3, 36)} = 0.5460$, $p = 0.6540$, *ns;* Holm-Sidak's multiple comparisons test: *ns*, $t = 0.09107$, df = 36, LM-4131 (mean ± s.e.m.: 4.900 ± 4.392, $N = 10$) vs. vehicle (mean ± s.e.m.: 5.300 ± 4.392, $N = 10$); *ns*, $t = 0.6375$, df = 36, LMX (mean ± s.e.m.: 2.500 ± 4.392, $N = 10$) or celecoxib (mean ± s.e.m.: 8.100 ± 4.392, $N = 10$) vs. vehicle (mean ± s.e.m.: 5.300 ± 4.392, $N = 10$); Fig. 2c (left panel)). However, when we tested the mice in the same cage environment 8 hours after being subjected to acute electric footshock stress,

we observed a decrease in feeding latency in mice treated with the substrate-selective COX-2 inhibitor, LM-4131, compared to those treated with vehicle (one-way ANOVA: $F_{(3, 36)} = 3.542$, $p = 0.0240$, $*p<0.05$; Holm-Sidak's multiple comparisons test: $**p<0.01$, $t = 3.161$, df = 36, LM-4131 (mean ± s.e.m.: 3.500 ± 2.404, $N = 10$) vs. vehicle (mean ± s.e.m.: 11.10 ± 2.404, $N = 10$); *ns*, $t = 2.163$, df = 36, LMX (mean ± s.e.m.: 5.900 ± 2.404, $N = 10$) vs. vehicle (mean ± s.e.m.: 11.10 ± 2.404, $N = 10$); *ns*, $t = 2.121$, df = 36, celecoxib (mean ± s.e.m.: 6.000 ± 2.404, $N = 10$) vs. vehicle (mean ± s.e.m.: 11.10 ± 2.404, $N = 10$); Fig. 2c (right panel)). Further analysis with an unpaired *t* test revealed a significant difference in the means of the LM-4131 or LMX treatment group compared to the vehicle treatment group ($p=0.0046$, $**p<0.01$, $t = 3.239$, df = 18, LM-4131 (mean ± s.e.m.: 3.500 ± 1.522, $N = 10$) vs. vehicle (mean ± s.e.m.: 11.10 ± 1.785, $N = 10$); $p=0.0438$, $*p<0.05$, $t = 2.168$, df = 18, LMX (mean ± s.e.m.: 5.900 ± 1.602, $N = 10$) vs. vehicle).

Since we observed decreased anxiety-like behavior in the juvenile male mice under stressed conditions in the home cage environment, we wanted to determine next if increasing the aversiveness or novelty of the cage environment would change the anxiolytic action of the SSCIs previously demonstrated in the non-stressful home cage environment. To increase the aversiveness or novelty of the cage, we removed all bedding and placed a white paper towel under the cage to amplify the intensity of the bright light illumination of the cage. This change in the environmental context of the cage can induce anxious behavior in mice since mice have a tendency to avoid well-lit areas in favor of ones that are dark and can exhibit neophobia (e.g., an animal's hesitation to explore a new or novel environment) in stressful or fear-inducing environments. Of all of the COX-2 inhibitors administered i.p. to the mice, only LM-4131 slightly decreased anxiety-like behavior in the mice under no stress in the mildly stressful, novel cage environment. According to the cumulative frequency distribution percentile plot of juvenile (5-7 weeks of age)

ICR male mice feeding in the NIFS assay (Fig. 2d (left panel)), 100% of vehicle-treated mice had a feeding latency ≤ 1755 s (e.g., 100th percentile), 100% of LM-4131-treated mice had a feeding latency ≤ 870 s, 100% of LMX-treated mice had a feeding latency ≤ 345 s, and 100% of celecoxib-treated mice had a feeding latency ≤ 255 s in the novel cage environment. A Kolmogorov-Smirnov (K-S) test of the feeding latency data presented in the cumulative frequency distribution percentile plot revealed significant differences between the cumulative frequency distribution for all COX-2 inhibitor treatment groups and the cumulative frequency distribution for the vehicle treatment group (D = 0.5950, ****p < 0.0001, LM-4131 at 10 mg/kg vs. vehicle; D = 0.7769, ****p < 0.0001, LMX at 1 mg/kg vs. vehicle; D = 0.8264, ****p < 0.0001, celecoxib at 10 mg/kg vs. vehicle; Fig. 2d (left panel)). Thus, there is a high likelihood that the two treatment groups (e.g., COX-2 inhibitor vs vehicle) are derived from different populations. This is based on the fact that the K-S test statistic, D (e.g., the maximum vertical deviation or distance between two distribution curves), is greater than the critical value of the comparisons being made between the COX-2 inhibitor and vehicle treatment groups. More specifically, the feeding latency data indicate that the feeding latency of mice treated with a COX-2 inhibitor is significantly less than the feeding latency of mice treated with vehicle. When the same set of feeding latency data was evaluated with one-way analysis of variance (ANOVA), we found that the results acquired with the one-way ANOVA was consistent only with the results for the LM-4131 treatment group obtained with the Kolmogorov-Smirnov test. There was a significant difference among the means for feeding latency between the LM-4131 treatment group and the vehicle treatment group (one-way ANOVA: $F_{(3, 108)}$ = 3.440, p = 0.0194, *p < 0.05; Holm-Sidak's multiple comparisons test: *p < 0.05, t = 2.528, df = 108, LM-4131 (mean ± s.e.m.: 192.7 ± 54.27, N = 46) vs. vehicle (mean ± s.e.m.: 329.9 ± 54.27, N = 45); *ns*, t = 2.222, df = 108, LMX (mean ± s.e.m.: 153.9 ± 79.21, N = 14) vs. vehicle

(mean ± s.e.m.: 329.9 ± 79.21, N = 45); *ns*, t = 2.109, df = 108, celecoxib (mean ± s.e.m.: 108.1 ± 105.2, N = 7) vs. vehicle (mean ± s.e.m.: 329.9 ± 105.2, N = 45); Fig. 2d (right panel)). A discrepancy between the results obtained from the K-S test and the one-way ANOVA may be due to the oversensitivity of the K-S test near the center as opposed to the tails of the distribution of the feeding latency data from the LMX and celecoxib treatment groups. It could also be due to the small sample size in the LMX and celecoxib treatment groups as compared to vehicle and LM-4131 treatment groups. One-way ANOVA with small sample sizes may not have enough power to detect significant differences among the samples even if the means are different. Power decreases as the sample variance increases and sample size decreases[168].

All COX-2 inhibitors decreased feeding latency when the mice were tested in the aversive, novel cage environment 8 hours after exposure to acute footshock stress. According to the cumulative frequency distribution percentile plot of juvenile ICR male mice feeding in the NIFS assay (Fig. 2e (left panel)), 100% of vehicle-treated mice had a feeding latency ≤ 1800 s, 100% of LM-4131-treated mice had a feeding latency ≤ 420 s, 100% of LMX-treated mice had a feeding latency ≤ 600 s, and 100% of celecoxib-treated mice had a feeding latency ≤ 465 s in the novel cage environment. A Kolmogorov-Smirnov test of the feeding latency data presented in the percentile plot revealed a significant difference between the cumulative frequency distributions for all COX-2 inhibitor treatment groups and the cumulative frequency distribution for the vehicle treatment group (D = 0.8430, ****p < 0.0001, LM-4131 at 10 mg/kg vs. vehicle; D = 0.6942, ****p < 0.0001, LMX at 1 mg/kg vs. vehicle; D = 0.7603, ****p < 0.0001, celecoxib at 10 mg/kg vs. vehicle; Fig. 2e (left panel)). There was a significant difference among the means for feeding latency between all COX-2 inhibitor treatment groups and the vehicle treatment group (one-way ANOVA: $F_{(3, 120)}$ = 8.165, ****p < 0.0001; Holm-Sidak's multiple comparisons test: ****p <

0.0001, $t = 4.671$, df = 120, LM-4131 (mean ± s.e.m.: 141.3 ± 74.02, $N = 36$) vs. vehicle (mean ± s.e.m.: 487.0 ± 74.02, $N = 54$); $^{**}p < 0.01$, $t = 2.980$, df = 120, LMX (mean ± s.e.m.: 231.7 ± 85.66, $N = 23$) vs. vehicle (mean ± s.e.m.: 487.0 ± 85.66, $N = 54$); $^{*}p < 0.05$, $t = 2.142$, df = 120, celecoxib (mean ± s.e.m.: 243.2 ± 113.8, $N = 11$) vs. vehicle (mean ± s.e.m.: 487.0 ± 113.8, $N = 54$); Fig. 2e (right panel)). Our findings thus far suggest that substrate-selective COX-2 inhibition can reduce anxiogenic behaviors in juvenile male mice under both basal and stressed conditions. However, the anxiolytic effects of SSCI in the mice were more robust when the mice were either exposed to environmental stress (e.g., environments with bright light illumination) or exposed to a form of physical stress that can induce anxiety or fear (e.g., electric footshock stress) in the mice. Thus, one plausible explanation for these results could be that COX-2 expression in the brain can be differentially modulated by stress exposure severity and duration. Various stressors, such as acute cold swim stress and immobilization stress, have been shown to cause a prolonged elevation and attenuated degradation in COX-2 protein levels and an increase in PGE2 levels, a biomarker for COX-2 activity[94,157,158,169,170]. Moreover, we have previously shown that components of the endocannabinoid system are sensitive to environmental stress, specifically bright light illumination, and, subsequently, can modulate anxiogenic behaviors in mice differentially[115]. Accordingly, our acute traumatic stress paradigm may have the potential to increase COX-2 expression in limbic brain regions, such as the amygdala, involved in modulating stress responses. If this is so, stress-induced increases in COX-2 expression levels in the brain could increase the availability of COX-2 protein to be acted upon by a substrate-selective COX-2 inhibitor, such as LM-4131 or LMX, thereby increasing the efficacy of the SSCIs in reducing anxiogenic behaviors in mice.

Pre-stress or trauma psychopathologies, such as anxiety or depression disorders, are believed to represent risk factors for the development and persistence of anxiety and stressor-related or trauma-related disorders. However, inter-individual variability in stress responses, such as anxiety-like behavioral phenotypes, may account for different vulnerability in humans and rodents to develop anxiety-like symptoms during or after stress exposure. In addition, anxiety-like behaviors under basal conditions are not always predictive of anxiety-like behavioral responses due to stress exposure. The behavioral response of an individual mouse to acute stress is multifaceted and involves genetic and environmental factors that play a major role in characterizing an individual behavioral response to stress exposure. Thus, a potential problem in interpreting the anxiolytic potential of a COX-2 inhibitor is individual variability within the ICR mouse strain regarding their anxiety-like behavioral responses in the NIFS assay or other behavioral assays that assess anxiety (i.e., elevated plus maze) after being subjected to the acute footshock stress paradigm. Accordingly, the efficacy of a COX-2 inhibitor in reducing stress-induced anxiety in the mice we used for our studies may be affected by the degree of individual variability in anxiety-like behavioral responses within each cohort of mice. To examine the degree to which the SSCI, LM-4131, in comparison to the other COX-2 inhibitors, LMX and celecoxib, can reduce feeding latency regardless of an animal's anxiety-like behavioral characteristics under control (no stress) conditions and after exposure to an external stressor (e.g., electric footshock) in the NIFS assay, we first measured feeding latency in a cohort of mice in the NIFS assay under basal conditions (trait anxiety or intrinsic basal anxiety characteristic) and then a week later after stress conditions (state anxiety or anxiety characteristic induced by an external stimulus, such as footshock stress) (Fig. 2f (left panel)). Next, we measured feeding latency again within the same cohort of mice after systemic administration of the different COX-2 inhibitors in the NIFS assay

and acute stress exposure (e.g., one week after assessing feeding latency in the NIFS assay after acute footshock stress exposure without systemic drug administration). We summarized these findings in a histogram (Fig. 2f (right panel)) that depicts the change in (Δ) feeding latency between the different treatment groups from the time the mice were exposed to acute footshock stress before drug administration to the time the same set of mice were exposed to acute footshock stress again and administered a COX-2 inhibitor by i.p. The change in feeding latency was calculated as follows: Δ in feeding latency = [feeding latency of a mouse after stress exposure and i.p. drug administration (S + 8h + Drug) – feeding latency of a mouse after stress exposure without i.p. drug administration (S + 8h)] divided by feeding latency of a mouse after stress exposure without i.p. drug administration (S + 8h). We found that regardless of an animal's anxiety-like behavioral responses at baseline and after exposure to an external stressor (Fig. 2f (left panel)), the SSCI, LM-4131, was more effective at reducing anxiety-like behavior in the mice subjected to acute stress in comparison to another SSCI, LMX (one-way ANOVA: $F_{(2, 65)} = 28.14$, ****$p < 0.0001$; Holm-Sidak's multiple comparisons test: ****$p < 0.0001$, $t = 7.496$, df = 65, LM-4131 (mean ± s.e.m.: -0.7672 ± 0.3096, $N = 45$) vs. LMX (mean ± s.e.m.: 1.553 ± 0.3096, $N = 12$); Fig. 2f (right panel)). There was no difference among the means for feeding latency between the LM-4131 treatment group and the celecoxib treatment group (Holm-Sidak's multiple comparisons test: *ns*, $t = 1.832$, df = 65, LM-4131 (mean ± s.e.m.: -0.7672 ± 0.3205, $N = 45$) vs. celecoxib (mean ± s.e.m.: -0.1802 ± 0.3205, $N = 11$); Fig. 2f (right panel)). Thus, celecoxib was just as effective as LM-4131 at reducing stress-induced anxiety-like behavior in the mice. Differences in the effectiveness of the COX-2 inhibitors to reduce stress-induced anxiety-like behaviors in mice with variable levels of trait and state anxiety may depend on where and how the COX-2 inhibitors bind to the COX-2 protein. Substrate-selective COX-2 inhibitors bind to one of two active sites of the COX-2

homodimer and induce a conformational change in the catalytic active site, inhibiting the oxygenation of the endocannabinoids, 2-AG and AEA, but not arachidonic acid. In particular, LMX binds in an inverted orientation in the active site of COX-2, forming hydrogen bonds between its carboxylic acid group and serine at position 530 and tyrosine at position 385 in the active site of COX-2[162,171]. LM-4131, on the other hand, has reduced hydrogen-bonding capacity since its carboxylic acid group has been converted to a tertiary amide that forms bonds with tyrosine at position 355 and arginine at position 120 in the active site of COX-2[162]. Moreover, COX-2's efficiency toward oxygenation of arachidonic acid or an endocannabinoid has been suggested to depend on if substrates for COX-2 bind to either the catalytic or allosteric sites of COX-2 or both sites and to what extent these substrates allosterically modulate COX-2[172].

We chose the 8h post-stress time point for testing the mice for anxiety-like behaviors due to the robustness of our preliminary findings that LM-4131 can reduce stress-induced anxiety-like behaviors in the NIFS assay more effectively at the 8h post-stress time point than at other time points (e.g., 4h, 24h, and 72h) and in comparison to the effects of the other COX-2 inhibitors on anxiety-like behavior in the NIFS assay under stressed conditions (Fig. 2g and see APPENDIX Fig. A). According to the cumulative frequency distribution percentile plot of mice feeding in the NIFS assay 4h post-footshock stress (Fig. Aa (left panel)), 100% of vehicle-treated mice had a feeding latency ≤ 750 s and 100% of LM-4131-treated mice had a feeding latency ≤ 390 s in the novel cage environment. A Kolmogorov-Smirnov test of the feeding latency data presented in the percentile plot revealed a significant difference between the cumulative frequency distribution for the LM-4131 treatment group and the cumulative frequency distribution for the vehicle treatment group ($D = 0.1983$, $p = 0.0171$, $^*p < 0.05$, LM-4131 at 10 mg/kg vs. vehicle). Thus, four hours post-footshock stress LM-4131 caused a decrease in feeding latency in mice. A Mann Whitney

test indicated that the feeding latency was greater for vehicle-treated mice (median = 238 s) than for the LM-4131-treated mice (median = 126 s), $U = 15.00$, $p = 0.0124$, $*p < 0.05$ (Fig. Aa (right panel)). According to the cumulative frequency distribution percentile plot of mice feeding in the NIFS assay 24h post-footshock stress (Fig. Ab (left panel)), 100% of vehicle-treated mice had a feeding latency ≤ 1095 s, 100% of LM-4131-treated mice had a feeding latency ≤ 390 s, and 100% of LMX-treated mice had a feeding latency ≤ 450 s in the novel cage environment. A Kolmogorov-Smirnov test of the feeding latency data presented in the percentile plot revealed a significant difference between the cumulative frequency distribution for the LM-4131 and LMX treatment groups and the cumulative frequency distribution for the vehicle treatment group ($D = 0.3884$, $****p < 0.0001$, LM-4131 at 10 mg/kg vs. vehicle; $D = 0.3554$, $****p < 0.0001$, LMX at 1 mg/kg vs. vehicle). Thus, 24 hours post-footshock stress LM-4131 and LMX caused a decrease in feeding latency in mice. A Mann Whitney test indicated that the feeding latency was greater for vehicle-treated mice than for the LM-4131-treated mice ($U = 117.0$, $p = 0.0007$, $***p < 0.001$; LM-4131 (median = 146.5 s) vs. vehicle (median = 319.0 s)) and the LMX-treated mice ($U = 59.00$, $p = 0.0081$, $**p < 0.01$; LMX (median = 140.5 s) vs. vehicle (median = 319.0 s); Fig. Ab (right panel)). According to the cumulative frequency distribution percentile plot of mice feeding in the NIFS assay 72h post-footshock stress (Fig. Ac (left panel)), 100% of vehicle-treated mice had a feeding latency ≤ 660 s and 100% of LM-4131-treated mice had a feeding latency ≤ 375 s in the novel cage environment. A Kolmogorov-Smirnov test of the feeding latency data presented in the percentile plot revealed no difference between the cumulative frequency distribution for the LM-4131 treatment group and the cumulative frequency distribution for the vehicle treatment group ($D = 0.1570$, $p = 0.1012$, *ns*, LM-4131 at 10 mg/kg vs. vehicle). Thus, 72 hours post-footshock stress LM-4131 caused no changes in feeding latency in mice. A Mann Whitney test indicated

that the feeding latency was similar for vehicle-treated mice (median = 268 s) and for the LM-4131-treated mice (median = 206 s), $U = 37.00$, $p = 0.3473$, *ns* (Fig. Ac (right panel)).

Since the COX-2 inhibitors were effective at reducing stress-induced anxiety-like behavior in the NIFS assay 8h after acute stress exposure, we determined if the anxiolytic potential of the COX-2 inhibitors remained before an animal was exposed to acute footshock stress and tested in the NIFS assay 8 hours later. Interestingly, none of the COX-2 inhibitors, LM-4131, LMX, or celecoxib, were able to prevent stress-induced anxiety-like behaviors in the NIFS assay (Fig. 2h) even though other studies have illustrated that COX-2 inhibitors are neuroprotective against stress-induced behavioral changes in animals[159,160]. According to the cumulative frequency distribution percentile plot of juvenile ICR male mice feeding in the NIFS assay (Fig. 2h (left panel)), 100% of vehicle-treated mice had a feeding latency ≤ 645 s, 100% of LM-4131-treated mice had a feeding latency ≤ 660 s, 100% of LMX-treated mice had a feeding latency ≤ 345 s, and 100% of celecoxib-treated mice had a feeding latency ≤ 285 s in the novel cage environment. A Kolmogorov-Smirnov test of the feeding latency data presented in the percentile plot revealed a significant difference only between the cumulative frequency distributions for the celecoxib treatment group and the cumulative frequency distribution for the vehicle treatment group ($D = 0.07438$, $p = 0.8914$, *ns*, LM-4131 at 10 mg/kg vs. vehicle; $D = 0.1653$, $p = 0.0733$, *ns*, LMX at 1 mg/kg vs. vehicle; $D = 0.1983$, $p = 0.0171$, $^*p < 0.05$, celecoxib at 10 mg/kg vs. vehicle; Fig. 2h (left panel)). There was no difference among the means for feeding latency between all COX-2 inhibitor treatment groups and the vehicle treatment group (one-way ANOVA: $F_{(3, 32)} = 0.4616$, $p = 0.7111$, *ns*; Holm-Sidak's multiple comparisons test: *ns*, $t = 0.04327$, df = 32, LM-4131 (mean ± s.e.m.: 241.2 ± 67.55, $N = 13$) vs. vehicle (mean ± s.e.m.: 238.3 ± 67.55, $N = 13$); *ns*, $t = 0.2152$, df = 32, LMX (mean ± s.e.m.: 218.8 ± 90.63, $N = 5$) vs. vehicle (mean ± s.e.m.: 238.3 ± 90.63, N

= 13); *ns*, $t = 1.074$, df = 32, celecoxib (mean ± s.e.m.: 238.3 ± 90.63, $N = 5$) vs. vehicle (mean ± s.e.m.: 238.3 ± 90.63, $N = 13$); Fig. 2h (right panel)). A discrepancy between the results obtained from the K-S test and the one-way ANOVA may be due to the oversensitivity of the K-S test near the center as opposed to the tails of the distribution of the feeding latency data from the celecoxib treatment group. It could also be due to the small sample size in the celecoxib treatment group as compared to vehicle and LM-4131 treatment groups. One-way ANOVA with small sample sizes may not have enough power to detect significant differences among the samples even if the means are different. Power decreases as the sample variance increases and sample size decreases[168].

Effects of SSCI on stress-induced anhedonia and despair-like behavior

Since anxiety-like behaviors have been suggested to be co-morbid with depressive-like behaviors[173-177], we wanted to determine the antidepressant potential of the SSCI, LM-4131. First, we measured anhedonia or loss of interest or pleasure in consuming a sweet, palatable ENSURE® vanilla shake in the NIH test. Anhedonia is a core feature of major depression in humans[178-180]. In addition, previous studies have suggested that hedonic deficits in rodents can occur after exposure to stress or placed in a stressful environmental context[181,182]. The NIH test can measure both anhedonia and hyponeophagia, a predictor of the anxiolytic effects of antidepressants, by determining how much of a sweet, palatable fluid an animal can consume in response to an anxiogenic, novel environment as opposed to a nonanxiogenic, familiar environment. In the NIH test, animals experience conflict between the desire to approach and consume a palatable liquid and the anxiety-induced avoidance of the novel environment (e.g., a new cage without bedding and illuminated by bright light)[183,184]. We have found that the NIH test in a mildly stressful, novel cage environment can induce both anhedonia and hyponeophagia. An unpaired *t* test revealed a

significant difference in the means of the amount of consumption of a sweet, palatable shake in mice tested in the nonanxiogenic and familiar, home cage environment compared to the same mice that were tested one day later in the anxiogenic, novel cage environment (****p<0.0001, t = 7.107, df = 54, novel (mean ± s.e.m.: 0.5321 ± 0.05682, N = 28) vs. home (mean ± s.e.m.: 1.521 ± 0.1271, N = 28); Fig. 2i). We also found that LM-4131 was able to decrease anhedonia in the NIH test only when the mice were previously exposed 8h earlier to an acute stressor regardless of the aversiveness of the cage environment in the NIH test. When the mice were tested in a safe, familiar cage environment (e.g., home cage) under basal conditions, we observed no changes in shake consumption between all COX-2 inhibitor treatment groups and the vehicle treatment group (one-way ANOVA: $F_{(3, 36)}$ = 1.003, p = 0.4028, *ns;* Holm-Sidak's multiple comparisons test: *ns*, t = 0.08231, df = 36, LM-4131 (mean ± s.e.m.: 1.330 ± 0.2430, N = 10) vs. vehicle (mean ± s.e.m.: 1.310 ± 0.2430, N = 10); *ns*, t = 0.8231, df = 36, LMX (mean ± s.e.m.: 1.510 ± 0.2430, N = 10) or celecoxib (mean ± s.e.m.: 1.090 ± 0.2430, N = 10) vs. vehicle (mean ± s.e.m.: 1.310 ± 0.2430, N = 10); Fig. 2j (left panel)). However, when we tested the mice in the same cage environment 8 hours after being subjected to acute electric footshock stress, we observed an increase in shake consumption in mice treated with the substrate-selective COX-2 inhibitor, LM-4131, compared to those treated with vehicle. An unpaired t test revealed a significant difference in the means of the LM-4131 treatment group compared to the vehicle treatment group (p=0.0319, *p<0.05, t = 2.326, df = 18, LM-4131 (mean ± s.e.m.: 1.440 ± 0.1536, N = 10) vs. vehicle (mean ± s.e.m.: 0.8500 ± 0.2018, N = 10); p=0.1340, *ns*, t = 1.569, df = 18, LMX (mean ± s.e.m.: 1.290 ± 0.1946, N = 10) vs. vehicle; p=0.0632, *ns*, t = 1.980, df = 18, celecoxib (mean ± s.e.m.: 1.370 ± 0.1680, N = 10) vs. vehicle; Fig. 2j (right panel)).

Since we observed decreased anhedonia in the juvenile male mice under stressed conditions in the home cage environment, we wanted to determine next the effect of the SSCI,

LM-4131, on hyponeophagia and if increasing the aversiveness or novelty of the cage environment would change the hedonic action of the SSCIs previously demonstrated in the non-stressful home cage environment. None of the COX-2 inhibitors administered by i.p. to the mice decreased anhedonia and hyponeophagia in the mice under no stress in the mildly stressful, novel cage environment. According to the cumulative frequency distribution percentile plot of juvenile (5-7 weeks of age) ICR male mice feeding in the NIFS assay (Fig. 2k (left panel)), 25% of vehicle-treated mice consumed ≤ 0.4 g of the shake (e.g., 25th percentile), 25% of LM-4131-treated mice consumed ≤ 0.55 g of the shake, 25% of LMX-treated mice consumed ≤ 0.575 g of the shake, and 25% of celecoxib-treated mice consumed ≤ 0.7 g of the shake in the novel cage environment. A Kolmogorov-Smirnov (K-S) test of the shake consumption data presented in the cumulative frequency distribution percentile plot revealed significant differences between the cumulative frequency distribution for the LMX and celecoxib treatment groups and the cumulative frequency distribution for the vehicle treatment group (D = 0.1563, p = 0.1918, *ns*, LM-4131 at 10 mg/kg vs. vehicle; D = 0.2604, p = 0.0030, $^{**}p < 0.01$, LMX at 1 mg/kg vs. vehicle; D = 0.2083, p = 0.0310, $^{*}p < 0.05$, celecoxib at 10 mg/kg vs. vehicle; Fig. 2k (left panel)). Thus, there is a likelihood that the two treatment groups (e.g., the COX-2 inhibitor, LMX or celecoxib, vs. vehicle) are derived from different populations. The shake consumption data indicate that the shake consumption in mice treated with the COX-2 inhibitor, LMX or celecoxib, is significantly greater than the shake consumption in mice treated with vehicle. When the same set of shake consumption data was evaluated with one-way analysis of variance (ANOVA), we found that the results acquired with the one-way ANOVA were not consistent with the results for the LMX or celecoxib treatment group obtained with the Kolmogorov-Smirnov test. There was no significant difference among the means for shake consumption between the LMX or celecoxib treatment group and the vehicle

treatment group (one-way ANOVA: $F_{(3, 91)} = 1.173$, $p = 0.3243$, *ns*; Holm-Sidak's multiple comparisons test: *ns*, $t = 1.649$, df = 91, LM-4131 (mean ± s.e.m.: 0.9000 ± 0.09668, $N = 37$) vs. vehicle (mean ± s.e.m.: 0.7405 ± 0.09668, $N = 37$); *ns*, $t = 1.003$, df = 91, LMX (mean ± s.e.m.: 0.8714 ± 0.1305, $N = 14$) vs. vehicle (mean ± s.e.m.: 0.7405 ± 0.1305, $N = 37$); *ns*, $t = 1.264$, df = 91, celecoxib (mean ± s.e.m.: 0.9571 ± 0.1714, $N = 7$) vs. vehicle (mean ± s.e.m.: 0.7405 ± 0.1714, $N = 37$); Fig. 2k (right panel)). A discrepancy between the results obtained from the K-S test and the one-way ANOVA may be due to the oversensitivity of the K-S test and the small sample size in the LMX and celecoxib treatment groups as compared to the vehicle and LM-4131 treatment groups.

Of all the COX-2 inhibitors, only LM-4131 decreased anhedonia and hyponeophagia when the mice were tested in the aversive, novel cage environment 8 hours after exposure to acute footshock stress. According to the cumulative frequency distribution percentile plot of juvenile ICR male mice feeding in the NIFS assay (Fig. 2l (left panel)), 100% of vehicle-treated mice consumed ≤ 1.12 g of the shake, 100% of LM-4131-treated mice consumed ≤ 1.62 g of the shake, 100% of LMX-treated mice consumed ≤ 0.92 g of the shake, and 100% of celecoxib-treated mice consumed ≤ 1.20 g of the shake in the novel cage environment. A Kolmogorov-Smirnov test of the shake consumption data presented in the percentile plot revealed a significant difference between the cumulative frequency distributions for the LM-4131 and LMX treatment groups and the cumulative frequency distribution for the vehicle treatment group ($D = 0.2970$, $p = 0.0003$, ***$p < 0.001$, LM-4131 at 10 mg/kg vs. vehicle; $D = 0.1980$, $p = 0.0381$, *$p < 0.05$, LMX at 1 mg/kg vs. vehicle; $D = 0.2153$, $p = 0.2153$, *ns*, celecoxib at 10 mg/kg vs. vehicle; Fig. 2l (left panel)). There was a significant difference among the means for feeding latency between the LM-4131 treatment group and the vehicle treatment group (one-way ANOVA: $F_{(3, 105)} = 5.731$, p =

0.0011, $^{**}p < 0.01$; Holm-Sidak's multiple comparisons test: $^{**}p < 0.01$, $t = 3.355$, df = 105, LM-4131 (mean ± s.e.m.: 0.8306 ± 0.09625, $N = 36$) vs. vehicle (mean ± s.e.m.: 0.5077 ± 0.09625, $N = 39$); *ns*, $t = 0.4674$, df = 105, LMX (mean ± s.e.m.: 0.4565 ± 0.1095, $N = 23$) vs. vehicle (mean ± s.e.m.: 0.5077 ± 0.1095, $N = 39$); *ns*, $t = 0.4378$, df = 105, celecoxib (mean ± s.e.m.: 0.4455 ± 0.1422, $N = 11$) vs. vehicle (mean ± s.e.m.: 0.5077 ± 0.1422, $N = 39$); Fig. 2l (right panel)).

We investigated the effects of substrate-selective COX-2 inhibition on stress-induced anhedonia and hyponeophagia in the NIH test after mice were subjected to acute footshock stress 4 h, 24 h, and 72 h prior to testing (see APPENDIX Fig. A). We found that the SSCI, LM-4131, decreased anhedonia and hyponeophagia in juvenile male mice 24 h and 72 h after acute footshock stress exposure. We compared these findings to another SSCI, LMX, and found similar results as regards to the 24 h post-footshock stress time point. According to the cumulative frequency distribution percentile plot of mice feeding in the NIFS assay 4h post-footshock stress (Fig. Ad (left panel)), 75% of vehicle-treated mice consumed ≤ 1.425 g of the shake (75^{th} percentile) and 75% of LM-4131-treated mice consumed ≤ 1.175 g of the shake in the novel cage environment. A Kolmogorov-Smirnov test of the shake consumption data presented in the percentile plot revealed a significant difference between the cumulative frequency distribution for the LM-4131 treatment group and the cumulative frequency distribution for the vehicle treatment group ($D = 0.2088$, $p = 0.0379$, $^{*}p < 0.05$, LM-4131 at 10 mg/kg vs. vehicle). However, a Mann Whitney test indicated that the shake consumption was similar for the vehicle-treated mice (median = 0.9000 g) and the LM-4131-treated mice (median = 0.8500 g), $U = 48.50$, $p = 0.9259$, *ns* (Fig. Ad (right panel)). According to the cumulative frequency distribution percentile plot of mice feeding in the NIFS assay 24h post-footshock stress (Fig. Ae (left panel)), 100% of vehicle-treated mice consumed ≤ 1.1 g of the shake (e.g., 100^{th} percentile), 100% of LM-4131-treated mice consumed

≤ 2.1 g of the shake, and 100% of LMX-treated mice consumed ≤ 0.8 g of the shake in the novel cage environment. A Kolmogorov-Smirnov test of the shake consumption data presented in the percentile plot revealed a significant difference between the cumulative frequency distribution for the LM-4131 and LMX treatment groups and the cumulative frequency distribution for the vehicle treatment group (D = 0.3465, ****p < 0.0001, LM-4131 at 10 mg/kg vs. vehicle; D = 0.2970, p = 0.0003, ***p < 0.001, LMX at 1 mg/kg vs. vehicle). Thus, 24 hours post-footshock stress LM-4131 caused an increase in shake consumption whereas LMX caused a decrease in shake consumption in mice. A Mann Whitney test indicated that the shake consumption was greater for LM-4131-treated mice than for the vehicle-treated mice (U = 117.0, p = 0.0007, ***p < 0.001; LM-4131 (median = 1.100 g) vs. vehicle (median = 0.6500 g)) and lesser for the LMX-treated mice than for the vehicle-treated mice (U = 58.00, p = 0.0141, *p < 0.05; LMX (median = 0.2500 g) vs. vehicle (median = 0.6500 g); Fig. Ae (right panel)). According to the cumulative frequency distribution percentile plot of mice feeding in the NIFS assay 72h post-footshock stress (Fig. Af (left panel)), 100% of vehicle-treated mice consumed ≤ 0.7 g of the shake and 100% of LM-4131-treated mice consumed ≤ 1.3 g of the shake in the novel cage environment. A Kolmogorov-Smirnov test of the shake consumption data presented in the percentile plot revealed a significant difference between the cumulative frequency distribution for the LM-4131 treatment group and the cumulative frequency distribution for the vehicle treatment group (D = 0.3125, p = 0.0002, ***p < 0.001, LM-4131 at 10 mg/kg vs. vehicle). Thus, 72 hours post-footshock stress LM-4131 increased shake consumption in the mice. A Mann Whitney test indicated that the shake consumption was lesser for vehicle-treated mice (median = 0.5000 g) and for the LM-4131-treated mice (median = 0.7000 g), U = 20.00, p = 0.0178, *p < 0.05 (Fig. Af (right panel)). As observed in our findings regarding the anxiolytic potential of SSCI on stress-induced anxiety-like behavior

in the NIH test, we saw in these results that the SSCI, LM-4131, was more efficacious when mice were exposed to a form of physical stress. These results may again imply that COX-2 catalytic activity and expression levels may be differentially regulated by the severity of an external stressor, whether it's a physical form or an environmental form of stress. Further investigation into how various stressors affect COX-2's catalytic activity and expression levels in the brain is needed to determine the relationship between COX-2 catalytic activity and expression levels and anxiogenic behaviors in animals after stress exposure.

Next, we performed the tail suspension test and the sucrose preference test under basal and stressed conditions to measure the effects of LM-4131 on despair-like behavior in juvenile male ICR mice. Although previous studies in both humans and rodents have illustrated the antidepressive effects of the selective COX-2 inhibitor, celecoxib[185-191], we found no changes in behavioral despair between the mice treated with vehicle or a COX-2 inhibitor. At first glance, LM-4131 at 10 mg/kg appeared to increase despair-like behavior in the mice under non stressed conditions compared to vehicle-treated mice. Two-way ANOVA revealed no effect of 1 min time bins x drug interaction ($F_{(11, 336)} = 0.7055$, $p = 0.7333$, *ns*; Fig. 3a (1st left panel)) but a significant main effect of drug dose ($F_{(1, 336)} = 12.26$, $p = 0.0005$, ***$p < 0.001$ (LM-4131 vs vehicle); Fig. 3a (1st left panel)) on duration of immobility over all 1 min bins in the tail suspension test. However, further statistical analysis of the main treatment group effect on duration of immobility for each minute of behavioral testing revealed no differences between the vehicle-treated and LM-4131-treated mice (unpaired *t* test: $p = 0.0929$, $t = 1.757$, df = 22, LM-4131 vs. vehicle; Fig. 3a (2nd left panel)). Neither LMX at 1 mg/kg or celecoxib at 10 mg/kg affected duration of immobility over

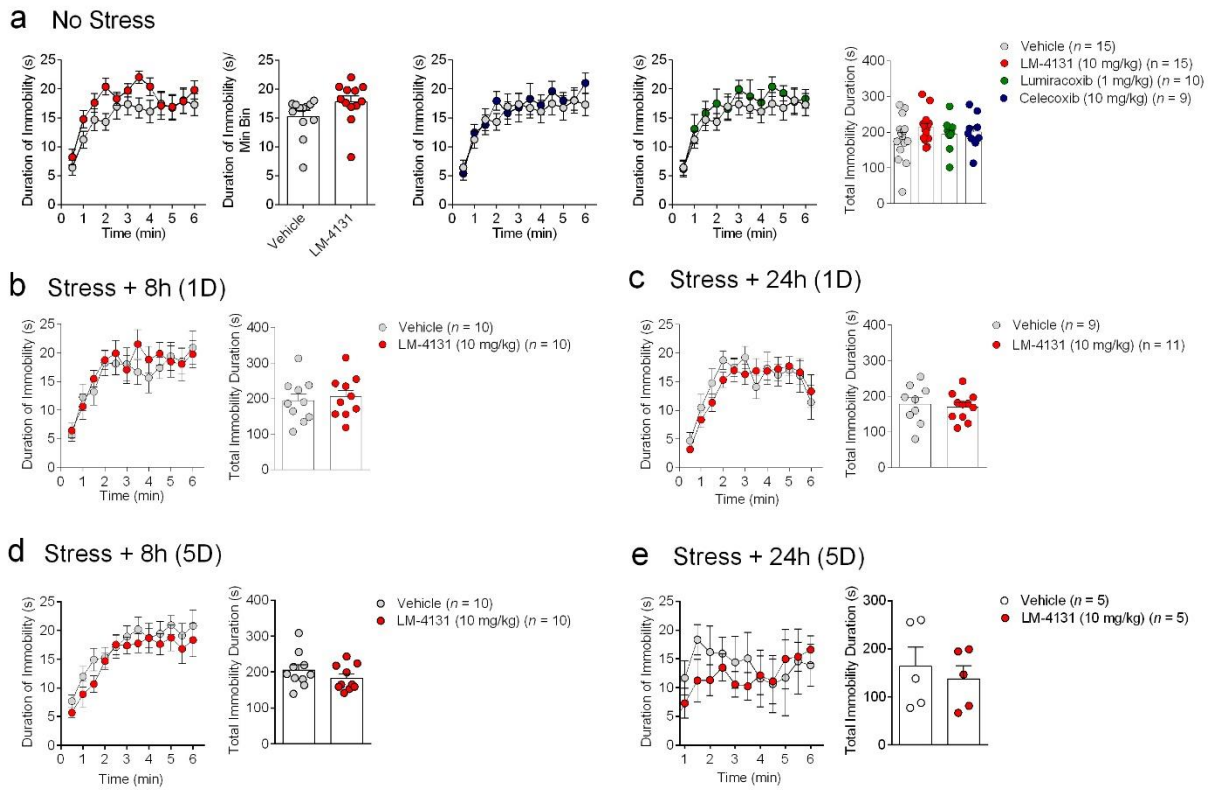

Figure 3. Effects of SSCI on despair-like behavior in the tail suspension test. (**a**) Effects of LM-4131, Lumiracoxib (LMX), and Celecoxib on immobility duration in the tail suspension test under control non-stressed conditions. (**b, c**) Effects of LM-4131 on immobility duration in the tail suspension test 8 and 24 hours after acute foot-shock exposure (1 day). (**d, e**) Effects of LM-4131 on immobility duration in the tail suspension test 8 and 24 hours after chronic foot-shock exposure (5 days). No drug effects on immobility were observed under any condition, except 8 hours after chronic stress exposure. Data are shown as the mean ± s.e.m. Stress (e.g., stress exposure in the form of an electric footshock administered 8h or 24h prior to testing). Statistical significance was calculated by two-tailed unpaired Student's t-test or two-way ANOVA with post hoc Holm-Sidak's multiple comparisons test.

all 1 min bins (two-way ANOVA: main effect of drug dose, $F_{(1, 276)} = 1.394$, $p = 0.2387$, *ns* (LMX vs vehicle) and $F_{(1, 264)} = 3.239$, $p = 0.0730$, *ns* (celecoxib vs. vehicle); effect of 1 min time bins x drug interaction, $F_{(11, 276)} = 0.3841$, $p = 0.9616$, *ns* (LMX vs vehicle) and $F_{(11, 264)} = 0.1927$, $p = 0.9979$, *ns* (celecoxib vs. vehicle); Fig. 3a (left panel)). None of the COX-2 inhibitors affected total immobility duration (one-way ANOVA: $F_{(3, 45)} = 0.8929$, $p = 0.4521$, *ns*; $t = 1.610$, df = 45, $p < 0.05$, *ns*, LM-4131 vs. vehicle; $t = 0.5363$, df = 45, $p < 0.05$, *ns*, LMX vs. vehicle; $t = 0.8352$, df = 45, $p < 0.05$, *ns*, celecoxib vs. vehicle; Fig. 3a (right panel)) under control (no stress) conditions in the tail suspension test. Acute footshock stress subjected to the mice 8h prior to

behavioral testing did not affect duration of immobility over all 1 min bins (two-way ANOVA: main effect of drug dose, $F_{(1, 216)} = 0.9427$, $p = 0.3327$, *ns*; effect of 1 min time bins x drug interaction, $F_{(11, 216)} = 0.4010$, $p = 0.9546$, *ns*; Fig. 3b (left panel)) or total immobility duration (unpaired *t* test: $p = 0.6888$, $t = 0.4070$, df = 18, LM-4131 at 10 mg/kg vs. vehicle; Fig. 3b (right panel)). Increasing the time length between the acute stress exposure and start of behavioral testing to 24 h did not affect duration of immobility over all 1 min bins (two-way ANOVA: main effect of drug dose, $F_{(1, 216)} = 0.5606$, $p = 0.4548$, *ns*; effect of 1 min time bins x drug interaction, $F_{(11, 216)} = 0.5363$, $p = 0.8773$, *ns*; Fig. 3c (left panel)) or total immobility duration (unpaired *t* test: $p = 0.7258$, $t = 0.3563$, df = 18, LM-4131 at 10 mg/kg vs. vehicle; Fig. 3c (right panel)). Nevertheless, increasing the intensity of the stress exposure from 1 day to 5 days if behavioral testing occurred 8 h after stress exposure slightly decreased duration of immobility over the 6 min testing period (two-way ANOVA: main effect of drug dose, $F_{(1, 216)} = 5.311$, $p = 0.0221$, $^*p < 0.05$; 1 min time bin x drug interaction, $F_{(11, 216)} = 0.2150$, $p = 0.9965$, *ns*; Fig. 3d (left panel)) but caused no changes in total immobility duration (unpaired *t* test: $p = 0.2519$, *ns*, $t = 1.184$, df = 18, LM-4131 at 10 mg/kg vs. vehicle; Fig. 3d (right panel)). Thus, regardless of the time at which despair-like behavior was measured in the tail suspension test or occurred in the mice, LM-4131 at a dose of 10 mg/kg significantly decreased despair-like behavior in the mice only 8 hours after being subjected to 5 days of footshock stress (e.g., 6 footshocks/day separated by 58 seconds with each footshock lasting 2 seconds). Chronic stress exposure subjected to the mice 24 h prior to testing did not affect duration of immobility over time (two-way ANOVA: main effect of drug dose, $F_{(1, 96)} = 2.000$, $p = 0.1605$, *ns*; 1 min time bin x drug interaction, $F_{(11, 96)} = 0.4539$, $p = 0.9266$, *ns*; Fig. 3e (left panel)) or total immobility duration (unpaired *t* test: $p = 0.6055$, $t = 0.5376$, df = 8, LM-4131 at 10 mg/kg vs. vehicle; Fig. 3e (right panel)).

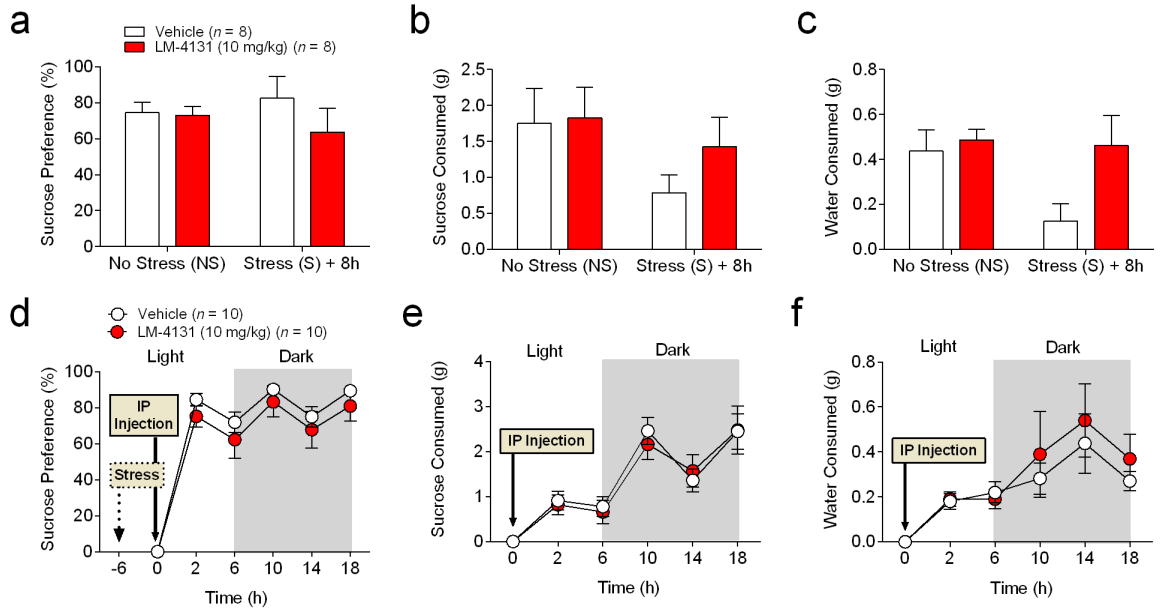

Figure 4. Effects of SSCI in the sucrose preference test. (**a-c**) 2 hour cumulative sucrose preference, sucrose consumption, and water consumption after vehicle or LM-4131 treatment in control non-stressed mice and in mice tested 8 hours after acute footshock exposure. Testing was conducted during the light phase of the circadian cycle. (**d-f**) Effects of LM-4131 or vehicle on sucrose consumption during the light and dark phase of the circadian cycle. Mice were treated with LM-4131 or vehicle 8 hours after acute foot shock exposure and tested time interval increments of 2 or 4 hours during the light cycle and the dark cycle. No drug effects on sucrose preference were observed under any condition. Data are shown as the mean ± s.e.m. NS = no stress, S = stress (e.g., stress exposure in the form of an electric footshock administered 8h prior to testing). Statistical significance was calculated by two-way ANOVA with post hoc Holm-Sidak's multiple comparisons test.

In regard to the sucrose preference test, we found no changes in percentage sucrose preference (two-way ANOVA: effect of drug dose, $F_{(1, 28)} = 1.062$, $p = 0.3115$, *ns*; effect of stress exposure, $F_{(1, 28)} = 0.005594$, $p = 0.9409$, *ns*; stress exposure condition x drug interaction, $F_{(1, 28)} = 0.7839$, $p = 0.3835$, *ns*; Fig. 4a) or the amount of sucrose consumed (two-way ANOVA: effect of drug dose, $F_{(1, 28)} = 0.7734$, $p = 0.3867$, *ns*; effect of stress exposure, $F_{(1, 28)} = 2.828$, $p = 0.1037$, *ns*; stress exposure condition x drug interaction, $F_{(1, 28)} = 0.4820$, $p = 0.4932$, *ns*; Fig. 4b) between the LM-4131 and vehicle treatment groups under both control, non-stressed and 8 hours after acute footshock stress exposure. LM-4131 treatment did restore the amount of water consumed (two-way ANOVA: effect of drug dose, $F_{(1, 28)} = 4.287$, $p = 0.0477$, $^*p < 0.05$; effect of stress exposure,

$F_{(1, 28)} = 3.252$, $p = 0.0821$, *ns*; stress exposure condition x drug interaction, $F_{(1, 28)} = 2.360$, $p = 0.1357$, *ns*; Fig. 4c) back to control, non-stressed levels since the amount of water consumed decreased in the vehicle treatment group 8 hours after acute footshock stress exposure. Even though the mice appeared to consume more sucrose than water in general, we found similar results irrespective of the time of day 8 hours after acute footshock stress exposure in percentage sucrose preference (two-way ANOVA: effect of drug dose, $F_{(1, 108)} = 3.670$, $p = 0.0580$, *ns*; time of day x drug interaction, $F_{(5, 108)} = 0.1616$, $p = 0.9760$, *ns*; Fig. 4d), the amount of sucrose consumed (two-way ANOVA: effect of drug dose, $F_{(1, 108)} = 0.07044$, $p = 0.7912$, *ns*; time of day x drug interaction, $F_{(5, 108)} = 0.1685$, $p = 0.9737$, *ns*; Fig. 4e), or the amount of water consumed (two-way ANOVA: effect of drug dose, $F_{(1, 108)} = 0.8032$, $p = 0.3721$, *ns*; time of day x drug interaction, $F_{(5, 108)} = 0.2183$, $p = 0.9540$, *ns*; Fig. 4f) between the LM-4131 and vehicle treatment groups.

Surprisingly, LM-4131 appeared to have some antidepressant properties only when the intensity of the stressor was increased. This finding is in line with previous studies that have shown chronic stress exposure instead of basal conditions can reverse depressive-like behavior in rodents administered the selective COX-2 inhibitor, celecoxib[188,191]. One plausible reason for this effect may be due to the ability of specific stress exposure protocols to upregulate PGE_2, a biomarker of COX-2 activity, and COX-2 transcript and protein expression levels, thus increasing the availability of COX-2 protein to be acted upon by COX-2 inhibitors. If this is so then LM-4131 may be more efficacious in treating despair-like behavior in animals when COX-2 expression is elevated compared to control levels. Studies have shown that upregulated COX-2 expression is found in patients with a depressive disorder[192] and COX-2 inhibitors are efficacious in the treatment of depressive disorders in humans[185,187,189,190]. Nevertheless, prolonged treatment with the SSCI, LM-4131, or a higher dose of LM-4131 may be necessary to rescue changes in

depressive-like behavior in animals exposed to no stress or acute stress. Santiago and others illustrated that prolonged treatment with celecoxib (e.g., up to 3 weeks) in an animal model of chronic mild stress restored sucrose preference in the sucrose preference test to control levels. Yet, these authors also demonstrated that acute administration of celecoxib at a dose of 10 mg/kg was sufficient to exhibit antidepressant-like properties in the forced swim test in rodents under basal conditions. Discrepancies between our finding that acute administration of celecoxib at a dose of 10 mg/kg does not improve despair-like behavior in mice under control (no stress) conditions and this study may depend on the time interval between drug administration and behavioral testing of despair-like behavior in the mice[191]. We administered the COX-2 inhibitor, celecoxib, 2 hours before behavioral testing whereas Santiago and others administered celecoxib 1 hour before behavioral testing.

Moreover, we may not have been able to observe robust changes in despair-like behavior in the mice due to COX-2 inhibition because our stress exposure protocols were not able to induce despair-like behavior in the mice in comparison to controls. This is evident in the sucrose preference test where our acute stress protocol did not cause a significant decrease but a decreasing trend (if not due to variability in animal behavioral responses and low sample size) in total sucrose consumption in the mice (see Fig. 4b). Even though our stress exposure protocols can induce anhedonia, which is a core symptom of depression, in the NIFS assay, modeling depression in animals is quite difficult. Depression is a complex affective disorder characterized by phenotypic heterogeneity and symptoms (e.g., anhedonia or loss of interest or pleasure, depressed mood, insomnia, fatigue, feelings of worthlessness, and diminished ability to concentrate) that are not pathognomonic but present in other neuropsychiatric disorders[193]. Depression has also been associated with dysregulation of the HPA axis due to previous studies finding increased cortisol

levels in depressed humans or corticosterone levels in animals exhibiting despair-like behavior[194-197]. Our stress exposure protocols did not induce any changes in plasma corticosterone (CORT) levels in mice when administered vehicle or LM-4131 (see APPENDIX Fig. F; unpaired *t* test: $p = 0.6345$, $t = 0.4836$, df = 18, LM-4131 at 10 mg/kg vs. vehicle; Fig. Aa (left panel); $p = 0.3805$, $t = 0.8873$, df = 38, LM-4131 at 10 mg/kg vs. vehicle; Fig. Ab (middle panel); $p = 0.6186$, $t = 0.5066$, df = 18, LM-4131 at 10 mg/kg vs. vehicle; Fig. Ac (right panel)), suggesting our animal model of stress-induced anxiety maybe a poor example for modeling depression when despair-like behavior in the mice is measured at least 8 hours after stress exposure. In fact, one-way ANOVA revealed no significant differences in plasma CORT levels in the mice subjected to acute stress (1 day) and chronic stress (5 days) conditions when compared to controls (one-way ANOVA: $F_{(2, 37)} = 0.2392$, $p = 0.7885$, *ns;* Holm-Sidak's multiple comparisons test: $t = 0.5446$, df = 37, S + 8h (1D) vs. control; $t = 0.6415$, df = 37, S + 8h (5D) vs. control).

Effects of age and sex on the anxiolytic potential of substrate-selective COX-2 inhibition

Previously, we have shown that the SSCI, LM-4131, can reduce anxiety-like behavior in juvenile male mice under basal and stressed conditions (see Fig. 2). Nevertheless, we wanted to examine the generalizability of these findings pertaining to the age and sex of mice. Thus, we determined if the anxiolytic potential of LM-4131 could be observed in aged male mice and juvenile and aged female mice. According to the cumulative frequency distribution percentile plot of adult (12-15 weeks of age) ICR male mice feeding in the NIFS assay (Fig. 5a (left panel)), 100% of vehicle-treated mice had a feeding latency $\leq$ 675 s, 100% of LM-4131-treated mice had a feeding latency $\leq$ 255 s, and 100% of LMX-treated mice had a feeding latency $\leq$ 135 s in the novel cage environment. A Kolmogorov-Smirnov test of these findings revealed a significant difference between both substrate-selective COX-2 inhibitor treatment groups, LM-4131 and LMX, and the

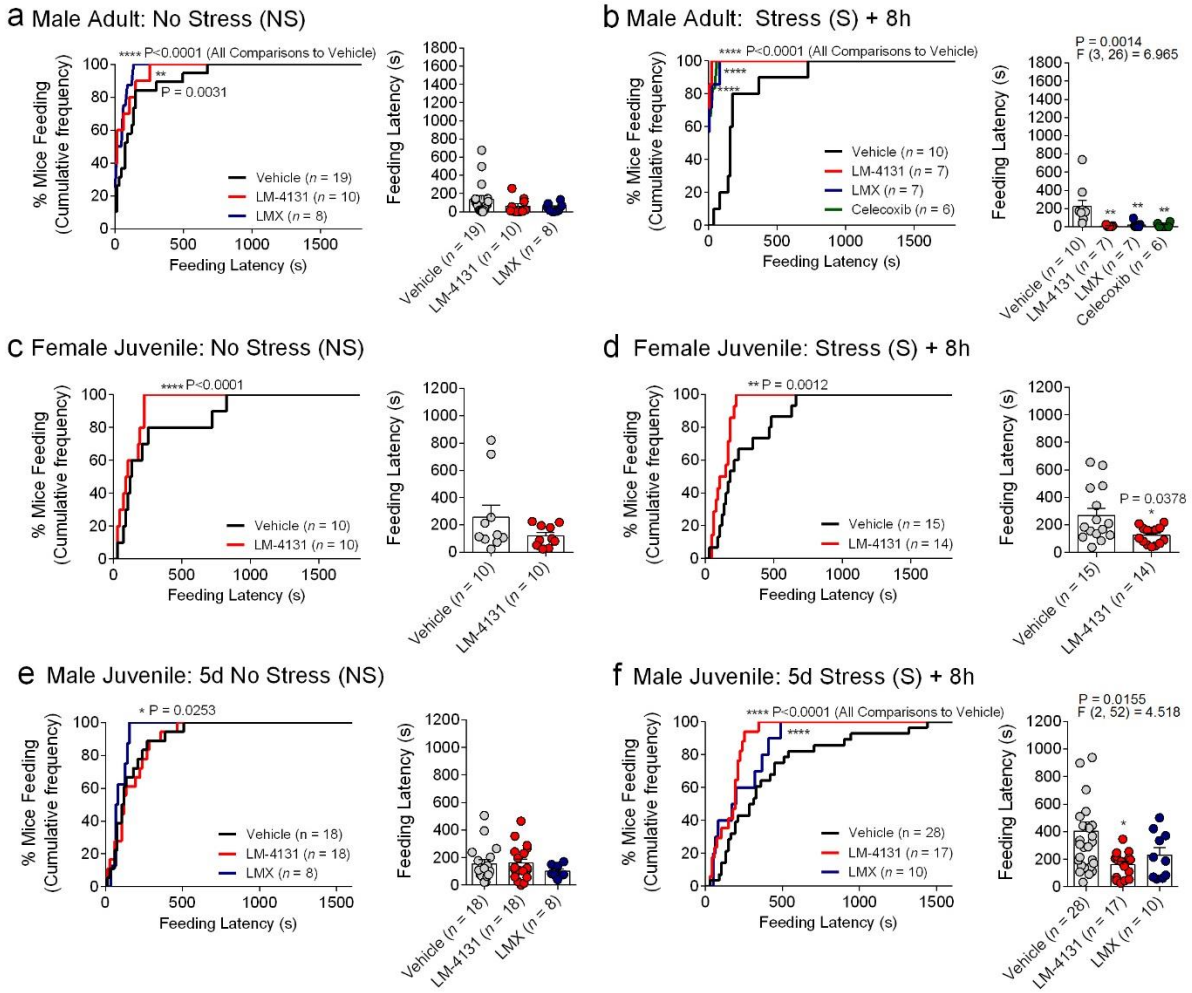

Figure 5. Anxiolytic effects of COX-2 inhibitors in aged and female mice and after chronic stress exposure. (**a,b**) Cumulative frequency of male adult mice feeding and latency to feed in novelty-induced feeding suppression (NIF test under non-stressful and acute stress conditions (six tone-shock pairings in one day). (**c,d**) Cumulative frequency of female juvenile mice feeding and latency to feed in novelty-induced feeding suppression (NIFS) test under non-stressful and acute stress conditions. (**e,f**) Cumulative frequency of male juvenile mice feeding and latency to feed in novelty-induced feeding suppression (NIFS) test under chronic non-stressful and stress conditions (six tone-shock pairings/day over five days). Data are shown as the mean ± s.e.m. NS = no stress, S = stress (e.g., stress exposure in the form of an electric footshock administered 8h prior to testing), *P < 0.05, **P < 0.01, ****P < 0.0001 (COX-2 inhibitor compared to vehicle). Statistical significance was calculated by two-tailed unpaired Student's *t*-test or Kolmogorov-Smirnov test (only for frequency plots) or one-way ANOVA with post hoc Holm-Sidak's multiple comparisons test.

vehicle treatment group (Kolmogorov-Smirnov test: $p = 0.0031$, $^{**}p < 0.01$, LM-4131 at 10 mg/kg vs. vehicle; $^{****}p < 0.0001$, LMX at 1 mg/kg vs. vehicle; Fig. 5a (left panel)). There was no significant difference among the means for feeding latency between the COX-2 inhibitor treatment groups and the vehicle treatment group (one-way ANOVA: $F_{(2, 34)} = 1.623$, $p = 0.2122$, *ns;* Holm-

Sidak's multiple comparisons test: *ns*, $t = 1.395$, df = 34, LM-4131 vs. vehicle; *ns*, $t = 1.526$, df = 34, LMX vs. vehicle; Fig. 5a (right panel)). When the adult male mice were subjected to acute footshock stress and tested for anxiety-like behavior in the NIFS assay 8 hours after stress exposure, the adult male mice exhibited a greater decrease in feeding latency in the novel cage environment. Similar effects were observed in adult mice administered by i.p. the SSCI, LMX, and the selective COX-2 inhibitor, celecoxib. According to the cumulative frequency distribution percentile plot of stressed adult male mice feeding in the NIFS assay (Fig. 5b (left panel)), 100% of vehicle-treated mice had a feeding latency ≤ 735 s, 100% of LM-4131-treated mice had a feeding latency ≤ 30 s, 100% of LMX-treated mice had a feeding latency ≤ 90 s, and 100% of celecoxib-treated mice had a feeding latency ≤ 60 s in the novel cage environment. A Kolmogorov-Smirnov test of these findings revealed a significant difference between all COX-2 inhibitor treatment groups, LM-4131, LMX, and celecoxib, and the vehicle treatment group (Kolmogorov-Smirnov test: $p < 0.0001$, ****$p < 0.0001$, LM-4131 at 10 mg/kg vs. vehicle; $p < 0.0001$, ****$p < 0.0001$, LMX at 1 mg/kg vs. vehicle; $p < 0.0001$, ****$p < 0.0001$, celecoxib at 10 mg/kg vs. vehicle; Fig. 5b (left panel)). The means for feeding latency between the COX-2 inhibitor treatment groups and the vehicle treatment group were significantly different (one-way ANOVA: $F_{(3, 26)} = 6.965$, $p = 0.0014$, **$p < 0.01$; Holm-Sidak's multiple comparisons test: **$p < 0.01$, $t = 3.705$, df = 26, LM-4131 vs. vehicle; **$p < 0.01$, $t = 3.504$, df = 26, LMX vs. vehicle; **$p < 0.01$, $t = 3.392$, df = 26, celecoxib vs. vehicle).

The effect of the SSCI, LM-4131, on feeding latency in juvenile ICR female mice in the novel cage environment was less pronounced compared to that in juvenile ICR male mice under both non stressed (control) and stressed conditions (see Fig. 2d, e). According to the cumulative frequency distribution percentile plot of juvenile (5-7 weeks of age) ICR female mice feeding in

the NIFS assay (Fig. 5c (left panel)), 100% of vehicle-treated mice had a feeding latency ≤ 825 s and 100% of LM-4131-treated mice had a feeding latency ≤ 225 s in the novel cage environment. A Kolmogorov-Smirnov test of these findings revealed a significant difference between the substrate-selective COX-2 inhibitor treatment group, LM-4131, and the vehicle treatment group (Kolmogorov-Smirnov test: $p < 0.0001$, ****$p < 0.0001$, LM-4131 at 10 mg/kg vs. vehicle; Fig. 5c (left panel)). In contrast to that found in juvenile male mice (see Fig. 2d), there was no significant difference among the means for feeding latency between the COX-2 inhibitor treatment group and the vehicle treatment group (unpaired *t* test: $p = 0.1575$, *ns*, $t = 1.475$, df = 18, LM-4131 vs. vehicle; Fig. 5c (right panel)). When the juvenile female mice were subjected to acute footshock stress and tested for anxiety-like behavior in the NIFS assay 8 hours after stress exposure, the juvenile female mice treated with LM-4131 exhibited a small decrease in feeding latency in the novel cage environment compared to vehicle-treated mice. According to the cumulative frequency distribution percentile plot of stressed adult male mice feeding in the NIFS assay (Fig. 5d (left panel)), 100% of vehicle-treated mice had a feeding latency ≤ 675 s and 100% of LM-4131-treated mice had a feeding latency ≤ 225 s in the novel cage environment. A Kolmogorov-Smirnov test of these findings revealed a significant difference between the LM-4131 treatment group and the vehicle treatment group (Kolmogorov-Smirnov test: $p = 0.0012$, **$p < 0.01$, LM-4131 at 10 mg/kg vs. vehicle; Fig. 5d (left panel)). The means for feeding latency between the COX-2 inhibitor treatment group and the vehicle treatment group were significantly different (unpaired *t* test: $p = 0.0154$, *$p < 0.05$, $t = 2.587$, df = 27, LM-4131 vs. vehicle; Fig. 5d (right panel)).

From these findings, we can conclude that the anxiolytic potential of LM-4131 in the female mice was less robust as observed previously in male mice of the same age in the NIFS

assay. To determine if these effects could be observed in female mice regardless of age, we measured anxiety-like behavior of adult female ICR mice in the elevated plus maze (EPM) under non stressed and acute stress conditions after i.p. administration of the COX-2 inhibitors, LM-4131, LMX, or celecoxib (see APPENDIX Fig. C). All COX-2 inhibitors decreased anxiety-like behaviors in the EPM only after the mice were exposed to acute footshock stress, with the exception of celecoxib which exhibited anxiolytic effects under both basal and stressed conditions. With respect to open arm time in the EPM, two-way ANOVA factoring drug dose and stress exposure revealed no effect of drug dose x stress exposure interaction ($F_{(3, 76)} = 0.2028$; $p = 0.8941$, *ns*), but a significant effect of stress exposure ($F_{(1, 76)} = 21.62$, ****$p < 0.0001$), or drug dose ($F_{(3, 76)} = 9.458$, ****$p < 0.0001$; Fig. Cc). Post hoc Holm-Sidak's multiple comparisons test revealed a significant increase in open arm time of the EPM at the 10 mg/kg dose of celecoxib compared to the vehicle treatment under basal conditions (**$p < 0.01$, $t = 3.610$, df = 76) and acute stress conditions (**$p < 0.01$, $t = 3.479$, df = 76). Relating to open arm latency in the EPM, two-way ANOVA factoring drug dose and stress exposure revealed no effect of drug dose x stress exposure interaction ($F_{(3, 75)} = 0.8824$; $p = 0.4542$, *ns*), but a significant effect of stress exposure ($F_{(1, 75)} = 4.750$, $p = 0.0324$, *$p < 0.05$), or drug dose ($F_{(3, 75)} = 7.046$, $p = 0.0003$, ***$p < 0.001$; Fig. Cf). Post hoc Holm-Sidak's multiple comparisons test revealed a significant decrease in open arm latency of the EPM at the 10 mg/kg dose of LM-4131, 1 mg/kg dose of LMX, and 10 mg/kg dose of celecoxib compared to the vehicle treatment only under acute stress conditions (***$p < 0.001$, $t = 3.689$, df = 75, LM-4131 vs. vehicle; ***$p < 0.001$, $t = 3.981$, df = 75, LMX vs. vehicle; **$p < 0.01$, $t = 2.739$, df = 75, celecoxib vs. vehicle). Concerning the closed arm latency in the EPM, two-way ANOVA factoring drug dose and stress exposure revealed no effect of drug dose x stress exposure interaction ($F_{(3, 76)} = 0.8551$; $p = 0.4682$, *ns*) and no effect of stress exposure ($F_{(1, 76)} =$

0.01881, $p = 0.8913$, *ns*), but a significant effect of drug dose ($F_{(3, 76)} = 5.490$, $^{**}p = 0.0018$; Fig. Cg). Post hoc Holm-Sidak's multiple comparisons test revealed a significant increase in closed arm latency of the EPM at the 10 mg/kg dose of LM-4131, 1 mg/kg dose of LMX, and the 10 mg/kg dose of celecoxib compared to the vehicle treatment only under acute stress conditions ($^{***}p < 0.001$, $t = 3.932$, df = 76, LM-4131 vs. vehicle; $^{**}p < 0.01$, $t = 2.848$, df = 76, LMX vs. vehicle; $^{**}p < 0.01$, $t = 3.054$, df = 76, celecoxib vs. vehicle). With respect to the start of the first freezing episode in the EPM, two-way ANOVA factoring drug dose and stress exposure revealed no effect of drug dose x stress exposure interaction ($F_{(3, 76)} = 1.086$; $p = 0.3604$, *ns*) and effect of stress exposure ($F_{(1, 76)} = 0.006470$, $p = 0.9361$, *ns*), but a significant effect of drug dose ($F_{(3, 76)} = 3.960$, $p = 0.0111$, $^{*}p < 0.05$; Fig. Ch). Post hoc Holm-Sidak's multiple comparisons test revealed a significant increase in the start of the first freezing episode in the EPM at the 10 mg/kg dose of celecoxib compared to the vehicle treatment only under basal (no stress) conditions ($^{*}p < 0.05$, $t = 1.874$, df = 76).

Also, LM-4131 at a dose of 10 mg/kg did not affect the anhedonic nature of the mice in the novel cage environment of the NIFS assay. There were no changes in the amount of the palatable shake consumed under basal (no stress) (unpaired *t* test: $p = 0.2186$, *ns*, $t = 1.275$, df = 18, LM-4131 vs. vehicle; see APPENDIX Fig. Ba (right panel)) or acute footshock stress (unpaired *t* test: $p = 0.3421$, *ns*, $t = 0.9671$, df = 27, LM-4131 vs. vehicle; see APPENDIX Fig. Bb (right panel)) conditions between vehicle and LM-4131 treatment groups.

Next, we determined if the anxiolytic potential of LM-4131 could be observed also in juvenile (5-7 weeks of age) ICR male mice subjected to no stress or electric footshock stress over 5 days. According to the cumulative frequency distribution percentile plot of juvenile male mice feeding in the NIFS assay (Fig. 5e (left panel)), 100% of vehicle-treated mice had a feeding latency

≤ 510 s, 100% of LM-4131-treated mice had a feeding latency ≤ 465 s, and 100% of LMX-treated mice had a feeding latency ≤ 165 s in the novel cage environment under basal (no stress) conditions. A Kolmogorov-Smirnov test of these findings revealed a significant difference only between the substrate-selective COX-2 inhibitor treatment group, LMX, and the vehicle treatment group (Kolmogorov-Smirnov test: $p > 0.9999$, *ns*, LM-4131 at 10 mg/kg vs. vehicle; $p = 0.0253$, $^{*}p < 0.05$, LMX at 1 mg/kg vs. vehicle; Fig. 5e (left panel)). There was no significant difference among the means for feeding latency between the COX-2 inhibitor treatment groups and the vehicle treatment group (one-way ANOVA: $F_{(2, 41)} = 0.7657$, $p = 0.4715$, *ns;* Holm-Sidak's multiple comparisons test: *ns*, $t = 0.1673$, df = 41, LM-4131 vs. vehicle; *ns*, $t = 1.062$, df = 41, LMX vs. vehicle; Fig. 5e (right panel)). When the juvenile male mice were subjected to chronic footshock stress and tested for anxiety-like behavior in the NIFS assay 8 hours after stress exposure, the juvenile male mice exhibited a greater decrease in feeding latency in the novel cage environment. Similar effects were observed in juvenile male mice administered by i.p. the SSCI, LMX. According to the cumulative frequency distribution percentile plot of stressed juvenile male mice feeding in the NIFS assay (Fig. 5f (left panel)), 100% of vehicle-treated mice had a feeding latency ≤ 1455 s, 100% of LM-4131-treated mice had a feeding latency ≤ 345 s, and 100% of LMX-treated mice had a feeding latency ≤ 495 s in the novel cage environment 8 hours after chronic stress exposure. A Kolmogorov-Smirnov test of these findings revealed a significant difference between all COX-2 inhibitor treatment groups, LM-4131 and LMX, and the vehicle treatment group (Kolmogorov-Smirnov test: $p < 0.0001$, $^{****}p < 0.0001$, LM-4131 at 10 mg/kg vs. vehicle; $p < 0.0001$, $^{****}p < 0.0001$, LMX at 1 mg/kg vs. vehicle; Fig. 5f (left panel)). The means for feeding latency between the COX-2 inhibitor treatment group, LM-4131, and the vehicle treatment group was significantly different (one-way ANOVA: $F_{(2, 52)} = 4.518$, $p = 0.0155$, $^{*}p <$

0.05*;* Holm-Sidak's multiple comparisons test: $p = 0.0114$, $^{*}p < 0.05$, $t = 2.883$, df = 52, LM-4131 vs. vehicle; $p = 0.0921$, *ns*, $t = 1.716$, df = 52, LMX vs. vehicle; Fig. 5f (right panel)).

Previous studies have suggested that increased CB_1R availability in humans that suffer from trauma-related disorders and animals subjected to stress paradigms may result from decreased stress-induced synaptic AEA levels. These studies also propose that basal AEA levels differ with regard to the age of an animal (e.g., aged animals have greater AEA levels than young animals)[198-200]. This could explain why our findings suggest that the SSCI, LM-4131, is more efficacious in reducing stress-induced anxiety and anhedonia in juvenile male mice as opposed to adult male mice and female mice. In addition, animal studies have noted sex differences in CB_1R regulation, with stress-induced upregulation of CB_1Rs seen mainly in limbic structures of female animals[201]. Moreover, since estradiol, the primary female sex hormone, has been suggested to not only alter emotionality in rodents but as well increase endocannabinoid signaling and AEA synthesis or release[202,203], the female mice may exhibit a less robust inverse relationship between brain AEA levels and stress-induced anxiety in the NIH assay in comparison with the male mice. Nevertheless, to gain an in-depth understanding of the mechanisms that govern stress-induced anxiety-like and anhedonic behaviors in male and female mice regardless of age, the availability of the receptors targeted by anandamide and anandamide levels in brain tissue should be examined before and after stress exposure.

The anxiolytic and hedonic potential of subchronic substrate-selective COX-2 inhibition

Since acute administration of the SSCIs, LM-4131 and LMX, exhibited anxiolytic potential in the NIFS assay, we wanted to determine if the same effect could be observed with subchronic i.p. administration of an SSCI. Thus, we administered by i.p. LMX daily for five days to juvenile male mice and tested them for anxiety-like behavior in the NIFS assay under basal and 8h after

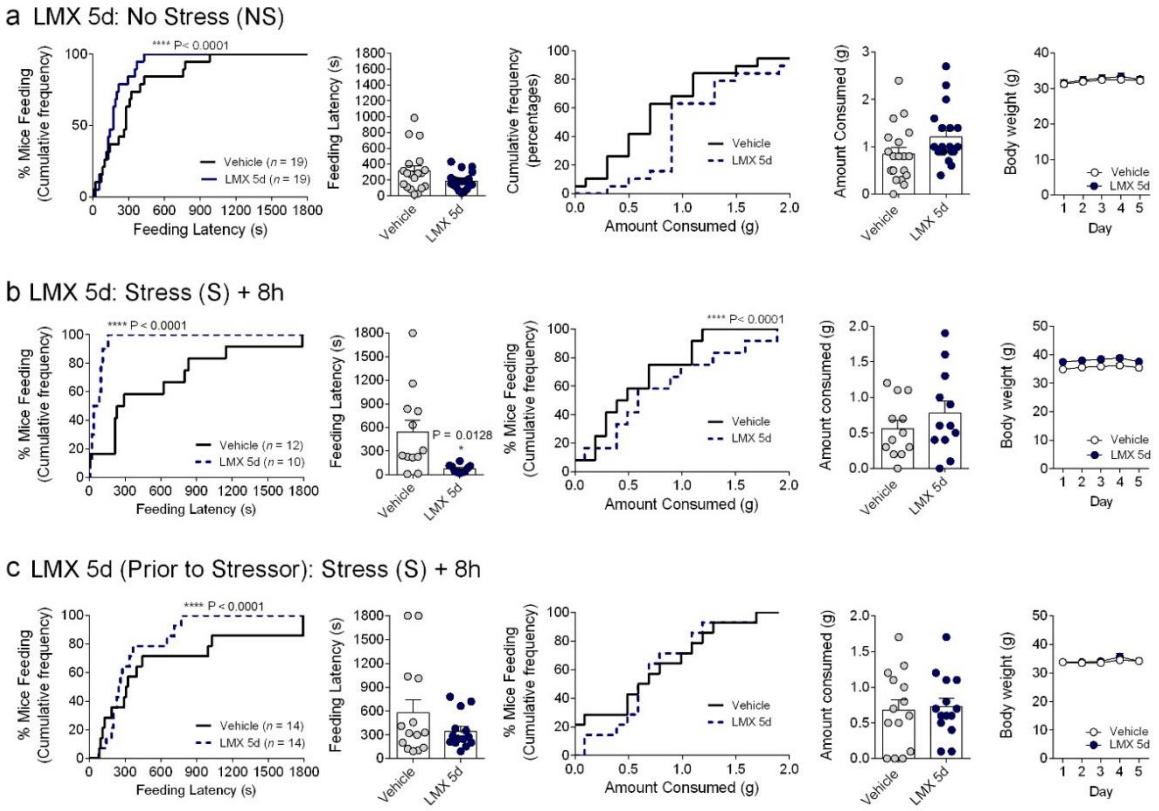

Figure 6. Anxiolytic and anti-hedonic effects of subchronic dose of COX-2 inhibitors in juvenile male mice. (**a**) Cumulative frequency of mice feeding, latency to feed, cumulative frequency of amount of palatable shake consumed, and total amount of shake consumption in novelty-induced feeding suppression (NIFS) test under non-stressful conditions (left to right). Body weight measured over five days of subchronic dosing of lumiracoxib or LMX (1 mg/kg). (**b,c**) Cumulative frequency of mice feeding, latency to feed, cumulative frequency of amount of palatable shake consumed, and total amount of shake consumption in novelty-induced feeding suppression (NIFS) test under acute stress conditions (six tone-shock pairings/day over five days) (left to right). Body weight measured over five days of subchronic dosing of lumiracoxib (1 mg/kg). Data are shown as the mean ± s.e.m. NS = no stress, S = stress (e.g., stress exposure in the form of an electric footshock administered 8h prior to testing), *P < 0.05, ****P < 0.0001 (LMX compared to vehicle). Statistical significance was calculated by two-tailed unpaired Student's *t*-test or Kolmogorov-Smirnov test (only for frequency plots).

acute footshock stress exposure. We chose to use LMX instead of LM-4131 since LM-4131 has less metabolic stability than LMX. Thus, the elimination half-life for LMX (e.g., 4-8 h) is longer than that for LM-4131 (e.g., 2-3 h)[125,204-208]. Only after exposure to a stressful external stimulus, the mice demonstrated a reduction in feeding latency in the NIFS test (Fig. 7b). According to the cumulative frequency distribution percentile plot of juvenile male mice feeding in the NIFS assay (Fig. 6a (1st left panel)), 100% of vehicle-treated mice had a feeding latency ≤ 990 s and 100% of subchronic LMX-treated mice had a feeding latency ≤ 435 s in the novel cage environment under

basal (no stress) conditions. A Kolmogorov-Smirnov test of these findings revealed a significant difference between the subchronic LMX and the vehicle treatment groups (Kolmogorov-Smirnov test: $p > 0.0001$, ****$p > 0.0001$, subchronic LMX at 1 mg/kg vs. vehicle; Fig. 6a (1st left panel)). There was no significant difference among the means for feeding latency between the subchronic LMX and the vehicle treatment groups (unpaired *t* test: $p = 0.0628$, *ns*, $t = 1.920$, df = 36, subchronic LMX vs. vehicle; Fig. 6a (2nd left panel)). Subchronic LMX treatment caused no changes in anhedonia in the mice in the NIFS assay. According to the cumulative frequency distribution percentile plot of juvenile male mice feeding in the NIFS assay (Fig. 6a (1st middle panel)), 100% of vehicle-treated mice consumed ≤ 2.4 g of the palatable shake and 100% of subchronic LMX-treated mice consumed ≤ 2.8 g in the novel cage environment under basal (no stress) conditions. A Kolmogorov-Smirnov test of these findings revealed no difference between the subchronic LMX and vehicle treatment groups (Kolmogorov-Smirnov test: $p = 0.9251$, *ns*, subchronic LMX at 1 mg/kg vs. vehicle; Fig. 6a (1st middle panel)). There was no significant difference among the means for the amount of the palatable shake consumed between the COX-2 inhibitor treatment group and the vehicle treatment group (unpaired *t* test: $p = 0.0670$, *ns*, $t = 1.889$, df = 36, subchronic LMX vs. vehicle; Fig. 6a (2nd middle panel)). Also, these findings were not confounded by changes in body weight due to subchronic administration of the COX-2 inhibitor or stress and physical discomfort caused by multiple i.p. injections (Fig. 6a (right panel)).

When the juvenile male mice were subjected to acute footshock stress and tested for anxiety-like behavior in the NIFS assay 8 hours after stress exposure, the juvenile male mice treated with subchronic LMX exhibited a significant decrease in feeding latency in the novel cage environment compared to vehicle-treated mice. According to the cumulative frequency distribution percentile plot of stressed juvenile male mice feeding in the NIFS assay (Fig. 6b (1st

left panel)), 100% of vehicle-treated mice had a feeding latency ≤ 1800 s and 100% of subchronic LMX-treated mice had a feeding latency ≤ 165 s in the novel cage environment 8 hours after acute stress exposure (6 footshocks in 1 day). A Kolmogorov-Smirnov test of these findings revealed a significant difference between the subchronic LMX and the vehicle treatment groups (Kolmogorov-Smirnov test: $p < 0.0001$, ****$p < 0.0001$, subchronic LMX at 1 mg/kg vs. vehicle; Fig. 6b (1st left panel)). The means for feeding latency between the subchronic LMX and vehicle treatment groups was significantly different (unpaired *t* test: $p = 0.0128$, *$p < 0.05$, $t = 2.733$, df = 20, subchronic LMX vs. vehicle; Fig. 6b (2nd left panel)). Regarding the effect of subchronic LMX on anhedonic behavior in the stressed mice, the cumulative frequency distribution percentile plot of juvenile male mice feeding in the NIFS assay (Fig. 6b (1st middle panel)) demonstrated that 100% of vehicle-treated mice consumed ≤ 1.22 g of the palatable shake whereas 100% of subchronic LMX-treated mice consumed a greater amount of the shake (e.g., ≤ 1.90 g) in the novel cage environment 8 hours after acute footshock stress exposure. A Kolmogorov-Smirnov test of these findings revealed a significant difference between the subchronic LMX and vehicle treatment groups (Kolmogorov-Smirnov test: $p < 0.0001$, ****$p < 0.0001$, subchronic LMX at 1 mg/kg vs. vehicle; Fig. 6b (1st middle panel)). There was no significant difference among the means for the amount of the palatable shake consumed between the COX-2 inhibitor treatment group and the vehicle treatment group (unpaired *t* test: $p = 0.3014$, *ns*, $t = 1.058$, df = 22, subchronic LMX vs. vehicle; Fig. 6b (2nd middle panel)). Also, these results were not affected by changes in body weight caused by multiple i.p. drug injections or subchronic LMX dosing (Fig. 6b (right panel)).

Also, the subchronic administration of the SSCI, LMX, before stress exposure was not able to prevent stress-induced anxiety or stress-induced hedonic deficits 8h after acute stress exposure in the NIFS assay (Fig. 6c). According to the cumulative frequency distribution percentile plot of

juvenile male mice feeding in the NIFS assay (Fig. 6c (1st left panel)), 100% of vehicle-treated mice had a feeding latency ≤ 1800 s and 100% of subchronic LMX-treated mice had a feeding latency ≤ 780 s in the novel cage environment under stressed conditions. A Kolmogorov-Smirnov test of these findings revealed a significant difference between the subchronic LMX and the vehicle treatment groups (Kolmogorov-Smirnov test: $p < 0.0001$, ****$p < 0.0001$, LMX at 1 mg/kg vs. vehicle; Fig. 6c (1st left panel)). However, there was no significant difference among the means for feeding latency between the COX-2 inhibitor treatment group and the vehicle treatment group (unpaired *t* test: $p = 0.1754$, *ns*, $t = 1.393$, df = 26, subchronic LMX vs. vehicle; Fig. 6c (2nd left panel)). Subchronic LMX treatment before acute stress exposure caused no changes in anhedonia in the mice in the NIFS assay. According to the cumulative frequency distribution percentile plot of juvenile male mice feeding in the NIFS assay (Fig. 6c (1st middle panel)), 100% of vehicle-treated and subchronic LMX-treated mice consumed the same amount of the palatable shake (e.g., ≤ 1.70 g) in the novel cage environment under acute stress conditions. Differences in the percentage of mice that consumed the palatable shake between the treatment groups occurred at lower amounts of the shake consumed. For instance, 29% of vehicle-treated mice consumed ≤ 0.10 g of the shake whereas 29% of subchronic LMX-treated mice consumed ≤ 0.50 g of the shake. A Kolmogorov-Smirnov test of these findings revealed a significant difference between the subchronic LMX and vehicle treatment groups (Kolmogorov-Smirnov test: $p = 0.0310$, *$p < 0.05$, subchronic LMX at 1 mg/kg vs. vehicle; Fig. 6c (1st middle panel)). There was no significant difference among the means for the amount of the palatable shake consumed between the COX-2 inhibitor treatment group and the vehicle treatment group (unpaired *t* test: $p = 0.7891$, *ns*, $t = 0.2702$, df = 26, subchronic LMX vs. vehicle; Fig. 6c (2nd middle panel)). Also, these results were not confounded by changes in body weight between the drug treatments (Fig. 6c (right panel)).

Effects of substrate-selective COX-2 inhibition on sensorimotor gating and locomotor activity

To ensure that the anxiolytic potential of the SSCIs was not an artifact or confounded by deficits in sensorimotor gating or increased locomotor activity in the mice when performing the NIFS assay or other behavioral tests of anxiety, we examined the effects of the SSCIs on sensorimotor function and locomotion in juvenile ICR male mice. We found no changes in sensorimotor function caused by the COX-2 inhibitors under basal (no stress) or acute stress conditions in the mice. With respect to percentage prepulse inhibition (%PPI) between the vehicle and COX-2 inhibitor treatment groups, two-way ANOVA factoring drug dose and stress exposure revealed no effect of drug dose x stress exposure interaction ($F_{(3, 118)} = 0.7896$; $p = 0.5020$, *ns*) and stress exposure ($F_{(1, 118)} = 0.9218$, $p = 0.3390$, *ns*), but a significant effect of drug dose ($F_{(3, 118)} = 3.086$, $p = 0.0299$, $^{*}p < 0.05$; Fig. 7a) under basal conditions. Post hoc Holm-Sidak's multiple comparisons test revealed no significant increase or decrease in %PPI at any dose of the COX-2 inhibitors compared to the vehicle treatment under control (no stress) conditions. Moreover, none of the COX-2 inhibitors compared to vehicle affected average startle responses in the mice under non stressed conditions or 8 hours after acute footshock stress exposure. Two-way ANOVA factoring drug dose and the prepulse intensity revealed no effect of drug dose x prepulse intensity interaction ($F_{(3, 174)} = 1.520$; $p = 0.2111$, *ns*) and drug dose ($F_{(3, 174)} = 0.2578$, $p = 0.8557$, *ns*), but a significant effect of prepulse intensity ($F_{(1, 174)} = 195.4$, $p < 0.0001$, $^{****}p < 0.0001$; Fig. 7b) under basal conditions. Two-way ANOVA factoring drug dose and stress exposure revealed no effect of drug dose x stress exposure interaction ($F_{(3, 64)} = 0.6285$; $p = 0.5993$, *ns*) and drug dose ($F_{(3, 64)} = 0.2440$, $p = 0.8553$, *ns*), but a significant effect of prepulse intensity ($F_{(1, 64)} = 143.6$, $p < 0.0001$, $^{****}p < 0.0001$; Fig. 7c) under acute stress conditions.

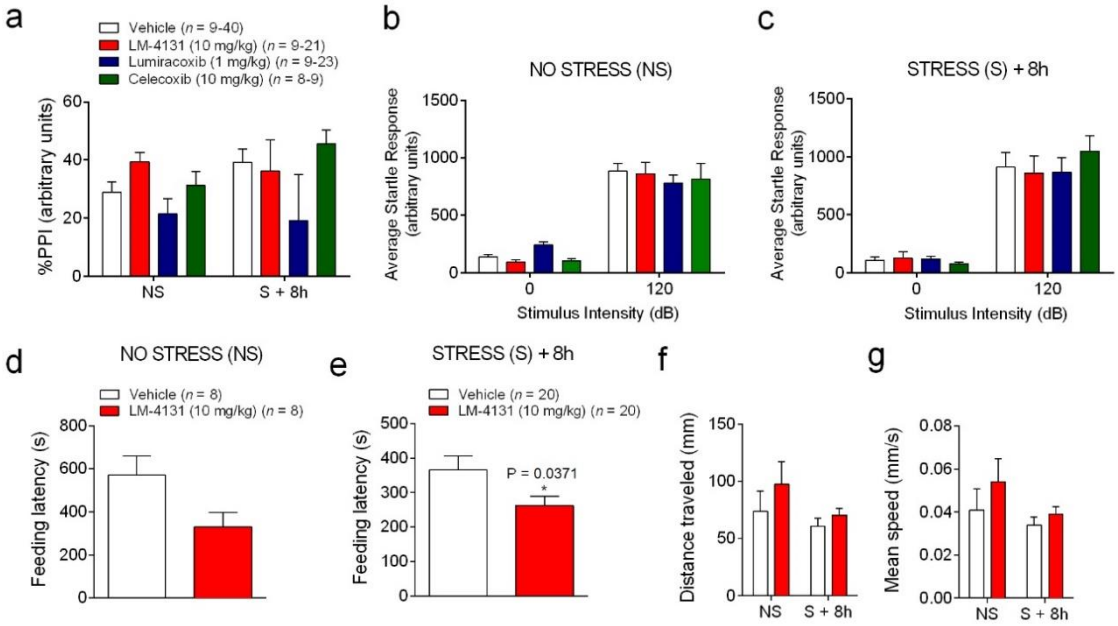

Figure 7. Sensorimotor effects of COX-2 inhibitors. (**a**) Percentage of composite prepulse inhibition (PPI) score collapsed across prepulse intensities under non-stressful and acute stress conditions. (**b, c**) Mean startle behavioral responses under non-stressful and acute stress conditions. (**d, e**) Latency to feed behavior in novelty-induced feeding suppression (NIFS) test using rat cages under non-stressful and acute stress conditions. (**f, g**) Distance traveled and mean speed in the rat cages during the NIFS test. Data are shown as the mean ± s.e.m. NS = no stress, S = stress (e.g., stress exposure in the form of an electric footshock administered 8h prior to testing), *P < 0.05 (LM-4131 compared to vehicle). Statistical significance was calculated by two-tailed unpaired Student's *t*-test or two-way ANOVA with post hoc Holm-Sidak's multiple comparisons test.

To determine if the effect of the COX-2 inhibitors on feeding latency was not due to increased movement or average speed in the novel cage while undergoing testing in the NIFS assay, we replaced the Allentown mouse cages with larger rat cages in the NIFS assay and tested the mice for anxiety-like behavior. We first ensured that the modifications made to the NIFS assay did not affect the anxiolytic potential of the COX-2 inhibitors observed previously in the original NIFS set up. We found a trending decrease in feeding latency (unpaired *t* test: $p = 0.0525$, *ns*, $t = 2.119$, df = 14, LM-4131 vs. vehicle; Fig. 7d) in mice treated with LM-4131 under control (no stress) conditions and a significant decrease in feeding latency (unpaired *t* test: $p = 0.0371$, $*p < 0.05$, $t = 2.161$, df = 38, LM-4131 vs. vehicle; Fig. 7e) in mice treated with LM-4131 8 hours after exposure to acute footshock stress. In addition, LM-4131 treated mice compared to vehicle treated

mice did not exhibit any signs of hyperactivity or increased average speed in the modified NIFS assay. Two-way ANOVA factoring drug dose and stress exposure revealed no effect of drug dose x stress exposure interaction ($F_{(1, 32)} = 0.3073$; $p = 0.5832$, *ns*), stress exposure ($F_{(1, 32)} = 2.458$, $p = 0.1267$, *ns*), or drug dose ($F_{(1, 32)} = 1.729$, $p = 0.1979$, *ns*; Fig. 7f) under basal conditions. Two-way ANOVA factoring drug dose and stress exposure also revealed no effect of drug dose x stress exposure interaction ($F_{(1, 32)} = 0.3057$; $p = 0.5842$, *ns*), stress exposure ($F_{(1, 32)} = 2.432$, $p = 0.1287$, *ns*), or drug dose ($F_{(1, 32)} = 1.664$, $p = 0.2063$, *ns* 5; Fig. 7g) under acute stress conditions. Thus, the reduction in the amount of time to approach and take the first sip of the palatable shake is not due to LM-4131 increasing the locomotion or speed of the mice under basal or stressed conditions.

To validate these findings, we examined the effect of the COX-2 inhibitors on locomotor activity in the open field assay under all stress exposures. We found no changes in locomotor activity caused by the COX-2 inhibitors under control (non-stressed), acute stress, or chronic stress conditions in the mice. One-way ANOVA did not reveal any effect of LM-4131 at 10 mg/kg, LMX at 1 mg/kg, or celecoxib at 10 mg/kg on total ambulatory or horizontal distance traveled in the open field test under basal conditions ($F_{(3, 46)} = 2.566$, $p = 0.0660$, ns; Holm-Sidak's multiple comparisons test: *ns*, $t = 0.2944$, df = 46, LM-4131 vs. vehicle; *ns*, $t = 2.249$, df = 46, LMX vs. vehicle; *ns*, $t = 2.052$, df = 46, celecoxib vs. vehicle; Fig. 8a), 8 hours after acute stress exposure ($F_{(3, 33)} = 0.9202$, $p = 0.4418$, ns; Holm-Sidak's multiple comparisons test: *ns*, $t = 0.03829$, df = 33, LM-4131 vs. vehicle; *ns*, $t = 0.9307$, df = 33, LMX vs. vehicle; *ns*, $t = 1.372$, df = 33, celecoxib vs. vehicle; Fig. 8a), and 8 hours after chronic stress exposure ($F_{(3, 34)} = 1.416$, $p = 0.2551$, ns; Holm-Sidak's multiple comparisons test: *ns*, $t = 0.1432$, df = 34, LM-4131 vs. vehicle; *ns*, $t = 0.5044$, df = 34, LMX vs. vehicle; *ns*, $t = 1.848$, df = 34, celecoxib vs. vehicle; Fig. 8a).

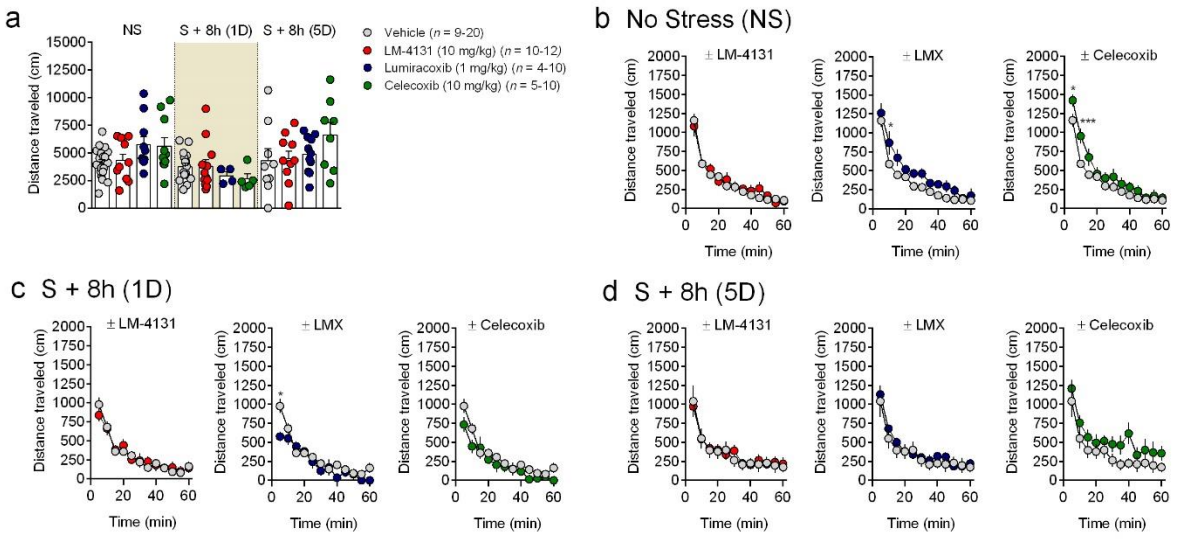

Figure 8. Effects of COX-2 Inhibitors on locomotor activity in the novel-open field assay. (**a**) Effects of LM-4131, Lumiracoxib (LMX), and Celecoxib under no stress (control) or 8h after acute (1 day) or chronic (5 days) stress exposure on total distance travelled in the open-field assay. (**b-d**) Effects of LM-4131, LMX, and Celecoxib compared to vehicle under no stress conditions (**b**) and 8h after acute stress exposure (**c**) or chronic stress exposure (**d**) on total distance travelled in the open-field assay over 60 minutes (data point/5 min). Data are shown as the mean ± s.e.m. NS = no stress, S = stress (e.g., stress exposure in the form of an electric footshock administered 8h prior to testing). Statistical significance was calculated by one-way or two-way ANOVA with post hoc Holm-Sidak's multiple comparisons test and time x treatment interaction as a source of variation between groups.

Concerning the effect of LM-4131 on distance traveled over all 5 min bins (60 min), two-way ANOVA factoring drug dose and time revealed no effect of drug dose ($F_{(11, 336)} = 0.5604$, $p = 0.4546$, *ns*) and drug dose x time interaction ($F_{(11, 336)} = 0.5480$; $p = 0.8697$, *ns*), but a significant effect of time ($F_{(11, 336)} = 44.17$, ****$p < 0.0001$; Fig. 8b) under no stress exposure. In regard to the effect of LMX on distance traveled over all 5 min bins (60 min), two-way ANOVA factoring drug dose and time revealed no effect of drug dose x time interaction ($F_{(11, 335)} = 0.5972$; $p = 0.8311$, *ns*), but a significant effect of drug dose ($F_{(1, 336)} = 27.61$, ****$p < 0.0001$) and time ($F_{(11, 336)} = 45.42$, ****$p < 0.0001$; Fig. 8b) under no stress exposure. Post hoc Holm-Sidak's multiple comparisons test revealed a slight increase in distance traveled during the 10 min bin of the open field assay at the 1 mg/kg dose of LMX compared to the vehicle treatment under basal conditions (*$p < 0.05$, $t = 3.042$, df = 336, LMX vs. vehicle; Fig. 8b). Pertaining to the effect of celecoxib on distance traveled over all 5 min bins (60 min), two-way ANOVA factoring drug dose and time

revealed no effect of dose x time interaction ($F_{(11, 336)} = 1.372$; $p = 0.1846$, *ns*), but a significant effect of drug dose ($F_{(1, 336)} = 23.62$, ****$p < 0.0001$) and time ($F_{(11, 336)} = 56.26$, ****$p < 0.0001$; Fig. 8b) under no stress exposure. Post hoc Holm-Sidak's multiple comparisons test revealed an increase in distance traveled during the first 5 min (*$p < 0.05$, $t = 2.884$, df = 336, celecoxib vs. vehicle; Fig. 8b) and 10 min (****$p < 0.0001$, $t = 4.025$, df = 336, celecoxib vs. vehicle; Fig. 8b) bins of the open field assay at the 10 mg/kg dose of celecoxib compared to the vehicle treatment under basal conditions.

With respect to the effect of LM-4131 on distance traveled over all 5 min bins (60 min), two-way ANOVA factoring drug dose and time revealed no effect of drug dose ($F_{(1, 312)} = 0.005497$, $p = 0.9409$, *ns*) and drug dose x time interaction ($F_{(11, 312)} = 0.4555$; $p = 0.9291$, *ns*), but a significant effect of time ($F_{(11, 312)} = 29.67$, ****$p < 0.0001$; Fig. 8c) 8 hours after acute stress exposure. With regard to the effect of LMX on distance traveled over all 5 min bins (60 min), two-way ANOVA factoring drug dose and time revealed no effect of drug dose x time interaction ($F_{(11, 204)} = 0.8993$; $p = 0.5420$, *ns*), but a significant effect of drug dose ($F_{(1, 204)} = 4.909$, $p = 0.0278$, *$p < 0.05$) and time ($F_{(11, 204)} = 12.15$, ****$p < 0.0001$; Fig. 8c) 8 hours after acute stress exposure. Post hoc Holm-Sidak's multiple comparisons test revealed a decrease in distance traveled during the first 5 min bin (*$p < 0.05$, $t = 3.010$, df = 204, LMX vs. vehicle; Fig. 8c) of the open field assay at the 1 mg/kg dose of LMX compared to the vehicle treatment under acute stress conditions. In connection with the effect of celecoxib on distance traveled over all 5 min bins (60 min), two-way ANOVA factoring drug dose and time revealed no effect of drug dose x time interaction ($F_{(11, 228)} = 0.7039$; $p = 0.7343$, *ns*), but a significant effect of drug dose ($F_{(1, 228)} = 8.749$, $p = 0.0034$, **$p < 0.01$) and time ($F_{(11, 228)} = 19.68$, ****$p < 0.0001$; Fig. 8c) 8 hours after acute stress exposure. Post hoc Holm-Sidak's multiple comparisons test revealed no changes in distance

traveled during all 5 min bins over a 60 min time frame of the open field assay at the 10 mg/kg dose of celecoxib compared to the vehicle treatment under acute stress conditions.

Pertaining to the effect of LM-4131 and LMX on distance traveled over all 5 min bins (60 min), two-way ANOVA factoring drug dose and time revealed no effect of drug dose (LM-4131: $F_{(1, 204)} = 0.1097$, $p = 0.7408$, *ns*; LMX: $F_{(1, 216)} = 1.603$, $p = 0.2069$, *ns*) and drug dose x time interaction (LM-4131: $F_{(11, 204)} = 0.1661$; $p = 0.9989$, *ns*; LMX: $F_{(11, 216)} = 0.2508$, $p = 0.9931$, *ns*), but a significant effect of time (LM-4131: $F_{(11, 204)} = 12.43$, ****$p < 0.0001$; LMX: $F_{(11, 216)} = 17.48$, ****$p < 0.0001$; Fig. 8d) 8 hours after chronic stress exposure. As regards to the effect of celecoxib on distance traveled over all 5 min bins (60 min), two-way ANOVA factoring drug dose and time revealed no effect of drug dose x time interaction ($F_{(11, 180)} = 0.2240$; $p = 0.9958$, *ns*), but a significant effect of drug dose ($F_{(1, 180)} = 16.76$, ****$p < 0.0001$) and time ($F_{(11, 180)} = 8.951$, ****$p < 0.0001$; Fig. 8d) 8 hours after chronic stress exposure. Post hoc Holm-Sidak's multiple comparisons test revealed no changes in distance traveled during all 5 min bins over a 60 min time frame of the open field assay at the 10 mg/kg dose of celecoxib compared to the vehicle treatment under chronic stress conditions.

Effects of substrate-selective COX-2 inhibition on neurotransmitter levels

Since cannabinoid receptor agonists or endocannabinoids, such as AEA, can affect synaptic neurotransmission when activating or inhibiting their receptor or ion channel targets[209,210], we examined the effects of the SSCI, LM-4131, on monoamine content in three brain regions known to modulate anxiety-like behaviors and fear responses in animals and humans (e.g., the amygdala, the prefrontal cortex, and the hippocampus). We found that our acute stress paradigm (8h post-footshock stress) compared to control (no stress) significantly increased dopamine (unpaired *t* test: $p = 0.0051$, **$p < 0.01$, $t = 3.168$, df = 19; Fig. 8a), noradrenaline (unpaired *t* test: $p = 0.0486$, *p

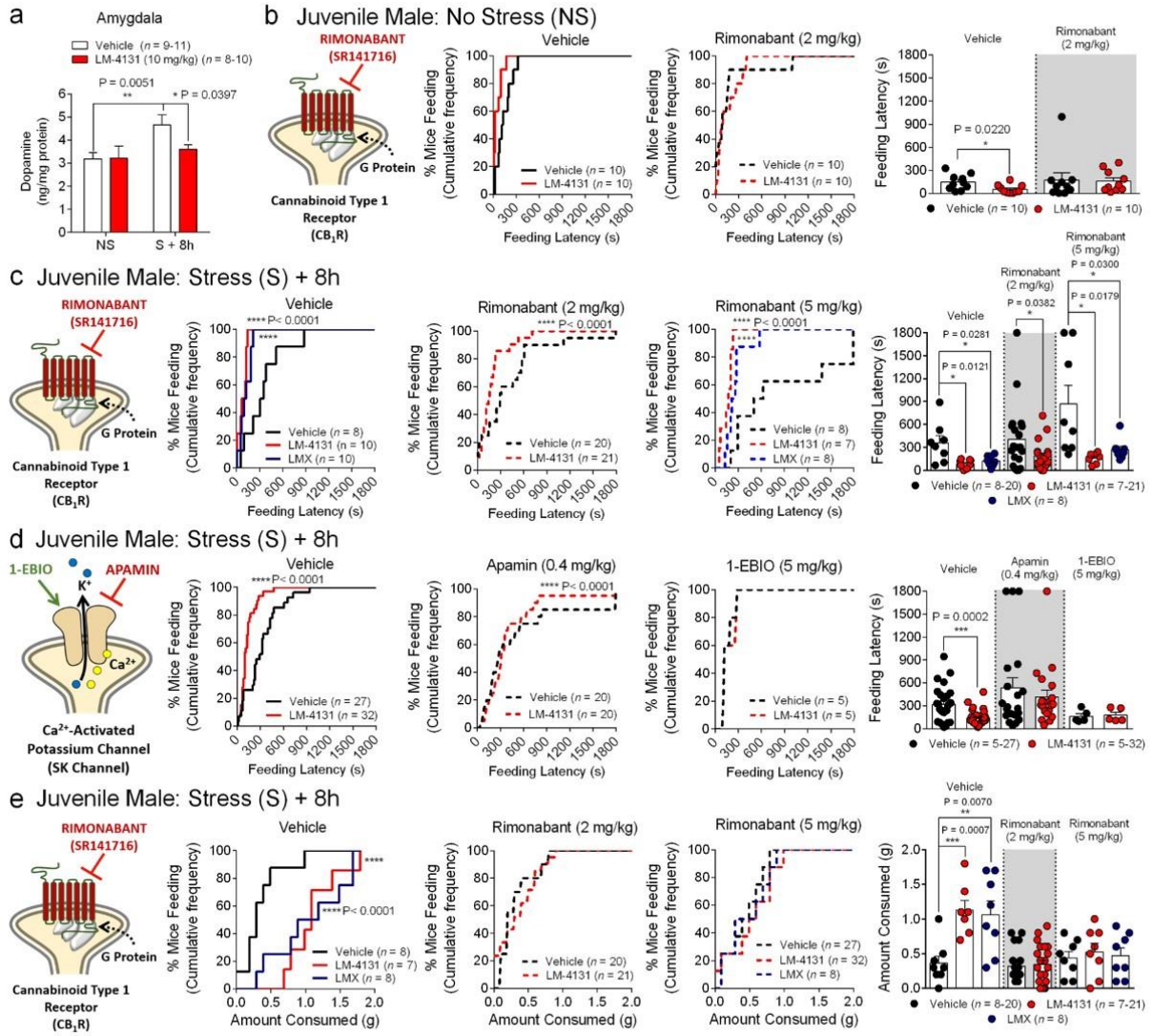

Figure 9. Receptor mechanisms mediating anxiolytic effects of COX-2 inhibition. (**a**) Dopamine levels in amygdala tissue sections determined by HPLC with electrochemical or fluorescent detection**.** (**b**) Cumulative feeding latency distribution curves for vehicle and LM-4131 treated mice in the presence of vehicle, Rimonabant (2 mg/kg) or Rimonabant (5 mg/kg) co-treatment. Mean ± S.E.M feeding latency for each group tested under non-stressful conditions. (**c**) Cumulative feeding latency distribution curves for vehicle, LM-4131, and Lumiracoxib (LMX) treated mice in the presence of vehicle, Rimonabant (2 mg/kg), or Rimonabant (5 mg/kg) co-treatment. Effects of the CB1 receptor antagonist Rimonabant (2 mg/kg and 5 mg/kg) on LM-4131- and LMX-induced reductions in feeding latency tested 8hours after stress exposure. Mean ± S.E.M feeding latency for each group tested 8h after stress exposure. (**d**) Cumulative feeding latency distribution curves for vehicle and LM-4131 treated mice in the presence of vehicle, Apamin (0.4 mg/kg), or 1-EBIO (5 mg/kg) co-treatment. Effects of the SK channel inhibitor Apamin (0.4 mg/kg), and SK channel activator 1-EBIO (5 mg/kg), on LM-4131-induced reductions in feeding latency tested 8h after stress exposure. Mean ± S.E.M feeding latency for each group tested 8h after stress exposure. (**e**) Cumulative food consumption distribution curves for vehicle, LM-4131, and LMX treated mice in the presence of vehicle or Rimonabant (2 mg/kg and 5 mg/kg) co-treatment. Effects of Rimonabant (2 mg/kg and 5 mg/kg) on LM-4131- or LMX-induced increases in shake consumption tested 8h after stress exposure. Mean ± S.E.M amount of shake consumed for each group tested 8h after stress exposure. Data are shown as the mean ± s.e.m. *P < 0.05, **P < 0.01, ***P<0.001, ****P<0.0001. Statistical significance was calculated by two-tailed unpaired Student's *t*-test or Kolmogorov-Smirnov test (only for frequency plots).

< 0.05, t = 2.100, df = 20; Fig. 8b), and serotonin (unpaired t test: p = 0.0011, **p < 0.01, t = 3.791, df = 20; Fig. 8c) levels in amygdala tissue sections. LM-4131 only reversed stress-induced increases in dopamine levels in the amygdala tissues sections back to control levels (unpaired t test: p = 0.0397, *p < 0.05, t = 2.228, df = 17, LM-4131 (acute S + 8h) vs. vehicle (acute S + 8h); unpaired t test: p = 0.1892, *ns*, t = 1.359, df = 20, LM-4131 (acute S + 8h) vs. vehicle (no stress); Fig. 8a). LM-4131 at a dose of 10 mg/kg did not alter levels of dopamine under chronic stress conditions (unpaired t test: p = 0.1168, *ns*, t = 1.643, df = 19, LM-4131 vs. vehicle; see APPENDIX Fig. Da). The SSCI was not able to affect the levels of other monoamines, such as noradrenaline and serotonin, under all stress exposures in the amygdala (Fig. Db, c) and the hippocampus (Fig. Dh, i). Also, there was no effect of LM-4131 on dopamine levels in the prefrontal cortex or the hippocampus (see APPENDIX Fig. Dd, g). In addition, LM-4131 did not affect the levels of the dopamine metabolite, 3,4-dihydroxyphenylacetic acid (DOPAC), the serotonin metabolite, 5-hydroxyindoleacetic acid (5-HIAA), or the DOPAC metabolite, homovanillic acid (HVA) levels in the amygdala (see APPENDIX Fig. Ea-c), even though our acute stress paradigm increased DOPAC levels in the amygdala (unpaired t test: p = 0.0051, **p < 0.01, t = 3.168, df = 19; Fig. Ea). In the prefrontal cortex, LM-4131 significantly decreased serotonin levels under basal conditions (unpaired t test: p = 0.0004, ***p < 0.001, t = 4.360, df = 18, LM-4131 at 10 mg/kg vs. vehicle; see APPENDIX Fig. Df). Our chronic stress paradigm also decreased serotonin levels in the prefrontal cortex (unpaired t test: p = 0.0015, **p<0.01, t = 3.725, df = 18, vehicle (no stress) vs. vehicle (chronic S + 8h); Fig. Df). LM-4131 reversed these effects and increased serotonin levels back to control levels 8 hours after 5 days of footshock stress (unpaired t test: p = 0.0225, *p < 0.05, t = 2.497, df = 18, LM-4131 (chronic S + 8h) vs. vehicle (chronic S + 8h); unpaired t test: p = 0.1672, *ns*, t = 1.429, df = 22, LM-4131 (chronic S + 8h) vs. vehicle (no stress); Fig. Df).

Our findings are consistent with previous studies that stress exposure can increase dopamine levels and its metabolism and decrease serotonin levels in the brain[211-213]. Interestingly, the SSCI, LM-4131, was able to restore these changes in neurotransmitter levels back to non-stressed or control levels. What remains unclear is whether or not these changes in neurotransmitter levels as a consequence of stress exposure directly correlates to anxiogenic behaviors in animals even though previous studies have suggested that serotonin and dopamine receptors can modulate anxiety-like behavior in animals[214-216].

Receptor-mediated mechanisms of SSCI on stress-induced anxiety and anhedonia

We have previously shown that under basal conditions SSCIs result in increased AEA levels in the brain and reduced anxiety-like behaviors in juvenile male ICR mice that were assessed for anxious behavior with the open field assay and the light-dark box. These effects were removed when the mice were co-administered by i.p. injection the SSCI, LM-4131 (10 mg/kg), and the CB_1R antagonist, rimonabant. These studies suggested that increased AEA levels and anxiolytic behaviors as a result of COX-2 inhibition was cannabinoid-receptor mediated[125]. Thus, we assumed that SSCIs can reduce anxiety-like behaviors in mice subjected to acute and chronic traumatic stress through a cannabinoid-receptor mediated mechanism. In order to examine this hypothesis, we subjected the same acute and chronic stress paradigms mentioned previously to juvenile ICR mice of both sexes and tested the mice for anxiety-like behavior in the NIH test. Before testing, we treated different cohorts of mice with either vehicle, LM-4131 (10 mg/kg), the CB_1R antagonist, rimonabant (2 mg/kg or 5 mg/kg), or both LM-4131 and rimonabant. We observed that the anxiolytic effects of the SSCI, LM-4131, is CB_1R-mediated under basal conditions. According to the cumulative frequency distribution percentile plots of mice feeding in the NIH test under basal (no stress) conditions (Fig. 9b (2 left panels)), 100% of vehicle-treated

mice had a feeding latency ≤ 327 s, 100% of LM-4131-treated mice had a feeding latency ≤ 176 s, 100% of rimonabant-treated mice had a feeding latency ≤ 998 s, and 100% of LM-4131 and rimonabant co-treated mice had a feeding latency ≤ 401 s in the novel cage environment. An independent samples (unpaired) *t* test revealed a significant difference between the vehicle and LM-4131 treatment groups, $t(18) = 2.507$; $p = 0.0220$, $^*p < 0.05$. The sample means are displayed in Figure 9b (right panel), which shows that the mice treated with LM-4131 (10 mg/kg) scored significantly lesser on feeding latency than did the mice treated with vehicle (for LM-4131 treatment group, means ± s.e.m. = 55.40 ± 17.88, $N = 10$; for vehicle treatment group, means ± s.e.m. = 146.7 ± 31.73, $N = 10$). An independent samples *t* test also revealed no significant difference between the vehicle treatment group and LM-4131 and rimonabant co-treatment group ($t(18) = 0.2215$; $p = 0.8272$, *ns*) and between the rimonabant treatment group and the rimonabant and rimonabant and LM-4131 treatment group ($t(18) = 0.1653$; $p = 0.8705$, *ns*). The sample means in Figure 9b (right panel) show that the vehicle-treated mice demonstrated scores on feeding latency similar to mice co-treated with rimonabant and LM-4131 (for vehicle treatment group, means ± s.e.m. = 146.7 ± 31.73, $N = 10$; for LM-4131 and rimonabant co-treatment group, means ± s.e.m. = 158.7 ± 43.92, $N = 10$). It also shows that the rimonabant-treated mice demonstrated scores on feeding latency similar to mice co-treated with rimonabant and LM-4131 (for rimonabant treatment group, means ± s.e.m. = 175.8 ± 93.64, $N = 10$; for LM-4131 and rimonabant co-treatment group, means ± s.e.m. = 158.7 ± 43.92, $N = 10$).

We found that the anxiolytic effects of the SSCIs, LM-4131 and LMX, was non-CB_1R-mediated under acute stress conditions. According to the cumulative frequency distribution percentile plots of mice feeding in the NIH test 8h after exposure to acute electric footshock stress (Fig. 9c (2 left panels)), 100% of vehicle-treated mice had a feeding latency ≤ 890 s, 100% of LM-

4131-treated mice had a feeding latency ≤ 150 s, 100% of LMX-treated mice had a feeding latency ≤ 221 s, 100% of rimonabant-treated mice had a feeding latency ≤ 1800 s, and 100% of LM-4131 and rimonabant co-treated mice had a feeding latency ≤ 716 s in the novel cage environment. A Kolmogorov-Smirnov test of the feeding latency data presented in the percentile plots revealed a significant difference between the cumulative frequency distribution for the LM-4131 or LMX treatment group and the cumulative frequency distribution for the vehicle treatment group (D = 0.4050, ****p < 0.0001, LM-4131 at 10 mg/kg vs. vehicle; D = 0.3636, ****p < 0.0001, LMX at 1 mg/kg vs. vehicle) and a significant difference between the cumulative frequency distribution for the rimonabant treatment group and the rimonabant and LM-4131 co-treatment group (D = 0.6942, ****p < 0.0001, rimonabant + LM-4131 vs. rimonabant at 2 mg/kg). An independent samples (unpaired) t test revealed a significant difference between the vehicle and LM-4131 or LMX treatment group (t (14) = 2.879; p = 0.0121, *p < 0.05, LM-4131 vs. vehicle; t (14) = 2.448, p = 0.0281, *p < 0.05, LMX vs. vehicle). The sample means are displayed in Figure 9b (right panel), which shows that the mice treated with LM-4131 (10 mg/kg) or LMX (1 mg/kg) scored significantly lesser on feeding latency than did the mice treated with vehicle (for LM-4131 treatment group, means ± s.e.m. = 87.00 ± 19.99, N = 8; for LMX treatment group, means ± s.e.m. = 125.0 ± 25.10, N = 8; for vehicle treatment group, means ± s.e.m. = 360.6 ± 92.91, N = 8). An independent samples t test also revealed a significant difference between the rimonabant treatment group and the rimonabant and rimonabant and LM-4131 treatment group (t (39) = 2.146; p = 0.0382, *p < 0.05), suggesting the CB_1R antagonist, rimonabant was not able to block the anxiolytic effects of LM-4131. The sample means in Figure 9b (right panel) show that the rimonabant-treated mice demonstrated scores on feeding latency which were significantly greater than those shown by mice co-treated with rimonabant and LM-4131 (for rimonabant treatment

group, means ± s.e.m. = 408.0 ± 96.96, $N = 20$; for LM-4131 and rimonabant co-treatment group, means ± s.e.m. = 188.0 ± 38.71, $N = 21$). We have previously shown that anxiety-like behavior exhibited by mice in the novel cage environment of the NIH test is dependent upon the dose of the CB_1R antagonist, rimonabant[115]. Thus, we increased our rimonabant dose from 2 mg/kg to 5 mg/kg and performed the NIH test in another cohort of juvenile male mice to determine whether or not the anxiolytic action of SSCIs is CB_1R-mediated. This enabled us to ensure the rimonabant dose we used in our behavioral testing was sufficient enough to produce anxiogenic effects in the mildly stressful, novel cage environment of the NIH test and block the anxiolytic effects of the SSCIs if they involve the CB_1R. Even treating the mice with a higher dose of rimonabant still did not block the anxiolytic effects of the SSCI, LM-4131, as well as LMX under acute stress conditions. According to the cumulative frequency distribution percentile plots of mice feeding in the NIH test 8h after exposure to acute electric footshock stress (Fig. 9c (3^{rd} left panel)), 100% of rimonabant-treated mice had a feeding latency ≤ 1800 s, 100% of LM-4131 and rimonabant co-treated mice had a feeding latency ≤ 242 s, and 100% of LMX and rimonabant co-treated mice had a feeding latency ≤ 584 s in the novel cage environment. A Kolmogorov-Smirnov test of the feeding latency data presented in the percentile plots revealed a significant difference between the cumulative frequency distribution for the rimonabant treatment group and the rimonabant and LMX or LM-4131 co-treatment group ($D = 0.8760$, $^{****}p < 0.0001$, rimonabant + LM-4131 vs. rimonabant at 5 mg/kg; $D = 0.8347$, $^{****}p < 0.0001$, rimonabant + LMX vs. rimonabant at 5 mg/kg). An independent samples t test also revealed a significant difference between the rimonabant treatment group and LM-4131 and rimonabant co-treatment group ($t\ (13) = 2.707$; $p = 0.0179$, $^{*}p < 0.05$) and between the rimonabant treatment group and the rimonabant and rimonabant and LMX treatment group ($t\ (14) = 2.415$; $p = 0.0300$, $^{*}p < 0.05$). The sample means

in Figure 9b (right panel) show that the rimonabant-treated mice demonstrated scores on feeding latency which were greater than those shown by mice co-treated with rimonabant and LM-4131 (for rimonabant treatment group, means ± s.e.m. = 867.0 ± 242.0, N = 8; for LM-4131 and rimonabant co-treatment group, means ± s.e.m. = 160.3 ± 26.10, N = 7). It also shows that the rimonabant-treated mice demonstrated scores on feeding latency which were greater than those shown by mice co-treated with rimonabant and LMX (for rimonabant treatment group, means ± s.e.m. = 867.0 ± 242.0, N = 8; for LMX and rimonabant co-treatment group, means ± s.e.m. = 271.0 ± 48.48, N = 8).

Anandamide (AEA) is an agonist of both cannabinoid type 1 and 2 receptors as well as the transient receptor potential cation channel subfamily V member 1 (TRPV1) and can activate other targets besides the cannabinoid receptors, such as small conductance calcium-activated potassium (SK) channels[217-219]. Thus, we repeated the NIH test in juvenile male ICR mice to rule out the contribution of theses receptors or ion channels in the anxiolytic behaviors illustrated by the mice after stress exposure as a result of substrate-selective COX-2 inhibition. We treated the mice with a CB_2R antagonist, SR144528 (3 mg/kg), the TRPV1 antagonist, capsazepine (10 mg/kg), or the SK channel antagonist, apamin (0.4 mg/kg) and examined the anxiolytic potential of the SSCI, LM-4131, after acute and chronic stress exposure as to whether or not it can be mediated by other receptors or ion channels besides the CB_1R. We found that the SSCI, LM-4131, can reduce anxiety-like behaviors after acute stress exposure through a non-CB_1 receptor-mediated mechanism in male ICR mice, specifically SK channels. This finding is in accordance with a recent study that has suggested that SK channels can modulate anxiogenic behaviors in animals after stress exposure. In particular, Rau and others showed that SK channel activation in the amygdala can reduce stress-induced anxiety-like behavior in an animal model of chronic early-life

stress[220]. According to the cumulative frequency distribution percentile plots of mice feeding in the NIH test 8h after exposure to acute electric footshock stress (Fig. 9d (3 left panels)), 100% of vehicle-treated mice had a feeding latency ≤ 946 s, 100% of LM-4131-treated mice had a feeding latency ≤ 482 s, 100% of apamin-treated mice had a feeding latency ≤ 1800 s, and 100% of apamin and LM-4131 co-treated mice had a feeding latency ≤ 1800 s in the novel cage environment. A Kolmogorov-Smirnov test of the feeding latency data presented in the percentile plots revealed a significant difference between the cumulative frequency distribution for the LM-4131 treatment group and the cumulative frequency distribution for the vehicle treatment group (D = 0.3306, ****p < 0.0001, LM-4131 at 10 mg/kg vs. vehicle) and no difference between the cumulative frequency distribution for the apamin treatment group and the apamin and LM-4131 co-treatment group (D = 0.2000, p = 0.8186, *ns*, apamin + LM-4131 vs. apamin at 0.4 mg/kg). An independent samples (unpaired) t test revealed a significant difference between the vehicle and LM-4131 treatment group (t (57) = 4.055; p = 0.0002, ***p < 0.001, LM-4131 vs. vehicle). The sample means are displayed in Figure 9d (right panel), which shows that the mice treated with LM-4131 (10 mg/kg) scored significantly lesser on feeding latency than did the mice treated with vehicle (for LM-4131 treatment group, means ± s.e.m. = 140.9 ± 17.20, N = 32; for vehicle treatment group, means ± s.e.m. = 320.9 ± 43.87, N = 27). An independent samples t test also revealed no significant difference between the apamin treatment group and LM-4131 and apamin co-treatment group (t (38) = 0.7658; p = 0.4485, *ns*) and between the vehicle treatment group and LM-4131 and apamin co-treatment group (t (45) = 1.074; p = 0.2884, *ns*). The sample means in Figure 9d (right panel) show that the apamin-treated mice demonstrated scores on feeding latency similar to mice co-treated with apamin and LM-4131 (for apamin treatment group, means ± s.e.m. = 537.3 ± 131.2, N = 20; for LM-4131 and apamin co-treatment group, means ± s.e.m. = 417.2 ± 85.86, N = 20). It

also shows that the vehicle-treated mice demonstrated scores on feeding latency similar to mice co-treated with apamin and LM-4131 (for vehicle treatment group, means ± s.e.m. = 320.9 ± 43.87, N = 27; for LM-4131 and apamin co-treatment group, means ± s.e.m. = 417.2 ± 85.86, N = 20). To further validate that the anxiolytic action of the SSCI, LM-4131, is mediated through the SK channels once mice have been subjected to acute stress exposure, we treated another cohort of juvenile male ICR mice with the SK channel agonist, 1-EBIO, to determine if it could mimic the anxiolytic effects of LM-4131 in the NIH test. We found that activating the SK channels reduced stress-induced anxiety-like behavior in the mice similar to LM-4131. According to the cumulative frequency distribution percentile plots of mice feeding in the NIH test 8h after exposure to acute electric footshock stress (Fig. 9d (3rd left panels)), 100% of 1-EBIO-treated mice had a feeding latency ≤ 287 s and 100% of 1-EBIO and LM-4131 co-treated mice had a feeding latency ≤ 280 s in the novel cage environment. A Kolmogorov-Smirnov test of the feeding latency data presented in the percentile plots revealed no difference between the cumulative frequency distribution for the 1-EBIO treatment group and the 1-EBIO and LM-4131 co-treatment group (D = 0.04132, p > 0.9999, *ns*, 1-EBIO + LM-4131 vs. 1-EBIO at 5 mg/kg). An independent samples t test also revealed no significant difference between the 1-EBIO treatment group and LM-4131 and 1-EBIO co-treatment group (t (8) = 0.2948; p = 0.7756, *ns*) and between the LM-4131 treatment group and LM-4131 and 1-EBIO co-treatment group (t (35) = 0.8318; p = 0.4112, *ns*). The sample means in Figure 9d (right panel) show that the 1-EBIO-treated mice demonstrated scores on feeding latency similar to mice co-treated with 1-EBIO and LM-4131 (for 1-EBIO treatment group, means ± s.e.m. = 163.8 ± 35.60, N = 5; for LM-4131 and 1-EBIO co-treatment group, means ± s.e.m. = 179.4 ± 39.15, N = 5). It also shows that the LM-4131-treated mice demonstrated scores on feeding latency similar mice co-treated with 1-EBIO and LM-4131 (for LM-4131 treatment group, means ± s.e.m.

= 140.9 ± 17.20, *N* = 32; for LM-4131 and 1-EBIO co-treatment group, means ± s.e.m. = 179.4 ± 39.15, *N* = 5).

We also investigated whether or not the effects of substrate-selective COX-2 inhibition on stress-induced anhedonia and hyponeophagia in the NIH test after mice were subjected to acute footshock stress 8 h prior to testing as mediated by the CB_1R. Both SSCIs, LM-4131 and LMX, decreased anhedonia and hyponeophagia when the mice were tested in the aversive, novel cage environment 8 hours after exposure to acute footshock stress. However, these effects were reversed when the mice were co-treated with LM-4131 or LMX and the CB_1R antagonist, rimonabant. Thus, the SSCIs, LM-4131 and LMX, decreased stress-induced anhedonia and hyponeophagia when the mice in a CB_1R-mediated manner. According to the cumulative frequency distribution percentile plots of juvenile ICR male mice feeding in the NIFS assay (Fig. 9e (3 left panels)), 100% of vehicle-treated mice consumed ≤ 1.0 g of the shake, 100% of LM-4131-treated mice consumed ≤ 1.8 g of the shake, 100% of LMX-treated mice consumed ≤ 1.7 g of the shake, 100% of rimonabant-treated mice consumed ≤ 0.8 g (for rimonabant at 2 or 5 mg/kg) of the shake, 100% of LM-4131 and rimonabant co-treated mice consumed ≤ 0.9 g (for rimonabant at 2 mg/kg) or ≤ 1.0 g (for rimonabant at 5 mg/kg) of the shake, and 100% of LMX and rimonabant co-treated mice consumed ≤ 0.9 g (for rimonabant at 5 mg/kg) of the shake in the novel cage environment. A Kolmogorov-Smirnov test of the shake consumption data presented in the percentile plots revealed a significant difference between the cumulative frequency distributions for the LM-4131 and LMX treatment groups and the cumulative frequency distribution for the vehicle treatment group ($D = 0.7143$, $^{***}p < 0.001$, LM-4131 at 10 mg/kg vs. vehicle; $D = 0.6593$, $^{****}p < 0.0001$, LMX at 1 mg/kg vs. vehicle). It also revealed no difference between the cumulative frequency distribution for the rimonabant treatment group and the cumulative

frequency distribution for the LM-4131 or LMX and rimonabant co-treatment group (D = 0.09901, p = 7052, *ns*, rimonabant at 2 mg/kg vs. rimonabant + LM-4131 at 10 mg/kg; D = 0.09901, p = 0.7052, *ns*, rimonabant at 5 mg/kg vs. rimonabant + LM-4131; D = 0.04950, p = 0.9997, rimonabant at 5 mg/kg vs. rimonabant + LMX at 1 mg/kg). An independent samples (unpaired) t test revealed a significant difference between the vehicle and LM-4131 or LMX treatment group (t (13) = 4.427, p = 0.0007, ***p < 0.001, LM-4131 vs. vehicle; t (14) = 3.155, p = 0.0070, **p < 0.01, LMX vs. vehicle). The sample means are displayed in Figure 9e (right panel), which shows that the mice treated with LM-4131 (10 mg/kg) or LMX (1 mg/kg) scored significantly greater on shake consumption than did the mice treated with vehicle (for LM-4131 treatment group, means ± s.e.m. = 1.129 ± 0.1409, N = 7; for LMX treatment group, means ± s.e.m. = 1.063 ± 0.1954, N = 8; for vehicle treatment group, means ± s.e.m. = 0.3625 ± 0.1051, N = 8). An independent samples t test also revealed no significant difference between the rimonabant treatment group and LM-4131 or LMX and rimonabant co-treatment group (t (39) = 0.2758; p = 0.7841, *ns*, LM-4131 + rimonabant at 2 mg/kg vs. rimonabant; t (14) = 0.5670; p = 0.5797, *ns*, LM-4131 + rimonabant at 5 mg/kg vs. rimonabant; t (14) = 0.2590; p = 0.7994, *ns*, LMX + rimonabant at 5 mg/kg vs. rimonabant) and between the vehicle treatment group and LM-4131 or LMX and rimonabant co-treatment group (t (27) = 0.1630; p = 0.8717, *ns*, vehicle vs. LM-4131 + rimonabant at 2 mg/kg; t (14) = 1.002; p = 0.3335, *ns*, vehicle vs. LM-4131 + rimonabant at 5 mg/kg; t (14) = 0.7345; p = 0.4748, *ns*, vehicle vs. LMX + rimonabant at 5 mg/kg). The sample means in Figure 9e (right panel) show that the rimonabant-treated mice demonstrated scores on shake consumption similar to mice co-treated with rimonabant and LM-4131 or LMX (for

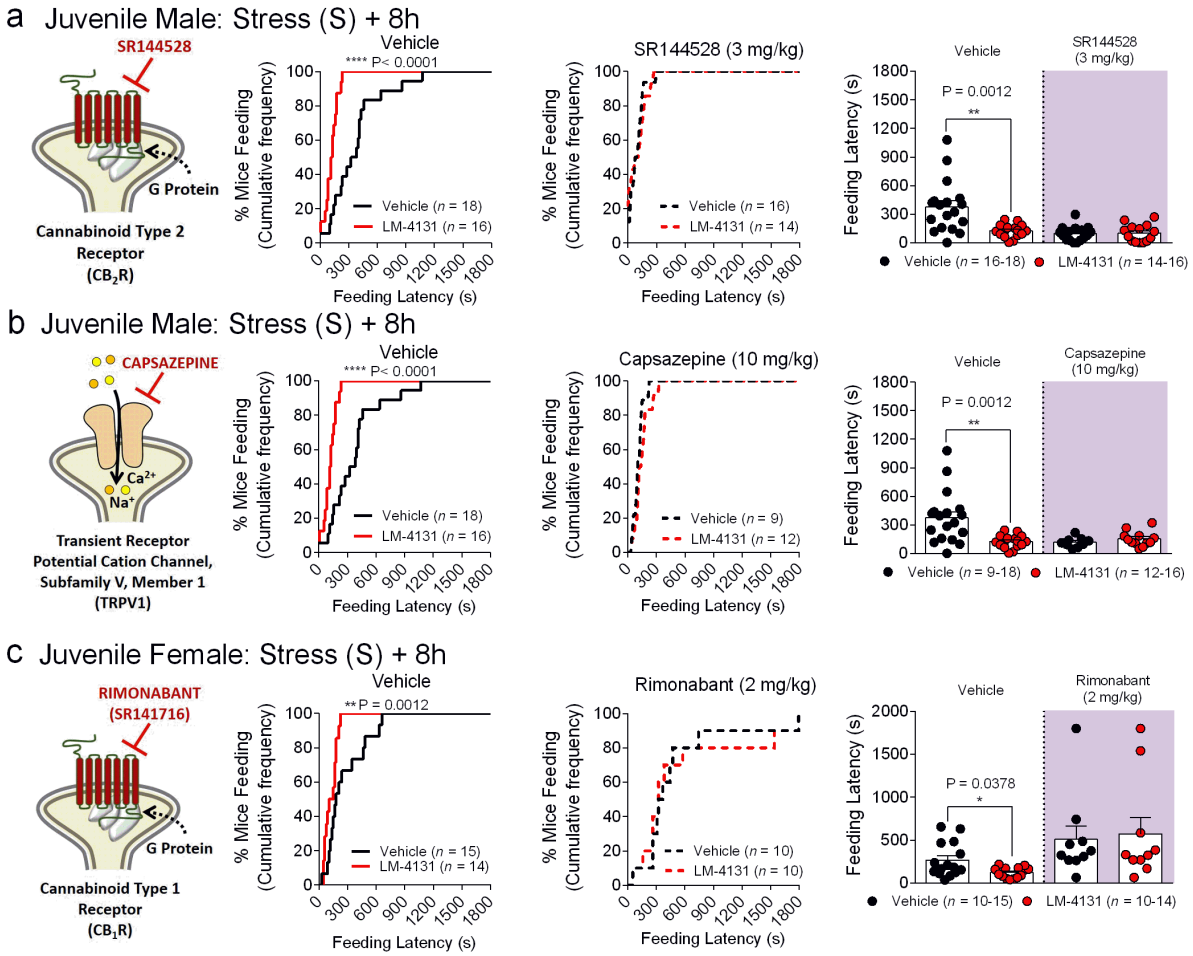

Figure 10. Anxiolytic effects of COX-2 inhibition is non-CB1R mediated only in male mice. (**a**) Cumulative feeding latency distribution curves for vehicle and LM-4131 treated male mice in the presence of vehicle or CB2 antagonist SR144528 (3 mg/kg) co-treatment. Mean ± S.E.M feeding latency for each group tested under acute footshock stress conditions. (**b**) Cumulative feeding latency distribution curves for vehicle and LM-4131 treated male mice in the presence of vehicle or TRPV1 antagonist capsazepine (10 mg/kg) co-treatment. Mean ± S.E.M feeding latency for each group tested under acute footshock stress conditions. (**c**) Cumulative feeding latency distribution curves for vehicle and LM-4131 treated female mice in the presence of vehicle or CB1 antagonist Rimonabant (2 mg/kg) co-treatment. Mean ± S.E.M feeding latency for each group tested under acute footshock stress conditions. Mean ± S.E.M amount of shake consumed for each group tested 8h after stress exposure. Data are shown as the mean ± s.e.m. *P < 0.05, **P < 0.01, ****P<0.0001. Statistical significance was calculated by two-tailed unpaired Student's *t*-test or Kolmogorov-Smirnov test (only for frequency plots).

rimonabant (2 mg/kg) treatment group, means ± s.e.m. = 0.3200 ± 0.05361, *N* = 20; for LM-4131 and rimonabant (2 mg/kg) co-treatment group, means ± s.e.m. = 0.3429 ± 0.06271, *N* = 21; for rimonabant (5 mg/kg) treatment group, means ± s.e.m. = 0.4375 ± 0.09246, *N* = 8; for LM-4131 and rimonabant (5 mg/kg) co-treatment group, means ± s.e.m. = 0.5250 ± 0.1236, *N* = 8; for LMX

and rimonabant (5 mg/kg) co-treatment group, means ± s.e.m. = 0.4750 ± 0.1114, $N = 8$). It also shows that the vehicle-treated mice demonstrated scores on shake consumption were similar to those shown by mice co-treated with rimonabant and LM-4131 or LMX (for vehicle treatment group, means ± s.e.m. = 0.3625 ± 0.1051, $N = 8$; for LM-4131 and rimonabant at 2 mg/kg co-treatment group, means ± s.e.m. = 0.3429 ± 0.06271, $N = 20$; for LM-4131 and rimonabant at 5 mg/kg co-treatment group, means ± s.e.m. = 0.5250 ± 0.1236, $N = 8$; for LMX and rimonabant at 5 mg/kg co-treatment group, means ± s.e.m. = 0.4750 ± 0.1114, $N = 8$).

Although the CB_2R or TRPV1 has been suggested to modulate anxiety-like behavior in rodents[221-226], we found that the SSCI, LM-4131, does not reduce anxiety-like behaviors after acute stress exposure through a CB_2 receptor-mediated mechanism in juvenile male ICR mice. According to the cumulative frequency distribution percentile plots of mice feeding in the NIH test 8h after exposure to acute electric footshock stress (Fig. 10a (2 left panels)), 100% of vehicle-treated mice had a feeding latency ≤ 1081 s, 100% of LM-4131-treated mice had a feeding latency ≤ 245 s, 100% of SR144528-treated mice had a feeding latency ≤ 297 s, and 100% of SR144528 and LM-4131 co-treated mice had a feeding latency ≤ 271 s in the novel cage environment. A Kolmogorov-Smirnov test of the feeding latency data presented in the percentile plots revealed a significant difference between the cumulative frequency distribution for the LM-4131 treatment group and the cumulative frequency distribution for the vehicle treatment group ($D = 0.4628$, ****$p < 0.0001$, LM-4131 at 10 mg/kg vs. vehicle) and no difference between the cumulative frequency distribution for the SR144528 treatment group and the SR144528 and LM-4131 co-treatment group ($D = 0.05785$, $p = 0.9874$, *ns*, SR144528 + LM-4131 vs. SR144528 at 3 mg/kg). An independent samples (unpaired) *t* test revealed a significant difference between the vehicle and LM-4131 treatment group (t (32) = 3.555; $p = 0.0012$, **$p < 0.01$, LM-4131 vs. vehicle). The

sample means are displayed in Figure 10a (right panel), which shows that the mice treated with LM-4131 (10 mg/kg) scored significantly lesser on feeding latency than did the mice treated with vehicle (for LM-4131 treatment group, means ± s.e.m. = 125.6 ± 16.90, N = 16; for vehicle treatment group, means ± s.e.m. = 374.9 ± 64.26, N = 18). An independent samples t test also revealed no significant difference between the SR144528 treatment group and LM-4131 and SR144528 co-treatment group (t (28) = 0.1819; p = 0.8569, *ns*), but a significant difference between the vehicle treatment group and LM-4131 and SR144528 co-treatment group (t (30) = 3.595; p = 0.0011, $^{**}p < 0.01$). The sample means in Figure 10a (right panel) show that the SR144528-treated mice demonstrated scores on feeding latency similar to mice co-treated with SR144528 and LM-4131 (for SR144528 treatment group, means ± s.e.m. = 95.50 ± 19.24, N = 16; for LM-4131 and SR144528 co-treatment group, means ± s.e.m. = 101.1 ± 24.27, N = 14). It also shows that the vehicle-treated mice demonstrated greater scores on feeding latency than mice co-treated with SR144528 and LM-4131 (for vehicle treatment group, means ± s.e.m. = 374.9 ± 64.26, N = 18; for LM-4131 and SR144528 co-treatment group, means ± s.e.m. = 101.1 ± 24.27, N = 14).

We also found that the SSCI, LM-4131, does not reduce anxiety-like behaviors after acute stress exposure through a TRPVI-mediated mechanism in juvenile male ICR mice. According to the cumulative frequency distribution percentile plots of mice feeding in the NIH test 8h after exposure to acute electric footshock stress (Fig. 10b (2 left panels)), 100% of vehicle-treated mice had a feeding latency ≤ 1081 s, 100% of LM-4131-treated mice had a feeding latency ≤ 245 s, 100% of capsazepine-treated mice had a feeding latency ≤ 219 s, and 100% of capsazepine and LM-4131 co-treated mice had a feeding latency ≤ 323 s in the novel cage environment. A Kolmogorov-Smirnov test of the feeding latency data presented in the percentile plots revealed a significant difference between the cumulative frequency distribution for the LM-4131 treatment

group and the cumulative frequency distribution for the vehicle treatment group (D = 0.4628, ****p < 0.0001, LM-4131 at 10 mg/kg vs. vehicle) and no difference between the cumulative frequency distribution for the capsazepine treatment group and the capsazepine and LM-4131 co-treatment group (D = 0.06612, p = 0.9541, *ns*, capsazepine + LM-4131 vs. capsazepine at 10 mg/kg). An independent samples (unpaired) t test revealed a significant difference between the vehicle and LM-4131 treatment group (t (32) = 3.555; p = 0.0012, **p < 0.01, LM-4131 vs. vehicle). The sample means are displayed in Figure 10a (right panel), which shows that the mice treated with LM-4131 (10 mg/kg) scored significantly lesser on feeding latency than did the mice treated with vehicle (for LM-4131 treatment group, means ± s.e.m. = 125.6 ± 16.90, N = 16; for vehicle treatment group, means ± s.e.m. = 374.9 ± 64.26, N = 18). An independent samples t test also revealed no significant difference between the capsazepine treatment group and LM-4131 and capsazepine co-treatment group (t (19) = 1.180; p = 0.2525, *ns*), but a significant difference between the vehicle treatment group and LM-4131 and capsazepine co-treatment group (t (28) = 2.724; p = 0.0110, *p < 0.05). The sample means in Figure 10b (right panel) show that the capsazepine-treated mice demonstrated scores on feeding latency similar to mice co-treated with capsazepine and LM-4131 (for capsazepine treatment group, means ± s.e.m. = 117.7 ± 17.12, N = 9; for LM-4131 and capsazepine co-treatment group, means ± s.e.m. = 153.4 ± 22.79, N = 12). It also shows that the vehicle-treated mice demonstrated scores on feeding latency which were greater than those shown by mice co-treated with capsazepine and LM-4131 (for vehicle treatment group, means ± s.e.m. = 374.9 ± 64.26, N = 18; for LM-4131 and capsazepine co-treatment group, means ± s.e.m. = 153.4 ± 22.79, N = 12).

In addition, we found that these findings were sex-specific since the anxiolytic behaviors displayed by female mice as a result of SSCI was CB_1R mediated after the juvenile female ICR

mice were exposed to acute footshock stress (Fig. 10c). This may be due to there being sex differences in CB_1R regulation, with stress-induced upregulation of CB_1Rs seen mainly in limbic structures of female animals[201]. According to the cumulative frequency distribution percentile plots of juvenile female ICR mice feeding in the NIH test 8 h after exposure to acute electric footshock stress (Fig. 10c (3 left panels)), 100% of vehicle-treated mice had a feeding latency ≤ 655 s, 100% of LM-4131-treated mice had a feeding latency ≤ 219 s, 100% of rimonabant-treated mice had a feeding latency ≤ 1800 s, and 100% of rimonabant and LM-4131 co-treated mice had a feeding latency ≤ 1800 s in the novel cage environment. A Kolmogorov-Smirnov test of the feeding latency data presented in the percentile plots revealed a significant difference between the cumulative frequency distribution for the LM-4131 treatment group and the cumulative frequency distribution for the vehicle treatment group ($D = 0.2479$, $p = 0.0012$, $^{**}p < 0.01$, LM-4131 at 10 mg/kg vs. vehicle) and no difference between the cumulative frequency distribution for the rimonabant treatment group and the rimonabant and LM-4131 co-treatment group ($D = 0.1000$, $p > 0.9999$, *ns*, rimonabant + LM-4131 vs. rimonabant at 2 mg/kg). An independent samples (unpaired) *t* test revealed a significant difference between the vehicle and LM-4131 treatment group (t (27) = 2.587; $p = 0.0154$, $^{*}p < 0.05$, LM-4131 vs. vehicle). The sample means are displayed in Figure 10c (right panel), which shows that the mice treated with LM-4131 (10 mg/kg) scored significantly lesser on feeding latency than did the mice treated with vehicle (for LM-4131 treatment group, means ± s.e.m. = 124.6 ± 16.48, $N = 14$; for vehicle treatment group, means ± s.e.m. = 268.7 ± 51.51, $N = 15$). An independent samples *t* test also revealed no significant difference between the rimonabant treatment group and LM-4131 and rimonabant co-treatment group (t (18) = 0.2684; $p = 0.7915$, *ns*) and between the vehicle treatment group and LM-4131 and rimonabant co-treatment group (t (23) = 1.855; $p = 0.0764$, *ns*). The sample means in Figure 10c

(right panel) show that the rimonabant-treated mice demonstrated scores on feeding latency similar to mice co-treated with rimonabant and LM-4131 (for rimonabant treatment group, means ± s.e.m. = 509.5 ± 153.8, N = 10; for LM-4131 and rimonabant co-treatment group, means ± s.e.m. = 574.8 ± 188.5, N = 10). It also shows that the vehicle-treated mice demonstrated scores on feeding latency similar to mice co-treated with rimonabant and LM-4131 (for vehicle treatment group, means ± s.e.m. = 268.7 ± 51.51, N = 15; for LM-4131 and rimonabant co-treatment group, means ± s.e.m. = 574.8 ± 188.5, N = 10).

Moreover, the chronic stress-induced anxiogenic and anhedonic effects in the NIFS assay were decreased in a non-cannabinoid-receptor and cannabinoid-receptor mediated manner, respectively, demonstrating a context-dependent dissociation between stress-induced anxiety-like and anhedonic behaviors concerning cannabinoid-receptor mediated mechanisms. We found that the SSCI, LM-4131, can reduce anxiety-like behaviors after chronic stress exposure through a non-CB_1 receptor-mediated mechanism in juvenile male ICR mice, specifically SK channels. According to the cumulative frequency distribution percentile plots of mice feeding in the NIH test 8h after exposure to chronic (5 days) electric footshock stress (Fig. 11a (2 left panels)), 100% of vehicle-treated mice had a feeding latency ≤ 1800 s, 100% of LM-4131-treated mice had a feeding latency ≤ 345 s, 100% of rimonabant-treated mice had a feeding latency ≤ 1800 s, and 100% of rimonabant and LM-4131 co-treated mice had a feeding latency ≤ 1800 s in the novel cage environment. A Kolmogorov-Smirnov test of the feeding latency data presented in the percentile plots revealed a significant difference between the cumulative frequency distribution

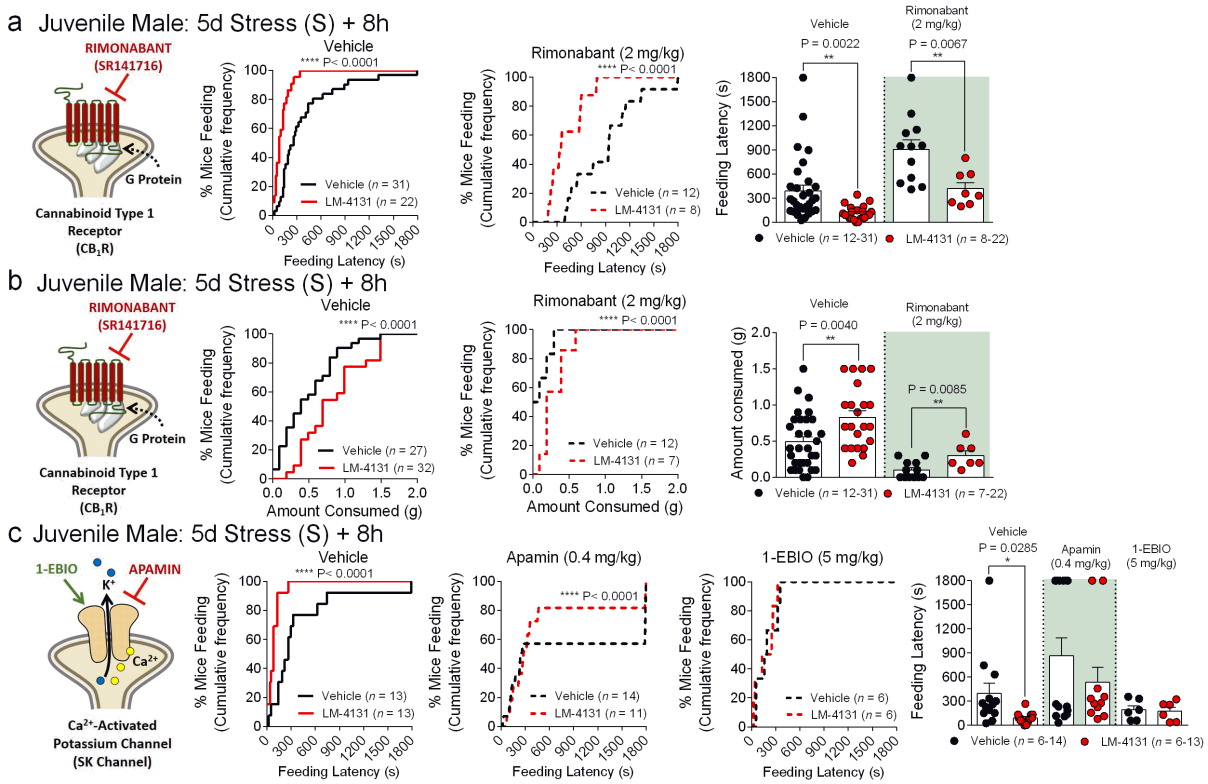

Figure 11. Receptor mechanisms mediating anxiolytic and hedonic effects of COX-2 inhibition after chronic stress exposure. (**a**) Cumulative feeding latency distribution curves for vehicle and LM-4131 treated mice in the presence of vehicle or Rimonabant (2 mg/kg) co-treatment. Mean ± S.E.M feeding latency for each group tested under acute stress conditions. (**b**) Cumulative feeding latency distribution curves for vehicle and LM-4131treated mice in the presence of vehicle or Rimonabant (2 mg/kg) co-treatment. Effects of the CB1 receptor antagonist Rimonabant (2 mg/kg on LM-4131-induced increases in shake consumption tested 8hours after 5 days of daily electric footshock stress exposure. Mean ± S.E.M feeding latency for each group tested 8h after stress exposure. (**c**) Cumulative feeding latency distribution curves for vehicle and LM-4131 treated mice in the presence of vehicle, Apamin (0.4 mg/kg), or 1-EBIO (5 mg/kg) co-treatment. Effects of the SK channel inhibitor Apamin (0.4 mg/kg), and SK channel activator 1-EBIO (5 mg/kg), on LM-4131-induced reductions in feeding latency tested 8h after5 days of daily electric footshock stress exposure. Mean ± S.E.M feeding latency/amount consumed for each group tested 8h after chronic stress exposure. Data are shown as the mean ± s.e.m. **P < 0.01, ****P<0.0001. Statistical significance was calculated by two-tailed unpaired Student's *t*-test or Kolmogorov-Smirnov test (only for frequency plots).

for the LM-4131 treatment group and the cumulative frequency distribution for the vehicle treatment group ($D = 0.8017$, ****$p < 0.0001$, LM-4131 at 10 mg/kg vs. vehicle) and between the cumulative frequency distribution for the rimonabant treatment group and the rimonabant and LM-4131 co-treatment group ($D = 0.5537$, ****$p < 0.0001$, rimonabant + LM-4131 vs. rimonabant at 2 mg/kg). An independent samples (unpaired) *t* test revealed a significant difference between the vehicle and LM-4131 treatment group (t (51) = 3.233; $p = 0.0022$, **$p < 0.01$, LM-4131 vs.

vehicle). The sample means are displayed in Figure 11a (right panel), which shows that the mice treated with LM-4131 (10 mg/kg) scored significantly lesser on feeding latency than did the mice treated with vehicle (for LM-4131 treatment group, means ± s.e.m. = 115.8 ± 18.78, N = 22; for vehicle treatment group, means ± s.e.m. = 391.6 ± 70.44, N = 31). An independent samples t test also revealed a significant difference between the rimonabant treatment group and LM-4131 and rimonabant co-treatment group (t (18) = 3.060; p = 0.0067, $^{**}p < 0.01$) and no significant difference between the vehicle treatment group and LM-4131 and rimonabant co-treatment group (t (37) = 0.1879; p = 0.8520, *ns*). The sample means in Figure 10a (right panel) show that the rimonabant-treated mice demonstrated scores on feeding latency which were significantly greater than those shown by mice co-treated with rimonabant and LM-4131 (for rimonabant treatment group, means ± s.e.m. = 909.2 ± 119.7, N = 12; for LM-4131 and rimonabant co-treatment group, means ± s.e.m. = 418.9 ± 76.62, N = 8). It also shows that the vehicle-treated mice demonstrated scores on feeding latency similar to mice co-treated with rimonabant and LM-4131 (for vehicle treatment group, means ± s.e.m. = 391.6 ± 70.44, N = 31; for LM-4131 and rimonabant co-treatment group, means ± s.e.m. = 418.9 ± 76.62, N = 8).

We also examined whether or not the effects of substrate-selective COX-2 inhibition on chronic stress-induced anhedonia and hyponeophagia in the NIH test after mice were subjected to chronic (5 days) footshock stress 8 h prior to testing was mediated by the CB_1R. The SSCI, LM-4131, decreased anhedonia and hyponeophagia when the mice were tested in the aversive, novel cage environment 8 hours after exposure to chronic footshock stress. However, these effects were reversed when the mice were co-treated with LM-4131 and the CB_1R antagonist, rimonabant. Thus, the SSCI, LM-4131, decreased chronic stress-induced anhedonia and hyponeophagia in the mice in a CB_1R-mediated manner. According to the cumulative frequency distribution percentile

plots of juvenile ICR male mice feeding in the NIFS assay 8h after chronic stress exposure (Fig. 11b (2 left panels)), 50% (50^{th} percentile) of vehicle-treated mice consumed ≤ 0.4 g of the shake, 50% of LM-4131-treated mice consumed ≤ 0.7 g of the shake, 50% of rimonabant-treated mice consumed ≤ 0.05 g of the shake, and 50% of LM-4131 and rimonabant co-treated mice consumed ≤ 0.2 g of the shake in the novel cage environment. A Kolmogorov-Smirnov test of the shake consumption data presented in the percentile plots revealed a significant difference between the cumulative frequency distributions for the LM-4131 treatment group and the cumulative frequency distribution for the vehicle treatment group ($D = 0.3465$, ****$p < 0.0001$, LM-4131 at 10 mg/kg vs. vehicle). It also revealed no difference between the cumulative frequency distribution for the rimonabant treatment group and the cumulative frequency distribution for the LM-4131 and rimonabant co-treatment group ($D = 0.1485$, $p = 0.2153$, *ns*, rimonabant at 2 mg/kg vs. rimonabant + LM-4131 at 10 mg/kg). An independent samples (unpaired) *t* test revealed a significant difference between the vehicle and LM-4131 treatment group (t (51) = 3.016, $p = 0.0040$, **$p < 0.01$, LM-4131 vs. vehicle). The sample means are displayed in Figure 11b (right panel), which shows that the mice treated with LM-4131 (10 mg/kg) scored significantly greater on shake consumption than did the mice treated with vehicle (for vehicle treatment group, means ± s.e.m. = 0.4903 ± 0.06884, $N = 31$; for LM-4131 treatment group, means ± s.e.m. = 0.8273 ± 0.09050, $N = 22$). An independent samples *t* test also revealed a significant difference between the rimonabant treatment group and LM-4131 and rimonabant co-treatment group (t (17) = 2.974; $p = 0.0085$, **$p < 0.01$, LM-4131 + rimonabant at 2 mg/kg vs. rimonabant), but no significant difference between the vehicle treatment group and LM-4131 and rimonabant co-treatment group (t (36) = 1.274; $p = 0.2108$, *ns*, vehicle vs. LM-4131 + rimonabant at 2 mg/kg). The sample means in Figure 11b (right panel) show that the rimonabant-treated mice demonstrated scores on shake consumption which

were lesser than those shown by mice co-treated with rimonabant and LM-4131 (for rimonabant (2 mg/kg) treatment group, means ± s.e.m. = 0.1000 ± 0.03482, N = 12; for LM-4131 and rimonabant (2 mg/kg) co-treatment group, means ± s.e.m. = 0.3000 ± 0.06547, N = 7). It also shows that the vehicle-treated mice demonstrated scores on shake consumption were similar to those shown by mice co-treated with rimonabant and LM-4131 (for vehicle treatment group, means ± s.e.m. = 0.4903 ± 0.06884, N = 31; for LM-4131 and rimonabant at 2 mg/kg co-treatment group, means ± s.e.m. = 0.3000 ± 0.06547, N = 7).

We found that the SSCI, LM-4131, can reduce anxiety-like behaviors after chronic (5 days) stress exposure through a non-CB_1 receptor-mediated mechanism in male ICR mice, specifically SK channels. According to the cumulative frequency distribution percentile plots of mice feeding in the NIH test 8h after exposure to acute electric footshock stress (Fig. 11c (3 left panels)), 100% of vehicle-treated mice had a feeding latency ≤ 1800 s, 100% of LM-4131-treated mice had a feeding latency ≤ 269 s, 100% of apamin-treated mice had a feeding latency ≤ 1800 s, and 100% of apamin and LM-4131 co-treated mice had a feeding latency ≤ 1800 s in the novel cage environment. A Kolmogorov-Smirnov test of the feeding latency data presented in the percentile plots revealed a significant difference between the cumulative frequency distribution for the LM-4131 treatment group and the cumulative frequency distribution for the vehicle treatment group (D = 0.9174, ****p < 0.0001, LM-4131 at 10 mg/kg vs. vehicle) and between the cumulative frequency distribution for the apamin treatment group and the apamin and LM-4131 co-treatment group (D = 0.8099, ****p < 0.0001, apamin + LM-4131 vs. apamin at 0.4 mg/kg). An independent samples (unpaired) t test revealed a significant difference between the vehicle and LM-4131 treatment group (t (24) = 2.330; p = 0.0285, *p < 0.05, LM-4131 vs. vehicle). The sample means are displayed in Figure 11c (right panel), which shows that the mice treated with LM-4131 (10

mg/kg) scored significantly lesser on feeding latency than did the mice treated with vehicle (for LM-4131 treatment group, means ± s.e.m. = 91.23 ± 19.25, $N = 13$; for vehicle treatment group, means ± s.e.m. = 397.3 ± 129.9, $N = 13$). An independent samples *t* test also revealed no significant difference between the apamin treatment group and LM-4131 and apamin co-treatment group ($t(23) = 1.084$, $p = 0.2896$, *ns*) and between the vehicle treatment group and LM-4131 and apamin co-treatment group ($t(22) = 0.6064$; $p = 0.5505$, *ns*). The sample means in Figure 11c (right panel) show that the apamin-treated mice demonstrated scores on feeding latency similar to mice co-treated with apamin and LM-4131 (for apamin treatment group, means ± s.e.m. = 865.6 ± 225.0, $N = 14$; for LM-4131 and apamin co-treatment group, means ± s.e.m. = 534.1 ± 191.6, $N = 11$). It also shows that the vehicle-treated mice demonstrated scores on feeding latency similar to mice co-treated with apamin and LM-4131 (for vehicle treatment group, means ± s.e.m. = 397.3 ± 129.9, $N = 13$; for LM-4131 and apamin co-treatment group, means ± s.e.m. = 534.1 ± 191.6, $N = 11$). To further validate that the anxiolytic action of the SSCI, LM-4131, is mediated through the SK channels once mice have been subjected to chronic stress exposure, we treated another cohort of juvenile male ICR mice with the SK channel agonist, 1-EBIO, to determine if it could mimic the anxiolytic effects of LM-4131 in the NIH test. We found that activating the SK channels reduced chronic stress-induced anxiety-like behavior in the mice similar to LM-4131. According to the cumulative frequency distribution percentile plots of mice feeding in the NIH test 8h after exposure to chronic electric footshock stress (Fig. 11c (3rd left panel)), 100% of 1-EBIO-treated mice had a feeding latency ≤ 355 s and 100% of 1-EBIO and LM-4131 co-treated mice had a feeding latency ≤ 324 s in the novel cage environment. A Kolmogorov-Smirnov test of the feeding latency data presented in the percentile plots revealed no difference between the cumulative frequency distribution for the 1-EBIO treatment group and the 1-EBIO and LM-4131 co-treatment group (*D*

= 0.03306, $p > 0.9999$, *ns*, 1-EBIO + LM-4131 vs. 1-EBIO at 5 mg/kg). An independent samples *t* test also revealed no significant difference between the 1-EBIO treatment group and LM-4131 and 1-EBIO co-treatment group ($t(10) = 0.2418$; $p = 0.8138$, *ns*) and between the vehicle treatment group and LM-4131 and 1-EBIO co-treatment group ($t(22) = 1.125$; $p = 0.2762$, *ns*). The sample means in Figure 11c (right panel) show that the 1-EBIO-treated mice demonstrated scores on feeding latency similar to mice co-treated with 1-EBIO and LM-4131 (for 1-EBIO treatment group, means ± s.e.m. = 193.2 ± 52.16, $N = 6$; for LM-4131 and 1-EBIO co-treatment group, means ± s.e.m. = 175.7 ± 50.17, $N = 6$). It also shows that the vehicle-treated mice demonstrated scores on feeding latency similar to mice co-treated with 1-EBIO and LM-4131 (for vehicle treatment group, means ± s.e.m. = 397.3 ± 129.9, $N = 13$; for LM-4131 and 1-EBIO co-treatment group, means ± s.e.m. = 175.7 ± 50.17, $N = 6$).

Our finding that SK channels are able to facilitate the anxiolytic effects of the SSCI, LM-4131, after acute stress exposure was not confounded by increased locomotor activity in the mice as a result of i.p. administration with the SK channel antagonist, apamin, or the SK channel agonist, 1-EBIO. Administration of the SK channel antagonist, apamin, did not cause any changes in horizontal activity under control (no stress) conditions (Fig. 12a). One-way ANOVA did not reveal any effect of apamin at 0.2, 0.4, or 1 mg/kg on horizontal counts ($F_{(3, 36)} = 2.688$, $p = 0.0608$; Fig. 12a (left panel)) or horizontal time ($F_{(3, 36)} = 2.245$, $p = 0.0997$; Fig. 12a (middle panel)) in the open field assay. Horizontal or ambulatory distance traveled was only decreased at the highest dose of apamin (one-way ANOVA: $F_{(3, 36)} = 2.929$, $p = 0.0467$; 1 mg/kg vs. vehicle, $p<0.05$ by Holm-Sidak post hoc test; Fig. 12a (right panel)), which was not used in the experiments aimed at determining the mechanism of action of LM-3131 in reducing stress-induced anxiety in the NIFS

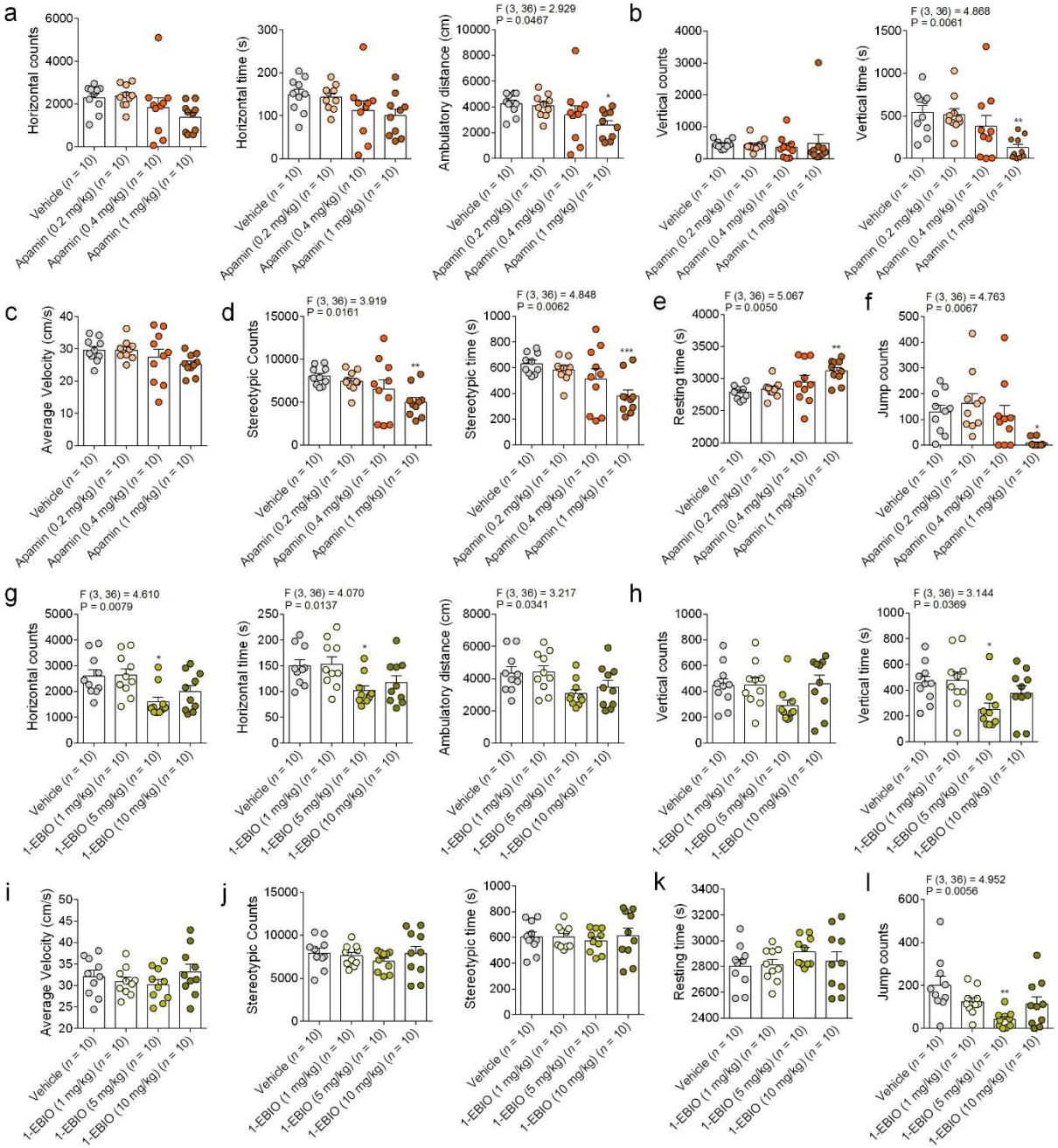

Figure 12. Locomotor effects of SK channel antagonists and agonists. Horizontal activity, vertical activity, average velocity, groom behavior, resting time, and jump counts measured in the open field assay under non-stressful conditions for the SK channel antagonist, apamin (**a-f**), and the SK channel agonist, 1-EBIO (**g-l**), at varying concentrations in juvenile male mice. Data are shown as the mean ± s.e.m. NS = no stress, S = stress (e.g., stress exposure in the form of an electric footshock administered 8h prior to testing), *P < 0.05 (SK channel antagonist/agonist compared to vehicle). Statistical significance was calculated by two-tailed unpaired Student's *t*-test.

test. Also, post hoc Holm-Sidak's test revealed no differences in horizontal distance traveled

during the 60 min testing period in the open-field assay at the 0.2 mg/kg and 0.4 mg/kg doses of apamin compared to the vehicle treatment. Moreover, administration of apamin did not cause any changes in vertical activity under control (no stress) conditions (Fig. 12b). One-way ANOVA did not reveal any effect of apamin at 0.2, 0.4, or 1 mg/kg on vertical counts ($F_{(3, 36)} = 0.1038$, $p = 0.9573$; Fig. 12b (left panel)) in the open field assay. Vertical time was only decreased at the highest dose of apamin (one-way ANOVA: $F_{(3, 36)} = 4.868$, $p = 0.0061$; 1 mg/kg vs. vehicle, $p<0.01$ by Holm-Sidak post hoc test; Fig. 12b (right panel)). Also, post hoc Holm-Sidak's test revealed no differences in vertical time during the 60 min testing period in the open-field assay at the 0.2 mg/kg and 0.4 mg/kg doses of apamin compared to the vehicle treatment. Apamin did not affect average velocity (one-way ANOVA: $F_{(3, 36)} = 1.794$, $p = 0.1657$; Fig. 12c) at any dose tested. Apamin only reduced grooming or stereotypic counts (one-way ANOVA: $F_{(3, 36)} = 3.919$, $p = 0.0161$; 1 mg/kg vs. vehicle, $p<0.01$ by Holm-Sidak post hoc test; Fig. 12d (left panel)) and stereotypic time (one-way ANOVA: $F_{(3, 36)} = 4.848$, $p = 0.0062$; 1 mg/kg vs. vehicle, $p<0.01$ by Holm-Sidak post hoc test; Fig. 12d (right panel)) at the highest dose. Apamin appeared to make the mice slightly lethargic by increasing resting time at the highest dose tested (one-way ANOVA: $F_{(3, 36)} = 5.067$, $p = 0.0050$; 1 mg/kg vs. vehicle, $p<0.01$ by Holm-Sidak post hoc test; Fig. 12de). Also, apamin decreased total jump counts at the highest dose tested in the open-field assay time (one-way ANOVA: $F_{(3, 36)} = 4.763$, $p = 0.0067$; 1 mg/kg vs. vehicle, $p<0.05$ by Holm-Sidak post hoc test; Fig. 12f).

Although administration of the SK channel agonist, 1-EBIO, at 5 mg/kg decreased horizontal counts (one-way ANOVA: $F_{(3, 36)} = 4.610$, $p = 0.0079$; 5 mg/kg vs. vehicle, $p<0.05$ by Holm-Sidak post hoc test; Fig. 12g (left panel)) and time (one-way ANOVA: $F_{(3, 36)} = 4.070$, $p = 0.0137$; 5 mg/kg vs. vehicle, $p<0.05$ by Holm-Sidak post hoc test; Fig. 12g (right panel)), this dose

of 1-EBIO did not cause any changes in horizontal distance traveled under control (no stress) conditions (one-way ANOVA: $F_{(3, 36)} = 3.217$, $p = 0.0341$; 5 mg/kg vs. vehicle, *ns* by Holm-Sidak post hoc test; Fig. 12g) in the open-field test. Also, post hoc Holm-Sidak's test revealed no differences in horizontal distance traveled during the 60 min testing period in the open-field assay at the 1 mg/kg and 10 mg/kg doses of 1-EBIO compared to the vehicle treatment. Moreover, administration of 1-EBIO did not cause any changes in vertical activity counts under control (no stress) conditions (one-way ANOVA: $F_{(3, 36)} = 2.141$, $p = 0.1121$; Fig. 12h) at any dose tested. Vertical time was only decreased at the 5 mg/kg dose of apamin (one-way ANOVA: $F_{(3, 36)} = 3.144$, $p = 0.0369$; 5 mg/kg vs. vehicle, $p<0.05$ by Holm-Sidak post hoc test; Fig. 12h (right panel)). Also, post hoc Holm-Sidak's test revealed no differences in vertical time during the 60 min testing period in the open-field assay at the 1 mg/kg and 10 mg/kg doses of 1-EBIO compared to the vehicle treatment. 1-EBIO did not affect average velocity (one-way ANOVA: $F_{(3, 36)} = 0.8780$, $p = 0.4616$; Fig. 12i), grooming or stereotypic counts (one-way ANOVA: $F_{(3, 36)} = 0.6029$, $p = 0.6174$; Fig. 12j (left panel)), stereotypic time (one-way ANOVA: $F_{(3, 36)} = 0.1697$, $p = 0.9162$; Fig. 12j (right panel)), or resting time (one-way ANOVA: $F_{(3, 36)} = 0.9059$, $p = 0.4478$; Fig. 12k) at any dose tested. Also, 1-EBIO decreased total jump counts at the 5 mg/kg dose tested in the open-field assay time (one-way ANOVA: $F_{(3, 36)} = 4.952$, $p = 0.0056$; 5 mg/kg vs. vehicle, $p<0.01$ by Holm-Sidak post hoc test; Fig. 12l).

Effects of substrate-selective COX-2 inhibition on stress-induced fear-related behavior

When a human or an animal encounters an aversive or stressful life event, a fear response can be produced until the aversion subsides. Fear responses can develop into pathological anxiety when they are chronically dysfunctional or exaggerated[227,228]. Lesion studies have shown that the amygdala is one of several brain structures involved in modulating fear-related behaviors in

animals, such as phasic immobility or freezing. In particular, these studies have illustrated that lesions of the lateral, basolateral, and central nuclei of the amygdala can disrupt fear responses conditioned to a cue (e.g., a tone paired with an electric footshock) and a context (e.g., a chamber in which tone-electric footshock pairings occur) and disrupt subsequent expression of stress-induced freezing[229-233]. Our study suggests that COX-2 inhibitors can reduce anxiety in mice after being subjected to an acute aversive life event, such as a series of electric footshocks in one day. Thus, one would expect that COX-2 inhibitors may as well be able to enhance extinction of conditioned fear responses in mice to the same acute aversive life event in an amygdala-dependent manner. To test this hypothesis, we examined the effects of the SSCI, LM-4131 (10 mg/kg), on freezing behavior in mice when we returned them to the same chamber they experienced the acute aversive life event (e.g., six tone-electric footshock pairings) in the presence of a conditioned stimulus (e.g., a 30 second tone repeated 15 times). We found no significant differences in the freezing behavior of the mice before i.p. administration of vehicle or LM-4131 after subjecting the mice to six tone-footshock pairings. Relating to the effect of six tone-electric footshock pairings on freezing behavior, two-way ANOVA factoring drug dose and time revealed no effect of drug dose x time interaction ($F_{(6, 308)} = 1.446$; $p = 0.1967$, *ns*), but a significant effect of drug dose ($F_{(1, 308)} = 6.843$, $p = 0.0093$, $^{**}p < 0.01$) and time ($F_{(6, 308)} = 53.38$, $^{****}p < 0.0001$; Fig. 13a (left panel)). Post hoc Holm-Sidak's multiple comparisons test revealed a slight decrease in percentage freezing after the administration of the last tone-footshock pairing in a cohort of mice that will be treated with LM-4131 at a dose of 10 mg/kg compared to the mice that will be treated with vehicle ($^{*}p < 0.05$, $t = 3.200$, df = 308, LM-4131 vs. vehicle; for vehicle treatment group, means ± s.e.m. = 62.06 ± 5.181, $N = 23$; for LM-4131 treatment group, means ± s.e.m. = 45.48 ± 5.181, $N = 23$). We also found no significant differences in the freezing

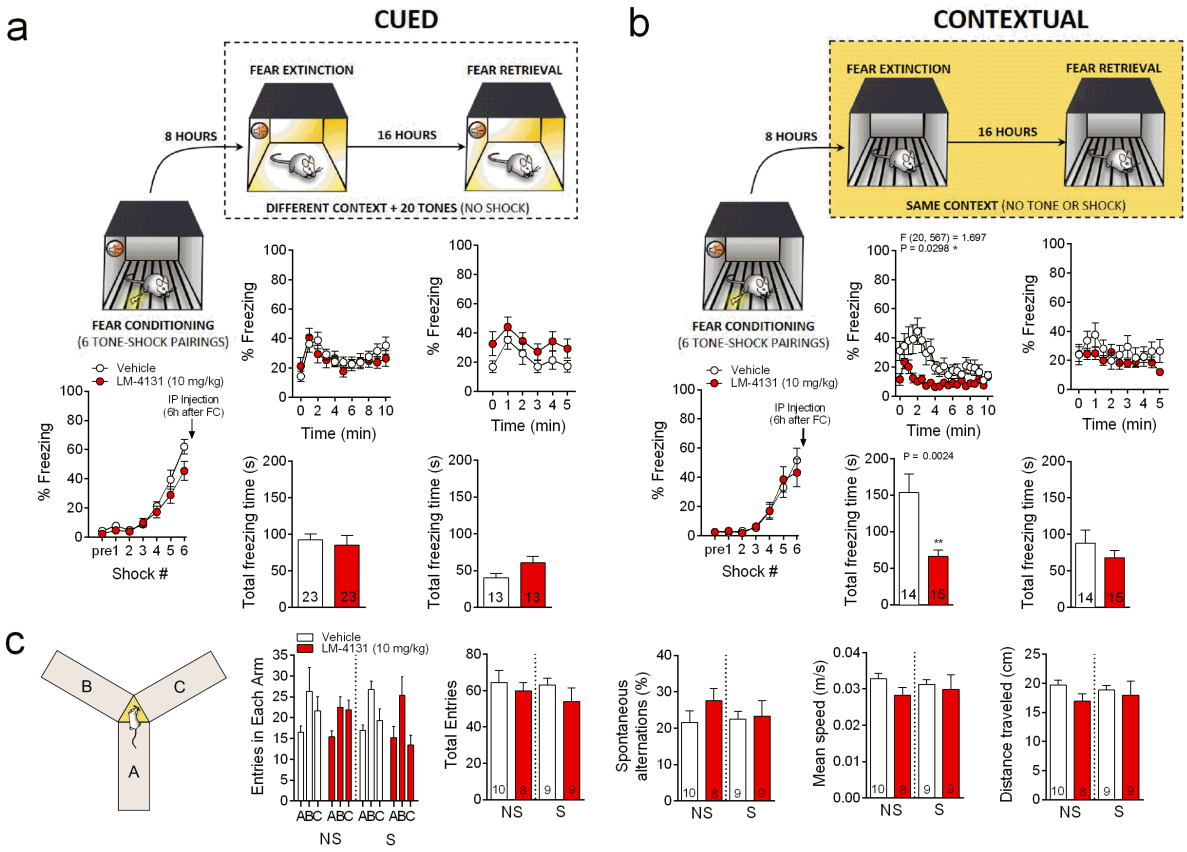

Figure 13. Cognitive effects of substrate-selective COX-2 inhibition. (**a, b**) Diagrams (top) of experimental design for context conditioning and cued or contextual fear extinction and retrieval. (**a**) Freezing behavior during context conditioning (left) and cued fear extinction (middle) and retrieval (right). During context conditioning, a tone, the conditional stimulus (CS), was paired with a footshock, the unconditional stimulus (US), six times. (**b**) Freezing behavior during context conditioning (left) and contextual fear extinction (middle) and retrieval (right). (**c**) Number of entries in each arm, number of total arm entries, percentage of spontaneous alternations, mean speed, and total distance traveled in the Y-maze (left to right). Data are shown as the mean ± s.e.m. NS = no stress, S = stress (e.g., stress exposure in the form of an electric footshock administered 8h prior to testing), *P < 0.05, **P < 0.01. Statistical significance was calculated by two-tailed unpaired Student's *t*-test or two-way ANOVA with post hoc Holm-Sidak's multiple comparisons test and time x treatment interaction as a source of variation between groups.

behavior of the vehicle-treated or LM-4131-treated mice elicited by a tone that was paired with the electric footshock once we placed the mice in the same chamber in which the aversive electric footshock was previously experienced. Two-way ANOVA factoring drug dose and time revealed no significant effect of drug dose ($F_{(1, 484)} = 1.136$; $p = 0.2870$, *ns*) and dose x time interaction ($F_{(10, 484)} = 0.6668$; $p = 0.7555$, *ns*), but a significant effect of time ($F_{(10, 484)} = 3.056$; $p = 0.0009$, ***$p < 0.001$; Fig.13a (middle top panel)). An independent samples (unpaired) *t* test revealed no

significant difference in total freezing time during the fear extinction test between the vehicle and LM-4131 treatment group (t (44) = 0.4572, p = 0.6498, *ns*, LM-4131 vs. vehicle). The sample means are displayed in Figure 13a (right bottom panel), which shows that the mice treated with LM-4131 (10 mg/kg) scored similar on total freezing time to the mice treated with vehicle (for LM-4131 treatment group, means ± s.e.m. = 84.97 ± 13.42, N = 23; for vehicle treatment group, means ± s.e.m. = 92.14 ± 8.133, N = 23). We obtained similar results in the freezing behavior of the mice when we examined the effects of LM-4131 on the recovery of the extinguished fear (e.g., fear retrieval or recall) in the mice. Two-way ANOVA factoring drug dose and time revealed a significant effect of drug dose ($F_{(1, 144)}$ = 10.61; p = 0.0014, **p < 0.01) and time ($F_{(5, 144)}$ = 2.279; p = 0.0498, *p < 0.05), but no significant effect of dose x time interaction ($F_{(5, 144)}$ = 0.1014; p = 0.9917, *ns*; Fig.13a (right top panel)). Post hoc Holm-Sidak's multiple comparisons test revealed no changes in percentage freezing at any time point in the vehicle-treated mice compared to the LM-4131-treated mice. An independent samples (unpaired) t test revealed no significant difference in total freezing time during the fear retrieval test between the vehicle and LM-4131 treatment group (t (24) = 1.913, p = 0.0678, *ns*, LM-4131 vs. vehicle). The sample means are displayed in Figure 13a (right bottom panel), which shows that the mice treated with LM-4131 (10 mg/kg) scored similar on total freezing time to the mice treated with vehicle (for LM-4131 treatment group, means ± s.e.m. = 60.49 ± 8.851, N = 13; for vehicle treatment group, means ± s.e.m. = 39.96 ± 6.078, N = 13). These results suggest that the SSCI, LM-4131, does not affect stress-induced fear-related behavior in an amygdala-dependent fashion. LM-4131 may be selectively affecting subregions of the amygdala after an animal has been exposed to a stressful external stimulus, such as a series of electric footshocks, or only affects fear-related behavior in animals in a context-dependent manner. Several studies have suggested that the basolateral

subregion of the amygdala is not restricted to a single sensory modality and is required for memories of contextual representations of an environment, especially in the case of memories acquired after contextual fear conditioning where an environment is associated with an aversive electric footshock[234-236].

Since impaired extinction of contextual fear memories is thought to contribute to the development and maintenance of anxiety, trauma-related, and stressor-related disorders, we next assessed whether or not COX-2 inhibitors could enhance contextual fear extinction and recall. To investigate the effects of LM-4131 on contextual fear extinction, we measured freezing behavior in vehicle-treated and LM-4131-treated mice when we returned them to the same chamber they experienced the acute aversive life event (e.g., six tone-electric footshock pairings). We found no significant differences in the freezing behavior of the mice before i.p. administration of vehicle or LM-4131 after subjecting the mice to six tone-footshock pairings. Concerning the effect of six tone-electric footshock pairings on freezing behavior, two-way ANOVA factoring drug dose and time revealed no effect of drug dose x time interaction ($F_{(18, 385)} = 0.4368$, $p = 0.9795$, *ns*) and drug dose ($F_{(13\ 385)} = 0.8664$, $p = 0.4586$, *ns*), but a significant effect of time ($F_{(6, 385)} = 63.69$, ****$p < 0.0001$; Fig. 13b (left panel)). We found that the SSCI, LM-4131, significantly increased contextual fear extinction by decreasing freezing behavior in the mice only 8 hours after exposure to the acute stress paradigm. Two-way ANOVA factoring drug dose and time revealed a significant effect of drug dose ($F_{(1, 567)} = 89.09$, ****$p < 0.0001$), time ($F_{(20, 567)} = 3.495$, ****$p < 0.0001$), and dose x time interaction ($F_{(20, 567)} = 1.697$, $p = 0.0298$, *$p < 0.05$; Fig.13b (middle top panel)). Post hoc Holm-Sidak's multiple comparisons test revealed a significant decrease in percentage freezing in the juvenile male ICR mice during the 1.5 min (t (567) = 3.948, **$p < 0.01$, for LM-4131 treatment group, means ± s.e.m. = 12.51 ± 6.746, $N = 15$; for vehicle treatment group,

means ± s.e.m. = 39.14 ± 6.746, N = 14), 2.0 min (t (567) = 5.100, ****p < 0.0001, for LM-4131 treatment group, means ± s.e.m. = 10.05 ± 6.746; for vehicle treatment group, means ± s.e.m. = 44.45 ± 6.746), 2.5 min (t (567) = 3.983, **p < 0.01, for LM-4131 treatment group, means ± s.e.m. = 11.55 ± 6.746; for vehicle treatment group, means ± s.e.m. = 38.41 ± 6.746), 3.0 min (t (567) = 3.322, *p < 0.05, for LM-4131 treatment group, means ± s.e.m. = 7.163 ± 6.746; for vehicle treatment group, means ± s.e.m. = 29.57 ± 6.746), and 3.5 min (t (567) = 3.358, *p < 0.05, for LM-4131 treatment group, means ± s.e.m. = 9.245 ± 6.746; for vehicle treatment group, means ± s.e.m. = 31.90 ± 6.746) bins of the fear extinction test at the 10 mg/kg dose of LM-4131 compared to vehicle treatment. An independent samples (unpaired) t test revealed a significant difference in total freezing time during the fear extinction test between the vehicle and LM-4131 treatment group (t (27) = 3.356, p = 0.0024, **p < 0.01, LM-4131 vs. vehicle). The sample means are displayed in Figure 13b (middle bottom panel), which shows that the mice treated with LM-4131 (10 mg/kg) scored significantly lesser on total freezing time than did the mice treated with vehicle (for LM-4131 treatment group, means ± s.e.m. = 66.31 ± 8.775, N = 15; for vehicle treatment group, means ± s.e.m. = 153.8 ± 25.33, N = 14). We found no significant differences in the freezing behavior of the mice during fear retrieval 24 hours after exposure to the acute stress protocol. Two-way ANOVA factoring drug dose and time revealed a significant effect of drug dose ($F_{(1, 297)}$ = 6.559, p = 0.0109, *p < 0.05), but no significant effect of time ($F_{(10, 297)}$ = 0.8374, p = 0.5928, *ns*) and dose x time interaction ($F_{(10, 297)}$ = 0.6363, p = 0.7824, *ns*; Fig.13b (middle top panel)). Post hoc Holm-Sidak's multiple comparisons test revealed no significant difference in percentage freezing at any time point in the juvenile male ICR mice of the fear retrieval test at the 10 mg/kg dose of LM-4131 compared to vehicle treatment. An independent samples (unpaired) test revealed no significant difference in total freezing time during the fear retrieval test between the vehicle

and LM-4131 treatment group (t (27) = 0.9954, p = 0.3284, *ns*, LM-4131 vs. vehicle). The sample means are displayed in Figure 13b (right bottom panel), which shows that the mice treated with LM-4131 (10 mg/kg) scored similar on total freezing time to the mice treated with vehicle (for LM-4131 treatment group, means ± s.e.m. = 68.26 ± 9.947, N = 15; for vehicle treatment group, means ± s.e.m. = 88.08 ± 17.66, N = 14). These results suggest that LM-4131 can decrease stress-induced fear in a context-dependent manner. Also, the effects of LM-4131 on contextual fear extinction is dependent upon not only the amygdala, but as well as the hippocampus, since we did not find similar changes with cued fear extinction and recall, which is mainly amygdala-dependent (Fig. 13a (middle panel)). Phillips and LeDoux illustrated in rats that both the amygdala and the hippocampus are involved in the conditioning of fear-related behavior as a consequence of complex, polymodal sensory stimuli. When they lesioned the amygdala and hippocampus, both brain regions disrupted conditioning of fear responses in the rats when the stress-induced fear responses were associated with a particular environment (e.g., the chamber where an electric footshock occurred)[230].

The effects of the SSCI, LM-4131, on stress-induced fear-related behavior in the mice were not confounded by cognitive deficits in spatial learning and memory or an animal's willingness to explore a novel environment. LM-4131 at a dose of 10 mg/kg compared to vehicle did not cause any changes in the number of entries in each arm in the Y-maze test under both basal and acute stress exposure conditions (Fig, 13c, left panel). With respect to the effect of LM-4131 on the number of entries in each arm of the Y-maze under basal (no stress) conditions, two-way ANOVA factoring drug dose and time revealed no significant effect of drug dose ($F_{(1, 48)}$ = 0.3075, p = 0.5818, *ns*) and dose x arm interaction ($F_{(2, 48)}$ = 0.1829, p = 0.8334, *ns*), but a significant effect of which arm was entered ($F_{(2, 48)}$ = 3.196, p = 0.0498, *p < 0.05). Relating to the effect of LM-4131

on the number of entries in each arm of the Y-maze 8h after acute stress exposure, two -way ANOVA factoring drug dose and time also revealed no significant effect of drug dose ($F_{(1, 48)}$ = 1.836, p = 0.1818, *ns*) and dose x arm interaction ($F_{(2, 48)}$ = 0.4066, p = 0.6682, *ns*), but a significant effect of which arm was entered ($F_{(2, 48)}$ = 8.511, p = 0.0007, ***p < 0.001). LM-4131 at a dose of 10 mg/kg compared to vehicle did not cause any changes in the total number of arm entries in the Y-maze test under both basal and acute stress exposure conditions (Fig, 13c, middle left panel). Pertaining to the effect of LM-4131 on the total number of arm entries in the Y-maze under basal conditions, an independent samples (unpaired) *t* test revealed no significant difference between the vehicle and LM-4131 treatment groups (t (16) = 0.5525; p = 0.5883, *ns*). The sample means are displayed in Figure 13c, which shows that the mice treated with LM-4131 (10 mg/kg) scored similar on the total number of arm entries in the Y-maze to the mice treated with vehicle (for LM-4131 treatment group, means ± s.e.m. = 59.75 ± 4.515, N = 8; for vehicle treatment group, means ± s.e.m. = 64.40 ± 6.580, N = 10). In connection with the effect of LM-4131 on the total number of arm entries in the Y-maze 8h after acute stress exposure, an independent samples (unpaired) *t* test revealed no significant difference between the vehicle and LM-4131 treatment groups (t (16) = 1.090; p = 0.2921, *ns*). The sample means are displayed in Figure 13c, which shows that the mice treated with LM-4131 (10 mg/kg) scored similar on the total number of arm entries in the Y-maze to the mice treated with vehicle (for LM-4131 treatment group, means ± s.e.m. = 54.00 ± 7.461, N = 9; for vehicle treatment group, means ± s.e.m. = 63.11 ± 3.777, N = 9). LM-4131 at a dose of 10 mg/kg compared to vehicle did not cause any changes in percentage spontaneous alternation in the Y-maze test under both basal and acute stress exposure conditions (Fig, 13c, middle panel). About the effect of LM-4131 on percentage spontaneous alternation in the Y-maze under basal conditions, an independent samples (unpaired) *t* test revealed no significant difference

between the vehicle and LM-4131 treatment groups (t (16) = 1.255; p = 0.2274, *ns*). The sample means are displayed in Figure 13c, which shows that the mice treated with LM-4131 (10 mg/kg) scored similar on percentage spontaneous alternation in the Y-maze to the mice treated with vehicle (for LM-4131 treatment group, means ± s.e.m. = 27.50 ± 3.410, N = 8; for vehicle treatment group, means ± s.e.m. = 21.60 ± 3.201, N = 10). In regard to the effect of LM-4131 on percentage spontaneous alternation in the Y-maze 8h after acute stress exposure, an independent samples (unpaired) t test revealed no significant difference between the vehicle and LM-4131 treatment groups (t (16) = 0.1551; p = 0.8787, *ns*). The sample means are displayed in Figure 13c, which shows that the mice treated with LM-4131 (10 mg/kg) scored similar on percentage spontaneous alternation in the Y-maze to the mice treated with vehicle (for LM-4131 treatment group, means ± s.e.m. = 23.30 ± 4.291, N = 9; for vehicle treatment group, means ± s.e.m. = 22.55 ± 2.140, N = 9). LM-4131 at a dose of 10 mg/kg compared to vehicle did not cause any changes in mean speed in the Y-maze test under both basal and acute stress exposure conditions (Fig, 13c, middle right panel). In connection with the effect of LM-4131 on mean speed in the Y-maze under basal conditions, an independent samples (unpaired) t test revealed no significant difference between the vehicle and LM-4131 treatment groups (t (16) = 1.844; p = 0.0838, *ns*). The sample means are displayed in Figure 13c, which shows that the mice treated with LM-4131 (10 mg/kg) scored similar on mean speed in the Y-maze to the mice treated with vehicle (for LM-4131 treatment group, means ± s.e.m. = 0.02825 ± 0.002102, N = 8; for vehicle treatment group, means ± s.e.m. = 0.0328 ± 0.001436, N = 10). With respect to the effect of LM-4131 on mean speed in the Y-maze 8h after acute stress exposure, an independent samples (unpaired) t test revealed no significant difference between the vehicle and LM-4131 treatment groups (t (16) = 0.3315; p = 0.7446, *ns*). The sample means are displayed in Figure 13c, which shows that the mice treated

with LM-4131 (10 mg/kg) scored similar on mean speed in the Y-maze to the mice treated with vehicle (for LM-4131 treatment group, means ± s.e.m. = 0.02978 ± 0.004146, $N = 9$; for vehicle treatment group, means ± s.e.m. = 0.03122 ± 0.001341, $N = 9$). LM-4131 at a dose of 10 mg/kg compared to vehicle did not cause any changes in total distance traveled in the Y-maze test under both basal and acute stress exposure conditions (Fig, 13c, right panel). Pertaining to the effect of LM-4131 on total distance traveled in the Y-maze under basal conditions, an independent samples (unpaired) *t* test revealed no significant difference between the vehicle and LM-4131 treatment groups (t (16) = 1.887; $p = 0.0775$, *ns*). The sample means are displayed in Figure 13c, which shows that the mice treated with LM-4131 (10 mg/kg) scored similar on total distance traveled in the Y-maze to the mice treated with vehicle (for LM-4131 treatment group, means ± s.e.m. = 16.90 ± 1.271, $N = 8$; for vehicle treatment group, means ± s.e.m. = 19.68 ± 0.8419, $N = 10$). In regard to the effect of LM-4131 on total distance traveled in the Y-maze 8h after acute stress exposure, an independent samples (unpaired) *t* test revealed no significant difference between the vehicle and LM-4131 treatment groups (t (16) = 0.3526; $p = 0.7290$, *ns*). The sample means are displayed in Figure 13c, which shows that the mice treated with LM-4131 (10 mg/kg) scored similar on total distance traveled in the Y-maze to the mice treated with vehicle (for LM-4131 treatment group, means ± s.e.m. = 17.93 ± 2.474, $N = 9$; for vehicle treatment group, means ± s.e.m. = 18.84 ± 0.7769, $N = 9$).

Next, we wanted to ensure that the effect of the SSCI, LM-4131, on stress-induced fear-related behavior was not dependent upon the time cued fear extinction and retrieval was performed after fear conditioning. Thus, we performed cued fear extinction 24 hours after fear conditioning and cued fear retrieval 48 hours after fear conditioning. During the cued fear extinction and

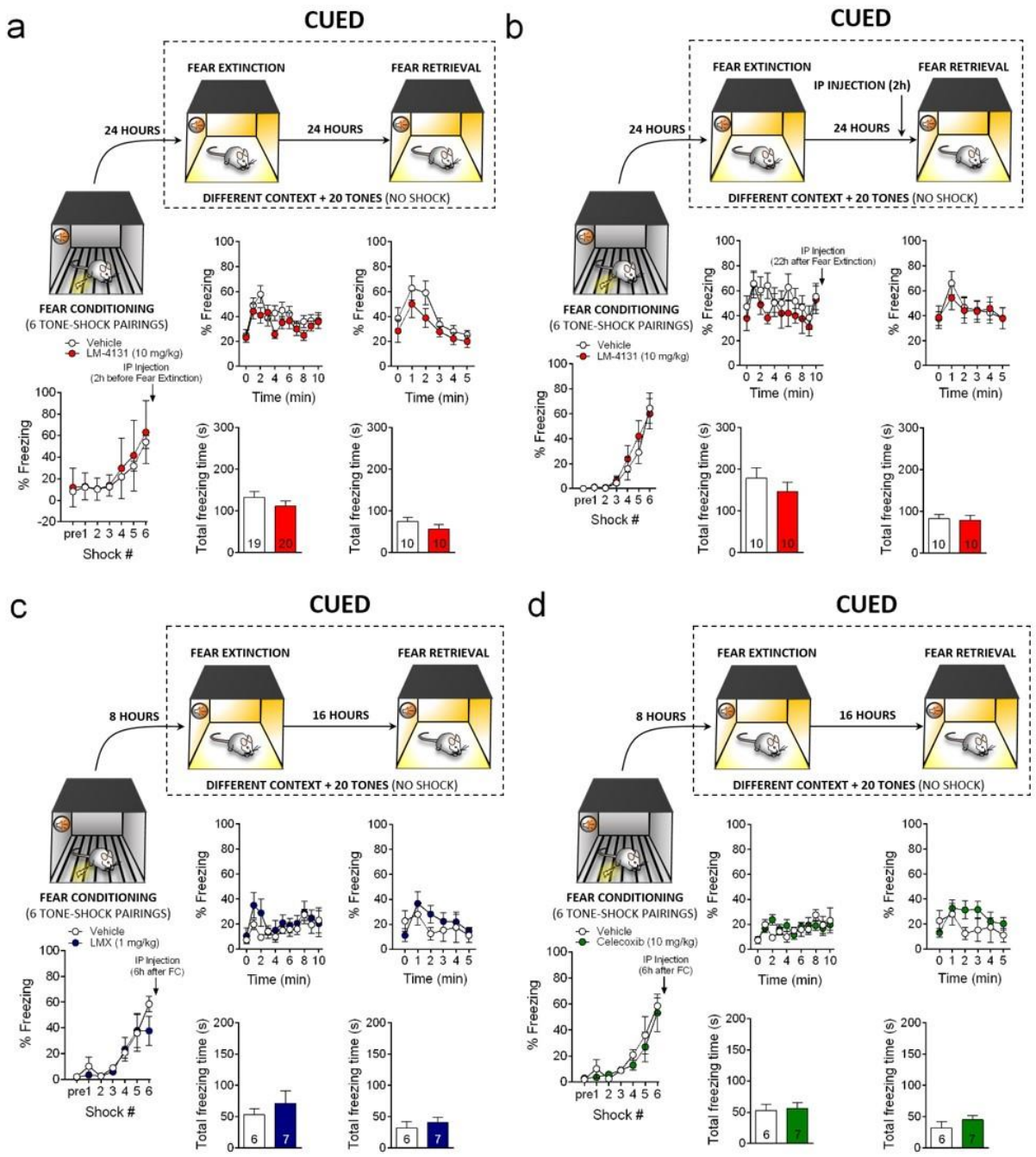

Figure 14. COX-2 inhibitors do not affect amygdala-dependent fear memory processes. (**a-d**) Diagram (top) of experimental design for context conditioning and cued fear extinction and retrieval. Freezing behavior (beneath diagram) during context conditioning (left) and cued fear extinction (middle) and retrieval (right). Data are shown as the mean ± s.e.m. Statistical significance was calculated by two-tailed unpaired Student's *t*-test or two-way ANOVA with post hoc Holm-Sidak's multiple comparisons test and time x treatment effect as a source of variation between vehicle and COX-2 inhibitor treatment groups (LM-4131, LMX, or celecoxib).

retrieval tests, we found no changes in the freezing behavior of the mice treated with LM-4131 compared to mice treated with vehicle. We found no significant differences in the freezing

behavior of the mice before i.p. administration of vehicle or LM-4131 after subjecting the mice to six tone-footshock pairings. Concerning the effect of six tone-electric footshock pairings on freezing behavior, two-way ANOVA factoring drug dose and time revealed no effect of drug dose x time interaction ($F_{(6, 245)} = 0.4506$; $p = 0.8442$, *ns*), but a significant effect of drug dose ($F_{(1, 245)} = 4.075$, $p = 0.0446$, $^{*}p < 0.05$) and time ($F_{(6, 245)} = 35.37$, $^{****}p < 0.0001$; Fig. 14a (left panel)). Post hoc Holm-Sidak's multiple comparisons test revealed no difference in percentage freezing after the administration of each tone-footshock pairing in a cohort of mice that will be treated with LM-4131 at a dose of 10 mg/kg compared to mice that will be treated with vehicle. We also found no significant differences in the freezing behavior of the vehicle-treated or LM-4131-treated mice elicited by a tone that was paired with the electric footshock once we placed the mice in the same chamber in which the aversive electric footshock was previously experienced but with a white smooth floor contextual insert that was positioned over the grid floor and a white curved wall contextual insert. Two-way ANOVA factoring drug dose and time revealed a significant effect of drug dose ($F_{(1, 407)} = 7.356$; $p = 0.0070$, $^{**}p < 0.01$) and time ($F_{(10, 407)} = 3.651$; $p = 0.0001$, $^{***}p < 0.001$), but no significant effect of dose x time interaction ($F_{(10, 407)} = 0.7554$; $p = 0.6719$, *ns*; Fig.14a (middle top panel)). Post hoc Holm-Sidak's multiple comparisons test revealed no difference in percentage freezing during any time point of the fear extinction test in LM-4131-treated mice compared to vehicle-treated mice. An independent samples (unpaired) *t* test revealed no significant difference in total freezing time during the fear extinction test between the vehicle and LM-4131 treatment group (t (37) = 1.160, $p = 0.2536$, *ns*, LM-4131 vs. vehicle). The sample means are displayed in Figure 14a (right bottom panel), which shows that the mice treated with LM-4131 (10 mg/kg) scored similar on total freezing time to the mice treated with vehicle (for LM-4131 treatment group, means ± s.e.m. = 111.5 ± 11.72, $N = 20$; for vehicle treatment group,

means ± s.e.m. = 132.3 ± 13.74, N = 19). We obtained similar results in the freezing behavior of the mice when we examined the effects of LM-4131 on the recovery of the extinguished fear (e.g., fear retrieval or recall) in the mice. Two-way ANOVA factoring drug dose and time revealed a significant effect of drug dose ($F_{(1, 108)}$ = 5.493; p = 0.0209, *p < 0.05) and time ($F_{(5, 108)}$ = 6.785; ****p < 0.0001), but no significant effect of dose x time interaction ($F_{(5, 108)}$ = 0.3130; p = 0.9043, *ns*; Fig.13a (right top panel)). Post hoc Holm-Sidak's multiple comparisons test revealed no changes in percentage freezing at any time point in the vehicle-treated mice compared to the LM-4131-treated mice. An independent samples (unpaired) *t* test revealed no significant difference in total freezing time during the fear retrieval test between the vehicle and LM-4131 treatment group (t (18) = 1.176, p = 0.2550, *ns*, LM-4131 vs. vehicle). The sample means are displayed in Figure 14a (right bottom panel), which shows that the mice treated with LM-4131 (10 mg/kg) scored similar on total freezing time to the mice treated with vehicle (for LM-4131 treatment group, means ± s.e.m. = 56.20 ± 10.83, N = 10; for vehicle treatment group, means ± s.e.m. = 74.10 ± 10.71, N = 10).

We also investigated if the effect of the SSCI, LM-4131, on stress-induced fear-related behavior was dependent upon when the SSCI was administered after fear conditioning. Thus, we performed cued fear extinction 24 hours after fear conditioning and cued fear retrieval 48 hours after fear conditioning, but administered LM-4131 two hours before performing the fear retrieval test. During the cued fear retrieval test, we found no changes in the freezing behavior of the mice treated with LM-4131 compared to mice treated with vehicle. We found no significant differences in the freezing behavior of the mice before i.p. administration of vehicle or LM-4131 after subjecting the mice to six tone-footshock pairings. With respect to the effect of six tone-electric footshock pairings on freezing behavior, two-way ANOVA factoring drug dose and time revealed

no effect of drug dose x time interaction ($F_{(6, 112)} = 0.3056$; $p = 0.9329$, *ns*) and drug dose ($F_{(1, 112)} = 0.4689$; $p = 0.4949$, *ns*), but a significant effect of time ($F_{(6, 112)} = 20.17$, ****$p < 0.0001$; Fig. 14b (left panel)). We also found no significant differences in the freezing behavior of the mice elicited by a tone that was paired with the electric footshock once we placed the mice in the same chamber in which the aversive electric footshock was previously experienced but with a white smooth floor contextual insert that was positioned over the grid floor and a white curved wall contextual insert. Two-way ANOVA factoring drug dose and time revealed a significant effect of drug dose ($F_{(1, 154)} = 5.309$; $p = 0.0226$, *$p < 0.05$), but no significant effect of time ($F_{(10, 154)} = 1.355$; $p = 0.2064$, *ns*) and dose x time interaction ($F_{(10, 154)} = 0.3267$; $p = 0.9730$, *ns*; Fig.14b (middle top panel)). Post hoc Holm-Sidak's multiple comparisons test revealed no difference in percentage freezing during any time point of the fear extinction test in the LM-4131-treated mice compared to the vehicle-treated mice. An independent samples (unpaired) *t* test revealed no significant difference in total freezing time during the fear extinction test between the vehicle and LM-4131 treatment group (t (14) = 0.9080, $p = 0.3792$, *ns*, LM-4131 vs. vehicle). The sample means are displayed in Figure 14b (right bottom panel), which shows that the mice that will be treated with LM-4131 (10 mg/kg) scored similar on total freezing time to the mice that will be treated with vehicle (for LM-4131 treatment group, means ± s.e.m. = 146.2 ± 22.79, $N = 7$; for vehicle treatment group, means ± s.e.m. = 178.2 ± 25.45, $N = 9$). We obtained similar results in the freezing behavior of the mice when we examined the effects of LM-4131 on fear retrieval in the mice. Two-way ANOVA factoring drug dose and time revealed no significant effect of drug dose ($F_{(1, 108)} = 0.1410$, $p = 0.7080$, *ns*), time ($F_{(5, 108)} = 1.803$, $p = 0.1183$, *ns*), and dose x time interaction ($F_{(5, 108)} = 0.1900$, $p = 0.9658$, *ns*; Fig.14b (right top panel)). An independent samples (unpaired) *t* test revealed no significant difference in total freezing time during the fear retrieval

test between the vehicle and LM-4131 treatment group (t (18) = 0.2173, p = 0.8305, *ns*, LM-4131 vs. vehicle). The sample means are displayed in Figure 14b (right bottom panel), which shows that the mice treated with LM-4131 (10 mg/kg) scored similar on total freezing time to the mice treated with vehicle (for LM-4131 treatment group, means ± s.e.m. = 79.37 ± 11.75, N = 10; for vehicle treatment group, means ± s.e.m. = 82.71 ± 9.938, N = 10).

Since the SSCI, LM-4131, had no effect on cued fear extinction in juvenile male ICR mice 8h after fear conditioning, we determined if the other COX-2 inhibitors, LMX and celecoxib, would have a similar effect on cued fear extinction in the mice. We found no significant differences in the freezing behavior of the mice before i.p. administration of vehicle or LMX after subjecting the mice to six tone-footshock pairings. With regard to the effect of six tone-electric footshock pairings on freezing behavior, two-way ANOVA factoring drug dose and time revealed no effect of drug dose x time interaction ($F_{(6, 77)}$ = 0.6293; p = 0.7063, *ns*) or drug dose ($F_{(1, 77)}$ = 0.9836, p = 0.3244, *ns*), but a significant effect of time ($F_{(6, 77)}$ = 12.86, ****p < 0.0001; Fig. 14c (left panel)). We also found no significant differences in the freezing behavior of the vehicle-treated or LMX-treated mice during the fear extinction test. Two-way ANOVA factoring drug dose and time revealed no significant effect of drug dose ($F_{(1, 121)}$ = 3.523; p = 0.0629, *ns*), dose x time interaction ($F_{(10, 121)}$ = 0.4461, p = 0.9206, *ns*), or time ($F_{(10, 121)}$ = 1.461, p = 0.1622, *ns*; Fig. 14c (middle top panel)). An independent samples (unpaired) t test revealed no significant difference in total freezing time during the fear extinction test between the vehicle and LMX treatment group (t (11) = 0.7747, p = 0.4549, *ns*, LMX vs. vehicle). The sample means are displayed in Figure 14c (right bottom panel), which shows that the mice treated with LMX (1 mg/kg) scored similar on total freezing time to the mice treated with vehicle (for LMX treatment group, means ± s.e.m. = 71.40 ± 20.10, N = 7; for vehicle treatment group, means ± s.e.m. = 53.13

± 9.680, N = 6). We obtained similar results in the freezing behavior of the mice when we examined the effects of LMX on fear retrieval in the mice. Two-way ANOVA factoring drug dose and time revealed no significant effect of drug dose ($F_{(1, 66)}$ = 1.143, p = 0.2890, *ns*), time ($F_{(5, 66)}$ = 1.539, p = 0.1899, *ns*), or dose x time interaction ($F_{(5, 66)}$ = 0.7258, p = 0.6065, *ns*; Fig.14c (right top panel)). An independent samples (unpaired) t test revealed no significant difference in total freezing time during the fear retrieval test between the vehicle and LMX treatment group (t (11) = 0.6171, p = 0.5497, *ns*, LMX vs. vehicle). The sample means are displayed in Figure 14c (right bottom panel), which shows that the mice treated with LMX (1 mg/kg) scored similar on total freezing time to the mice treated with vehicle (for LMX treatment group, means ± s.e.m. = 40.37 ± 8.885, N = 7; for vehicle treatment group, means ± s.e.m. = 32.09 ± 10.14, N = 6). These results suggest that the SSCI, LMX, does not affect stress-induced fear-related behavior in an amygdala-dependent fashion.

We also found no significant differences in the freezing behavior of the mice before i.p. administration of vehicle or celecoxib after subjecting the mice to six tone-footshock pairings. Pertaining to the effect of six tone-electric footshock pairings on freezing behavior, two-way ANOVA factoring drug dose and time revealed no effect of drug dose x time interaction ($F_{(6, 77)}$ = 0.2328; p = 0.9646, *ns*) or drug dose ($F_{(1, 77)}$ = 0.8567, p = 0.3576, *ns*), but a significant effect of time ($F_{(6, 77)}$ = 15.03, ****p < 0.0001; Fig. 14d (left panel)). We as well found no significant differences in the freezing behavior of the vehicle-treated or celecoxib-treated mice during the fear extinction test. Two-way ANOVA factoring drug dose and time revealed no significant effect of drug dose ($F_{(1, 121)}$ = 0.2185, p = 0.6410, *ns*), dose x time interaction ($F_{(10, 121)}$ = 0.9731, p = 0.4704, *ns*), or time ($F_{(10, 121)}$ = 1.610, p = 0.1115, *ns*; Fig. 14d (middle top panel)). An independent samples (unpaired) t test revealed no significant difference in total freezing time during the fear extinction

test between the vehicle and celecoxib treatment group (t (11) = 0.2272, p = 0.8245, *ns*, celecoxib vs. vehicle). The sample means are displayed in Figure 14d (right bottom panel), which shows that the mice treated with celecoxib (10 mg/kg) scored similar on total freezing time to the mice treated with vehicle (for celecoxib treatment group, means ± s.e.m. = 56.16 ± 9.120, N = 7; for vehicle treatment group, means ± s.e.m. = 53.13 ± 9.680, N = 6). We obtained similar results in the freezing behavior of the mice when we examined the effects of celecoxib on fear retrieval in the mice. Two-way ANOVA factoring drug dose and time revealed no significant effect of drug dose ($F_{(1, 66)}$ = 3.310, p = 0.0734, *ns*), time ($F_{(5, 66)}$ = 1.088, p = 0.3756, *ns*), or dose x time interaction ($F_{(5, 66)}$ = 1.061, p = 0.3900, *ns*; Fig.14d (right top panel)). An independent samples (unpaired) t test revealed no significant difference in total freezing time during the fear retrieval test between the vehicle and celecoxib treatment group (t (11) = 1.119, p = 0.2870, *ns*, celecoxib vs. vehicle). The sample means are displayed in Figure 14d (right bottom panel), which shows that the mice treated with celecoxib (10 mg/kg) scored similar on total freezing time to the mice treated with vehicle (for celecoxib treatment group, means ± s.e.m. = 45.26 ± 6.624, N = 7; for vehicle treatment group, means ± s.e.m. = 32.09 ± 10.14, N = 6). These results suggest that the selective COX-2 inhibitor, celecoxib, does not affect stress-induced fear-related behavior in an amygdala-dependent fashion.

Next, we wanted to ensure that the effect of the SSCI, LM-4131, on stress-induced fear-related behavior was not dependent upon the time contextual fear extinction and retrieval was performed after fear conditioning. Thus, we performed contextual fear extinction 24 hours after fear conditioning and contextual fear retrieval 48 hours after fear conditioning. During the contextual fear extinction and retrieval tests, we found no changes in the freezing behavior of the mice treated with LM-4131 compared to mice treated with vehicle. We found a few

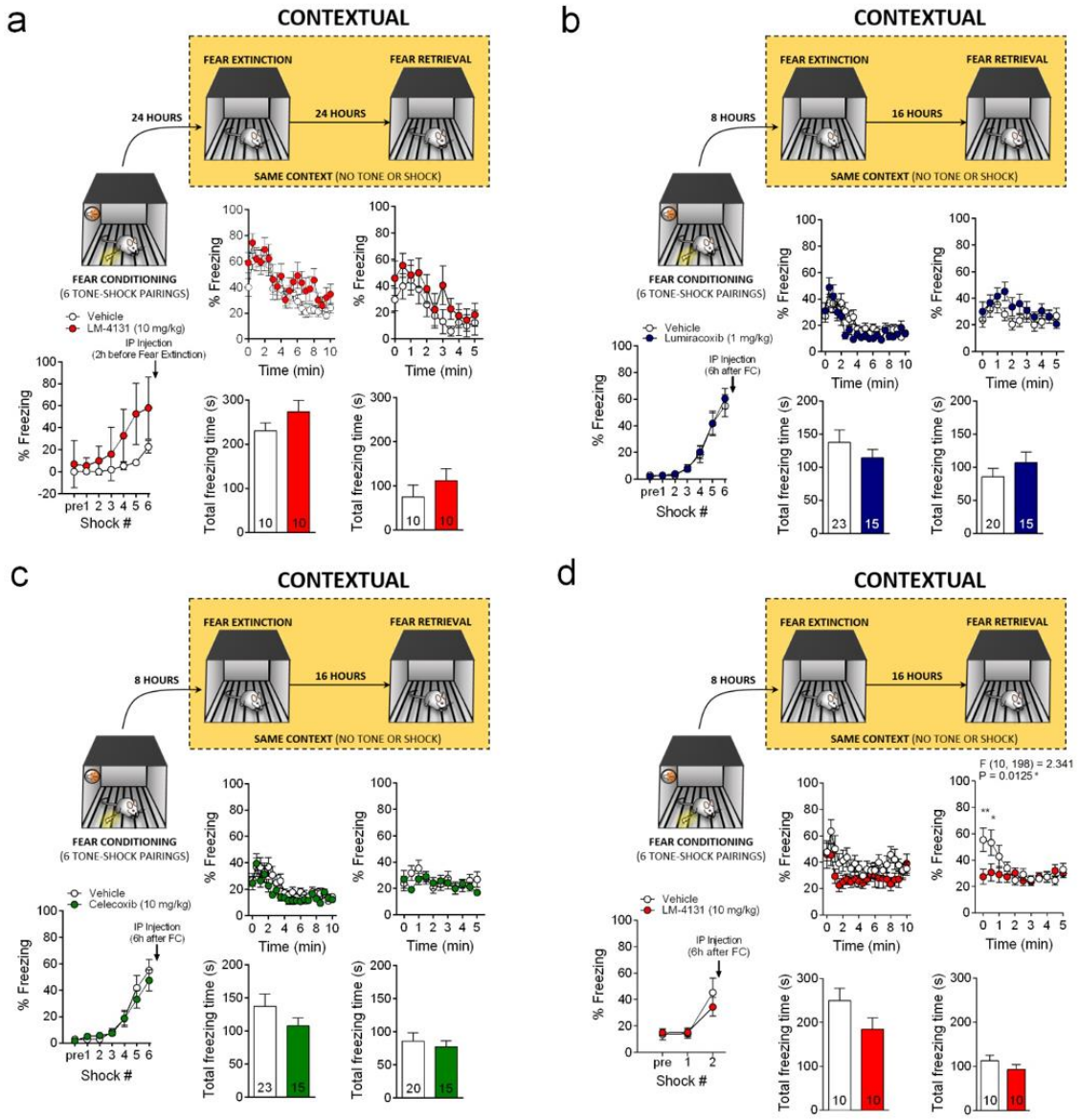

Figure 15. COX-2 inhibitors differentially affect both amygdala-dependent and hippocampal-dependent fear memory processes. (**a-d**) Diagram (top) of experimental design for context conditioning and contextual fear extinction and retrieval. Freezing behavior (beneath diagram) during context conditioning (left) and contextual fear extinction (middle) and retrieval (right) in ICR (CD-1) (**a-c**) and C57Bl/6J (**d**) juvenile male mice. Data are shown as the mean ± s.e.m. Statistical significance was calculated by two-tailed unpaired Student's *t*-test or two-way ANOVA with post hoc Holm-Sidak's multiple comparisons test and time x treatment effect as a source of variation between vehicle and COX-2 inhibitor treatment groups (LM-4131, LMX, or celecoxib).

significant differences in the freezing behavior of the mice before i.p. administration of vehicle or LM-4131 after subjecting the mice to six tone-footshock pairings. About the effect of six tone-electric footshock pairings on freezing behavior, two-way ANOVA factoring drug dose and time

revealed a significant effect of drug dose x time interaction ($F_{(6, 119)}$ = 3.825, p = 0.0016, **p < 0.01), drug dose ($F_{(1\ 119)}$ = 47.65, ****p < 0.0001), and time ($F_{(6, 119)}$ = 14.16, ****p < 0.0001; Fig. 15a (left panel)). Post hoc Holm-Sidak's multiple comparisons test revealed a significant decrease in percentage freezing in the juvenile male ICR mice after the 4th tone-footshock pairing (t (119) = 3.521, **p < 0.01, for LM-4131 treatment group, means ± s.e.m. = 32.77 ± 7.838, N = 10; for vehicle treatment group, means ± s.e.m. = 5.172 ± 7.838, N = 9), the 5th tone-footshock pairing (t (119) = 5.644, ****p < 0.0001, for LM-4131 treatment group, means ± s.e.m. = 52.52 ± 7.838; for vehicle treatment group, means ± s.e.m. = 8.286 ± 7.838), and the 6th tone-footshock pairing (t (119) = 4.505, ****p < 0.0001, for LM-4131 treatment group, means ± s.e.m. = 57.88 ± 7.838; for vehicle treatment group, means ± s.e.m. = 22.57 ± 7.838) of the fear conditioning session that will be treated at the 10 mg/kg dose of LM-4131 compared to the vehicle treatment. We found that the SSCI, LM-4131, did not affect contextual fear extinction in the mice 24 hours after exposure to the acute stress paradigm. Two-way ANOVA factoring drug dose and time revealed a significant effect of drug dose ($F_{(1, 367)}$ = 16.98, ****p < 0.0001) and time ($F_{(20, 367)}$ = 6.783, ****p < 0.0001), but no significant effect of dose x time interaction ($F_{(20, 367)}$ = 0.5172, p = 0.9593, *ns*; Fig.15a (middle top panel)). Post hoc Holm-Sidak's multiple comparisons test revealed no significant changes in percentage freezing in the juvenile male ICR mice during the fear extinction test at the 10 mg/kg dose of LM-4131 compared to the vehicle treatment. An independent samples (unpaired) t test revealed no significant difference in total freezing time during the fear extinction test between the vehicle and LM-4131 treatment group (t (18) = 1.348, p = 0.1943, *ns*, LM-4131 vs. vehicle). The sample means are displayed in Figure 15a (middle bottom panel), which shows that the mice treated with LM-4131 (10 mg/kg) scored similar on total freezing time compare to the mice treated with vehicle (for LM-4131 treatment group, means ± s.e.m. = 273.3 ± 26.29, N =

10; for vehicle treatment group, means ± s.e.m. = 230.2 ± 18.12, $N = 10$). We found no significant differences in the freezing behavior of the mice during fear retrieval 24 hours after exposure to the acute stress protocol. Two-way ANOVA factoring drug dose and time revealed a significant effect of drug dose ($F_{(1, 198)} = 6.974$, $p = 0.0089$, $^{**}p < 0.01$) and time ($F_{(10, 198)} = 3.846$, $p = 0.5928$, *ns*), but no significant effect of dose x time interaction ($F_{(10, 297)} = 0.6363$, $^{****}p < 0.0001$; Fig.15a (middle top panel)). Post hoc Holm-Sidak's multiple comparisons test revealed no significant difference in percentage freezing at any time point in the juvenile male ICR mice of the fear retrieval test at the 10 mg/kg dose of LM-4131 compared to the vehicle treatment. An independent samples (unpaired) *t* test revealed no significant difference in total freezing time during the fear retrieval test between the vehicle and LM-4131 treatment group (t (18) = 0.9704, $p = 0.3447$, *ns*, LM-4131 vs. vehicle). The sample means are displayed in Figure 15a (right bottom panel), which shows that the mice treated with LM-4131 (10 mg/kg) scored similar on total freezing time to the mice treated with vehicle (for LM-4131 treatment group, means ± s.e.m. = 111.8 ± 27.45, $N = 10$; for vehicle treatment group, means ± s.e.m. = 74.60 ± 26.69, $N = 10$).

Since the SSCI, LM-4131, had a significant effect on contextual fear extinction in juvenile male ICR mice 8h after fear conditioning, we determined if the other COX-2 inhibitors, LMX and celecoxib, would have a similar effect on contextual fear extinction in the mice. We found no significant differences in the freezing behavior of the mice before i.p. administration of vehicle or LMX after subjecting the mice to six tone-footshock pairings. With respect to the effect of six tone-electric footshock pairings on freezing behavior, two-way ANOVA factoring drug dose and time revealed no effect of drug dose x time interaction ($F_{(6, 189)} = 0.1034$, $p = 0.9960$, *ns*) and drug dose ($F_{(1\ 189)} = 0.1022$, $p = 0.7496$, *ns*), but a significant effect of time ($F_{(6, 189)} = 38.38$, $^{****}p < 0.0001$; Fig. 15b (left panel)). We found that the SSCI, LMX, slightly increased contextual fear

extinction by decreasing freezing behavior in the mice only 8 hours after exposure to the acute stress paradigm. Two-way ANOVA factoring drug dose and time revealed a significant effect of drug dose ($F_{(1, 693)}$ = 6.576, p = 0.0105, *p < 0.05) and time ($F_{(20, 693)}$ = 7.792, ****p < 0.0001), but no significant effect of dose x time interaction ($F_{(20, 693)}$ = 1.131, p = 0.3112, *ns*; Fig.15b (middle top panel)). An independent samples (unpaired) *t* test revealed no significant difference in total freezing time during the fear extinction test between the vehicle and LM-4131 treatment group (*t* (33) = 0.9626, p = 0.3428, *ns*, LMX vs. vehicle). The sample means are displayed in Figure 15b (middle bottom panel), which shows that the mice treated with LMX (1 mg/kg) scored similar on total freezing time compared to mice treated with vehicle (for LMX treatment group, means ± s.e.m. = 113.9 ± 12.92, N = 15; for vehicle treatment group, means ± s.e.m. = 137.3 ± 18.64, N = 20). We found no significant differences in the freezing behavior of the mice during fear retrieval 24 hours after exposure to the acute stress protocol. Two-way ANOVA factoring drug dose and time revealed a significant effect of drug dose ($F_{(1, 363)}$ = 7.377, p = 0.0069, **p < 0.01), but no significant effect of time ($F_{(10, 363)}$ = 1.620, p = 0.0989, *ns*) or dose x time interaction ($F_{(10, 363)}$ = 0.6414, p = 0.7782, *ns*; Fig.15b (middle top panel)). Post hoc Holm-Sidak's multiple comparisons test revealed no significant difference in percentage freezing at any time point in the juvenile male ICR mice of the fear retrieval test at the 1 mg/kg dose of LMX compared to the vehicle treatment. An independent samples (unpaired) *t* test revealed no significant difference in total freezing time during the fear retrieval test between the vehicle and LMX treatment group (*t* (33) = 1.067, p = 0.2939, *ns*, LMX vs. vehicle). The sample means are displayed in Figure 15b (right bottom panel), which shows that the mice treated with LMX (1 mg/kg) scored similar on total freezing time to the mice treated with vehicle (for LMX treatment group, means ± s.e.m. = 107.1 ± 15.90, N = 15; for vehicle treatment group, means ± s.e.m. = 85.55 ± 12.83, N = 20).

Thus, these results suggest that LMX can slightly decrease stress-induced fear-related behavior in a context-dependent manner. We found similar results with the selective COX-2 inhibitor, celecoxib. There were no significant differences in the freezing behavior of the mice before i.p. administration of vehicle or celecoxib after subjecting the mice to six tone-footshock pairings. Relating to the effect of six tone-electric footshock pairings on freezing behavior, two-way ANOVA factoring drug dose and time revealed no effect of drug dose x time interaction ($F_{(6, 189)}$ = 0.0.4124, p = 0.8703, *ns*) and drug dose ($F_{(1\ 189)}$ = 0.5459, p = 0.4609, *ns*), but a significant effect of time ($F_{(6, 189)}$ = 29.85, ****p < 0.0001; Fig. 15c (left panel)). We found that celecoxib slightly increased contextual fear extinction by decreasing freezing behavior in the mice 8 hours after exposure to the acute stress paradigm. Two-way ANOVA factoring drug dose and time revealed a significant effect of drug dose ($F_{(1, 693)}$ = 11.56, p = 0.0007, ***p < 0.001) and time ($F_{(20, 693)}$ = 5.949, ****p < 0.0001), but no significant effect of dose x time interaction ($F_{(20, 693)}$ = 0.6024, p = 0.9126, *ns*; Fig.15c (middle top panel)). An independent samples (unpaired) *t* test revealed no significant difference in total freezing time during the fear extinction test between the vehicle and celecoxib treatment group (t (33) = 1.244, p = 0.2223, *ns*, celecoxb vs. vehicle). The sample means are displayed in Figure 15c (middle bottom panel), which shows that the mice treated with celecoxib (10 mg/kg) scored similar on total freezing time compared to mice treated with vehicle (for celecoxib treatment group, means ± s.e.m. = 107.4 ± 12.10, N = 15; for vehicle treatment group, means ± s.e.m. = 137.3 ± 18.64, N = 20). We found no significant differences in the freezing behavior of the mice during fear retrieval 24 hours after exposure to the acute stress protocol. Two-way ANOVA factoring drug dose and time revealed no significant effect of drug dose ($F_{(1, 363)}$ = 1.399, p = 0.2377, *ns*), time ($F_{(10, 363)}$ = 0.8092, p = 0.6199, *ns*), or dose x time interaction ($F_{(10, 363)}$ = 0.6603, p = 0.7612, *ns*; Fig.15c (middle top panel)). An independent samples (unpaired)

t test revealed no significant difference in total freezing time during the fear retrieval test between the vehicle and celecoxib treatment group (t (33) = 0.4881, p = 0.6287, *ns*, celecoxib vs. vehicle). The sample means are displayed in Figure 15c (right bottom panel), which shows that the mice treated with celecoxib (10 mg/kg) scored similar on total freezing time to the mice treated with vehicle (for celecoxib treatment group, means ± s.e.m. = 77.33 ± 9.144, N = 15; for vehicle treatment group, means ± s.e.m. = 85.55 ± 12.83, N = 20).

Moreover, the effects of LM-4131 on contextual fear extinction and retrieval were not restricted to only the ICR mouse strain but could as well be observed in the C57BL/6J mouse strain. LM-4131 enhanced contextual fear extinction and retrieval in juvenile male C57BL/6J mice. We found no significant differences in the freezing behavior of the mice before i.p. administration of vehicle or LM-4131 after subjecting the mice to six tone-footshock pairings. Concerning the effect of six tone-electric footshock pairings on freezing behavior, two-way ANOVA factoring drug dose and time revealed no effect of drug dose x time interaction ($F_{(2, 48)}$ = 0.7317, p = 0.4864, *ns*) and drug dose ($F_{(1, 48)}$ = 0.3643, p = 0.5490, *ns*), but a significant effect of time ($F_{(2, 48)}$ = 12.95, ****p < 0.0001; Fig. 15d (left panel)). We found that the SSCI, LM-4131, significantly increased contextual fear extinction by decreasing freezing behavior in the C57BL/6J mice only 8 hours after exposure to the acute stress paradigm. Two-way ANOVA factoring drug dose and time revealed a significant effect of drug dose ($F_{(1, 378)}$ = 27.25, ****p < 0.0001) and time ($F_{(20, 378)}$ = 1.815, p = 0.0177), but no significant effect of dose x time interaction ($F_{(20, 378)}$ = 0.5734, p = 0.9302, *ns*; Fig.15d (middle top panel)). An independent samples (unpaired) t test revealed no significant difference in total freezing time during the fear extinction test between the vehicle and LM-4131 treatment group (t (18) = 1.701, p = 0.1061, *ns*, LM-4131 vs. vehicle). The sample means are displayed in Figure 15d (middle bottom panel), which shows that the mice treated with

LM-4131 (10 mg/kg) scored similar on total freezing time compared to the mice treated with vehicle (for LM-4131 treatment group, means ± s.e.m. = 184.7 ± 25.87, N = 10; for vehicle treatment group, means ± s.e.m. = 249.8 ± 28.15, N = 10). We found significant differences in the freezing behavior of the C57BL/6J mice during fear retrieval 24 hours after exposure to the acute stress protocol. Two-way ANOVA factoring drug dose and time revealed a significant effect of drug dose ($F_{(1, 198)}$ = 7.322, p = 0.0074, **p < 0.01), time ($F_{(10, 198)}$ = 2.729, p = 0.0036, **p < 0.01), and dose x time interaction ($F_{(10, 198)}$ = 2.341, p = 0.0125, *p < 0.05; Fig.15d (middle top panel)). Post hoc Holm-Sidak's multiple comparisons test revealed a significant difference in percentage freezing at the start of the fear retrieval test (e.g., 0.0 min time bin) (t (198) = 3.823, **p < 0.01, *ns*, LM-4131 vs. vehicle; for LM-4131 treatment group, means ± s.e.m. = 27.46 ± 7.326, N = 10; for vehicle treatment group, means ± s.e.m. = 55.47 ± 7.326, N = 10) and at the first 0.5 min time (t (198) = 3.089, *p < 0.05, *ns*, LM-4131 vs. vehicle; for LM-4131 treatment group, means ± s.e.m. = 30.65 ± 7.326, N = 10; for vehicle treatment group, means ± s.e.m. = 53.28 ± 7.326, N = 10) bin in the juvenile male C57BL/6J mice of the fear retrieval test at the 10 mg/kg dose of LM-4131 compared to the vehicle treatment. An independent samples (unpaired) t test revealed no significant difference in total freezing time during the fear retrieval test between the vehicle and LM-4131 treatment group (t (18) = 1.183, p = 0.2523, *ns*, LM-4131 vs. vehicle). The sample means are displayed in Figure 15d (right bottom panel), which shows that the mice treated with LM-4131 (10 mg/kg) scored similar on total freezing time to the mice treated with vehicle (for LM-4131 treatment group, means ± s.e.m. = 92.86 ± 10.70, N = 10; for vehicle treatment group, means ± s.e.m. = 112.6 ± 12.78, N = 10).

Since the SSCI, LM-4131, had a significant effect on contextual fear extinction, but no effect on cued fear extinction, in juvenile male ICR mice 8h after acute (1 day) fear conditioning,

we determined if LM-4131 would have a similar effect in the mice 8h after chronic (5 days) fear conditioning. We found no significant differences in the freezing behavior of the mice before i.p. administration of vehicle or LM-4131 after subjecting the mice to five days of six tone-footshock pairings per day. With reference to the effect of six tone-electric footshock pairings per day on freezing behavior, two-way ANOVA factoring drug dose and time revealed no effect of drug dose x time interaction ($F_{(13, 196)} = 1.147$, $p = 0.3220$, *ns*) and drug dose ($F_{(1, 196)} = 0.4780$, $p = 0.4901$, *ns*), but a significant effect of time ($F_{(13, 196)} = 19.96$, ****$p < 0.0001$; Fig. 16a (left panel)). We found that the SSCI, LM-4131, did not affect cued fear extinction in the mice only 8 hours after exposure to the chronic stress paradigm. Two-way ANOVA factoring drug dose and time revealed no significant effect of drug dose ($F_{(1, 154)} = 3.451$, $p = 0.0651$, *ns*) and dose x time interaction ($F_{(10, 154)} = 0.3604$, $p = 0.9616$, *ns*), but a slightly significant effect of time ($F_{(10, 154)} = 2.172$, $p = 0.0222$, *$p < 0.05$; Fig.16a (middle top panel)). An independent samples (unpaired) *t* test revealed no significant difference in total freezing time during the fear extinction test between the vehicle and LM-4131 treatment group (t (14) = 0.9251, $p = 0.3706$, *ns*, LM-4131 vs. vehicle). The sample means are displayed in Figure 16a (middle bottom panel), which shows that the mice treated with LM-4131 (10 mg/kg) scored similar on total freezing time compared to mice treated with vehicle (for LM-4131 treatment group, means ± s.e.m. = 107.7 ± 22.74, $N = 8$; for vehicle treatment group, means ± s.e.m. = 132.9 ± 14.94, $N = 8$). We found no significant differences in the freezing behavior of the mice during fear retrieval 24 hours after exposure to the chronic stress protocol. Two-way ANOVA factoring drug dose and time revealed no significant effect of drug dose ($F_{(1, 84)} = 0.8466$, $p = 0.3601$, *ns*) or dose x time interaction ($F_{(5, 84)} = 0.1843$, $p = 0.9678$, *ns*), but a

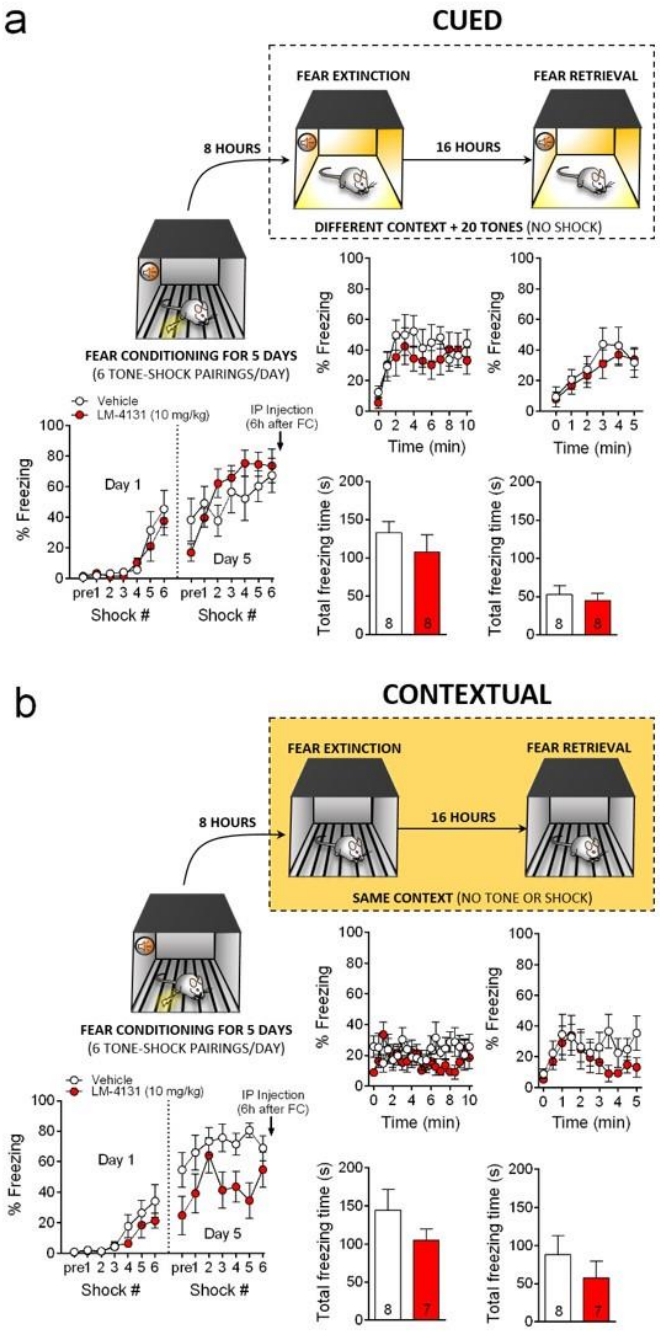

Figure 16. Substrate-selective COX-2 inhibition does not affect amygdala-dependent fear memory processes after chronic stress exposure. (**a, b**) Diagram (top) of experimental design for context conditioning and cued fear extinction and retrieval. Freezing behavior (beneath diagram) during context conditioning (left) and cued fear extinction (middle) and retrieval (right). During context conditioning, a tone, the conditional stimulus (CS), was paired with a footshock, the unconditional stimulus (US), six times daily for five days. Data are shown as the mean ± s.e.m. Statistical significance was calculated by two-tailed unpaired Student's *t*-test or two-way ANOVA with post hoc Holm-Sidak's multiple comparisons test and time x treatment effect as a source of variation between vehicle and LM-4131 treatment groups.

significant effect of time ($F_{(5, 84)} = 4.210$, $p = 0.0018$, $^{**}p < 0.01$); Fig.16a (middle top panel)). An

independent samples (unpaired) *t* test revealed no significant difference in total freezing time during the fear retrieval test between the vehicle and LM-4131 treatment group (t (14) = 0.5354, p = 0.6008, *ns*, LM-4131 vs. vehicle). The sample means are displayed in Figure 16a (right bottom panel), which shows that the mice treated with LM-4131 (10 mg/kg) scored similar on total freezing time to the mice treated with vehicle (for LM-4131 treatment group, means ± s.e.m. = 44.91 ± 9.142, N = 8; for vehicle treatment group, means ± s.e.m. = 52.78 ± 11.51, N = 8). Thus, these results suggest that LM-4131 does not affect chronic stress-induced fear-related behavior in an amygdala-dependent manner. We found similar results with LM-4131 when mice were subjected to chronic fear conditioning and tested for contextual fear extinction and retrieval. There were slight significant differences in the freezing behavior of the mice before i.p. administration of vehicle or LM-4131 after subjecting the mice to five days of six tone-footshock pairings per day. With respect to the effect of five days of six tone-electric footshock pairings on freezing behavior, two-way ANOVA factoring drug dose and time revealed no effect of drug dose x time interaction ($F_{(13, 182)}$ = 1.644, p = 0.0768, *ns*), but a significant effect of drug dose ($F_{(1, 182)}$ = 26.07, ****p < 0.0001) and time ($F_{(13, 182)}$ = 20.26, ****p < 0.0001; Fig. 16b (left panel)). Post hoc Holm-Sidak's multiple comparisons test revealed a significant decrease in percentage freezing in the juvenile male ICR mice after the 3rd tone-footshock pairing of the last day (e.g., day 5) of fear conditioning (t (182) = 2.977, *p < 0.05, for LM-4131 treatment group, means ± s.e.m. = 41.34 ± 11.55, N = 7; for vehicle treatment group, means ± s.e.m. = 75.73 ± 11.55, N = 8) and the 5th tone-footshock pairing of the last day of fear conditioning (t (182) = 3.985, **p < 0.01, for LM-4131 treatment group, means ± s.e.m. = 34.61 ± 11.55; for vehicle treatment group, means ± s.e.m. = 80.64 ± 11.55) of the chronic fear conditioning session that will be treated at the 10 mg/kg dose of LM-4131 compared to the vehicle treatment. We found that LM-4131 slightly increased

contextual fear extinction by decreasing freezing behavior in the mice 8 hours after exposure to the chronic stress paradigm. Two-way ANOVA factoring drug dose and time revealed a significant effect of drug dose ($F_{(1, 273)} = 8.992$, $p = 0.0030$, $^{**}p < 0.01$), but no significant effect of time ($F_{(20, 273)} = 0.3257$, $p = 0.9977$, *ns*) and dose x time interaction ($F_{(20, 273)} = 1.035$, $p = 0.4204$, *ns*; Fig.16b (middle top panel)). An independent samples (unpaired) *t* test revealed no significant difference in total freezing time during the fear extinction test between the vehicle and LM-4131 treatment group (t (13) = 1.232, $p = 0.2397$, *ns*, LM-4131 vs. vehicle). The sample means are displayed in Figure 16b (middle bottom panel), which shows that the mice treated with LM-4131 (10 mg/kg) scored similar on total freezing time compared to mice treated with vehicle (for LM-4131 treatment group, means ± s.e.m. = 105.2 ± 14.45, $N = 7$; for vehicle treatment group, means ± s.e.m. = 144.6 ± 26.95, $N = 8$). We found a slight significant difference in the freezing behavior of the mice during fear retrieval 24 hours after exposure to the chronic stress protocol. Two-way ANOVA factoring drug dose and time revealed a significant effect of drug dose ($F_{(1, 143)} = 5.752$, $p = 0.0178$, $^{*}p < 0.05$), but no significant effect of time ($F_{(10, 143)} = 1.279$, $p = 0.2476$, *ns*) or dose x time interaction ($F_{(10, 143)} = 0.4936$, $p = 0.8920$, *ns*; Fig.16b (middle top panel)). An independent samples (unpaired) *t* test revealed no significant difference in total freezing time during the fear retrieval test between the vehicle and LM-4131 treatment group (t (13) = 0.9011, $p = 0.3839$, *ns*, LM-4131 vs. vehicle). The sample means are displayed in Figure 16b (right bottom panel), which shows that the mice treated with LM-4131 (10 mg/kg) scored similar on total freezing time to the mice treated with vehicle (for LM-4131 treatment group, means ± s.e.m. = 57.80 ± 21.44, $N = 7$; for vehicle treatment group, means ± s.e.m. = 88.02 ± 25.10, $N = 8$).

Since stress-induced anxiety-like behavior reduced by substrate-selective COX-2 inhibition is mediated in a non-cannabinoid receptor fashion, we wanted to determine if stress-

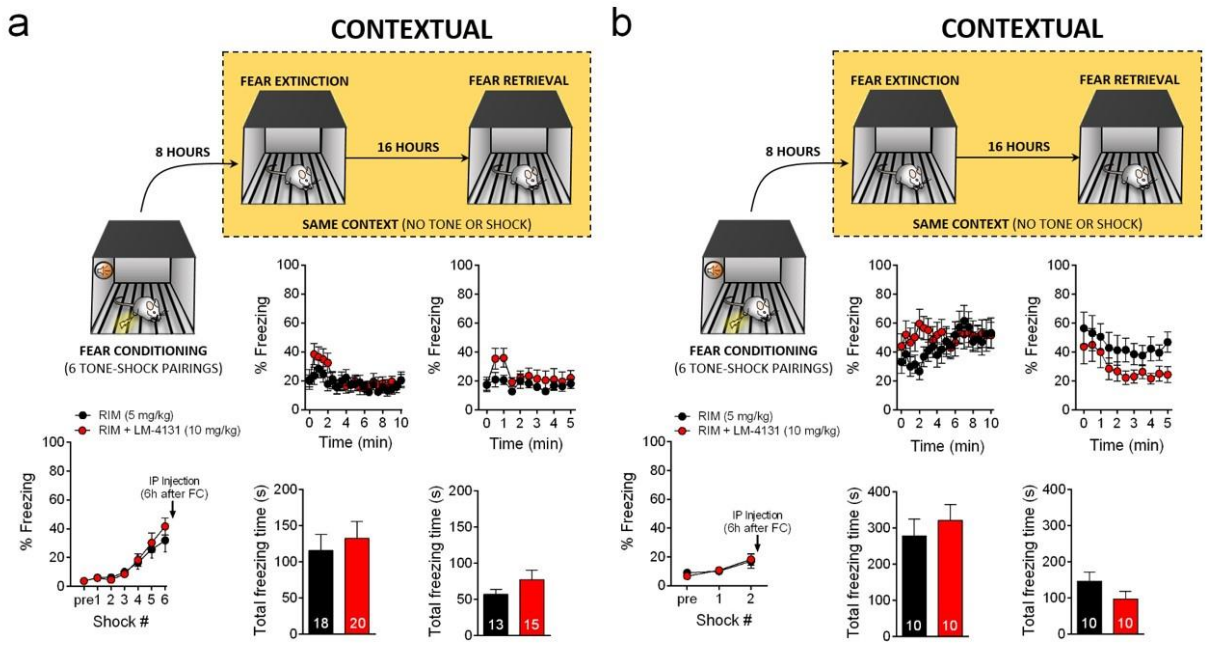

Figure 17. Modulation of contextual fear memory processes by substrate-selective COX-2 inhibition is CB_1 receptor-dependent. (**a, b**) Diagram (top) of experimental design for context conditioning and contextual fear extinction and retrieval. Freezing behavior (beneath diagram) during context conditioning (left) and contextual fear extinction (middle) and retrieval (right) in ICR (CD-1) (**a**) and C57Bl/6J (**b**) juvenile male mice. Data are shown as the mean ± s.e.m. Statistical significance was calculated by two-tailed unpaired Student's *t*-test or two-way ANOVA with post hoc Holm-Sidak's multiple comparisons test and time x treatment effect as a source of variation between rimonbant and co-administered rimonabant and LM-4131 treatment groups.

induced fear-related behavior was also mediated in a non-cannabinoid receptor manner. We found that regardless of mouse strain, stress-induced fear-related behavior is mediated by the cannabinoid type 1 receptor when it is context dependent. During fear conditioning of juvenile male ICR mice, we found no significant differences in the freezing behavior of the mice before i.p. administration of the CB_1R antagonist, rimonabant (5 mg/kg), or co-administration of rimonabant and LM-4131 after subjecting the mice to six tone-footshock pairings. Regarding the effect of six tone-electric footshock pairings on freezing behavior, two-way ANOVA factoring drug dose and time revealed no effect of drug dose x time interaction ($F_{(6, 252)} = 0.4851$, $p = 0.8192$, *ns*) and drug dose ($F_{(1, 252)} = 0.6801$, $p = 0.4103$, *ns*), but a significant effect of time ($F_{(6, 252)} = 18.96$, ****$p < 0.0001$; Fig. 17a (left panel)). We found that the CB_1R antagonist, rimonabant, blocked the previously observed increase in contextual fear extinction (see Fig. 13b (middle panel)) by increasing freezing behavior

in the mice co-treated with LM-4131 and rimonabant only 8 hours after exposure to the acute stress paradigm. Two-way ANOVA factoring drug dose and time revealed no significant effect of drug dose ($F_{(1, 756)} = 2.988$, $p = 0.0843$, *ns*) or dose x time interaction ($F_{(20, 756)} = 0.5714$, $p = 0.9329$, *ns*), but a significant effect of time ($F_{(20, 756)} = 2.224$, $^{**}p < 0.01$; Fig.17a (middle top panel)). An independent samples (unpaired) *t* test revealed no significant difference in total freezing time during the fear extinction test between the rimonabant treatment group and the rimonabant and LM-4131 treatment group (t (36) = 0.5272, $p = 0.6013$, *ns*, rimonabant + LM-4131 vs. rimonabant). The sample means are displayed in Figure 17a (middle bottom panel), which shows that the mice co-treated with rimonabant (5 mg/kg) and LM-4131 (10 mg/kg) scored similar on total freezing time compared to the mice treated with rimonabant (for rimonabant and LM-4131 co-treatment group, means ± s.e.m. = 132.6 ± 23.02, $N = 20$; for rimonabant treatment group, means ± s.e.m. = 115.6 ± 22.54, $N = 18$). We found no significant differences in the freezing behavior of the mice during fear retrieval 24 hours after exposure to the acute stress protocol. Two-way ANOVA factoring drug dose and time revealed a significant effect of drug dose ($F_{(1, 286)} = 8.521$, $p = 0.0038$, $^{**}p < 0.01$), but no significant effect of time ($F_{(10, 286)} = 1.438$, $p = 0.1629$, *ns*) and dose x time interaction ($F_{(10, 286)} = 0.4615$, $p = 0.9138$, *ns*; Fig.17a (middle top panel)). Post hoc Holm-Sidak's multiple comparisons test revealed no significant difference in percentage freezing at any time point in the juvenile male ICR mice of the fear retrieval test at the 10 mg/kg dose of LM-4131 combined with the 5 mg/kg dose of rimonabant compared to the rimonabant treatment. An independent samples (unpaired) *t* test revealed no significant difference in total freezing time during the fear retrieval test between the rimonabant treatment group and the rimonabant and LM-4131 co-treatment group (t (26) = 1.338, $p = 0.1924$, *ns*, rimonabant + LM-4131 vs. rimonabant). The sample means are displayed in Figure 17a (right bottom panel), which

shows that the mice co-treated with rimonabant (5 mg/kg) and LM-4131 (10 mg/kg) scored similar on total freezing time to the mice treated with rimonabant (for rimonabant and LM-4131 co-treatment group, means ± s.e.m. = 77.25 ± 12.97, $N = 15$; for rimonabant treatment group, means ± s.e.m. = 56.83 ± 6.632, $N = 13$). These results suggest that the CB_1R mediates LM-4131-induced decreases in fear elicited by acute stress exposure in a context-dependent manner.

In the juvenile male C57BL/6J mice, we found that the CB_1R also mediates the action of LM-4131 on stress-induced fear-related behavior when it is context dependent. During fear conditioning of juvenile male C57BL/6J mice, we found no significant differences in the freezing behavior of the mice before i.p. administration of the CB_1R antagonist, rimonabant (5 mg/kg), or co-administration of rimonabant and LM-4131 after subjecting the mice to six tone-footshock pairings. As to the effect of six tone-electric footshock pairings on freezing behavior, two-way ANOVA factoring drug dose and time revealed no effect of drug dose x time interaction ($F_{(2, 54)} = 0.2055$, $p = 0.8149$, *ns*) and drug dose ($F_{(1, 54)} = 0.002349$, $p = 0.9615$, *ns*), but a significant effect of time ($F_{(2, 54)} = 5.993$, $p = 0.0045$, $^{**}p < 0.01$; Fig. 17b (left panel)). As seen in the juvenile male ICR mice, we found that the CB_1R antagonist, rimonabant, blocked the previously observed increase in contextual fear extinction (see Fig. 15d (middle panel)) by increasing freezing behavior in the C57BL/6J mice co-treated with LM-4131 and rimonabant only 8 hours after exposure to the acute stress paradigm. Two-way ANOVA factoring drug dose and time revealed no significant effect of drug dose ($F_{(1, 18)} = 0.4501$, $p = 0.5108$, *ns*), but a slightly significant effect of dose x time interaction ($F_{(20, 360)} = 1.786$, $p = 0.0207$, $^{*}p < 0.05$) and time ($F_{(20, 360)} = 1.718$, , $p = 0.0288$, $^{*}p < 0.05$; Fig.17b (middle top panel)). An independent samples (unpaired) *t* test revealed no significant difference in total freezing time during the fear extinction test between the rimonabant treatment group and the rimonabant and LM-4131 treatment group (t (18) = 0.6712, $p = 0.5106$, *ns*,

rimonabant + LM-4131 vs. rimonabant). The sample means are displayed in Figure 17b (middle bottom panel), which shows that the mice co-treated with rimonabant (5 mg/kg) and LM-4131 (10 mg/kg) scored similar on total freezing time compared to the mice treated with rimonabant (for rimonabant and LM-4131 co-treatment group, means ± s.e.m. = 321.6 ± 43.29, N = 10; for rimonabant treatment group, means ± s.e.m. = 279.0 ± 46.44, N = 10). We found no significant differences in the freezing behavior of the mice during fear retrieval 24 hours after exposure to the acute stress protocol. Two-way ANOVA factoring drug dose and time revealed no significant effect of drug dose ($F_{(1, 18)}$ = 2.240, p = 0.1518, *ns*) or dose x time interaction ($F_{(10, 180)}$ = 0.4587, p = 0.9145, *ns*), but a significant effect of time ($F_{(10, 180)}$ = 5.130, ****p < 0.0001; Fig.17b (middle top panel)). An independent samples (unpaired) t test revealed no significant difference in total freezing time during the fear retrieval test between the rimonabant treatment group and the rimonabant and LM-4131 co-treatment group (t (18) = 1.497, p = 0.1518, *ns*, rimonabant + LM-4131 vs. rimonabant). The sample means are displayed in Figure 17b (right bottom panel), which shows that the mice co-treated with rimonabant (5 mg/kg) and LM-4131 (10 mg/kg) scored similar on total freezing time to the mice treated with rimonabant (for rimonabant and LM-4131 co-treatment group, means ± s.e.m. = 97.71 ± 20.83, N = 10; for rimonabant treatment group, means ± s.e.m. = 147.0 ± 25.48, N = 10).

Our acute and chronic stress paradigms using Pavlovian fear conditioning models maladaptive fear, which is fear that is continual or easily generalized to a nonthreatening stimulus. Maladaptive fear is associated with anxiety-related, trauma-related, and stressor-related disorders in humans. In addition, impaired fear extinction can be reversed in mice by pharmacological augmentation of AEA signaling[22], which is how SSCIs are suggested to reduce anxiety-like behaviors in animals[237]. Our studies appear to be in line with previous studies that suggest

increased AEA signaling through pharmacological manipulation of the endocannabinoid system can modulate stress-induced fear-related behaviors in mice. Moreover, similar to previous studies[238,239], our findings in this research endeavor suggest that stress-induced fear-related behavior in mice is mediated by the cannabinoid type 1 receptor.

Conclusion

Through our studies, we have observed the potential of substrate-selective COX-2 inhibitors, such as LM-4131, to not only serve as a therapeutic alternative to reduce anxiety-like and anhedonic behaviors in animals under basal conditions but as well after acute and chronic stress exposure regardless of sex (only with respect to anxiety-like behaviors). In particular, the SSCI, LM-4131, reduced anxiety-like behavior in the NIFS assay in the juvenile ICR male mice subjected to acute stress or under basal conditions only when the mice were exposed to an aversive environment. When we repeated the NIFS assay in another cohort of juvenile male ICR mice subjected to no stress or acute footshock stress to compare the efficacy of LM-4131 to the SSCI, lumiracoxib (1 mg/kg), and the FDA approved selective COX-2 inhibitor, celecoxib (10 mg/kg), which served as a reference drug to increase the translational implications of these experiments, we observed similar changes in feeding latency. However, LM-4131 appeared more efficacious at reducing anxiety-like behavior. Nevertheless, the mechanisms for the anxiolytic and hedonic action of these drugs are mediated through cannabinoid receptors under context-dependent conditions. This can be due to differential expression of receptor or ion channel targets in specific brain regions as a consequence of the magnitude and length of stress exposure as well as sex hormones.

CHAPTER III

SYNAPTIC AND ANXIOLYTIC BEHAVIORAL CORRELATES OF SUBSTRATE-SELECTIVE COX-2 INHIBITION IN AN ANIMAL MODEL OF ACUTE TRAUMATIC STRESS

Introduction

Excitatory neurotransmission, mediated mostly by glutamate, can be enhanced by stress and induce anxiety-like behaviors in animals and humans[240-242]. Thus, an increased ratio of synaptic excitation/inhibition in the hippocampus or prefrontal cortex-amygdala neural circuits may play a role in the pathophysiology of anxiety, trauma-related, and stressor-related disorders. Enhanced AEA signaling, possibly on glutamatergic neurons, has been shown to modulate stress-induced anxiety-like behaviors in animals[125,133,243]. Thus, SSCIs, which increase AEA levels in the brain, may enhance AEA signaling on glutamatergic neurons and, subsequently alter glutamatergic and GABAergic neurotransmission in key limbic brain structures, such as the amygdala. In order to examine this, we will discuss in this chapter the effects of SSCI on synaptic changes in the amygdala and how such alterations relate to the anxiolytic actions of SSCI observed in our previous studies (see CHAPTER II).

Experimental

Animals. Male ICR (CD-1) mice between 4-7 weeks of age (juvenile) or between 12-15 weeks of age (adult) were used for all experiments (Harlan, Indianapolis, IN) unless otherwise noted. All mice were housed on a 12:12 light-dark cycle (lights on at 6:00 a.m.) with food and water available *ad libitum*. All studies were carried out in accordance with the National Institute of Health Guide for the Care and Use of Laboratory Animals and approved by the Vanderbilt University

Institutional Animal Care and Use Committee. All behavioral testing was performed during the inactive light phase of the mouse circadian cycle (between 6:00 a.m. and 6:00 p.m.).

Drugs and treatment. The following drugs were used for the experiments: the COX-2 inhibitors, LM-4131 (10 mg/kg; gift from Dr. Lawrence Marnett laboratory) and lumiracoxib (1 mg/kg; Selleck Chemicals, Houston, TX). Drugs or vehicle (dimethyl sulfoxide or DMSO) were administered by i.p. injection. Drugs were dissolved in DMSO at a volume of 1 mL/kg. Drug pretreatment times were two hours prior to behavioral testing.

Behavioral testing.

Elevated plus maze. The elevated plus maze apparatus was elevated 47 cm from the ground, and consisted of two open arms (30 × 5 cm; 90 lux) and two closed arms (30 × 5 × 15 cm; 20 lux) extending from a 5 × 5 cm central area (San Diego Instruments). The walls and floor were made from black ABS (acrylonitrile butadiene styrene) plastic. To begin the 5-min test for animals without cannulization or 10-min test for animals cannulized for *in vivo* electrophysiological recordings, each mouse was placed in the center, facing an open arm. Time spent and entries into the open and closed arms were recorded using CinePlex Behavioral Research System (Plexon Inc, Dallas TX) and scored offline by the experimenter or using Any Maze tracking software. The mouse was considered to be in an arm when all four paws were in the arm. "Risk Assessment" was defined as when a mouse placed its front paws into an open arm while its back paws were in the center, but returned to the center without entering the open arm.

In vivo electrophysiology. Male Hsd:ICR (CD-1) outbred mice were obtained from Harlan Laboratories (Indianapolis, IN). Mice were 4 weeks of age upon arrival, and were given one week to acclimate prior to any surgical or behavioral procedures. They were housed in pairs in a temperature (72 ± 5°F) and humidity (45±15%) controlled vivarium, under a 12-hr light/dark cycle

(lights on at 0630 h). All experimental procedures carried out were approved by the NIAAA Animal Care and Use Committee under animal study protocol #LIN-AH-31 and followed the NIH guidelines outlined in Using Animals in Intramural Research and the local Animal Care and Use Committees.

Mice were anesthetized with 2% Isoflurane (Baxter Healthcare, Deerfield, IL) and implanted with 2x8 electrode (35um tungsten) micro-arrays (Innovative Neurophysiology Inc, Durham, NC) targeted at the basolateral amygdala (3.1mm lateral, 1.2-2.2mm posterior, and 4.5mm ventral relative to Bregma). Following surgery, mice were housed singly, and allowed at least one week to recover prior to behavioral testing.

Animals were exposed to stress individually, between the hours of 700 and 930am. Stress exposure took place in 27 × 27 × 11cm conditioning chambers (Med Associates, St. Albans, VT), with a metal-rod floor. Mice received 6 parings of a pure tone CS with a .7mA foot shock. Stimulus presentation and automated motion scoring were controlled by the Med Associates VideoFreeze system.

Five and a half hours following stress exposure, each animal received a pre-drug baseline recording session in its homecage. Individual units were identified and recorded for 5 min using Omniplex Neural Data Acquisition System (Plexon Inc, Dallas, TX). Exactly 6 hours after stress exposure, animals received an injection of either LM-4131 (10mg/kg, 1mg/ml in DMSO), or vehicle. Two hours following the injection (8 hours after stress exposure), animals received a 5-min post-drug baseline recording session in its homecage, using the same parameters for cell identification as each animal's pre-drug baseline recording session. Immediately following the post-drug baseline session, animals were placed on the elevated plus maze (EPM) for a 10-min recorded EPM session. In addition to neural recordings on the EPM, video acquisition monitored

behavior using CinePlex Behavioral Research System software (Plexon Inc, Dallas, TX). Neural data was sorted using Offline Sorter (Plexon Inc, Dallas, TX) and analyzed using NeuroExplorer 5.0 (Nex Technologies, Madison, AL).

Statistical analyses. For single unit analysis, neural data was acquired and recorded using Omniplex Neural Data Acquisition System (Plexon, Inc, Dallas, TX). Waveforms were isolated manually, using principal component analysis (Offline Sorter, Plexon Inc). To be included in the analyses, spikes had to exhibit a refractory period of at least 1 ms. Autocorrelograms from simultaneously recorded units were examined to ensure that no cell was counted twice. "Responsiveness" to arm entries for each unit was analyzed by generating perievent histograms (100ms bins) of firing rates in the 2 s surrounding arm entry (NeuroExplorer, Nex Technologies). Firing rates were normalized to baseline (1 s prior to entry) using z-score transformation. If z-scores for any of the time bins in the 1 second following arm entry was greater than 2 or less than -2, the cell was considered to be responsive (excitatory or inhibitory, respectively). Analysis of arm entry responsiveness included 67 cells in vehicle-treated animals, and 72 cells in LM-4131-treated animals. Data reported for raw firing rates included only putative principal neurons; any unit with a baseline firing rate over 7Hz was excluded (5 veh and 3 LM-4131; see Likhtik, E, *et al*., 2006)[244]. Statistical analyses were conducted by either Student's *t*-test or by ANOVA followed by Holm-Sidak post hoc multiple comparisons test.

Results and Discussion

Correlates of SSCI in stress-induced anxiety and synaptic transmission

To correlate our findings described in Chapter II in relation to the anxiolytic potential of SSCI after acute stress exposure with synaptic changes in the amygdala, a brain region known to

modulate anxiety-like behaviors in animals and humans, we performed *in vivo* electrophysiology in the basolateral nucleus of the amygdala in mice subjected to the elevated plus maze paradigm, which is depicted in Figure 18a, after exposure to the acute footshock paradigm and i.p. administration of either vehicle or the SSCI, LM-4131 (10 mg/kg). To ensure implanting of the cannula for the *in vivo* electrophysiology did not interfere with the anxiety-like behaviors exhibited by the mice after acute stress exposure, we tested the mice in the EPM with and without cannulization to compare findings. We found that regardless of the cannulization the mice exhibited a reduction in stress-induced anxiety-like behavior in the EPM when administered LM-4131 in comparison to vehicle-treated mice. Regarding the mice that were not cannulized, all substrate-selective COX-2 inhibitors, LM-4131 and LMX, compared to vehicle treatment decreased anxiety-like behaviors in the EPM by decreasing the latency to open arm entry and increasing the latency to closed arm entry after the mice were exposed to acute footshock stress (Fig. 18b). A one-way ANOVA was conducted to compare the effect of LM-4131 and LMX on open arm latency in juvenile male ICR mice 8h after acute stress exposure. It showed that the difference in open arm latency between the vehicle treatment group (means ± s.e.m. = 27.90 ± 5.355, $N = 17$), the LM-4131 treatment group (means ± s.e.m. = 0.6000 ± 0.4030, $N = 13$), and the LMX treatment group (means ± s.e.m. = 2.287 ± 1.053, $N = 15$) were statistically significant ($F_{(2, 42)} = 19.26$; ****$p < 0.0001$). Post hoc Holm-

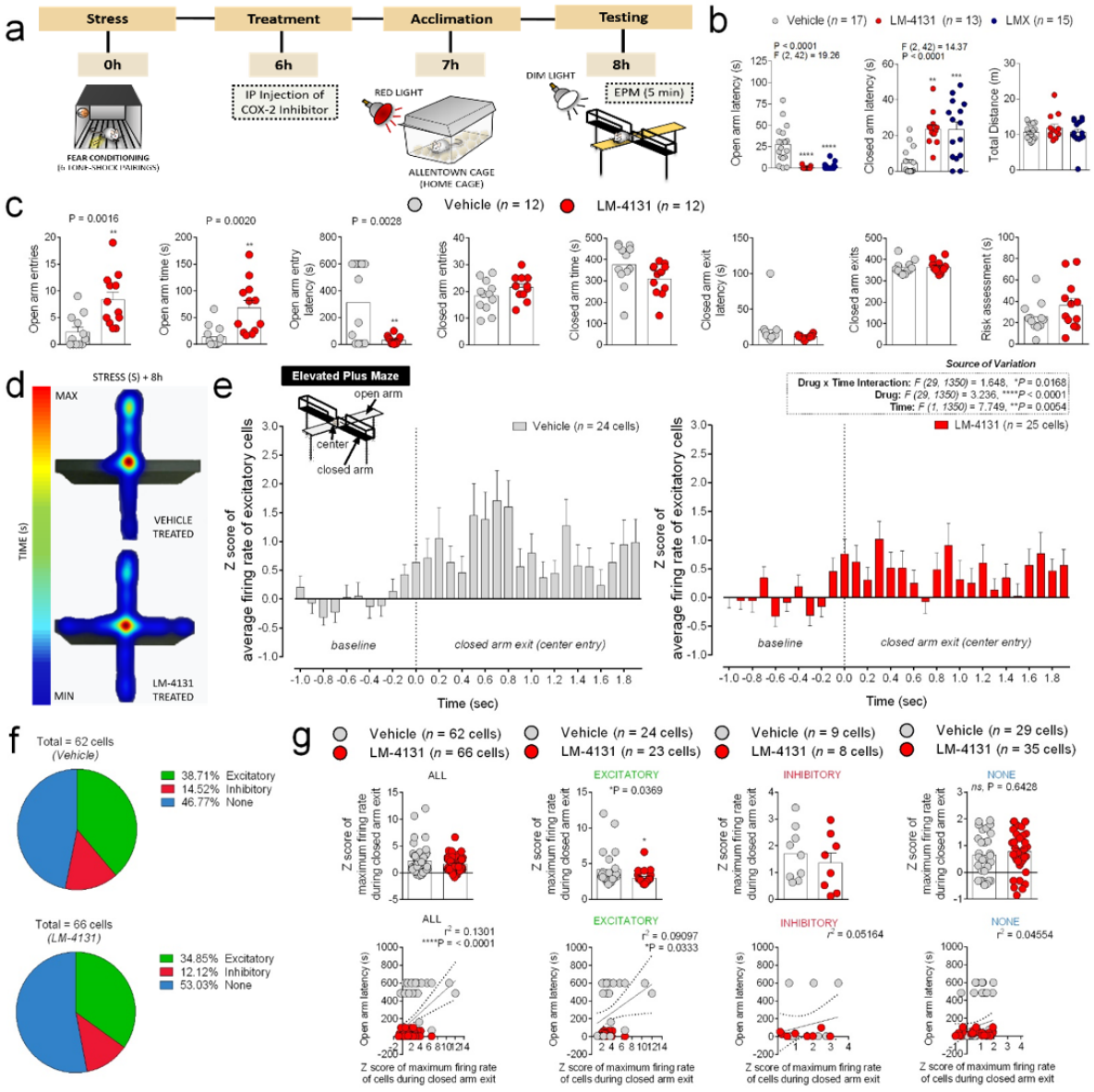

Figure 18. Synaptic effects of substrate-selective COX-2 inhibition in stress-induced anxiety-like behaviors. (**a**) Diagram of experimental design using the elevated plus maze (EPM), a behavioral test for anxiety. **(b**) Open arm latency, closed arm latency, and total distance traveled by mice in the EPM that have not undergone cannulization. (**c**) Closed or open arm entries or time, closed or open arm latency, closed arm exits, and risk assessment by ice in the EPM that have undergone cannulization for *in vivo* electrophysiology. (**d**) Schematic of heat map of elevated plus for vehicle-treated or LM-4131 treated mouse after stress exposure. (**e**) Z score of average firing rate of excitatory cells in vehicle-treated and LM-4131-treated mice as the mice enter the center of the EPM. (f) Number of cell types in vehicle and LM-4131-treated animals. (**g**) Correlation plots of open arm latency and Data are shown as the mean ± s.e.m. *P < 0.05, **P < 0.01, ***P<0.001, ****P<0.0001 (COX-2 inhibitor compared to vehicle). Statistical significance was calculated by two-tailed unpaired Student's *t*-test *or* one-way or two-way ANOVA with post hoc Holm-Sidak's multiple comparisons test.

Sidak's multiple comparisons test revealed a significant decrease in open arm latency of the EPM

at the 10 mg/kg dose of LM-4131 (****$p < 0.0001$, $t = 5.350$, df = 42, LM-4131 vs. vehicle) and at the 1 mg/kg dose of LMX (****$p < 0.0001$, $t = 5.220$, df = 42, LMX vs. vehicle) compared to vehicle treatment under acute stress conditions. A one-way ANOVA was also conducted to compare the effect of LM-4131 and LMX on closed arm latency in the mice 8h after acute stress exposure. It showed that the difference in closed arm latency between the vehicle treatment group (means ± s.e.m. = 4.600 ± 1.787, $N = 17$), the LM-4131 treatment group (means ± s.e.m. = 23.58 ± 2.516, $N = 13$), and the LMX treatment group (means ± s.e.m. = 23.27 ± 4.150, $N = 15$) were statistically significant ($F_{(2, 42)} = 14.37$; ****$p < 0.0001$). Post hoc Holm-Sidak's multiple comparisons test revealed a significant increase in closed arm latency of the EPM at the 10 mg/kg dose of LM-4131 (****$p < 0.0001$, $t = 4.512$, df = 42, LM-4131 vs. vehicle) and at the 1 mg/kg dose of LMX (****$p < 0.0001$, $t = 4.618$, df = 42, LMX vs. vehicle) compared to vehicle treatment under acute stress conditions. These results were not confounded by changes in total distance traveled in the EPM, suggesting that the drug effects on anxiety-like behavior in the EPM were not an artifact of motor deficits or abnormalities. A one-way ANOVA was conducted to compare the effect of LM-4131 and LMX on total distance traveled in the mice 8h after acute stress exposure. It showed that the difference in total distance traveled between the vehicle treatment group (means ± s.e.m. = 10.65 ± 0.5166, $N = 17$), the LM-4131 treatment group (means ± s.e.m. = 11.92 ± 0.9740, $N = 13$), and the LMX treatment group (means ± s.e.m. = 10.66 ± 0.9433, $N = 15$) were not statistically significant ($F_{(2, 42)} = 0.7595$; $p = 0.4742$, *ns*). Post hoc Holm-Sidak's multiple comparisons test revealed no significant changes in total distance traveled in the EPM at the 10 mg/kg dose of LM-4131 (*ns*, $t = 1.104$, df = 42, LM-4131 vs. vehicle) and at the 1 mg/kg dose of LMX (*ns*, $t = 0.007873$, df = 42, LMX vs. vehicle) compared to vehicle treatment under acute stress conditions.

We also found that the SSCIs, LM-4131 and LMX, reduced anxiety-like behavior in the EPM in both juvenile and adult male ICR mice that were not cannulized regardless of stress exposure, even though the most robust effects were observed in stressed and juvenile mice (see APPENDIX Fig. G). Non-stressed juvenile male ICR mice showed significant differences in open arm entries (one-way ANOVA: $F_{(2, 58)} = 4.972$, $p = 0.0102$, $^{*}p < 0.05$) and closed arm latency (one-way ANOVA: $F_{(2, 52)} = 12.55$, $^{****}p < 0.0001$) in the EPM. The sample means are displayed in Figure Ga, which shows that the mice treated with an SSCI, LM-4131 (10 mg/kg) or LMX (1 mg/kg), scored greater on open arm entries and closed arm latency than mice treated with vehicle (t (58) = 3.070 (open arm entries), t (51) = 5.006 (closed arm latency); for vehicle treatment group: means ± s.e.m. = 6.391 ± 1.895 (open arm entries), 2.576 ± 2.493 (closed arm latency), $N = 23$; for LM-4131 treatment group: means ± s.e.m. = 15.05 ± 2.493 (closed arm latency), $N = 13$; for LMX treatment group: means ± s.e.m. = 12.21 ± 1.895 (open arm entries), $N = 24$). Stressed juvenile male ICR mice showed significant differences in latency to freeze (one-way ANOVA: $F_{(2, 52)} = 7.184$, $p = 0.0018$, $^{**}p < 0.01$) in the EPM. The sample means are displayed in Figure Gb, which shows that the mice treated with the SSCI, LM-4131 (10 mg/kg), scored greater on latency to freeze than mice treated with vehicle (t (52) = 3.789, for vehicle treatment group: means ± s.e.m. = 0.3875 ± 1.910, $N = 16$; for LM-4131 treatment group: means ± s.e.m. = 7.626 ± 1.910, $N = 19$). Non-stressed adult male ICR mice showed significant differences in open arm latency (one-way ANOVA: $F_{(2, 58)} = 17.06$, $^{****}p < 0.0001$), closed arm latency (one-way ANOVA: $F_{(2, 64)} = 8.275$, $p = 0.0006$, $^{***}p < 0.001$), and latency to freeze (one-way ANOVA: $F_{(2, 61)} = 8.448$, $p = 0.0006$, $^{***}p < 0.001$) in the EPM. The sample means are displayed in Figure Gc, which shows that the mice treated with an SSCI, LM-4131 (10 mg/kg) or LMX (1 mg/kg), scored lesser on open arm latency and greater on closed arm latency and latency to freeze than mice treated with vehicle

(t (52) = 5.188 (LM-4131 vs. vehicle) or 4.942 (LMX vs. vehicle) (open arm latency), t (64) = 4.056 (LM-4131 vs. vehicle) or 2.590 (LMX vs. vehicle) (closed arm latency), t (61) = 3.794 (latency to freeze); for vehicle treatment group: means ± s.e.m. = 20.31 ± 4.530 (open arm latency), 7.128 ± 2.202 (closed arm latency), 1.253 ± 0.4512 (latency to freeze), N = 18; for LM-4131 treatment group: means ± s.e.m. = 1.028 ± 0.2234 (open arm latency), 23.94 ± 3.114 (closed arm latency), 8.856 ± 1.870 (latency to freeze), N = 24; for LMX treatment group: means ± s.e.m. = 2.184 ± 0.6974 (open arm latency), 17.77 ± 2.729 (closed arm latency), N = 25). Stressed adult male ICR mice showed significant differences in open arm latency (one-way ANOVA: $F_{(2, 39)}$ = 8.922, p = 0.0006, ***p < 0.001), closed arm latency (one-way ANOVA: $F_{(2, 36)}$ = 8.354, p = 0.0010, **p < 0.01), and latency to freeze (one-way ANOVA: $F_{(2, 36)}$ = 10.84, p = 0.0002, ***p < 0.001) in the EPM. The sample means are displayed in Figure Gd, which shows that the mice treated with an SSCI, LM-4131 (10 mg/kg) or LMX (1 mg/kg), scored lesser on open arm latency and greater on closed arm latency and latency to freeze than mice treated with vehicle (t (39) = 3.032 (LM-4131 vs. vehicle) or 4.026 (LMX vs. vehicle) (open arm latency), t (36) = 3.367 (LM-4131 vs. vehicle) or 3.860 (LMX vs. vehicle) (closed arm latency), t (36) = 4.484 (latency to freeze); for vehicle treatment group: means ± s.e.m. = 42.55 ± 10.50 (open arm latency), 0.3000 ± 0.2191 (closed arm latency), 0.5333 ± 0.3163 (latency to freeze), N = 10; for LM-4131 treatment group: means ± s.e.m. = 12.37 ± 5.121 (open arm latency), 20.59 ± 3.428 (closed arm latency), N = 15; for LMX treatment group: means ± s.e.m. = 1.685 ± 0.5418 (open arm latency), 23.90 ± 5.435 (closed arm latency), 9.164 ± 2.002 (latency to freeze), N = 14).

We were able to replicate some of the effects of LM-4131 on stress-induced anxiety-like behavior in the mice that were cannulized for use in the *in vivo* electrophysiology experiments. The substrate-selective COX-2 inhibitor, LM-4131, compared to vehicle treatment decreased

anxiety-like behaviors in the EPM by increasing the number of open arm entries and time spent in the open arms while decreasing the latency to open arm entry after the mice were exposed to acute footshock stress (Fig. 18c). An independent (unpaired) samples *t* test showed that the difference in open arm entries in juvenile male ICR mice 8h after acute stress exposure between the vehicle treatment group (means ± s.e.m. = 2.333 ± 0.8646, *N* = 12) and the LM-4131 treatment group (means ± s.e.m. = 8.333 ± 1.421, *N* = 12) were statistically significant (*t* (22) = 3.607, *p* = 0.0016, ***p* < 0.01, 95% CI [2.550, 9.450], *d* = 6.000 ± 1.664). It also illustrated that the difference in open arm time in the mice 8h after acute stress exposure between the vehicle treatment group (means ± s.e.m. = 14.11 ± 5.910, *N* = 12) and the LM-4131 treatment group (means ± s.e.m. = 68.13 ± 14.22, *N* = 12) were statistically significant (*t* (22) = 3.506, *p* = 0.0020, ***p* < 0.01, 95% CI [22.07, 85.96], *d* = 54.01 ± 15.40). An independent (unpaired) samples *t* test also revealed a significant difference in open arm entry latency in the mice 8h after acute stress exposure between the vehicle treatment group and the LM-4131 treatment group (*t* (22) = 3.366, *p* = 0.0028, ***p* < 0.01, 95% CI [-451.9, -107.3], *d* = -279.6 ± 83.07). The sample means are displayed in Figure 18c, which shows that the mice treated with LM-4131 (10 mg/kg) scored lower on open arm entry latency than the mice treated with vehicle (for LM-4131 treatment group, means ± s.e.m. = 32.15 ± 8.714, *N* = 12; for vehicle treatment group, means ± s.e.m. = 311.7 ± 82.61, *N* = 12). There were no significant differences in closed arm entries (unpaired samples *t* test: *t* (22) = 1.498, *p* = 0.1483, *ns*), closed arm time (unpaired samples *t* test: *t* (22) = 1.817, *p* = 0.0828, *ns*), closed arm latency (unpaired samples *t* test: *t* (22) = 1.326, *p* = 0.1983, *ns*), closed arm exits or center entries (unpaired samples *t* test: *t* (22) = 0.1962, *p* = 0.8462, *ns*), and risk assessment (unpaired samples *t* test: *t* (22) = 1.399, *p* = 0.1757, *ns*). The sample means are displayed in Figure 18c, which shows that the mice treated with LM-4131 (10 mg/kg) scored similar on closed arm entries, closed arm latency,

closed arm exits, and risk assessment compared to the mice treated with vehicle (for vehicle treatment group: means ± s.e.m. = 18.42 ± 1.663 (closed arm entries), 376.0 ± 28.61 (closed arm time), 21.29 ± 7.283 (closed arm latency), 362.2 ± 9.147 (closed arm exits), 25.35 ± 4.076 (risk assessment), N = 12; for LM-4131 treatment group: means ± s.e.m. = 21.58 ± 1.305 (closed arm entries), 310.4 ± 22.00 (closed arm time), 11.57 ± 0.7971 (closed arm latency), 364.6 ± 8.330 (closed arm exits), 36.16 ± 6.564 (risk assessment), N = 12).

Since excitatory neurotransmission can be enhanced by stress and induce anxiety-like behaviors in animals and humans[240-242], we wanted to determine if our acute stress paradigm, which we have shown to induce anxiety-like behavior in the juvenile ICR mice (Fig. 2e), could induce changes in the levels of glutamate or GABA in the amygdala of these mice. Using high performance liquid chromatography (HPLC), we measured glutamate and GABA levels in the amygdala from mice under non-stressed (control) or acute footshock stress conditions (see APPENDIX H). We found that the acute footshock stress paradigm did not affect amygdala glutamate or GABA levels compared to non-stressed (control) conditions. An independent (unpaired) samples t test showed that the difference in amygdala glutamate levels in juvenile male ICR mice between the non-stressed group (means ± s.e.m. = 101.7 ± 3.323, N = 10) and the stressed group (means ± s.e.m. = 93.15 ± 2.450, N = 10) was not statistically significant (t (18) = 2.069, p = 0.0533, *ns*, 95% CI [-17.21, 0.1338], d = -8.540 ± 4.129; see APPENDIX Ha). It also illustrated that the difference in amygdala GABA levels in juvenile male ICR mice between the non-stressed group (means ± s.e.m. = 19.93 ± 1.025, N = 10) and the stressed group (means ± s.e.m. = 19.74 ± 0.4566, N = 10) was not statistically significant (t (18) = 0.1685, p = 0.8681, *ns*, 95% CI [-2.546, 2.168], d = -0.1890 ± 1.122; see APPENDIX Hb). The unexpected findings may be due to the limitations of HPLC to accurately measure the effects of stress exposure on amygdala glutamate

or GABA levels, especially since site specificity of changes in neurotransmitter levels is lost in brain tissue sections that have subregions characterized by cell type differences. The technique of microdialysis may be better suited to quantitatively measure neurotransmitters, such as glutamate or GABA, from tissue preparations, especially since it more precisely characterizes the quantity and distribution of an analyte, such as a neurotransmitter, and can measure the temporal pattern of the release of neurotransmitters in specific brain regions in an awake animal[245].

A schematic heat map of the elevated plus maze for vehicle-treated and LM-4131-treated mice after acute footshock stress exposure is depicted in Figure 18d, which shows that the juvenile male ICR mice exposed to acute footshock stress spent most of their time in the center or open arms after they exited a closed arm. Since increased amygdala cell excitability has been suggested to be correlated to anxiogenic phenotypes in animals[220,246-249], we wanted to determine if the SSCI, LM-4131, could reduce stress-induced anxiety-like behavior exhibited by the mice in the EPM by reducing cell excitability in the basolateral nucleus of the amygdala (BLA) of the mice. Thus, we examined the average firing rate of excitatory neurons in the BLA in the mice exposed to acute footshock stress and administered either vehicle or the LM-4131 by i.p. (see APPENDIX Fig. Ia). To ensure that the baseline firing rate (spikes/s) of responsive excitatory cells before and after intraperitoneal (IP) injection were similar between vehicle-treated and LM-4131-treated mice exposed to acute footshock stress 8h prior to testing for anxiety-like behavior in the EPM and simultaneously recording firing rate of excitatory BLA cells, we performed two-way ANOVA factoring drug dose and time of i.p. injection, which revealed no significant effect of drug dose x time of i.p. injection interaction ($F_{(1, 254)} = 0.01199$, $p = 0.9129$, *ns*) and drug dose ($F_{(1, 254)} = 3.063$, $p = 0.0813$, *ns*), but a significant effect of time of i.p. injection ($F_{(1, 254)} = 4.241$, $p = 0.0405$, $^*p < 0.05$; see APPENDIX Fig. Ib). After performing the *in vivo* electrophysiology experiments, we

discovered that LM-4131 induced a reduction in the firing rate when the mice exited a closed arm to enter the center of the maze, which is a more aversive area of the EPM as opposed to the dimly lit closed arms (Fig. 18e and see APPENDIX Fig. Ic). With respect to the effects of LM-4131 on the *Z* score of the average firing rate of excitatory cells in the BLA of mice exposed to acute footshock stress, two-way ANOVA factoring drug dose and time of exit from the closed arm (center entry) of the EPM revealed a significant effect of drug dose x time interaction ($F_{(29, 1350)}$ = 1.648; p = 0.0168, *p < 0.05), time of exit from the closed arm (center entry) of the EPM ($F_{(29, 1350)}$ = 3.236, ****p < 0.0001), and drug dose ($F_{(1, 1350)}$ = 7.749, **p < 0.01; Fig. 18e). Post hoc Holm-Sidak's multiple comparisons test revealed at the 10 mg/kg dose of LM-4131 compared to vehicle treatment a significant decrease in the average firing rate of excitatory cells in the BLA in the mice exposed to acute footshock stress when they exited a closed arm of the EPM (**p < 0.01, t = 3.835, df = 1350, at 0.7 s time bin; for LM-4131 treatment group, means ± s.e.m. = 0.07138 ± 0.4274, N = 23 cells; for vehicle treatment group, means ± s.e.m. = 1.711 ± 0.4274, N = 24 cells). As depicted in the pie charts in Figure 18f, of all 62 BLA responsive cells recorded from in vehicle-treated mice, 24% were excitatory, 9% were inhibitory, and 29% were neither excitatory nor inhibitory, and of all 66 BLA responsive cells recorded from in vehicle-treated mice, 35% were excitatory, 12% were inhibitory, and 53% were neither excitatory nor inhibitory. From the cells that were recorded for firing rate, we found a positive correlation between open arm latency and maximum firing rate when the animals exited the closed arms in the EPM (Fig. 18g). An independent (unpaired) samples *t* test showed that the difference in the Z score of maximum firing rate of all BLA responsive cells during closed arm exit from the EPM in juvenile male ICR mice 8h after acute stress exposure between the vehicle treatment group (means ± s.e.m. = 2.174 ± 0.2986, N = 62) and the LM-4131 treatment group (means ± s.e.m. = 1.616 ± 0.1671, N = 66) were

not statistically significant (*t* (126) = 1.657, *p* = 0.1001, *ns*, 95% CI [-1.224, 0.1086], *d* = -0.5580 ± 0.3368). For the 128 BLA responsive cells from mice exposed to acute footshock stress, the Z scores of maximum firing rate of the cells during closed arm exit from the EPM (means ± s.e.m. = 1.886 ± 0.1695, *N* = 128 cells) and the latency to open arm entry of the EPM (means ± s.e.m. = 166.5 ± 20.16, *N* = 12 animals) were strongly and significantly correlated, *r* = 0.3607, ****p < 0.0001. An independent (unpaired) samples *t* test showed that the difference in the Z score of maximum firing rate of excitatory BLA responsive cells during closed arm exit from the EPM in juvenile male ICR mice 8h after acute stress exposure between the vehicle treatment group (means ± s.e.m. = 4.195 ± 0.5109, *N* = 24) and the LM-4131 treatment group (means ± s.e.m. = 2.990 ± 0.2069, *N* = 23) was statistically significant (*t* (45) = 2.151, *p* = 0.0369, **p* < 0.05, 95% CI [-2.333, -0.07678], *d* = -1.205 ± 0.5600). For the 47 excitatory BLA responsive cells from mice exposed to acute footshock stress, the Z scores of maximum firing rate of the cells during closed arm exit from the EPM (means ± s.e.m. = 3.465 ± 0.2844, *N* = 47 cells) and the latency to open arm entry of the EPM (means ± s.e.m. = 244.9 ± 37.90, *N* = 12 animals) were significantly correlated, *r* = 0.3016, *p* = 0.0333, **p* < 0.05. An independent (unpaired) samples *t* test showed that the difference in the Z score of maximum firing rate of inhibitory BLA responsive cells during closed arm exit from the EPM in juvenile male ICR mice 8h after acute stress exposure between the vehicle treatment group (means ± s.e.m. = 1.695 ± 0.3316, *N* = 9) and the LM-4131 treatment group (means ± s.e.m. = 1.363 ± 0.3759, *N* = 8) was not statistically significant (*t* (15) = 0.6642, *p* = 0.5166, *ns*, 95% CI [-1.395, 0.7324], *d* = -0.3315 ± 0.4991). For the 47 inhibitory BLA responsive cells from mice exposed to acute footshock stress, the Z scores of maximum firing rate of the cells during closed arm exit from the EPM (means ± s.e.m. = 1.539 ± 0.2448, *N* = 17 cells) and the latency to open arm entry of the EPM (means ± s.e.m. = 121.4 ± 55.72, *N* = 12 animals) were not

significantly correlated, $r = 0.2273$, $p = 0.3804$, *ns*. An independent (unpaired) samples *t* test showed that the difference in the Z score of maximum firing rate of "none" BLA responsive cells (e.g., neither excitatory nor inhibitory) during closed arm exit from the EPM in juvenile male ICR mice 8h after acute stress exposure between the vehicle treatment group (means ± s.e.m. = 0.6500 ± 0.1477, $N = 29$) and the LM-4131 treatment group (means ± s.e.m. = 0.7706 ± 0.1334, $N = 35$) was statistically significant (t (62) = 0.6064, $p = 0.5464$, *ns*, 95% CI [-0.2770, 0.5183], $d = 0.1206$ ± 0.1989). For the 47 "none" BLA responsive cells (e.g., neither excitatory nor inhibitory) from mice exposed to acute footshock stress, the Z scores of maximum firing rate of the cells during closed arm exit from the EPM (means ± s.e.m. = 0.7160 ± 0.09852, $N = 64$ cells) and the latency to open arm entry of the EPM (means ± s.e.m. = 114.5 ± 23.13, $N = 12$ animals) were not significantly correlated, $r = 0.2134$, $p = 0.0904$, *ns*.

Conclusion

As illustrated in this chapter the anxiolytic potential of SSCI after an animal has been exposed to acute footshock stress is related to a decrease in the firing of excitatory cells in the amygdala. Nevertheless, the mechanisms responsible or the sequence of events that leads up to this phenomenon is unknown and requires further investigation. A recent study by Rau and others has suggested that activation of SK channels in the BLA can reduce BLA pyramidal cell excitability in an animal model of chronic early-life stress[220]. This study supports our observation that stress-induced anxiety-like behavior in mice is mediated by the SK channel. It also reinforces the notion that the SSCI, LM-4131, may be a target of the SK channels located possibly in the amygdala, specifically the BLA. From our findings, we can construct a hypothetical model of cellular and molecular occurrences as a result of SSCI action under acute stress conditions in male

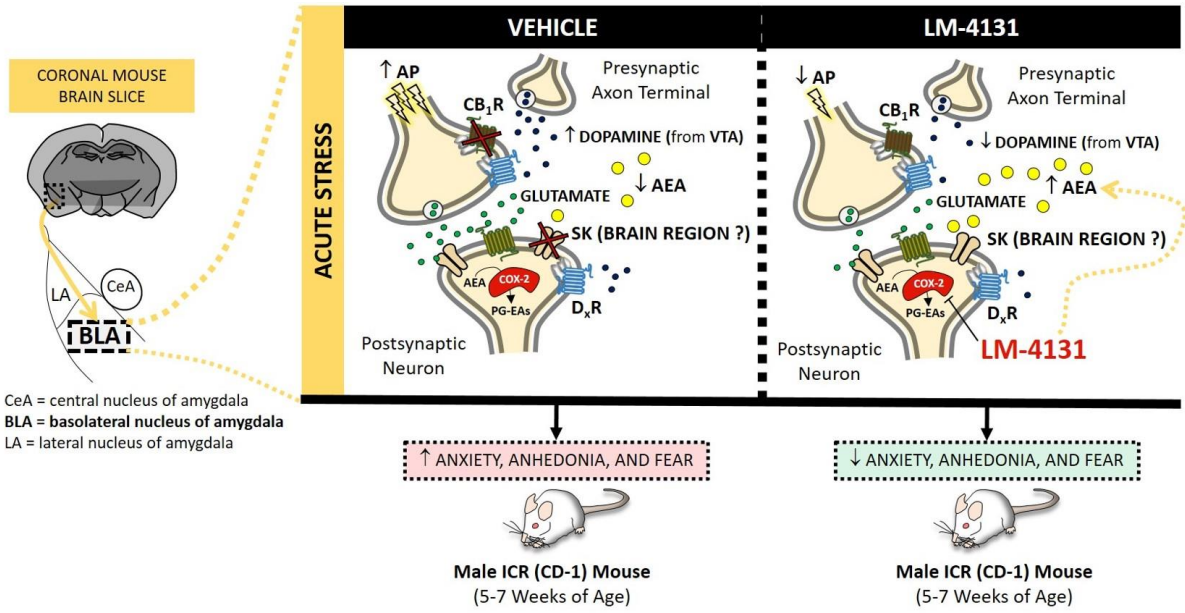

Figure 19. Hypothetical working model of synaptic and behavioral effects of substrate-selective COX-2 inhibition in the amygdala. Acute stress exposure induces an increase in action potential firing in excitatory pyramidal neurons located in the basolateral nucleus of the amygdala and release of dopamine from the ventral tegmental area (VTA) onto neurons in the BLA. Consequently, the endocannabinoid, anandamide, is reduced in content possibly by degradation of the enzyme cyclooxygenase-2 (COX-2) or other surrounding enzymes and the calcium activated potassium (SK) channel is decreased in content at the plasma membrane surface in either the amygdala or other brain regions involved in modulating anxiety, anhedonia, and/or fear in animals. Due to these synaptic changes, animals exhibit an increase in anxiety, anhedonia, and/or contextual fear. LM-4131, a substrate-selective COX-2 inhibitor, counteracts these synaptic and behavioral effects.

mice of juvenile age (5-7 weeks of age) (Fig. 19). Through this hypothetical reconstruction, we have assumed that an increase of dopamine release in the amygdala from axon terminals originating in the ventral tegmental area of the brain is induced by the acute stress exposure and, subsequently, is restored by elevations of AEA via SSCI. This increase in dopamine release may induce an increase in the firing of excitatory neurons along with other molecular changes at the synaptic level. LM-4131 through AEA signaling reduces such increases and/or synaptic molecular changes by targeting calcium-activated potassium channels, resulting in a reduction in anxiogenic, anhedonic, and/or fearful behavioral responses in the mice. Future studies will examine how applicable this model is to the cellular and molecular events occurring in the amygdala and other associated brain regions involved in modulating fear and stress responses in mice in relation to stress-induced anxiogenic, anheonic, and fear-related behaviors in animals.

APPENDIX

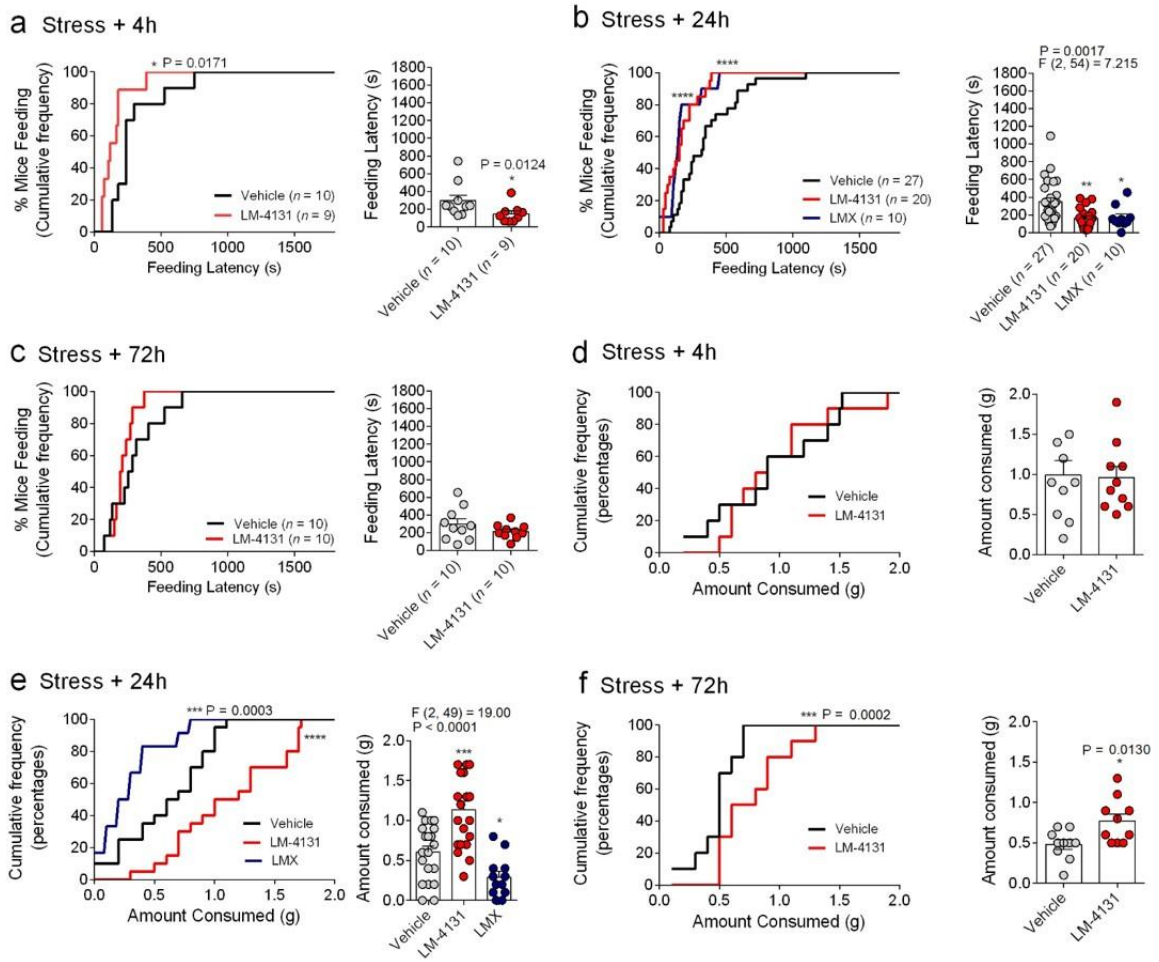

Figure A. Time-dependent anxiolytic and anhedonic effects of COX-2 inhibitors in juvenile male mice. (**a-c**) Cumulative frequency of mice feeding and latency to feed in novelty-induced feeding suppression (NIFS) test at four, 24, and 72 hours after acute stress exposure. (**d-f**) Cumulative frequency of mice consuming palatable shake and amount of shake consumed in novelty-induced feeding suppression (NIFS) test at four, 24, and 72 hours after acute stress exposure. Data are shown as the mean ± s.e.m. NS = no stress, S = stress (e.g., stress exposure in the form of an electric footshock administered 4/24/72h prior to testing), *P < 0.05, **P < 0.01, ***P < 0.001, ****P < 0.0001 (COX-2 inhibitor compared to vehicle). Statistical significance was calculated by two-tailed unpaired Student's *t*-test or Kolmogorov-Smirnov test (only for frequency plots) or one-way ANOVA with post hoc Holm-Sidak's multiple comparisons test.

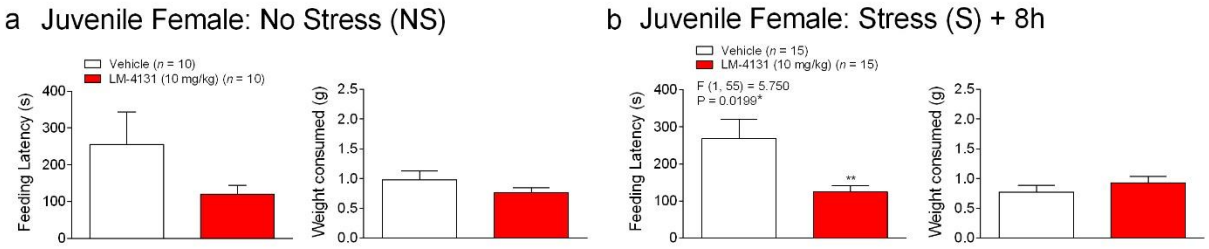

Figure B. Anxiolytic effects of COX-2 inhibitors in the NIFS assay on juvenile female mice. (**a)** Mean latency to feed and amount of shake consumed in the novelty-induced feeding suppression (NIFS) test under basal (no stress) conditions in juvenile ICR (CD-1) female mice, and (**b**) Mean latency to feed and amount of shake consumed in the novelty-induced feeding suppression (NIFS) test at 8 hours after acute stress exposure in juvenile ICR (CD-1) mice. Data are shown as the mean ± s.e.m. NS = no stress, S = stress (e.g., stress exposure in the form of an electric footshock administered 8h prior to testing), *P < 0.05, **P < 0.01 (COX-2 inhibitor compared to vehicle). Statistical significance was calculated by unpaired, two-tailed *t* test.

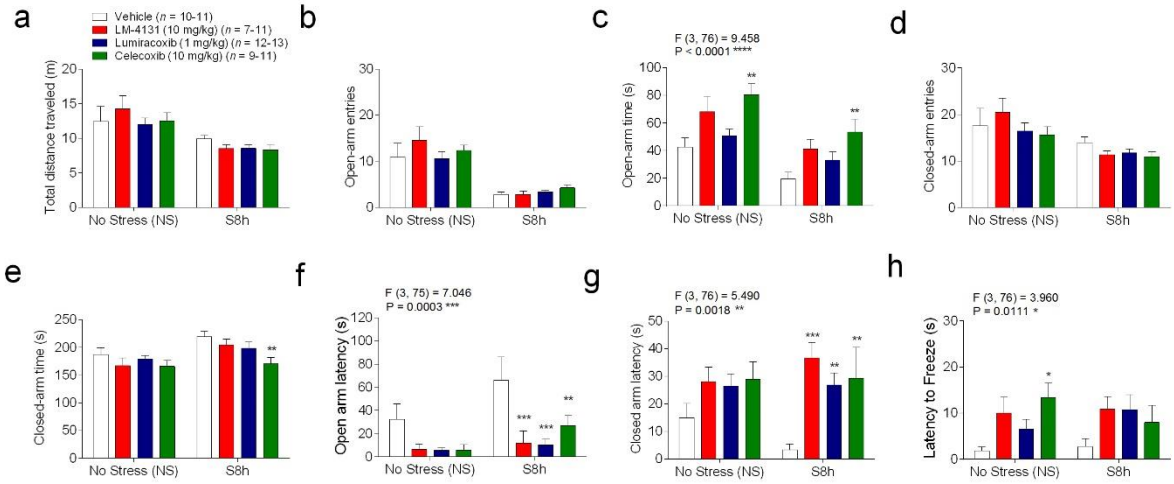

Figure C. Anxiolytic effects of COX-2 inhibitors in the elevated plus maze on adult female mice. (**a)** Total distance traveled, (**b**) open arm entries, (**c**) open arm time, (**d**) closed arm entries, (**e**) closed arm time, (**f**) open arm latency, (**g**) closed arm latency, and (**h**) latency to freeze in adult female mice under non-stressful conditions and after acute stress exposure in the elevated plus maze. Data are shown as the mean ± s.e.m. NS = no stress, S = stress (e.g., stress exposure in the form of an electric footshock administered 8h prior to testing), *P < 0.05, **P < 0.01, ***P<0.001, ****P<0.0001 (COX-2 inhibitor compared to vehicle). Statistical significance was calculated by two-way ANOVA with post hoc Holm-Sidak's multiple comparisons test.

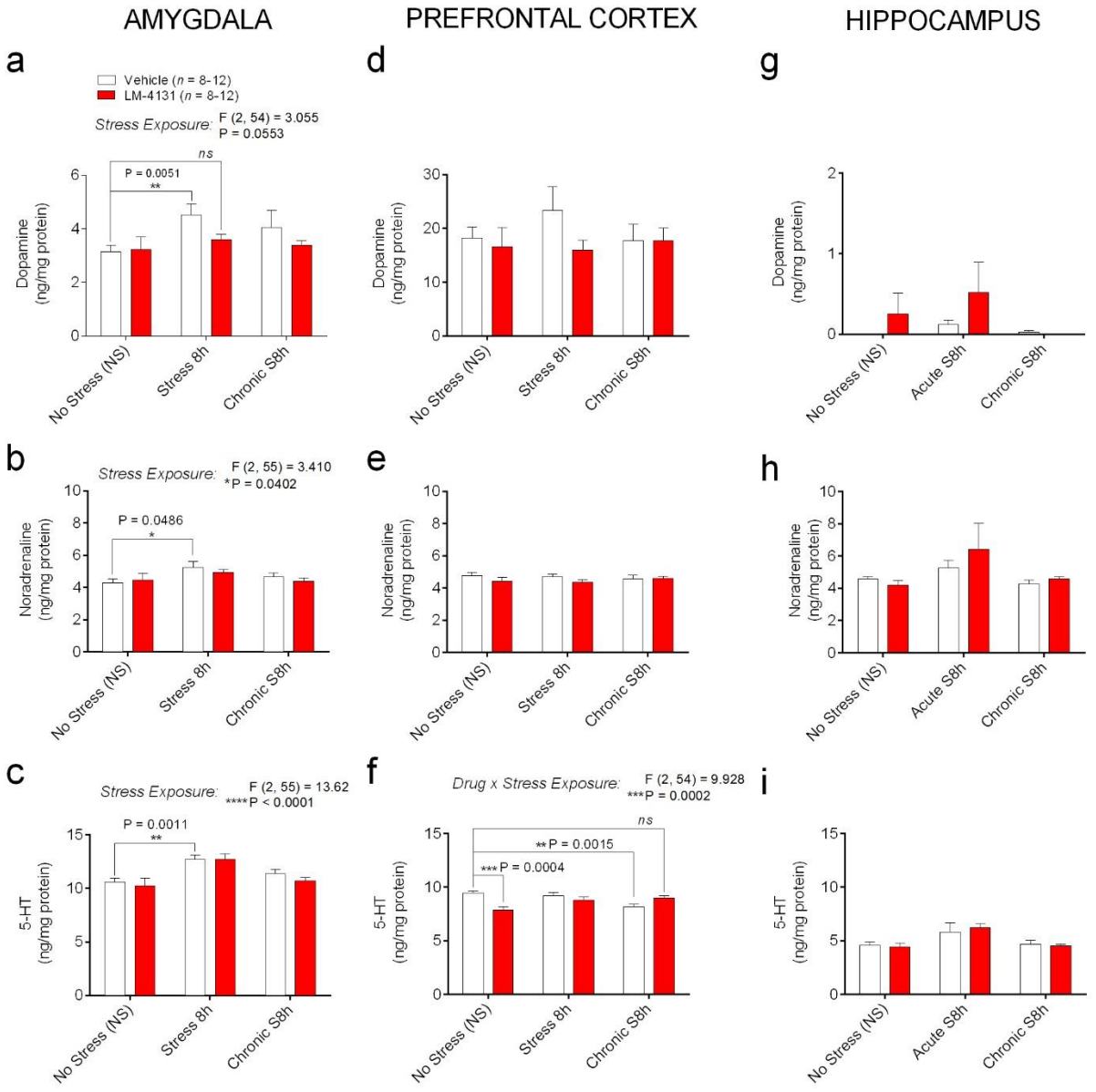

Figure D. Effects of SSCI on amygdala, PFC, and HPC monoamine levels. Effects of LM-4131 under control (non-stressed) conditions and 8 hours after acute (1 day) and chronic (5 days) foot-shock stress on dopamine (**a**), noradrenaline (**b**) and serotonin (5-HT) (**c**) levels in the amygdala. Effects of LM-4131 under control (non-stressed) conditions and 8 hours after acute and chronic foot-shock stress on dopamine (**d**), Noradrenaline (**e**) and Serotonin (5-HT) (**f**) levels in the PFC. Effects of LM-4131 under control (non-stressed) conditions and 8 hours after acute and chronic foot-shock stress on dopamine (**g**), Noradrenaline (**h**) and Serotonin (5-HT) (**i**) levels in the HPC. Significant F and P values for Two-way ANOVA shown above figures. *ns*, not significant, **p*<0.05, ***p*<0.01, ****p*<0.001, *****p*<0.0001 by Holm-Sidak multiple comparisons test after two-way ANOVA.

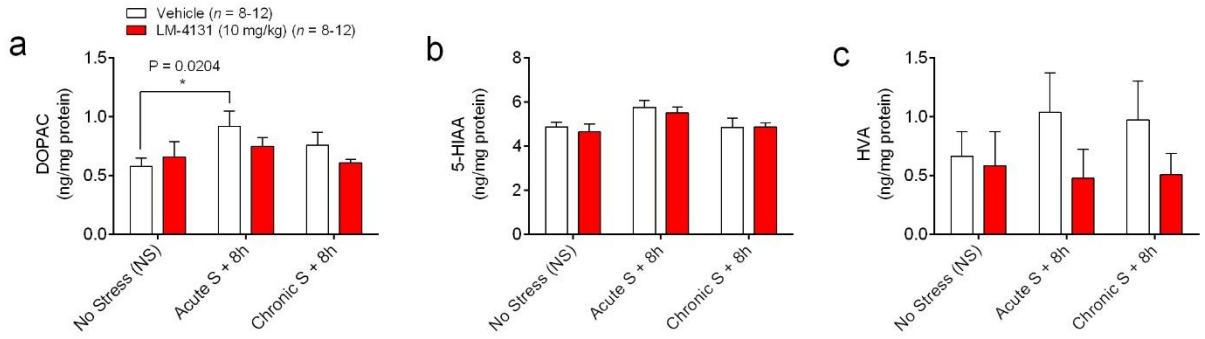

Figure E. Effects of SSCI on amygdala serotonin and dopamine metabolite levels. Effects of LM-4131 under control (non-stressed) conditions and 8 hours after acute (1 day) and chronic (5 days) foot-shock stress on the dopamine metabolite, 3,4-dihydroxyphenylacetic acid (DOPAC) (**a**), the serotonin metabolite, 5-hydroxyindoleacetic acid (5-HIAA), (**b**) and the DOPAC metabolite, homovanillic acid (HVA) (**c**) levels in the amygdala. Data are shown as the mean ± s.e.m. NS = no stress, S = stress (e.g., stress exposure in the form of an electric footshock administered 8h prior to HPLC experiment), *P<0.05 (COX-2 inhibitor compared to vehicle or no stress compared to acute and/or chronic stress exposure paradigm). Statistical significance was calculated by unpaired, two-tailed *t* test.

Figure F. Effects of SSCI on CORT levels. Effects of LM-4131 under control (non-stressed) conditions (**a**) and 8 hours after acute (1 day) (**b**) and chronic (5 days) foot-shock stress (**c**) on plasma corticosterone (CORT) levels in juvenile male ICR mice. Data are shown as the mean ± s.e.m. NS = no stress, S = stress (e.g., stress exposure in the form of an electric footshock administered 8h prior to ELISA experiment). Statistical significance was calculated by unpaired two-tailed *t* test.

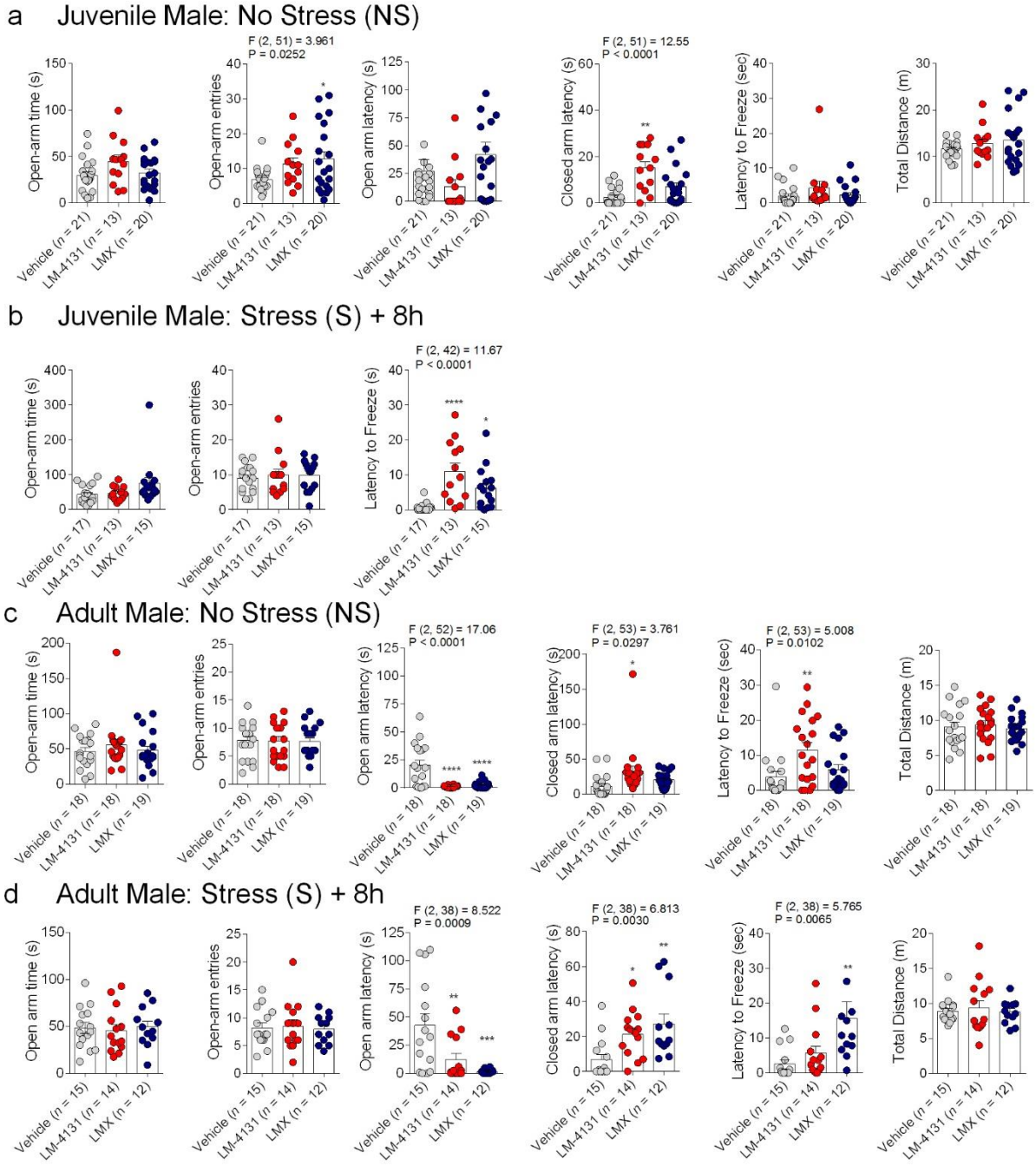

Figure G. Anxiolytic effects of COX-2 inhibitors in the elevated plus maze. (**a-d)** Open arm time, entries, and latency, closed arm latency, latency to freeze, and/or total distance traveled by juvenile (**a**) and adult (**c**) male mice under non-stressful conditions and juvenile (**b**) and adult (**d**) male mice after acute stress exposure in the elevated plus maze. Data are shown as the mean ± s.e.m. NS = no stress, S = stress (e.g., stress exposure in the form of an electric footshock administered 8h prior to testing), *P < 0.05, **P < 0.01, ***P<0.001, ****P<0.0001 (COX-2 inhibitor compared to vehicle). Statistical significance was calculated by one-way ANOVA with post hoc Holm-Sidak's multiple comparisons test.

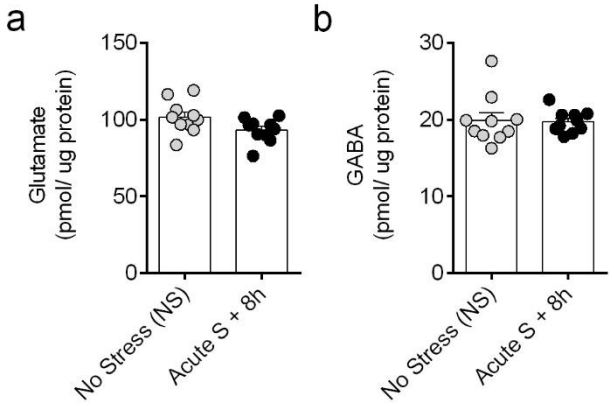

Figure H. Effects of acute footshock stress on amygdala amino acid levels. Effects of no stress (n = 10) and acute (1 day) stress (n = 10) on the amino acids, glutamate (**a**) and gamma-aminobutyric acid (GABA) (**b**). Data are shown as the mean ± s.e.m. NS = no stress, S = stress (e.g., stress exposure in the form of an electric footshock administered 8h prior to HPLC experiment), Statistical significance was calculated by unpaired, two-tailed t test.

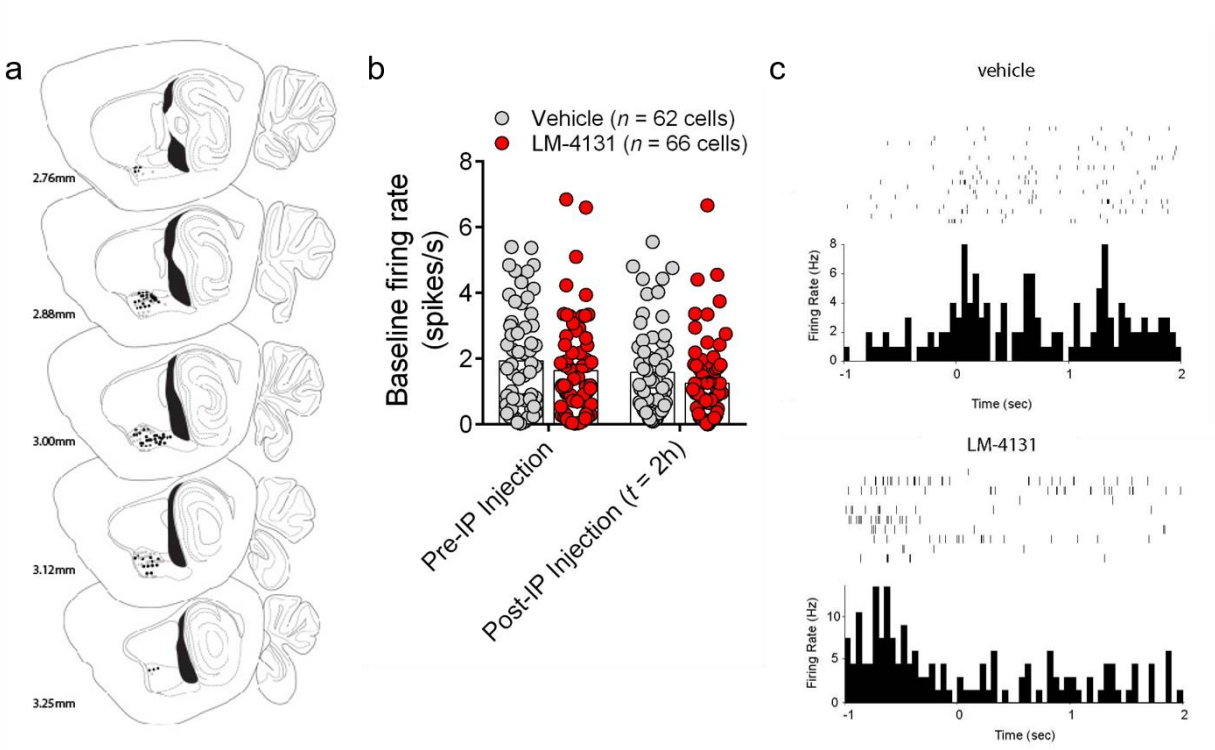

Figure I. Representative plots of cellular recordings using *in vivo* electrophysiology. (**a**) Histological reconstruction of the recording sites in the basolateral nucleus of the amygdala (BLA) with corresponding coordinates relative to bregma. (**b**) Baseline firing rate (spikes/s) of responsive excitatory cells before and after intraperitoneal (IP) injection. (**c**) Spike rasters (top) and peristimulus time histograms (PSTHs) (bottom) for representative responsive excitatory cell that is from a vehicle-treated animal versus an LM-4131-treated animal.

REFERENCES

1. Anxiety and Depression Association of America. Facts & Statistics. Vol. 2014 (Anxiety and Depression Association of America, Silver Spring, 2014).

2. National Institute of Mental Health. Anxiety Disorders. Vol. 2014 (National Institutes of Health, Bethesda, 2014).

3. Kessler, R.C., *et al.* The global burden of mental disorders: an update from the WHO World Mental Health (WMH) surveys. *Epidemiologia e psichiatria sociale* **18**, 23-33 (2009).

4. Melchior, M., *et al.* Work stress precipitates depression and anxiety in young, working women and men. *Psychological medicine* **37**, 1119-1129 (2007).

5. Greenberg, P.E., *et al.* The economic burden of anxiety disorders in the 1990s. *J Clin Psychiatry* **60**, 427-435 (1999).

6. Lepine, J.P. The epidemiology of anxiety disorders: prevalence and societal costs. *J Clin Psychiatry* **63 Suppl 14**, 4-8 (2002).

7. Crippa, J.A., *et al.* Neural basis of anxiolytic effects of cannabidiol (CBD) in generalized social anxiety disorder: a preliminary report. *J Psychopharmacol* **25**, 121-130.

8. Bergamaschi, M.M., *et al.* Cannabidiol reduces the anxiety induced by simulated public speaking in treatment-naive social phobia patients. *Neuropsychopharmacology* **36**, 1219-1226.

9. Das, R.K., *et al.* Cannabidiol enhances consolidation of explicit fear extinction in humans. *Psychopharmacology (Berl)* **226**, 781-792.

10. Nakano, S., Gillespie, H.K. & Hollister, L.E. A model for evaluation of antianxiety drugs with the use of experimentally induced stress: Comparison of nabilone and diazepam. *Clin Pharmacol Ther* **23**, 54-62 (1978).

11. Fabre, L.F. & McLendon, D. The efficacy and safety of nabilone (a synthetic cannabinoid) in the treatment of anxiety. *J Clin Pharmacol* **21**, 377S-382S (1981).

12. Rabinak, C.A., *et al.* Cannabinoid facilitation of fear extinction memory recall in humans. *Neuropharmacology* **64**, 396-402.

13. Viveros, M.P., Marco, E.M. & File, S.E. Endocannabinoid system and stress and anxiety responses. *Pharmacol Biochem Behav* **81**, 331-342 (2005).

14. Berrendero, F. & Maldonado, R. Involvement of the opioid system in the anxiolytic-like effects induced by Delta(9)-tetrahydrocannabinol. *Psychopharmacology (Berl)* **163**, 111-117 (2002).

15. Onaivi, E.S., Green, M.R. & Martin, B.R. Pharmacological characterization of cannabinoids in the elevated plus maze. *J Pharmacol Exp Ther* **253**, 1002-1009 (1990).

16. Valjent, E., Mitchell, J.M., Besson, M.J., Caboche, J. & Maldonado, R. Behavioural and biochemical evidence for interactions between Delta 9-tetrahydrocannabinol and nicotine. *Br J Pharmacol* **135**, 564-578 (2002).

17. Arevalo, C., de Miguel, R. & Hernandez-Tristan, R. Cannabinoid effects on anxiety-related behaviours and hypothalamic neurotransmitters. *Pharmacol Biochem Behav* **70**, 123-131 (2001).

18. Marin, S., *et al.* Involvement of the kappa-opioid receptor in the anxiogenic-like effect of CP 55,940 in male rats. *Pharmacol Biochem Behav* **74**, 649-656 (2003).

19. Genn, R.F., Tucci, S., Marco, E.M., Viveros, M.P. & File, S.E. Unconditioned and conditioned anxiogenic effects of the cannabinoid receptor agonist CP 55,940 in the social interaction test. *Pharmacol Biochem Behav* **77**, 567-573 (2004).

20. Marco, E.M., *et al.* Involvement of 5-HT1A receptors in behavioural effects of the cannabinoid receptor agonist CP 55,940 in male rats. *Behav Pharmacol* **15**, 21-27 (2004).

21. Hill, M.N. & Gorzalka, B.B. Enhancement of anxiety-like responsiveness to the cannabinoid CB(1) receptor agonist HU-210 following chronic stress. *Eur J Pharmacol* **499**, 291-295 (2004).

22. Gunduz-Cinar, O., *et al.* Convergent translational evidence of a role for anandamide in amygdala-mediated fear extinction, threat processing and stress-reactivity. *Mol Psychiatry* **18**, 813-823 (2013).

23. Busquets-Garcia, A., *et al.* Differential role of anandamide and 2-arachidonoylglycerol in memory and anxiety-like responses. *Biol Psychiatry* **70**, 479-486.

24. Sumislawski, J.J., Ramikie, T.S. & Patel, S. Reversible gating of endocannabinoid plasticity in the amygdala by chronic stress: a potential role for monoacylglycerol lipase inhibition in the prevention of stress-induced behavioral adaptation. *Neuropsychopharmacology* **36**, 2750-2761.

25. Aliczki, M., *et al.* Monoacylglycerol lipase inhibition-induced changes in plasma corticosterone levels, anxiety and locomotor activity in male CD1 mice. *Horm Behav* **63**, 752-758.

26. Kinsey, S.G., O'Neal, S.T., Long, J.Z., Cravatt, B.F. & Lichtman, A.H. Inhibition of endocannabinoid catabolic enzymes elicits anxiolytic-like effects in the marble burying assay. *Pharmacol Biochem Behav* **98**, 21-27.

27. Kathuria, S., *et al.* Modulation of anxiety through blockade of anandamide hydrolysis. *Nat Med* **9**, 76-81 (2003).

28. Hill, M.N., *et al.* Disruption of fatty acid amide hydrolase activity prevents the effects of chronic stress on anxiety and amygdalar microstructure. *Mol Psychiatry* **18**, 1125-1135.

29. Di Marzo, V. Biosynthesis and inactivation of endocannabinoids: relevance to their proposed role as neuromodulators. *Life Sci* **65**, 645-655 (1999).

30. Vaughan, C.W. & Christie, M.J. Retrograde signalling by endocannabinoids. *Handb Exp Pharmacol*, 367-383 (2005).

31. Di Marzo, V. & Deutsch, D.G. Biochemistry of the endogenous ligands of cannabinoid receptors. *Neurobiol Dis* **5**, 386-404 (1998).

32. Bisogno, T., Ligresti, A. & Di Marzo, V. The endocannabinoid signalling system: biochemical aspects. *Pharmacol Biochem Behav* **81**, 224-238 (2005).

33. Gorzalka, B.B., Hill, M.N. & Hillard, C.J. Regulation of endocannabinoid signaling by stress: implications for stress-related affective disorders. *Neurosci Biobehav Rev* **32**, 1152-1160 (2008).

34. Sugiura, T., Kishimoto, S., Oka, S. & Gokoh, M. Biochemistry, pharmacology and physiology of 2-arachidonoylglycerol, an endogenous cannabinoid receptor ligand. *Prog Lipid Res* **45**, 405-446 (2006).

35. Matsuda, L.A., Lolait, S.J., Brownstein, M.J., Young, A.C. & Bonner, T.I. Structure of a cannabinoid receptor and functional expression of the cloned cDNA. *Nature* **346**, 561-564 (1990).

36. Sah, P., Faber, E.S., Lopez De Armentia, M. & Power, J. The amygdaloid complex: anatomy and physiology. *Physiol Rev* **83**, 803-834 (2003).

37. Matsuda, L.A., Bonner, T.I. & Lolait, S.J. Localization of cannabinoid receptor mRNA in rat brain. *J Comp Neurol* **327**, 535-550 (1993).

38. Puente, N., *et al.* Localization and function of the cannabinoid CB1 receptor in the anterolateral bed nucleus of the stria terminalis. *PLoS One* **5**, e8869.

39. Martin, A.B., *et al.* Expression and function of CB1 receptor in the rat striatum: localization and effects on D1 and D2 dopamine receptor-mediated motor behaviors. *Neuropsychopharmacology* **33**, 1667-1679 (2008).

40. Cristino, L., *et al.* Immunohistochemical localization of cannabinoid type 1 and vanilloid transient receptor potential vanilloid type 1 receptors in the mouse brain. *Neuroscience* **139**, 1405-1415 (2006).

41. Matyas, F., *et al.* Subcellular localization of type 1 cannabinoid receptors in the rat basal ganglia. *Neuroscience* **137**, 337-361 (2006).

42. Katona, I., *et al.* Distribution of CB1 cannabinoid receptors in the amygdala and their role in the control of GABAergic transmission. *J Neurosci* **21**, 9506-9518 (2001).

43. Patel, S., Cravatt, B.F. & Hillard, C.J. Synergistic interactions between cannabinoids and environmental stress in the activation of the central amygdala. *Neuropsychopharmacology* **30**, 497-507 (2005).

44. Freund, T.F., Katona, I. & Piomelli, D. Role of endogenous cannabinoids in synaptic signaling. *Physiol Rev* **83**, 1017-1066 (2003).

45. Chhatwal, J.P., Davis, M., Maguschak, K.A. & Ressler, K.J. Enhancing cannabinoid neurotransmission augments the extinction of conditioned fear. *Neuropsychopharmacology* **30**, 516-524 (2005).

46. Kodirov, S.A., *et al.* Endogenous cannabinoids trigger the depolarization-induced suppression of excitation in the lateral amygdala. *Learn Mem* **17**, 43-49 (2010).

47. Carter, M. & Shieh, J.C. *Guide to research techniques in neuroscience*, (Elsevier/Academic Press, Amsterdam ; Boston).

48. Domenici, M.R., *et al.* Cannabinoid receptor type 1 located on presynaptic terminals of principal neurons in the forebrain controls glutamatergic synaptic transmission. *J Neurosci* **26**, 5794-5799 (2006).

49. Martina, M., Royer, S. & Pare, D. Physiological properties of central medial and central lateral amygdala neurons. *J Neurophysiol* **82**, 1843-1854 (1999).

50. Washburn, M.S. & Moises, H.C. Electrophysiological and morphological properties of rat basolateral amygdaloid neurons in vitro. *J Neurosci* **12**, 4066-4079 (1992).

51. Millhouse, O.E. & DeOlmos, J. Neuronal configurations in lateral and basolateral amygdala. *Neuroscience* **10**, 1269-1300 (1983).

52. Cassell, M.D., Gray, T.S. & Kiss, J.Z. Neuronal architecture in the rat central nucleus of the amygdala: a cytological, hodological, and immunocytochemical study. *J Comp Neurol* **246**, 478-499 (1986).

53. Faber, E.S., Callister, R.J. & Sah, P. Morphological and electrophysiological properties of principal neurons in the rat lateral amygdala in vitro. *J Neurophysiol* **85**, 714-723 (2001).

54. Schiess, M.C., Callahan, P.M. & Zheng, H. Characterization of the electrophysiological and morphological properties of rat central amygdala neurons in vitro. *J Neurosci Res* **58**, 663-673 (1999).

55. McDonald, A.J. Cytoarchitecture of the central amygdaloid nucleus of the rat. *J Comp Neurol* **208**, 401-418 (1982).

56. McDonald, A.J. & Betette, R.L. Parvalbumin-containing neurons in the rat basolateral amygdala: morphology and co-localization of Calbindin-D(28k). *Neuroscience* **102**, 413-425 (2001).

57. Schiess, M.C., Asprodini, E.K., Rainnie, D.G. & Shinnick-Gallagher, P. The central nucleus of the rat amygdala: in vitro intracellular recordings. *Brain Res* **604**, 283-297 (1993).

58. Marsicano, G. & Lutz, B. Expression of the cannabinoid receptor CB1 in distinct neuronal subpopulations in the adult mouse forebrain. *Eur J Neurosci* **11**, 4213-4225 (1999).

59. Vogel, Z., *et al.* Anandamide, a brain endogenous compound, interacts specifically with cannabinoid receptors and inhibits adenylate cyclase. *J Neurochem* **61**, 352-355 (1993).

60. Dalton, G.D. & Howlett, A.C. Cannabinoid CB1 receptors transactivate multiple receptor tyrosine kinases and regulate serine/threonine kinases to activate ERK in neuronal cells. *Br J Pharmacol* **165**, 2497-2511 (2012).

61. Pertwee, R.G., *et al.* International Union of Basic and Clinical Pharmacology. LXXIX. Cannabinoid receptors and their ligands: beyond CB(1) and CB(2). *Pharmacological reviews* **62**, 588-631 (2010).

62. Valjent, E., Pages, C., Herve, D., Girault, J.A. & Caboche, J. Addictive and non-addictive drugs induce distinct and specific patterns of ERK activation in mouse brain. *Eur J Neurosci* **19**, 1826-1836 (2004).

63. Marsicano, G., *et al.* CB1 cannabinoid receptors and on-demand defense against excitotoxicity. *Science* **302**, 84-88 (2003).

64. Rubino, T., *et al.* Cellular mechanisms underlying the anxiolytic effect of low doses of peripheral Delta9-tetrahydrocannabinol in rats. *Neuropsychopharmacology* **32**, 2036-2045 (2007).

65. Sugiura, T., *et al.* 2-Arachidonoylglycerol: a possible endogenous cannabinoid receptor ligand in brain. *Biochem Biophys Res Commun* **215**, 89-97 (1995).

66. Childers, S.R., Sexton, T. & Roy, M.B. Effects of anandamide on cannabinoid receptors in rat brain membranes. *Biochem Pharmacol* **47**, 711-715 (1994).

67. Weidenfeld, J., Feldman, S. & Mechoulam, R. Effect of the brain constituent anandamide, a cannabinoid receptor agonist, on the hypothalamo-pituitary-adrenal axis in the rat. *Neuroendocrinology* **59**, 110-112 (1994).

68. Devane, W.A., *et al.* Isolation and structure of a brain constituent that binds to the cannabinoid receptor. *Science* **258**, 1946-1949 (1992).

69. Azad, S.C., *et al.* Activation of the cannabinoid receptor type 1 decreases glutamatergic and GABAergic synaptic transmission in the lateral amygdala of the mouse. *Learn Mem* **10**, 116-128 (2003).

70. Haring, M., Guggenhuber, S. & Lutz, B. Neuronal populations mediating the effects of endocannabinoids on stress and emotionality. *Neuroscience* **204**, 145-158 (2012).

71. Azad, S.C., *et al.* Circuitry for associative plasticity in the amygdala involves endocannabinoid signaling. *J Neurosci* **24**, 9953-9961 (2004).

72. Juranek, J., *et al.* Association between amygdala volume and anxiety level: magnetic resonance imaging (MRI) study in autistic children. *J Child Neurol* **21**, 1051-1058 (2006).

73. de Kloet, E.R., Joels, M. & Holsboer, F. Stress and the brain: from adaptation to disease. *Nat Rev Neurosci* **6**, 463-475 (2005).

74. Vyas, A., Pillai, A.G. & Chattarji, S. Recovery after chronic stress fails to reverse amygdaloid neuronal hypertrophy and enhanced anxiety-like behavior. *Neuroscience* **128**, 667-673 (2004).

75. Shekhar, A., Truitt, W., Rainnie, D. & Sajdyk, T. Role of stress, corticotrophin releasing factor (CRF) and amygdala plasticity in chronic anxiety. *Stress* **8**, 209-219 (2005).

76. Rainnie, D.G., *et al.* Corticotrophin releasing factor-induced synaptic plasticity in the amygdala translates stress into emotional disorders. *J Neurosci* **24**, 3471-3479 (2004).

77. Vermetten, E. & Bremner, J.D. Circuits and systems in stress. I. Preclinical studies. *Depress Anxiety* **15**, 126-147 (2002).

78. Phelps, E.A. & LeDoux, J.E. Contributions of the amygdala to emotion processing: from animal models to human behavior. *Neuron* **48**, 175-187 (2005).

79. LeDoux, J. The emotional brain, fear, and the amygdala. *Cell Mol Neurobiol* **23**, 727-738 (2003).

80. LeDoux, J.E. Emotion circuits in the brain. *Annu Rev Neurosci* **23**, 155-184 (2000).

81. McDonald, A.J. Cortical pathways to the mammalian amygdala. *Prog Neurobiol* **55**, 257-332 (1998).

82. Vyas, A., Jadhav, S. & Chattarji, S. Prolonged behavioral stress enhances synaptic connectivity in the basolateral amygdala. *Neuroscience* **143**, 387-393 (2006).

83. Mitra, R. & Sapolsky, R.M. Acute corticosterone treatment is sufficient to induce anxiety and amygdaloid dendritic hypertrophy. *Proc Natl Acad Sci U S A* **105**, 5573-5578 (2008).

84. Vyas, A., Mitra, R., Shankaranarayana Rao, B.S. & Chattarji, S. Chronic stress induces contrasting patterns of dendritic remodeling in hippocampal and amygdaloid neurons. *J Neurosci* **22**, 6810-6818 (2002).

85. Mitra, R., Jadhav, S., McEwen, B.S., Vyas, A. & Chattarji, S. Stress duration modulates the spatiotemporal patterns of spine formation in the basolateral amygdala. *Proc Natl Acad Sci U S A* **102**, 9371-9376 (2005).

86. Hill, M.N., Hillard, C.J. & McEwen, B.S. Alterations in corticolimbic dendritic morphology and emotional behavior in cannabinoid CB1 receptor-deficient mice parallel the effects of chronic stress. *Cereb Cortex* **21**, 2056-2064 (2011).

87. Patel, S., Kingsley, P.J., Mackie, K., Marnett, L.J. & Winder, D.G. Repeated homotypic stress elevates 2-arachidonoylglycerol levels and enhances short-term endocannabinoid signaling at inhibitory synapses in basolateral amygdala. *Neuropsychopharmacology* **34**, 2699-2709 (2009).

88. Gilabert-Juan, J., Castillo-Gomez, E., Perez-Rando, M., Molto, M.D. & Nacher, J. Chronic stress induces changes in the structure of interneurons and in the expression of molecules related to neuronal structural plasticity and inhibitory neurotransmission in the amygdala of adult mice. *Exp Neurol* **232**, 33-40.

89. Rodriguez Manzanares, P.A., Isoardi, N.A., Carrer, H.F. & Molina, V.A. Previous stress facilitates fear memory, attenuates GABAergic inhibition, and increases synaptic plasticity in the rat basolateral amygdala. *J Neurosci* **25**, 8725-8734 (2005).

90. Duvarci, S. & Pare, D. Glucocorticoids enhance the excitability of principal basolateral amygdala neurons. *J Neurosci* **27**, 4482-4491 (2007).

91. Faber, E.S., Delaney, A.J. & Sah, P. SK channels regulate excitatory synaptic transmission and plasticity in the lateral amygdala. *Nat Neurosci* **8**, 635-641 (2005).

92. Mitra, R., Ferguson, D. & Sapolsky, R.M. SK2 potassium channel overexpression in basolateral amygdala reduces anxiety, stress-induced corticosterone secretion and dendritic arborization. *Mol Psychiatry* **14**, 847-855, 827 (2009).

93. Faber, E.S., *et al.* Modulation of SK channel trafficking by beta adrenoceptors enhances excitatory synaptic transmission and plasticity in the amygdala. *J Neurosci* **28**, 10803-10813 (2008).

94. Madrigal, J.L., *et al.* Induction of cyclooxygenase-2 accounts for restraint stress-induced oxidative status in rat brain. *Neuropsychopharmacology* **28**, 1579-1588 (2003).

95. Gilad, G.M., Gilad, V.H., Wyatt, R.J. & Tizabi, Y. Region-selective stress-induced increase of glutamate uptake and release in rat forebrain. *Brain Res* **525**, 335-338 (1990).

96. Rosenkranz, J.A., Venheim, E.R. & Padival, M. Chronic stress causes amygdala hyperexcitability in rodents. *Biol Psychiatry* **67**, 1128-1136.

97. Etkin, A. & Wager, T.D. Functional neuroimaging of anxiety: a meta-analysis of emotional processing in PTSD, social anxiety disorder, and specific phobia. *Am J Psychiatry* **164**, 1476-1488 (2007).

98. Karst, H., Berger, S., Erdmann, G., Schutz, G. & Joels, M. Metaplasticity of amygdalar responses to the stress hormone corticosterone. *Proc Natl Acad Sci U S A* **107**, 14449-14454.

99. Gabr, R.W., Birkle, D.L. & Azzaro, A.J. Stimulation of the amygdala by glutamate facilitates corticotropin-releasing factor release from the median eminence and activation of the hypothalamic-pituitary-adrenal axis in stressed rats. *Neuroendocrinology* **62**, 333-339 (1995).

100. Hill, M.N., *et al.* Suppression of amygdalar endocannabinoid signaling by stress contributes to activation of the hypothalamic-pituitary-adrenal axis. *Neuropsychopharmacology* **34**, 2733-2745 (2009).

101. Patel, S., Roelke, C.T., Rademacher, D.J. & Hillard, C.J. Inhibition of restraint stress-induced neural and behavioural activation by endogenous cannabinoid signalling. *Eur J Neurosci* **21**, 1057-1069 (2005).

102. Ligresti, A., Cascio, M.G. & Di Marzo, V. Endocannabinoid metabolic pathways and enzymes. *Curr Drug Targets CNS Neurol Disord* **4**, 615-623 (2005).

103. Sutt, S., *et al.* Cat odour-induced anxiety--a study of the involvement of the endocannabinoid system. *Psychopharmacology (Berl)* **198**, 509-520 (2008).

104. Chopra, G.S. & Smith, J.W. Psychotic reactions following cannabis use in East Indians. *Arch Gen Psychiatry* **30**, 24-27 (1974).

105. Howlett, A.C., *et al.* International Union of Pharmacology. XXVII. Classification of cannabinoid receptors. *Pharmacological reviews* **54**, 161-202 (2002).

106. Onaivi, E.S., Chakrabarti, A., Gwebu, E.T. & Chaudhuri, G. Neurobehavioral effects of delta 9-THC and cannabinoid (CB1) receptor gene expression in mice. *Behav Brain Res* **72**, 115-125 (1995).

107. Hill, M.N. & Gorzalka, B.B. Increased sensitivity to restraint stress and novelty-induced emotionality following long-term, high dose cannabinoid exposure. *Psychoneuroendocrinology* **31**, 526-536 (2006).

108. Haller, J., Varga, B., Ledent, C. & Freund, T.F. CB1 cannabinoid receptors mediate anxiolytic effects: convergent genetic and pharmacological evidence with CB1-specific agents. *Behav Pharmacol* **15**, 299-304 (2004).

109. Rubino, T., *et al.* CB1 receptor stimulation in specific brain areas differently modulate anxiety-related behaviour. *Neuropharmacology* **54**, 151-160 (2008).

110. Ganon-Elazar, E. & Akirav, I. Cannabinoids prevent the development of behavioral and endocrine alterations in a rat model of intense stress. *Neuropsychopharmacology* **37**, 456-466 (2012).

111. Ganon-Elazar, E. & Akirav, I. Cannabinoid receptor activation in the basolateral amygdala blocks the effects of stress on the conditioning and extinction of inhibitory avoidance. *J Neurosci* **29**, 11078-11088 (2009).

112. Phan, K.L., *et al.* Cannabinoid modulation of amygdala reactivity to social signals of threat in humans. *J Neurosci* **28**, 2313-2319 (2008).

113. Blasio, A., *et al.* Rimonabant precipitates anxiety in rats withdrawn from palatable food: role of the central amygdala. *Neuropsychopharmacology* **38**, 2498-2507 (2013).

114. Navarro, M., *et al.* Acute administration of the CB1 cannabinoid receptor antagonist SR 141716A induces anxiety-like responses in the rat. *Neuroreport* **8**, 491-496 (1997).

115. Gamble-George, J.C., *et al.* Dissociable effects of CB1 receptor blockade on anxiety-like and consummatory behaviors in the novelty-induced hypophagia test in mice. *Psychopharmacology (Berl)* **228**, 401-409 (2013).

116. Haller, J., Bakos, N., Szirmay, M., Ledent, C. & Freund, T.F. The effects of genetic and pharmacological blockade of the CB1 cannabinoid receptor on anxiety. *Eur J Neurosci* **16**, 1395-1398 (2002).

117. MacLean, K.I. & Littleton, J.M. Environmental stress as a factor in the response of rat brain catecholamine metabolism to delta8-tetrahydrocannabinol. *Eur J Pharmacol* **41**, 171-182 (1977).

118. Hollister, L.E. Health aspects of cannabis. *Pharmacological reviews* **38**, 1-20 (1986).

119. Gregg, J.M., Small, E.W., Moore, R., Raft, D. & Toomey, T.C. Emotional response to intravenous delta9tetrahydrocannabinol during oral surgery. *J Oral Surg* **34**, 301-313 (1976).

120. Talbott, J.A. & Teague, J.W. Marihuana psychosis. Acute toxic psychosis associated with the use of Cannabis derivatives. *JAMA : the journal of the American Medical Association* **210**, 299-302 (1969).

121. Kotin, J., Post, R.M. & Goodwin, F.K. 9 -Tetrahydrocannabinol in depressed patients. *Arch Gen Psychiatry* **28**, 345-348 (1973).

122. Rey, A.A., Purrio, M., Viveros, M.P. & Lutz, B. Biphasic effects of cannabinoids in anxiety responses: CB1 and GABA(B) receptors in the balance of GABAergic and glutamatergic neurotransmission. *Neuropsychopharmacology* **37**, 2624-2634.

123. Zoppi, S., *et al.* Regulatory role of cannabinoid receptor 1 in stress-induced excitotoxicity and neuroinflammation. *Neuropsychopharmacology* **36**, 805-818.

124. Cravatt, B.F., *et al.* Supersensitivity to anandamide and enhanced endogenous cannabinoid signaling in mice lacking fatty acid amide hydrolase. *Proc Natl Acad Sci U S A* **98**, 9371-9376 (2001).

125. Hermanson, D.J., *et al.* Substrate-selective COX-2 inhibition decreases anxiety via endocannabinoid activation. *Nat Neurosci* **16**, 1291-1298.

126. Cravatt, B.F., *et al.* Molecular characterization of an enzyme that degrades neuromodulatory fatty-acid amides. *Nature* **384**, 83-87 (1996).

127. Blankman, J.L., Simon, G.M. & Cravatt, B.F. A comprehensive profile of brain enzymes that hydrolyze the endocannabinoid 2-arachidonoylglycerol. *Chem Biol* **14**, 1347-1356 (2007).

128. Ueda, N., Tsuboi, K. & Uyama, T. Metabolism of endocannabinoids and related N-acylethanolamines: canonical and alternative pathways. *FEBS J* **280**, 1874-1894 (2013).

129. Thomas, E.A., Cravatt, B.F., Danielson, P.E., Gilula, N.B. & Sutcliffe, J.G. Fatty acid amide hydrolase, the degradative enzyme for anandamide and oleamide, has selective distribution in neurons within the rat central nervous system. *J Neurosci Res* **50**, 1047-1052 (1997).

130. Hillard, C.J., Wilkison, D.M., Edgemond, W.S. & Campbell, W.B. Characterization of the kinetics and distribution of N-arachidonylethanolamine (anandamide) hydrolysis by rat brain. *Biochim Biophys Acta* **1257**, 249-256 (1995).

131. Tsou, K., *et al.* Fatty acid amide hydrolase is located preferentially in large neurons in the rat central nervous system as revealed by immunohistochemistry. *Neurosci Lett* **254**, 137-140 (1998).

132. Gulyas, A.I., *et al.* Segregation of two endocannabinoid-hydrolyzing enzymes into pre- and postsynaptic compartments in the rat hippocampus, cerebellum and amygdala. *Eur J Neurosci* **20**, 441-458 (2004).

133. Bluett, R.J., *et al.* Central anandamide deficiency predicts stress-induced anxiety: behavioral reversal through endocannabinoid augmentation. *Transl Psychiatry* **4**, e408 (2014).

134. Bortolato, M., *et al.* Antidepressant-like activity of the fatty acid amide hydrolase inhibitor URB597 in a rat model of chronic mild stress. *Biol Psychiatry* **62**, 1103-1110 (2007).

135. Rademacher, D.J., *et al.* Effects of acute and repeated restraint stress on endocannabinoid content in the amygdala, ventral striatum, and medial prefrontal cortex in mice. *Neuropharmacology* **54**, 108-116 (2008).

136. Moreira, F.A., Kaiser, N., Monory, K. & Lutz, B. Reduced anxiety-like behaviour induced by genetic and pharmacological inhibition of the endocannabinoid-degrading enzyme fatty acid amide hydrolase (FAAH) is mediated by CB1 receptors. *Neuropharmacology* **54**, 141-150 (2008).

137. Rinaldi-Carmona, M., *et al.* SR141716A, a potent and selective antagonist of the brain cannabinoid receptor. *FEBS Lett* **350**, 240-244 (1994).

138. Mato, S., Pazos, A. & Valdizan, E.M. Cannabinoid receptor antagonism and inverse agonism in response to SR141716A on cAMP production in human and rat brain. *Eur J Pharmacol* **443**, 43-46 (2002).

139. Sim-Selley, L.J., Brunk, L.K. & Selley, D.E. Inhibitory effects of SR141716A on G-protein activation in rat brain. *Eur J Pharmacol* **414**, 135-143 (2001).

140. Haller, J., *et al.* Interactions between environmental aversiveness and the anxiolytic effects of enhanced cannabinoid signaling by FAAH inhibition in rats. *Psychopharmacology (Berl)* **204**, 607-616 (2009).

141. Chiang, K.P., Gerber, A.L., Sipe, J.C. & Cravatt, B.F. Reduced cellular expression and activity of the P129T mutant of human fatty acid amide hydrolase: evidence for a link between defects in the endocannabinoid system and problem drug use. *Hum Mol Genet* **13**, 2113-2119 (2004).

142. Sipe, J.C., Chiang, K., Gerber, A.L., Beutler, E. & Cravatt, B.F. A missense mutation in human fatty acid amide hydrolase associated with problem drug use. *Proc Natl Acad Sci U S A* **99**, 8394-8399 (2002).

143. Hariri, A.R., *et al.* Divergent effects of genetic variation in endocannabinoid signaling on human threat- and reward-related brain function. *Biol Psychiatry* **66**, 9-16 (2009).

144. Gunduz-Cinar, O., *et al.* Convergent translational evidence of a role for anandamide in amygdala-mediated fear extinction, threat processing and stress-reactivity. *Mol Psychiatry* **18**, 813-823.

145. Chanda, P.K., *et al.* Monoacylglycerol lipase activity is a critical modulator of the tone and integrity of the endocannabinoid system. *Mol Pharmacol* **78**, 996-1003.

146. Aliczki, M., Balogh, Z., Tulogdi, A. & Haller, J. The temporal dynamics of the effects of monoacylglycerol lipase blockade on locomotion, anxiety, and body temperature. *Behav Pharmacol* **23**, 348-357.

147. Schlosburg, J.E., *et al.* Chronic monoacylglycerol lipase blockade causes functional antagonism of the endocannabinoid system. *Nat Neurosci* **13**, 1113-1119.

148. Sciolino, N.R., Zhou, W. & Hohmann, A.G. Enhancement of endocannabinoid signaling with JZL184, an inhibitor of the 2-arachidonoylglycerol hydrolyzing enzyme monoacylglycerol lipase, produces anxiolytic effects under conditions of high environmental aversiveness in rats. *Pharmacol Res* **64**, 226-234.

149. Yu, M., Ives, D. & Ramesha, C.S. Synthesis of prostaglandin E2 ethanolamide from anandamide by cyclooxygenase-2. *J Biol Chem* **272**, 21181-21186 (1997).

150. Kozak, K.R., *et al.* Metabolism of the endocannabinoids, 2-arachidonylglycerol and anandamide, into prostaglandin, thromboxane, and prostacyclin glycerol esters and ethanolamides. *J Biol Chem* **277**, 44877-44885 (2002).

151. Kozak, K.R., Prusakiewicz, J.J., Rowlinson, S.W., Prudhomme, D.R. & Marnett, L.J. Amino acid determinants in cyclooxygenase-2 oxygenation of the endocannabinoid anandamide. *Biochemistry* **42**, 9041-9049 (2003).

152. Kozak, K.R., Rowlinson, S.W. & Marnett, L.J. Oxygenation of the endocannabinoid, 2-arachidonylglycerol, to glyceryl prostaglandins by cyclooxygenase-2. *J Biol Chem* **275**, 33744-33749 (2000).

153. Breder, C.D., Dewitt, D. & Kraig, R.P. Characterization of inducible cyclooxygenase in rat brain. *J Comp Neurol* **355**, 296-315 (1995).

154. Kaufmann, W.E., Worley, P.F., Pegg, J., Bremer, M. & Isakson, P. COX-2, a synaptically induced enzyme, is expressed by excitatory neurons at postsynaptic sites in rat cerebral cortex. *Proc Natl Acad Sci U S A* **93**, 2317-2321 (1996).

155. Ma, Y., Matsuwaki, T., Yamanouchi, K. & Nishihara, M. Cyclooxygenase-2-related signaling in the hypothalamus plays differential roles in response to various acute stresses. *Brain Res* **1508**, 23-33.

156. Yamagata, K., Andreasson, K.I., Kaufmann, W.E., Barnes, C.A. & Worley, P.F. Expression of a mitogen-inducible cyclooxygenase in brain neurons: regulation by synaptic activity and glucocorticoids. *Neuron* **11**, 371-386 (1993).

157. Garcia-Bueno, B., Madrigal, J.L., Perez-Nievas, B.G. & Leza, J.C. Stress mediators regulate brain prostaglandin synthesis and peroxisome proliferator-activated receptor-gamma activation after stress in rats. *Endocrinology* **149**, 1969-1978 (2008).

158. Smith, S.M. & Vale, W.W. The role of the hypothalamic-pituitary-adrenal axis in neuroendocrine responses to stress. *Dialogues in clinical neuroscience* **8**, 383-395 (2006).

159. Dhir, A., Padi, S.S., Naidu, P.S. & Kulkarni, S.K. Protective effect of naproxen (non-selective COX-inhibitor) or rofecoxib (selective COX-2 inhibitor) on immobilization stress-induced behavioral and biochemical alterations in mice. *Eur J Pharmacol* **535**, 192-198 (2006).

160. Kumari, B., Kumar, A. & Dhir, A. Protective effect of non-selective and selective COX-2-inhibitors in acute immobilization stress-induced behavioral and biochemical alterations. *Pharmacol Rep* **59**, 699-707 (2007).

161. Lee, T.T., Hill, M.N., Hillard, C.J. & Gorzalka, B.B. Temporal changes in N-acylethanolamine content and metabolism throughout the peri-adolescent period. *Synapse* **67**, 4-10.

162. Hermanson, D.J., Gamble-George, J.C., Marnett, L.J. & Patel, S. Substrate-selective COX-2 inhibition as a novel strategy for therapeutic endocannabinoid augmentation. *Trends Pharmacol Sci* **35**, 358-367 (2014).

163. Hefner, K., *et al.* Impaired fear extinction learning and cortico-amygdala circuit abnormalities in a common genetic mouse strain. *J Neurosci* **28**, 8074-8085 (2008).

164. Halsey, L.G., Curran-Everett, D., Vowler, S.L. & Drummond, G.B. The fickle P value generates irreproducible results. *Nat Methods* **12**, 179-185 (2015).

165. Liu, X., Tang, X. & Sanford, L.D. Stressor controllability and Fos expression in stress regulatory regions in mice. *Physiol Behav* **97**, 321-326 (2009).

166. Balderston, N.L., Schultz, D.H., Hopkins, L. & Helmstetter, F.J. Functionally distinct amygdala subregions identified using DTI and high-resolution fMRI. *Soc Cogn Affect Neurosci* (2015).

167. Jean-Richard-Dit-Bressel, P. & McNally, G.P. The role of the basolateral amygdala in punishment. *Learn Mem* **22**, 128-137 (2015).

168. Sheskin, D. *Handbook of parametric and nonparametric statistical procedures*, (Chapman & Hall/CRC, Boca Raton, 2004).

169. Noguchi, M., *et al.* Effect of celecoxib, a cyclooxygenase-2 inhibitor, on the pathophysiology of adjuvant arthritis in rat. *Eur J Pharmacol* **513**, 229-235 (2005).

170. Sood, R., *et al.* Underwater trauma causes a long-term specific increase in the expression of cyclooxygenase-2 in the ventral CA(1) of the hippocampus. *Psychoneuroendocrinology* **49**, 62-68 (2014).

171. Windsor, M.A., Valk, P.L., Xu, S., Banerjee, S. & Marnett, L.J. Exploring the molecular determinants of substrate-selective inhibition of cyclooxygenase-2 by lumiracoxib. *Bioorg Med Chem Lett* **23**, 5860-5864 (2013).

172. Mitchener, M.M., *et al.* Competition and allostery govern substrate selectivity of cyclooxygenase-2. *Proc Natl Acad Sci U S A* **112**, 12366-12371 (2015).

173. Kessler, R.C., *et al.* Co-morbid major depression and generalized anxiety disorders in the National Comorbidity Survey follow-up. *Psychol Med* **38**, 365-374 (2008).

174. Olino, T.M., Klein, D.N., Lewinsohn, P.M., Rohde, P. & Seeley, J.R. Longitudinal associations between depressive and anxiety disorders: a comparison of two trait models. *Psychol Med* **38**, 353-363 (2008).

175. Kvaal, K., *et al.* Co-occurrence of anxiety and depressive disorders in a community sample of older people: results from the MRC CFAS (Medical Research Council Cognitive Function and Ageing Study). *Int J Geriatr Psychiatry* **23**, 229-237 (2008).

176. Fava, M., *et al.* Anxiety disorders in major depression. *Compr Psychiatry* **41**, 97-102 (2000).

177. Kaufman, J. & Charney, D. Comorbidity of mood and anxiety disorders. *Depress Anxiety* **12 Suppl 1**, 69-76 (2000).

178. Kessler, R.C., *et al.* Lifetime and 12-month prevalence of DSM-III-R psychiatric disorders in the United States. Results from the National Comorbidity Survey. *Arch Gen Psychiatry* **51**, 8-19 (1994).

179. Klein, D.F. Endogenomorphic depression. A conceptual and terminological revision. *Arch Gen Psychiatry* **31**, 447-454 (1974).

180. Hamilton, M. Development of a rating scale for primary depressive illness. *Br J Soc Clin Psychol* **6**, 278-296 (1967).

181. D'Aquila, P.S., Brain, P. & Willner, P. Effects of chronic mild stress on performance in behavioural tests relevant to anxiety and depression. *Physiol Behav* **56**, 861-867 (1994).

182. Harkin, A., Houlihan, D.D. & Kelly, J.P. Reduction in preference for saccharin by repeated unpredictable stress in mice and its prevention by imipramine. *J Psychopharmacol* **16**, 115-123 (2002).

183. Duman, C.H. Models of depression. *Vitam Horm* **82**, 1-21 (2010).

184. Dulawa, S.C. & Hen, R. Recent advances in animal models of chronic antidepressant effects: the novelty-induced hypophagia test. *Neurosci Biobehav Rev* **29**, 771-783 (2005).

185. Mohammadinejad, P., *et al.* Celecoxib Versus Diclofenac in Mild to Moderate Depression Management Among Breast Cancer Patients: A Double-Blind, Placebo-Controlled, Randomized Trial. *Ann Pharmacother* **49**, 953-961 (2015).

186. Kurhe, Y., Mahesh, R. & Gupta, D. Effect of a selective cyclooxygenase type 2 inhibitor celecoxib on depression associated with obesity in mice: an approach using behavioral tests. *Neurochem Res* **39**, 1395-1402 (2014).

187. Muller, N., *et al.* The cyclooxygenase-2 inhibitor celecoxib has therapeutic effects in major depression: results of a double-blind, randomized, placebo controlled, add-on pilot study to reboxetine. *Mol Psychiatry* **11**, 680-684 (2006).

188. Guo, J.Y., *et al.* Chronic treatment with celecoxib reverses chronic unpredictable stress-induced depressive-like behavior via reducing cyclooxygenase-2 expression in rat brain. *Eur J Pharmacol* **612**, 54-60 (2009).

189. Akhondzadeh, S., *et al.* Clinical trial of adjunctive celecoxib treatment in patients with major depression: a double blind and placebo controlled trial. *Depress Anxiety* **26**, 607-611 (2009).

190. Na, K.S., Lee, K.J., Lee, J.S., Cho, Y.S. & Jung, H.Y. Efficacy of adjunctive celecoxib treatment for patients with major depressive disorder: a meta-analysis. *Prog Neuropsychopharmacol Biol Psychiatry* **48**, 79-85 (2014).

191. Santiago, R.M., *et al.* Antidepressant-like effect of celecoxib piroxicam in rat models of depression. *J Neural Transm (Vienna)* **121**, 671-682 (2014).

192. Galecki, P., Talarowska, M., Bobinska, K. & Szemraj, J. COX-2 gene expression is correlated with cognitive function in recurrent depressive disorder. *Psychiatry Res* **215**, 488-490 (2014).

193. Matthews, K., Christmas, D., Swan, J. & Sorrell, E. Animal models of depression: navigating through the clinical fog. *Neurosci Biobehav Rev* **29**, 503-513 (2005).

194. Zhao, Y., *et al.* A mouse model of depression induced by repeated corticosterone injections. *Eur J Pharmacol* **581**, 113-120 (2008).

195. Hohne, N., *et al.* Increased HPA axis response to psychosocial stress in remitted depression: the influence of coping style. *Biol Psychol* **103**, 267-275 (2014).

196. Herane Vives, A., *et al.* The relationship between cortisol, stress and psychiatric illness: New insights using hair analysis. *J Psychiatr Res* **70**, 38-49 (2015).

197. Ali, S.H., *et al.* Resveratrol ameliorates depressive-like behavior in repeated corticosterone-induced depression in mice. *Steroids* **101**, 37-42 (2015).

198. Pietrzak, R.H., *et al.* Cannabinoid type 1 receptor availability in the amygdala mediates threat processing in trauma survivors. *Neuropsychopharmacology* **39**, 2519-2528 (2014).

199. Neumeister, A., *et al.* Elevated brain cannabinoid CB1 receptor availability in post-traumatic stress disorder: a positron emission tomography study. *Mol Psychiatry* **18**, 1034-1040 (2013).

200. Lee, T.T., Hill, M.N., Hillard, C.J. & Gorzalka, B.B. Temporal changes in N-acylethanolamine content and metabolism throughout the peri-adolescent period. *Synapse* **67**, 4-10 (2013).

201. Reich, C.G., Taylor, M.E. & McCarthy, M.M. Differential effects of chronic unpredictable stress on hippocampal CB1 receptors in male and female rats. *Behav Brain Res* **203**, 264-269 (2009).

202. Hill, M.N., Karacabeyli, E.S. & Gorzalka, B.B. Estrogen recruits the endocannabinoid system to modulate emotionality. *Psychoneuroendocrinology* **32**, 350-357 (2007).

203. Maccarrone, M., Bari, M., Battista, N. & Finazzi-Agro, A. Estrogen stimulates arachidonoylethanolamide release from human endothelial cells and platelet activation. *Blood* **100**, 4040-4048 (2002).

204. Buvanendran, A. & Barkin, R. Lumiracoxib. *Drugs Today (Barc)* **43**, 137-147 (2007).

205. Mangold, J.B., *et al.* Pharmacokinetics and metabolism of lumiracoxib in healthy male subjects. *Drug Metab Dispos* **32**, 566-571 (2004).

206. Shi, S. & Klotz, U. Clinical use and pharmacological properties of selective COX-2 inhibitors. *Eur J Clin Pharmacol* **64**, 233-252 (2008).

207. Windsor, M.A., *et al.* Substrate-Selective Inhibition of Cyclooxygenase-2: Development and Evaluation of Achiral Profen Probes. *ACS Med Chem Lett* **3**, 759-763 (2012).

208. Duggan, K.C., *et al.* (R)-Profens are substrate-selective inhibitors of endocannabinoid oxygenation by COX-2. *Nat Chem Biol* **7**, 803-809 (2011).

209. Steffens, M., Engler, C., Zentner, J. & Feuerstein, T.J. Cannabinoid CB1 receptor-mediated modulation of evoked dopamine release and of adenylyl cyclase activity in the human neocortex. *Br J Pharmacol* **141**, 1193-1203 (2004).

210. Romero, J., *et al.* The endogenous cannabinoid receptor ligand, anandamide, inhibits the motor behavior: role of nigrostriatal dopaminergic neurons. *Life Sci* **56**, 2033-2040 (1995).

211. Dunn, A.J. Changes in plasma and brain tryptophan and brain serotonin and 5-hydroxyindoleacetic acid after footshock stress. *Life Sci* **42**, 1847-1853 (1988).

212. Herman, J.P., *et al.* Differential effects of inescapable footshocks and of stimuli previously paired with inescapable footshocks on dopamine turnover in cortical and limbic areas of the rat. *Life Sci* **30**, 2207-2214 (1982).

213. Speciale, S.G., Miller, J.D., McMillen, B.A. & German, D.C. Activation of specific central dopamine pathways: locomotion and footshock. *Brain Res Bull* **16**, 33-38 (1986).

214. Delgado, M., *et al.* Anxiolytic-like effect of a serotonergic ligand with high affinity for 5-HT1A, 5-HT2A and 5-HT3 receptors. *Eur J Pharmacol* **511**, 9-19 (2005).

215. Seo, J.H. & Kuzhikandathil, E.V. Dopamine D3 Receptor Mediates Preadolescent Stress-Induced Adult Psychiatric Disorders. *PLoS One* **10**, e0143908 (2015).

216. Hranilovic, D., Bucan, M. & Wang, Y. Emotional response in dopamine D2L receptor-deficient mice. *Behav Brain Res* **195**, 246-250 (2008).

217. Wang, W., *et al.* Enhancement of apamin-sensitive medium afterhyperpolarization current by anandamide and its role in excitability control in cultured hippocampal neurons. *Neuropharmacology* **60**, 901-909 (2011).

218. Goodfellow, C.E. & Glass, M. Anandamide receptor signal transduction. *Vitam Horm* **81**, 79-110 (2009).

219. Felder, C.C., *et al.* Anandamide, an endogenous cannabimimetic eicosanoid, binds to the cloned human cannabinoid receptor and stimulates receptor-mediated signal transduction. *Proc Natl Acad Sci U S A* **90**, 7656-7660 (1993).

220. Rau, A.R., Chappell, A.M., Butler, T.R., Ariwodola, O.J. & Weiner, J.L. Increased Basolateral Amygdala Pyramidal Cell Excitability May Contribute to the Anxiogenic Phenotype Induced by Chronic Early-Life Stress. *J Neurosci* **35**, 9730-9740 (2015).

221. Aguiar, D.C., Terzian, A.L., Guimaraes, F.S. & Moreira, F.A. Anxiolytic-like effects induced by blockade of transient receptor potential vanilloid type 1 (TRPV1) channels in the medial prefrontal cortex of rats. *Psychopharmacology (Berl)* **205**, 217-225 (2009).

222. Moreira, F.A. & Wotjak, C.T. Cannabinoids and anxiety. *Curr Top Behav Neurosci* **2**, 429-450 (2010).

223. Moreira, F.A., Aguiar, D.C., Terzian, A.L., Guimaraes, F.S. & Wotjak, C.T. Cannabinoid type 1 receptors and transient receptor potential vanilloid type 1 channels in fear and anxiety-two sides of one coin? *Neuroscience* **204**, 186-192 (2012).

224. Hakimizadeh, E., Oryan, S., Hajizadeh Moghaddam, A., Shamsizadeh, A. & Roohbakhsh, A. Endocannabinoid System and TRPV1 Receptors in the Dorsal Hippocampus of the Rats Modulate Anxiety-like Behaviors. *Iran J Basic Med Sci* **15**, 795-802 (2012).

225. Garcia-Gutierrez, M.S., Garcia-Bueno, B., Zoppi, S., Leza, J.C. & Manzanares, J. Chronic blockade of cannabinoid CB2 receptors induces anxiolytic-like actions associated with alterations in GABA(A) receptors. *Br J Pharmacol* **165**, 951-964 (2012).

226. Bahi, A., *et al.* beta-Caryophyllene, a CB2 receptor agonist produces multiple behavioral changes relevant to anxiety and depression in mice. *Physiol Behav* **135**, 119-124 (2014).

227. Rosen, J.B. & Schulkin, J. From normal fear to pathological anxiety. *Psychol Rev* **105**, 325-350 (1998).

228. Jovanovic, T., *et al.* Acute stress disorder versus chronic posttraumatic stress disorder: inhibition of fear as a function of time since trauma. *Depress Anxiety* **30**, 217-224 (2013).

229. Maren, S., Aharonov, G. & Fanselow, M.S. Retrograde abolition of conditional fear after excitotoxic lesions in the basolateral amygdala of rats: absence of a temporal gradient. *Behav Neurosci* **110**, 718-726 (1996).

230. Phillips, R.G. & LeDoux, J.E. Differential contribution of amygdala and hippocampus to cued and contextual fear conditioning. *Behav Neurosci* **106**, 274-285 (1992).

231. Kalin, N.H., Shelton, S.E. & Davidson, R.J. The role of the central nucleus of the amygdala in mediating fear and anxiety in the primate. *J Neurosci* **24**, 5506-5515 (2004).

232. Gale, G.D., *et al.* Role of the basolateral amygdala in the storage of fear memories across the adult lifetime of rats. *J Neurosci* **24**, 3810-3815 (2004).

233. LaBar, K.S. & LeDoux, J.E. Partial disruption of fear conditioning in rats with unilateral amygdala damage: correspondence with unilateral temporal lobectomy in humans. *Behav Neurosci* **110**, 991-997 (1996).

234. Onishi, B.K. & Xavier, G.F. Contextual, but not auditory, fear conditioning is disrupted by neurotoxic selective lesion of the basal nucleus of amygdala in rats. *Neurobiol Learn Mem* **93**, 165-174 (2010).

235. Akagi Jordao, E.M., Onishi, B.K. & Xavier, G.F. Pre-Training Reversible Inactivation of the Basal Amygdala (BA) Disrupts Contextual, but Not Auditory, Fear Conditioning, in Rats. *PLoS One* **10**, e0125489 (2015).

236. Flavell, C.R. & Lee, J.L. Post-training unilateral amygdala lesions selectively impair contextual fear memories. *Learn Mem* **19**, 256-263 (2012).

237. Hermanson, D.J., *et al.* Substrate-selective COX-2 inhibition decreases anxiety via endocannabinoid activation. *Nat Neurosci* **16**, 1291-1298 (2013).

238. Simone, J.J., Green, M.R., Hodges, T.E. & McCormick, C.M. Differential effects of CB1 receptor agonism in behavioural tests of unconditioned and conditioned fear in adult male rats. *Behav Brain Res* **279**, 9-16 (2015).

239. Kuhnert, S., Meyer, C. & Koch, M. Involvement of cannabinoid receptors in the amygdala and prefrontal cortex of rats in fear learning, consolidation, retrieval and extinction. *Behav Brain Res* **250**, 274-284 (2013).

240. Bagley, J. & Moghaddam, B. Temporal dynamics of glutamate efflux in the prefrontal cortex and in the hippocampus following repeated stress: effects of pretreatment with saline or diazepam. *Neuroscience* **77**, 65-73 (1997).

241. Simon, A.B. & Gorman, J.M. Advances in the treatment of anxiety: targeting glutamate. *NeuroRx* **3**, 57-68 (2006).

242. Alo, R., *et al.* Excitatory/inhibitory equilibrium of the central amygdala nucleus gates anti-depressive and anxiolytic states in the hamster. *Pharmacol Biochem Behav* **118**, 79-86 (2014).

243. Campos, A.C., Ferreira, F.R., Guimaraes, F.S. & Lemos, J.I. Facilitation of endocannabinoid effects in the ventral hippocampus modulates anxiety-like behaviors depending on previous stress experience. *Neuroscience* **167**, 238-246 (2010).

244. Likhtik, E., Pelletier, J.G., Popescu, A.T. & Pare, D. Identification of basolateral amygdala projection cells and interneurons using extracellular recordings. *J Neurophysiol* **96**, 3257-3265 (2006).

245. Chefer, V.I., Thompson, A.C., Zapata, A. & Shippenberg, T.S. Overview of brain microdialysis. *Curr Protoc Neurosci* **Chapter 7**, Unit7 1 (2009).

246. Hetzel, A. & Rosenkranz, J.A. Distinct effects of repeated restraint stress on basolateral amygdala neuronal membrane properties in resilient adolescent and adult rats. *Neuropsychopharmacology* **39**, 2114-2130 (2014).

247. Rosenkranz, J.A., Venheim, E.R. & Padival, M. Chronic stress causes amygdala hyperexcitability in rodents. *Biol Psychiatry* **67**, 1128-1136 (2010).

248. Davis, M., Rainnie, D. & Cassell, M. Neurotransmission in the rat amygdala related to fear and anxiety. *Trends Neurosci* **17**, 208-214 (1994).

249. Mozhui, K., *et al.* Strain differences in stress responsivity are associated with divergent amygdala gene expression and glutamate-mediated neuronal excitability. *J Neurosci* **30**, 5357-5367 (2010).